AD-A010 228

AIDS FOR THE STUDY OF ELECTROMAGNETIC BLACKOUT

Warren S. Knapp, et al

General Electric Company

Prepared for:

Defense Nuclear Agency

25 Febraury 1975

DNA 3499H

AIDS FOR THE STUDY OF ELECTROMAGNETIC BLACKOUT

General Electric Company — TEMPO
816 State Street
Santa Barbara, California 93102

25 February 1975

Handbook

CONTRACT No. DNA 001-72-C-0180

**APPROVED FOR PUBLIC RELEASE;
DISTRIBUTION UNLIMITED.**

THIS WORK SPONSORED BY THE DEFENSE NUCLEAR AGENCY
UNDER SUBTASK HE043-25.

Prepared for
Director
DEFENSE NUCLEAR AGENCY
Washington, D. C. 20305

UNCLASSIFIED

SECURITY CLASSIFICATION OF THIS PAGE (When Data Entered)

REPORT DOCUMENTATION PAGE	READ INSTRUCTIONS BEFORE COMPLETING FORM
1. REPORT NUMBER: DNA 3499H	2. GOVT ACCESSION NO.
3. RECIPIENT'S CATALOG NUMBER: AD-A010 228	
4. TITLE (and Subtitle): AIDS FOR THE STUDY OF ELECTROMAGNETIC BLACKOUT	5. TYPE OF REPORT & PERIOD COVERED: Handbook
6. PERFORMING ORG. REPORT NUMBER: GE74TMP-33	
7. AUTHOR(s): Warren S. Knapp Kenneth Schwartz	8. CONTRACT OR GRANT NUMBER(s): DNA 001-72-C-0180
9. PERFORMING ORGANIZATION NAME AND ADDRESS: General Electric Company—TEMPO 816 State Street Santa Barbara, California 93102	10. PROGRAM ELEMENT, PROJECT, TASK AREA & WORK UNIT NUMBERS: NWED Subtask HE043-25
11. CONTROLLING OFFICE NAME AND ADDRESS: Director Defense Nuclear Agency Washington, D.C. 20305	12. REPORT DATE: 25 February 1975
	13. NUMBER OF PAGES: ~~200~~ 199
14. MONITORING AGENCY NAME & ADDRESS(if different from Controlling Office)	15. SECURITY CLASS. (of this report): UNCLASSIFIED
	15a. DECLASSIFICATION/DOWNGRADING SCHEDULE

16. DISTRIBUTION STATEMENT (of this Report)

Approved for public release; distribution unlimited.

17. DISTRIBUTION STATEMENT (of the abstract entered in Block 20, if different from Report)

18. SUPPLEMENTARY NOTES

This work sponsored by the Defense Nuclear Agency under Subtask HE043-25.

19. KEY WORDS (Continue on reverse side if necessary and identify by block number)

Electromagnetic blackout	Thermal ionization
Nuclear weapon outputs	Deionization
Gamma rays	Absorption
X Rays	Refraction
Beta particles	Noise
Debris	Atmospheric properties

20. ABSTRACT (Continue on reverse side if necessary and identify by block number)

This report is a revision of DASA 2499 (same title) and replaces that document. The report is a compendium of selected graphs, charts, equations, and relations useful in the analysis of electromagnetic blackout caused by nuclear explosions. Information is provided on weapon outputs, ionization source functions, deionization, absorption, phase effects, and noise. The report also contains sections listing atmospheric properties, physical constants, definition of symbols, and a glossary of frequently used terms.

DD FORM 1 JAN 73 1473 EDITION OF [illegible]

UNCLASSIFIED

SECURITY CLASSIFICATION OF THIS PAGE (When Data Entered)

PREFACE

This version of the *Aids for the Study of Electromagnetic Blackout* contains new data on energy deposition, atmospheric air chemistry, and electromagnetic propagation effects caused by inhomogeneities in the propagation medium. This document is intended for use by those generally familiar with derivations and discussions presented in Defense Nuclear Agency (DNA) handbooks describing nuclear weapon effects on electromagnetic propagation. Equations and graphical data describe nominal values for weapon and atmospheric quantities obtained from current models. While uncertainties and limitations in the use of these data are indicated, the user should refer to the more detailed descriptions given in DNA handbooks for possible variations and predicted results.

Unless otherwise stated, the symbols and units used are as defined in Section 1. Section 1 also contains a glossary of terms frequently used in the nuclear weapon effects literature. Atmospheric properties used in the computations for this report are given in Section 8.

TABLE OF CONTENTS

LIST OF ILLUSTRATIONS

LIST OF ILLUSTRATIONS (Continued)

LIST OF ILLUSTRATIONS (Continued)

2

LIST OF ILLUSTRATIONS (Continued)

LIST OF ILLUSTRATIONS (Continued)

LIST OF ILLUSTRATIONS (Continued)

FIGURE PAGE LOCATOR

WEAPON OUTPUTS AND IONIZATION SOURCE FUNCTIONS

PHENOMENOLOGY OF HEATED REGIONS AND DEBRIS LOCATION

DEIONIZATION

ABSORPTION

PHASE EFFECTS

NOISE

PROPERTIES OF THE ATMOSPHERE

LIST OF TABLES

SECTION 1
SYMBOLS AND GLOSSARY

SYMBOLS

A	Atomic mass number or atomic weight; integral of the incremental radio wave absorption (dB); debris area (km^2); attachment rate (sec^{-1})
A_o, A_D	Initial signal amplitude and the disturbed signal amplitude, specifically after transmission through an ionized medium
a	Incremental absorption (dB km^{-1})
B_ν	Boltzmann distribution function $B_\nu = \frac{2h\nu^3}{c^2}\left[\exp\left(\frac{h\nu}{kT}\right) - 1\right]^{-1}$ see Figure 2-8
BT	Time bandwidth product
D	Detachment rate (sec^{-1}); doppler shift (Hz); great circle distance measured along earth's surface (km); normalized neutron energy deposition rate due to capture reactions (cm^2 ergs gm^{-1} sec^{-1})
ΔD_{rms}	Root-mean-square doppler frequency shift due to scintillation from striations (Hz)
d	Distance of closest approach between debris center and ray path (km); distance from radar to fireball clutter region or target (km)
Δd	Extent of clutter or depth of fireball (km)
E	Photon and particle energy (MeV, keV)
E_1	Exponential integral, $E_1(x) = \int_x^\infty \frac{e^{-t}}{t}\,dt$

(see Handbook of Mathematical Functions, NBS Applied Mathematics, Series 55)

$\bar{E}_n$	Average energy of neutron spectrum
$\bar{E}_\beta$	Average energy of beta spectrum (MeV)
E_γ	Gamma-ray energy release rate (MeV fission^{-1} sec^{-1})
F_n	Neutron flux (MeV cm^{-2})
F_T	Fraction of energy transmitted
F_x	X-Ray flux (MeV cm^{-2})
F_β	Beta particle flux (MeV cm^{-2} sec^{-1})
F_γ	Gamma ray flux (MeV cm^{-2}, MeV cm^{-2} sec^{-1})
f	Frequency (Hz)
f_n	Yield fraction for prompt neutrons
f_p	Plasma frequency (Hz)
f_x	Yield fraction for prompt X-rays
f_γ	Yield fraction for prompt gammas
G_T, G_R	Transmitter and receiver spatial gain function for an antenna
g	Acceleration of gravity at the earth's surface (980 cm sec^{-2} at sea level)
h	Altitude, Planck's constant (km)
h_B, h_D	Burst or detonation altitude (km)
h_{DB}	Debris altitude (km)
I_o	Intensity
I_γ	Gamma radiation intensity parameter (watts m^{-2})
K	Opacity (cm^{-1})
k	Boltzmann constant; rate of ion-atom interchange (cm^3 sec^{-1}); absorption coefficient (nepers)

L	Integrated absorption (nepers)
ρ_θ	Correlation length at the striation phase changing screen (km)
M	Penetrated or intervening mass (gms cm^{-2}); molecular weight
$[M^+]$	Concentration of positive molecular ions in the E- and F-region (cm^{-3})
N_A	Number density of striations (km^{-2})
N_c	Compton electron flux (cm^{-2} sec^{-1}); electron density corresponding to $\omega = \omega_p$
N_e	Electron density (cm^{-3})
$\overline{N}_{eb}$	Average background electron density (cm^{-3})
N_i	Positive and negative ion density (cm^{-3})
N_n	Ion pairs caused by neutrons (cm^{-3})
$N_{n\beta}$	Flux of neutron decay beta particles (cm^{-2} sec^{-1})
N_o	Avogadro's constant (gm mole)$^{-1}$, initial ion pairs produced by prompt radiation (cm^{-3})
N_x	Ion pairs caused by X-Rays (cm^{-3})
N_+	Positive ion number density (cm^{-3})
N_-	Negative ion number density (cm^{-3})
$[N^+]$	Number density of positive nitrogen ions (cm^{-3})
$[NO]$	Number density of nitric oxide molecules (cm^{-3})
n	Total number density of atmospheric particles (cm^{-3})
n_n	Normalized neutron spectrum (neutrons MeV^{-1} $neutron^{-1}$)
n_β	Beta particle disintegration rate (betas $fission^{-1}$ sec^{-1})
$n_{\beta E}$	Normalized beta-particle energy distribution function (betas MeV^{-1} $beta^{-1}$)
n_γ	Normalized photon energy distribution function (photons MeV^{-1} $photon^{-1}$)

$[O]$	Number density of oxygen atoms (cm^{-3})
$[O^+]$	Number density of positive oxygen ions (cm^{-3})
P	Air pressure (dynes cm^{-2})
P_a	Ambient air pressure (dynes cm^{-2})
P_R, P_T	Received or transmitted power (watts)
P_s	Pressure at shock front (dynes cm^{-2})
P_γ	Gamma-ray energy deposition rate in the atmosphere near the source (gm^{-1} sec^{-1} km^2)
q	Ion-pair production rate (cm^{-3} sec^{-1})
q_c	Ion-pair production rate due to Compton electrons in conjugate regions (cm^{-3} sec^{-1})
q_{nc}	Ion-pair production rate due to neutron capture reactions (cm^{-3} sec^{-1})
q_β	Ion-pair production rate due to beta particles (cm^{-3} sec^{-1})
q_γ	Ion-pair production rate due to gamma rays (cm^{-3} sec^{-1})
R	Radial distance from burst or debris center to point of interest (km); reflection coefficient
R_{DB}	Debris radius (km)
R_{FB}	Fireball radius (km)
R_o	Closest point of approach between detonation point and magnetic field line through the point of interest (km)
r_o	Characteristic distance for point explosion (cm)
r_s	Radius of spherical shock front (cm)
s	Position along a ray path (cm)
S	Total length of a ray path (cm)
T	Temperature (°K)
T_{ANT}	Effective antenna temperature (°K)

T_D	Striation decorrelation time $\left(=(2\pi f_D)^{-1}\right)$
T_e	Electron temperature (°K)
T_{FB}	Fireball temperature (°K)
T_s	Signal symbol period (sec)
T_x	Radiating temperature of weapon (κT_x in keV)
t_o	Characteristic time scale for a point explosion
V	Volume (km^3)
	Velocity ($m\ sec^{-1}$)
v_g	Group velocity ($m\ sec^{-1}$)
v_p	Phase velocity ($m\ sec^{-1}$)
v_t	Relative velocity between target and striations perpendicular to the line of sight between the radar and target ($km\ sec^{-1}$)
W	Total yield (MT)
W_F	Fission yield (MT)
W_H	Hydrodynamic yield (MT)
Z	Atomic number
Z_f	Fresnel distance $(=\lambda^2/d)$ where λ is the wavelength and d is the characteristic dimension of the scattering region
z	Distance in the direction of the gradient of the electron density
z_o'	Characteristic scale length for the electron density spatial variation
α	Ion-ion and ion-electron recombination coefficient ($cm^3\ sec^{-1}$); incremental absorption ($nepers\ km^{-1}$)
α_d	Ion-electron recombination coefficient ($cm^3\ sec^{-1}$)
α_i	Ion-ion recombination coefficient ($cm^3\ sec^{-1}$)
α_r	Radiative collisional recombination coefficient ($cm^3\ sec^{-1}$)

α_T, α'_T	Incremental absorption (nepers km^{-1})
β_o, β_n	Ion-atom interchange rate coefficients (sec^{-1})
$\Gamma(x)$	Gamma function (see Handbook of Mathematical Functions, NBS Applied Mathematics, Series 55)
γ	Radar beamwidths; air constant
η	Complex index of refraction; surface scattering coefficient ($\sigma_T = \eta A$ where A is area of scatterer)
κ	Opacity (cm^{-1})
κ_ν	Frequency dependent opacity (cm^{-1})
λ	Wavelength (cm); mean-free path (cm)
μ	Real part of the complex index of refraction
μ_D	Debris energy absorption coefficient (MeV cm^2 gm^{-1})
μ_n	Neutron energy absorption coefficient (cm^2 $gram^{-1}$)
μ_x	X-Ray energy absorption coefficient (cm^2 gm^{-1})
$\overline{\mu}_x$	Normalized energy deposition integral (cm^2 gm^{-1})
μ_β	Beta-particle energy absorption coefficient (cm^2 gm^{-1})
μ_γ	Gamma-ray energy absorption coefficient (cm^2 gm^{-1})
ν	Collisional frequency (sec^{-1}); frequency (Hz)
$\overline{\nu}_{em}$	Electron-neutral collision frequency (sec^{-1})
$\overline{\nu}_{ei}$	Electron-ion collision frequency (sec^{-1})
$\overline{\nu}_{eo}$	Electron-oxygen atom collision frequency (sec^{-1})
$\overline{\nu}_{im}$	Ion-neutral collision frequency (sec^{-1})
ρ	Mass density ($gm\ cm^{-3}$)
ρ_a	Ambient air density ($gm\ cm^{-3}$)
ρ_D	Air density at detonation altitude ($gm\ cm^{-3}$)
ρ_{FB}	Air density within the fireball ($gm\ cm^{-3}$)

ρ	Air density at shock front
ρ_o	Sea level air density (1.29×10^{-3} gm cm^{-3})
σ	Scattering cross section (m^2); initial standard deviation for a Gaussian pulse
σ_D	Standard deviation for a Gaussian pulse after propagation through an ionized medium
σ_s	Surface scattering coefficient (m^2/m^2)
σ_T	Total radar cross section (m^2)
σ_v	Volume scattering cross section (m^2/m^3)
τ	Time instant (sec)
ϕ	Magnetic dip angle (degrees)
$\Delta\phi_{rms}$	Root mean square phase fluctuation for a wave traversing a striation phase screen (radians)
ω	Radian frequency (radians sec^{-1})
ω_p	Radian plasma frequency ($2\pi f_p$)

GLOSSARY

ABSORPTION: As applied to electromagnetic radiation it is strictly the process resulting in the transfer of energy from the radiation to an absorbing material through which it passes. In this sense, absorption involves for radio waves the heating of the intervening material and for gamma- and X-Rays the photoelectric effect and pair production. However, the term is frequently used interchangeably with attenuation; absorption then includes both the removal and scattering of energy. See Attenuation, Scattering.

ABSORPTION COEFFICIENT: A number characterizing the ability of a given material to absorb (or attenuate) radiations of a specified energy. The linear absorption coefficient expresses this ability per unit thickness and is stated in units of reciprocal length (or thickness). The mass absorption coefficient is equal to the linear absorption coefficient divided by the density of the absorbing material; it is a measure of the absorption ability per unit mass.

ACTIVITY: The rate of decay of radioactive material expressed as the number of nuclear disintegrations per second.

AMBIENT: Surrouding; especially of or pertaining to the undisturbed atmosphere.

AMPLITUDE: The maximum displacement of an oscillating particle or wave from its position of equilibrium.

ANGLE OF INCIDENCE: The angle between the perpendicular to a surface and the direction of propagation of a wave.

ANGSTROM: A unit of length equal to 10^{-8} centimeter.

ATMOSPHERIC TRANSMISSIVITY: The fraction of the radiant energy received at a given distance after passing through the atmosphere relative to that which would have been received at the same distance if no atmosphere were present.

ATOM: The smallest particle of an element that still retains the characteristics of that element. Every atom consists of a positively charged central nucleus, which carries nearly all the mass of the atom, surrounded by a number of negatively charged electrons, so that the whole system is electrically neutral.

ATOMIC NUMBER: The number of protons in the nucleus of an atom.

ATOMIC WEIGHT: The relative weight of an atom of the given element. As a basis of reference, the atomic weight of the common isotope of carbon (carbon 12) is taken to be exactly 12; the atomic weight of hydrogen (the lightest element) is then 1.008. The atomic weight of any element is approximately the weight of an atom of that element relative to the weight of a hydrogen atom or the total number of protons and neutrons in the nucleus.

ATTENUATION: Decrease in intensity of a signal, beam, or wave as a result of absorption of energy and of scattering of energy out of the path of a detector, but not including the reduction due to geometric spreading, ie, the inverse square of distance effect. See Absorption, Inverse Square Law.

BAGATELLE: Computer code. Simulates an attack on an area defense system.

BALLISTIC RISE: The rapid rise experienced by a fireball whose diameter is a scale height or more and which is rapidly accelerated upward by pressure gradients.

BETA AURORA: Fluorescence caused by deposition of beta particle energy in the atmosphere.

BETA PARTICLE: A small particle ejected spontaneously from a nucleus of either natural or artificially radioactive elements. It carries a

negative charge of one electronic unit and has an atomic weight of 1/1840. See Electron.

BETA PATCH: The volume formed by the intersection of the beta tube and the D-region. This patch is characterized by high electron density.

BETA SHEATH: That region of cooler air surrounding the fireball that is ionized by beta particles.

BETA TUBE: That tubular shaped region surrounding the geomagnetic field lines through the burst region populated by spiraling charged particles.

BLACKBODY: An ideal body which would absorb all (and reflect none) of the radiation falling upon it. The spectral energy distribution of a blackbody is described in Planck's equation; the total rate of emission of radiant energy is proportional to the fourth power of the absolute temperature (Stefan-Boltzmann law).

BLAST WAVE: A pulse of air in which the pressure increases sharply at the front, accompanied by winds, propagated continuously from an explosion. See Shock Wave.

BOMB DEBRIS: See Weapon Debris.

BREAKAWAY: The onset of a condition in which the shock front (in the air), moves away from the exterior of the expanding fireball produced by the explosion of a nuclear (or atomic) weapon. See Fireball, Shock Front.

BREMSSTRAHLUNG: Literally "braking radiation." Radiations covering a range of wave lengths (and energies) in the X-Ray region resulting from the electrical interaction of fast (high-energy) electrons with atomic nuclei.

BUOYANT RISE: The rise due to buoyant forces experienced by a nuclear fireball.

BURST: Explosion or detonation.

BURST GEOMETRY: The location of a nuclear detonation with respect to a particular surface.

CHARGE TRANSFER: The movement of electric charge from one particle or atom to another. Charge transfer often results in the neutralization of high-energy debris particles from a nuclear explosion, allowing the debris to move out perpendicular to the ambient magnetic field direction.

CLUTTER: Unwanted signals, echoes, or images returned to a radar.

COLLISION FREQUENCY: The average number of collisions (involving momentum transfer) per second of a particle of a given species with particles of another or the same species.

COMPTON EFFECT: The scattering of photons (of gamma or X-Rays) by the orbital electrons of atoms. In a collision between a (primary) photon and an electron, some of the energy of the photon is transferred to the electron which is generally ejected from the atom. Another (secondary) photon, with less energy, then moves off in a new direction at an angle to the direction of motion of the primary photon.

COMPTON ELECTRON: An electron ejected from an atom as the result of a Compton interaction with a photon.

COMPTON SCATTERING: Scattering of photons by electrons by means of the Compton effect.

CONJUGATE POINTS: Points at the north and south ends of a geomagnetic field line which are either at corresponding altitudes or at corresponding field strength.

COUPLING: A term used to describe the way or ways in which the energy released by an explosion is transferred to the surrounding medium. The predominant mode may be hydrodynamic at low altitudes or magnetohydrodynamic at higher altitudes.

CRITICAL ELECTRON DENSITY: The electron density for which the plasma frequency equals the radio wave frequency.

CRITICAL FREQUENCY: For a given electron density, the radio frequency which is equal to the plasma frequency.

CROSS SECTION: The measure of the probability of interaction of a photon or energetic particle with matter.

D-REGION: The region of the ionosphere between about 40 and 90 kilometers altitude.

DEBRIS: Material constituting the weapon; its attendant mechanisms, and the carrier.

DEBRIS RADIATION: Radiation emitted after the first few hundred microseconds after a burst. It is primarily gamma ray and beta radiation.

DECAY (OR RADIOACTIVE DECAY): The decrease in activity of any radioactive material with the passage of time, due to spontaneous emission from the atomic nuclei of either alpha or beta particles, sometimes accompanied by gamma radiation. See Half-life, Radioactivity.

DEFOCUSING: The attenuation of an electromagnetic wave due to refraction or scattering away from the intended propagation direction.

DELAYED RADIATION: See Debris Radiation.

DIFFRACTION: The bending of waves around the edges of objects.

DIP ANGLE: The angle between the geomagnetic field and the local horizontal.

DISPERSION: Effects on an electromagnetic wave traversing a region in which the propagation characteristics are frequency dependent.

DISSOCIATION: The breaking up of a molecule to form two or more simpler ones.

E-FIELD: Electric field associated with an electromagnetic wave or created by a charge distribution.

E-REGION: The region of the ionosphere between about 90 and 160 kilometers altitude.

ELECTROMAGNETIC RADIATION: A traveling wave motion resulting from oscillating magnetic and electric fields. Familiar electromagnetic radiations range from X-Rays (and gamma rays) of short wavelength, through the ultraviolet, visible, and infrared regions, to radar and radio waves of relatively long wavelength. All electromagnetic radiations travel in a vacuum with the velocity of light.

ELECTROMAGNETIC SPECTRUM: The distribution of frequencies (or wave lengths) present in a given electromagnetic radiation.

ELECTRON: A particle of very small mass, carrying a unit negative or positive charge. Negative electrons, surrounding the nucleus, are present in all atoms; their number is equal to the number of positive charges (or protons) in the particular nucleus. The term electron, where used alone, commonly refers to these negative electrons. A positive electron is usually called a positron,

ELECTRON VOLT (eV): The energy imparted to an electron when it is moved through a potential difference of 1 volt. It is equivalent to 1.6×10^{-12} erg.

ENERGY FLUX DENSITY: The energy of any radiation incident upon or flowing through a unit area, perpendicular to a radiation beam, per unit time.

ENERGY PARTITION: The distribution of the total energy released by a nuclear detonation among the various phenomena, eg, nuclear radiation,

thermal radiation, and blast. The exact distribution is a function of time, weapon yield, and the medium in which the weapon is detonated.

EXCITED STATE: A state having a higher energy than the normal or ground state.

F-REGION: The region of the ionosphere above about 160 kilometers.

FACTOR: A multiplier, frequently used to indicate range of coverage. For example, "correct within a factor of two" means correct within a possible range of values between twice and one-half the stated value.

FIREBALL: The luminous sphere of hot gases which forms a few millionths of a second after a nuclear (or atomic) explosion as the result of the absorption by the surrounding medium of the thermal X-Rays emitted by the extremely hot (several tens of millions degrees) weapon residues. The exterior of the fireball in air is initially sharply defined by the luminous shock front and later by the limits of the hot gases themselves (radiation front). See Breakaway.

FISSION: The splitting of a heavy nucleus into two or more nuclei of lighter elements—the fission products. Fission is accompanied by the emission of neutrons and the release of energy. It can be spontaneous or it can be caused by the impact of a neutron, a fast charged particle, or a photon.

FISSION DEBRIS: Radioactive debris.

FISSION FRACTION: The fraction (or percentage) of the total yield of a nuclear weapon which is due to fission. For thermonuclear weapons the nominal value of the fission fraction is about 50 percent.

FISSION PRODUCTS: A general term for the complex mixture of substances produced as a result of nuclear fission. A distinction should be made between these and the direct fission products or fission fragments which are formed by the actual splitting of the heavy-element nuclei. Something like 80 different fission fragments result from roughly 40 different modes of fission of a given nuclear species, eg, uranium-235 or plutonium-239. The fission fragments, being radioactive, immediately begin to decay, forming additional (daughter) products, with the result that the complex mixture of fission products so formed contains about 200 different isotopes of 36 elements.

FLUENCE: The number of particles or photons or the amount of energy that enters an imaginary sphere of unit cross-sectional area. It is the time-integrated flux.

FLUX: The flow of photons, particles, or energy per unit time through an imaginary sphere of unit cross-sectional area.

FREE CHARGE: The charge carriers that are capable of moving (ie, those which are not bound to atoms).

FUSION: The process whereby the nuclei of light elements, especially those of the isotopes of hydrogen, namely, deuterium and tritium, combine to form the nucleus of a heavier element with the release of substantial amounts of energy. See Thermonuclear.

GAMMA RAYS: Highly penetrating, high-frequency electromagnetic radiation from the nuclei of radioactive substances. They are of the same nature as X-Rays, but of nuclear rather than atomic origin, and are emitted with discrete. definite energies.

GROUND ZERO: The point on the surface of land or water vertically below the center of a burst of a nuclear weapon.

H-FIELD: Magnetic field associated with an electromagnetic wave or created by an electric current.

HALF-LIFE: The time required for the activity of a given radioactive species to decrease to half of its initial value due to radioactive decay. The half-life is a characteristic property of each radioactive species and is independent of its amount or condition.

HEIGHT OF BURST: The height above the surface of the earth at which a weapon is detonated. Altitude, by contrast, is the height above mean sea level.

HULL: Computer code. Calculates phenomenology for bursts at altitudes where hydrodynamics plays a dominant role.

HYDRODYNAMIC REGIME: Regime in which the air and debris motion can be described using the equations of motion of continuum fluid dynamics.

INELASTIC SCATTERING: Scattering in which the total kinetic energy of a two-particle system is decreased, and one or both of the particles are left in an excited state.

INTENSITY: The energy of any radiation incident upon or flowing through unit area, perpendicular to the radiation beam, in unit time. The intensity of thermal radiation is generally expressed in calories per square centimeter per second falling on a given surface at any specified instant.

INVERSE SQUARE LAW: The intensity of radiation emitted from a point source is inversely proportional to the square of distance between the source and point of observation assuming no other intervening attenuation.

ION: An atom with a net electric charge.

IONIZATION: The separation of a normally electrically neutral atom or molecule into electrically charged components. The term is also employed to describe the degree or extent to which this separation occurs.

IONIZING RADIATION: Electromagnetic radiation (gamma rays or X-Rays) or particulate radiation (alpha particles, beta particles, neutrons, etc) capable of producing ions, ie, electrically charged particles, directly or indirectly, in its passage through matter.

IONOSPHERE: The region of the atmosphere, extending from roughly 60 to 400 km altitude, in which there is appreciable ionization. The presence of charged particles in this region profoundly affects the propagation of long-wavelength electromagnetic radiation (radio and radar waves).

ION PAIR: A separated ion and electron resulting from ionization.

ISOTOPES: Forms of the same element having identical chemical properties but differing in their atomic masses (due to different numbers of neutrons in their respective nuclei) and in their nuclear properties, eg, radioactivity, fusion, etc.

JITTER: Short-time instability of a radar signal.

KELVIN SCALE: The absolute temperature scale for which the zero is -273°C. Conversion from centigrade to Kelvin is made by adding 273 to the centigrade reading.

KILO-ELECTRON VOLT (or keV): An amount of energy equal to 1000 electron volts. See Electron Volt.

KILOTON ENERGY: The energy of a nuclear (or atomic) explosion which is equivalent to that produced by the explosion of 1 kiloton (ie, 1000 tons) of TNT, ie, 10^{12} calories or 4.2×10^{19} ergs.

K-SHELL: The innermost and most tightly bound electrons surrounding an atomic nucleus.

LARMOR RADIUS: The gyroradius of a charged particle in a magnetic field.

LINEAR ABSORPTION COEFFICIENT: See Absorption Coefficient.

MAGNETIC CONJUGATE POINTS: Points at the north and south ends of a geomagnetic field line that are either at corresponding altitudes or at corresponding magnetic field strengths.

MAGNETOHYDRODYNAMIC REGIME: Regime in which ionized air and debris motion are described by continuum fluid equations of motions with magnetic

field coupling. Charge neutrality is assumed to exist as a first approximation.

MASS ABSORPTION COEFFICIENT: See Absorption Coefficient.

MEAN FREE PATH: Average distance traveled by particles before interaction or average distance a single particle travels between interactions.

MEGATON ENERGY: The energy of a nuclear (or atomic) explosion which is equivalent to 1,000,000 tons (or 1000 kilotons) ot TNT, ie, 10^{15} calories or 4.2×10^{22} ergs.

MeV (OR MILLION ELECTRON VOLT): A unit of energy commonly used in nuclear physics. It is equivalent to 1.6×10^{-6} erg. Approximately 200 MeV of energy are produced for every nucleus that undergoes fission.

MICE: A magnetohydrodynamic computer code primarily for high altitude phenomenology.

MICRON: A one-millionth part of a meter, ie, 10^{-6} meter or 10^{-4} centimeter.

MICROSECOND: A one-millionth part of a second.

MIRROR POINT: A point at which a charged particle, moving in a spiral path along the lines of a magnetic field, is reflected back as it enters a stronger magnetic field region. The actual location of the mirror point depends on the direction and energy of motion of the charged particle and the ratio of the magnetic field strengths.

MONTE CARLO METHOD: A method of solution of a group of physical problems by means of a series of statistical experiments which are performed by applying mathematical operations of random numbers.

MR HYDE: A three-dimension magnetohydrodynamic computer code used for numerically investigating high-altitude nuclear weapon effects.

MULTIPATH: Signals that reach a receiver by several paths each usually having amplitude and phase differences.

NEUTRALS: Unionized atoms and molecules, ie, without an electrical charge.

NEUTRON: An electrically neutral particle which is one of the fundamental particles making up the nucleus of all atoms except ordinary (light) hydrogen. It has nearly the same weight as the hydrogen nucleus (atomic weight 1).

NEUTRON CAPTURE: A basic interaction of neutrons with matter. Neutron capture can result in the generation of gamma rays and/or charged particles.

NEUTRON FLUENCE: The number of neutrons entering an imaginary sphere of unit cross-sectional area. It is equal to the time integrated neutron flux. It is generally expressed as n/cm^2. If expressed as Nvt, N is the neutron density (n/cm^3) in the beam, v is the average speed (cm/sec), and t is the time duration. The spectrum should be specified with the fluence, eg, n/cm^2 (fission spectrum).

NEUTRON FLUX: The flow of neutrons into an imaginary sphere of unit cross-sectional area. It is generally expressed as $n/cm^2/sec$. If expressed as Nv, N is the neutron density in the beam (n/cm^3), and v is the average speed (cm/sec). The spectrum should be specified with the flux, eg, $n/cm^2/sec$ (fission spectrum).

NUCLEAR RADIATION: Particulate and electromagnetic radiation emitted from atomic nuclei in various nuclear processes. The important nuclear radiations, from the weapons standpoint, are alpha and beta particles, gamma rays, and neutrons. All nuclear radiations are ionizing radiations, but the reverse is not true; X-Rays, for example, are included among ionizing radiations, but they are not nuclear radiations since they do not originate from atomic nuclei.

NUCLEAR WEAPON (OR BOMB): A general name given to any weapon in which the explosion results from the energy released by reactions involving atomic nuclei, either fission or fusion or both. Thus, the A- (or atomic) bomb and the H- (or hydrogen) bomb are both nuclear weapons. It would be equally true to call them atomic weapons, since it is the energy of atomic nuclei that is involved in each case.

NUCLEUS (OR ATOMIC NUCLEUS): The small, central, positively charged region of an atom which carries essentially all the mass. Except for the nucleus of ordinary (light) hydrogen, which is a single proton, all atomic nuclei contain both protons and neutrons. The number of protons determines the total positive charge, or atomic number; this is the same for all the atomic nuclei of a given chemical element. The total number of neutrons and protons, called the mass number, is closely related to the mass (or weight) of the atom. The nuclei of isotopes of a given element contain the same number of protons, but different numbers of neutrons. They thus have the same atomic number, and so are the same element, but they have different mass numbers (and masses). The nuclear properties, eg, radioactivity, fission, neutron capture, etc, of an isotope of a given element are determined by both the number of neutrons and the number of protons.

NUCOM: Computer code. Calculates HF propagation in a nuclear environment.

OPACITY: A measure of the property of matter to obstruct by absorption the transmission of radiant energy,

OVER(UNDER)DENSE REGION: In terms of electromagnetic wave propagation a region in which the plasma frequency, ω_p, is greater than (less than) the angular wave frequency, $\omega = 2\pi f$.

PAIR PRODUCTION: The process whereby a gamma-ray or X-Ray photon, with energy in excess of 1.02 MeV in passing near the nucleus of an atom is converted into a positive electron and a negative electron. As a result, the photon ceases to exist.

PHENOMENOLOGY: Description and classification of phenomena. As used in the blackout field, this word is nearly synonymous with the blackout environment. Such things as fireball growth and rise, debris spread, cloud rise, etc, are referred to as the phenomena.

PHOTOELECTRIC EFFECT: The process whereby a gamma-ray or X-Ray photon, with energy somewhat greater than that of the binding energy of an electron in an atom, transfers all its energy to the electron which is consequently removed from the atom. Since it has lost all its energy, the photon ceases to exist.

PHOTON: A unit or "particle" of electromagnetic radiation, possessing a quantum of energy which is characteristic of the particular radiation. If ν is the frequency of the radiation in cycles per second and λ is the wave length in centimeters, the energy quantum of the photon in ergs is $h\nu$ or hc/λ where h is Planck's constant, 6.62×10^{-27} erg-second and c is the velocity of light (3.00×10^{10} centimeters per second). For gamma rays, the photon energy is usually expressed in million electron volt (MeV) units, ie, $1.24 \times 10^{-10}/\lambda$ where λ is in centimeters or $1.24 \times 10^{-2}/\lambda$ if λ is in Angstroms.

PLANCKIAN RADIATION: The energy distribution of the radiation emitted by a blackbody radiator. The spectrum is determined by the temperature and is given by Planck's radiation law.

PROMPT GAMMA RAYS: Gamma rays produced in fission and fusion reactions and as a result of nuclear excitation of the weapon materials.

PROMPT NEUTRONS: Neutrons generated by the fission and fusion reactions of a nuclear weapon burst.

PROMPT RADIATION: Energy released during the first few microseconds after detonation.

PROTON: A positively charged particle with a mass approximately the same as that of a neutron. In nature, protons are bound in the nuclei of atoms.

RADIOACTIVITY: The spontaneous emission of radiation, generally alpha or beta particles, often accompanied by gamma rays, from the nuclei of

an (unstable) isotope. As a result of this emission the radioactive isotope is converted (or decays) into the isotope of a different (daughter) element which may (or may not) also be radioactive. Ultimately, as a result of one or more stages of radioactive decay, a stable (nonradioactive) end product is formed.

RANC: Computer code. Calculates radar performance in nuclear environment.

REACTION RATE: In chemical kinetics, the time derivative of the concentration of a given species is called the reaction rate of that species.

RECOMBINATION: A process by which a positive ion and an electron (or negative ion) join to produce a single neutral atom or molecule (or pair of neutrals). Recombination transitions may be radiative.

REFRACTION: Bending of an electromagnetic wave path when it traverses a region whose propagation characteristics are a function of position.

RIOMETER: An ionospheric research instrument. Measures the relative ionospheric opacity (riometer) by comparing the magnitude of incoming cosmic noise with an internal noise source.

SATL: Computer code. Calculates satellite to ground communication performance in a nuclear environment.

SATURATION: The level of prompt ionization that is so high that an increase in the radiation will neither add appreciably to the ionization or lengthen its duration.

SCALE HEIGHT: The scale height physically approximates the atmospheric pressure or density "e-folding height," ie, that change in altitude which causes the pressure or density to change by a factor of e.

SCALING LAW: A mathematical relationship which permits the effects of a nuclear explosion of given energy yield to be determined as a function of distance from the explosion, provided the corresponding effect is known as a function of distance for a reference explosion, eg, of 1-kiloton energy yield.

SCATTERING: The diversion of radiation from its original path as a result of interactions or collisions with atoms, molecules, larger particles in the atmosphere, or inhomogeneities in the medium between the source of the radiations, eg, a nuclear explosion, and a point at some distance away.

SCINTILLATION: Random fluctuations in the amplitude and direction of an electromagnetic wave as it traverses an inhomogeneous medium.

SECONDARY ELECTRON: An electron that is emitted as a result of bombardment of a material by high energy radiation.

SHAKE: A nonstandard unit of time used in nuclear physics, equal to 10^{-8} second.

SHOCK FRONT (OR PRESSURE FRONT): The fairly sharp boundary between the pressure disturbance created by an explosion (in air, water, or earth) and the ambient atmosphere, water, or earth, respectively. It constitutes the front of the shock (or blast) wave.

SHOCK STRENGTH: The ratio of the peak blast wave overpressure plus the ambient pressure to the ambient pressure.

SHOCK WAVE: A continuously propagated pressure pulse (or wave) in the surrounding medium which may be air, water, or earth, initiated by the expansion of the hot gases produced in an explosion. A shock wave in air is generally referred to as a blast wave, because it resembles and is accompanied by strong, but transient, winds.

SLANT RANGE: The direct distance between an explosion and a point of interest.

SMOG: Ionospheric smog is a term that has been used to describe the buildup of ozone, nitrogen dioxide, and nitric oxide due to weapon radiation in the upper atmosphere with a consequent effect on the intensity and duration of the resulting ionization.

SPUTTER: Computer code. Calculates early bomb debris expansion.

STOPPING ALTITUDE: That altitude near which radiation coming from the sun or from a high altitude nuclear explosion will deposit most of its energy in the earth's atmosphere.

STRIATIONS: The self-luminous magnetic-field-aligned filamentary structures observed after high-altitude nuclear explosions.

SYNCHROTRON RADIATION (NOISE): Electromagnetic radiation emitted by a high-energy electron moving in a magnetic field.

THERMAL ENERGY: The energy emitted from the fireball as thermal radiation.

THERMAL ENERGY YIELD (OR THERMAL YIELD): The part of the total energy yield of the nuclear explosion which is received as thermal energy usually within a minute or less. In an air burst, the thermal energy is, on the average, about one-third of the total energy of the explosion. For a high-altitude burst, roughly one-fourth of the total yield is received as thermal energy at a distance within about a minute.

THERMAL PULSE: Time integral of the radiated thermal power.

THERMAL RADIATION: Electromagnetic radiation emitted from the fireball as a consequence of its very high temperature; it consists essentially of ultraviolet, visible, and infrared radiations. In the early stages (first pulse of an air burst), when the temperature of the fireball is extremely high, the ultraviolet radiation predominates; in the second pulse, the temperatures are lower and most of the thermal radiation lies in the visible and infrared regions of the spectrum. From a high-altitude burst, the thermal radiation is emitted in a single short pulse.

THERMAL X-RAYS: The electromagnetic radiation, mainly in the soft (low-energy) X-ray region, emitted by the extremely hot weapon debris in virtue of its extremely high temperature; it is also referred to as the primary thermal radiation. It is the absorption of this radiation by the ambient medium, accompanied by an increase in temperature, which results in the formation of the fireball which then emits thermal radiation.

THERMONUCLEAR: An adjective referring to the process (or processes) in which very high temperatures are used to bring about the fusion of light nuclei, such as those of the hydrogen isotopes (deuterium and tritium), with the accompanying liberation of energy. A thermonuclear bomb is a weapon in which part of the explosion energy results from thermonuclear fusion reactions. The high temperatures required are obtained by means of a fission explosion.

TRAVELING WAVES: Gravity wave generated in E- and F-region by high-altitude nuclear detonations.

TORUS: That characteristic ring-like structure into which a nuclear fireball will in many cases transform itself.

TRANSMITTANCE (ATMOSPHERIC): The fraction (or percentage) of the energy received at a given location after passage through the atmosphere relative to that which would have been received at the same location if no atmosphere were present.

TROPO: Computer code. Calculates troposcatter system performance in a nuclear environment.

TROPOSPHERE: The region of the atmosphere immediately above the earth's surface and up to the tropopause in which the temperature falls fairly regularly with increasing altitude, clouds form, convection is active, and mixing is continuous and more or less complete.

TURBULENCE: Highly irregular fluid flow characterized by fluctuations in the fluid velocity.

ULTRAVIOLET: Electromagnetic radiation of wave length between the shortest visible violet (about 3,850 Angstroms) and soft X-Rays (about 100 Angstroms).

VORTEX: A region within a body of fluid in which the individual fluid elements have an angular velocity about the center of the region.

WAVE LENGTH: The distance between two similar and successive points on an alternating wave, as between maxima.

WEAPON DEBRIS: The highly radioactive material, consisting of fission products, various products of neutron capture, and uranium and plutonium that have escaped fission, remaining after the explosion.

WEPH: Computer code. Calculates ionization and absorption in weapon disturbed ionosphere. Shares many phenomenology assumptions with RANC code.

X-RAYS: Electromagnetic radiations of high energy having wave lengths shorter than those in the ultraviolet region, ie, less than 10^{-6} cm or 100 Angstroms. X-Rays can be produced by any of three processes: radiation from a heated mass (eg, a blackbody); deceleration of a charged particle; electron transitions between atomic energy levels, usually excited by incident beams of high-energy particles, resulting in characteristic, discrete energy levels.

YIELD: The total effective energy released in a nuclear detonation (usually expressed in the equivalent tonnage of TNT required to produce the same energy release).

SECTION 2

WEAPON OUTPUTS AND IONIZATION SOURCE FUNCTIONS

FISSION DATA

Fissions per megaton—1.47×10^{28}.
Distribution of fission energy—see Table 2-1.
Fusion reactions and energy released—see Table 2-2.

ATMOSPHERIC INTERACTION PROCESSES

Photon cross sections in air—see Figure 2-1.
Electron energy loss cross section and total range—see Figure 2-2.
Atomic oxygen energy loss cross section and total range in nitrogen—see Figure 2-3.
Neutron elastic, inelastic, and capture cross sections— strong functions of neutron energy and interaction species.

PARTITION OF ENERGY DEPOSITION

Energy deposition below 100 km—see Tables 2-3 and 2-4.

Column labeled Ory and Gilmore, 1971, used in ionization calculations in this document.

Energy deposition above 100 km:

Initial species produced by photon and electron energy deposition dependent on atmospheric composition and lifetime of excited states. Heavy particle interactions provide a larger ratio of atomic to molecular ionization than photon and electron interactions.

PROMPT GAMMA RAYS

Yield fraction:

$$f_\gamma \approx 0.001 \quad .$$

Spectrum (gamma rays that escape the case are generally assumed to have a fission spectrum):

$$n_\gamma \approx 1.1e^{-1.1E} \quad \text{photons MeV}^{-1} \text{ photon}^{-1} \quad .$$

Thin-region energy absorption coefficient (same as delayed gammas):

$$\mu_\gamma = 0.025 \text{ cm}^2 \text{ gm}^{-1} .$$

Flux:

$$F_\gamma(h) = \frac{2 \times 10^{17} \text{ W } f_\gamma \text{ A(M)}}{R^2} \text{ MeV cm}^{-2} ,$$

where A(M) is

$$A(M) \approx \begin{cases} 1 & M \leq 10 \text{ gm cm}^{-2} \\ 1.4e^{-0.034M} & M > \text{gm cm}^{-2} \end{cases} .$$

M—see Section 8, Figure 8-4.

Energy release time is less than a microsecond; rate is dependent on weapon design.

Ionization:

$$N_\gamma(h) = \frac{1.5 \times 10^{20} \text{ W } f_\gamma \rho(h) \text{ A(M)}}{R^2} \text{ ion pairs cm}^{-3} .$$

Ionization for W f_γ = 0.01 MT—see Figures 2-4 through 2-7.

Uncertainty: The largest uncertainty in computed ionization is related to the specification of the gamma flux escaping the weapon case.

X RAYS

Yield fraction:

$$f_x \approx 0.75.$$

Blackbody spectrum—see Figure 2-8.

Approximate K-shell energy absorption coefficient in air (sea level composition, E in keV):

$$\mu_x \approx \begin{cases} \frac{4 \times 10^3}{E^3} \text{ cm}^2 \text{ gm}^{-1} , & E > 0.4 \text{ keV (nitrogen edge)} \\ \frac{10^2}{E^3} \text{ cm}^2 \text{ gm}^{-1} , & E \leq 0.4 \text{ keV} \end{cases}$$

Flux (blackbody spectrum, neglects scattering):

$$F_x(h) = \frac{2 \times 10^{17} \text{ Wf}_x}{R^2} F_T \text{ MeV cm}^{-2} .$$

F_T—see Figure 2-9.

Ionization (assuming local deposition of photoelectrons):

$$N_x(h) = \frac{6 \times 10^{21} \text{ Wf}_x \rho(h)}{R^2} \bar{\mu}_x \text{ ion pairs cm}^{-3}$$

or

$$N_x(h) = \frac{6 \times 10^{21} \text{ Wf}_x}{R^2} \frac{\rho(h)}{M} B \text{ ion pairs cm}^{-3} .$$

$\bar{\mu}_x$—see Figures 2-10 and 2-11.

B—see Figure 2-12.

Ionization for Wf_x = 0.75 MT—see Figures 2-13 through 2-16.

Uncertainty: Neglect of photon scattering for high energies may be important; use of single radiating temperature at very short or very long ranges may produce errors. Uncertainty in ionization is probably within a factor of 2 for h < 100 km.

DEBRIS

Yield fraction ≈ 0.25 .

Energy release rate:

Nonradiated weapon energy is converted to debris kinetic energy within a few microseconds.

Energy spectrum:

Velocities up to 2×10^8 cm sec^{-1}.

Thin-region energy absorption coefficient:

$$\mu_D = -\frac{dE}{dM} = \frac{1.4 \times 10^3 (Z_1 + Z_2)}{A_2} \left(\frac{v}{10^8}\right) \text{ MeV cm}^2 \text{ gm}^{-1} \quad .$$

Z_1 and Z_2 are the atomic numbers of incident and target particles, respectively, and A_1 and A_2 are the corresponding atomic weights. v is the relative velocity in cm sec^{-1}.

Single particle range:

$$\xi = 7 \times 10^{-6} \left(\frac{v}{10^8}\right) \frac{A_1 A_2}{(Z_1 + Z_2)} \text{ gm cm}^{-2} \quad .$$

Energy deposition:

Debris energy is locally deposited in fireball for detonations below about 200 km; for higher detonation altitudes, debris energy is distributed over a large region. Debris-air interaction results in radiation from the visible through X rays, which can produce ionization outside the fireball when the debris-air interaction occurs above about 100 km.

NEUTRONS

Yield fraction

$$f_n \approx 0.01 \quad .$$

Spectrum between 10^{-3} and 10 MeV (neutrons escaping the bomb):

$$n_n \approx 0.1\ E^{-1} \text{ neutrons MeV}^{-1} \text{ neutron}^{-1} \quad .$$

Spectrum is variable with weapon design. Neutron output in energy range below 10^{-3} MeV and above 10 MeV may be important for some problems.

Thin-region kinetic energy absorption coefficient:

$$\mu_n \approx 0.015 \text{ cm}^2 \text{ gm}^{-1} \quad .$$

Flux:

$$F_n(h) \approx \frac{2 \times 10^{17}\ W f_n\ A(M)\ G(h)\ F(h_B)}{R^2} \quad , \quad \text{MeV cm}^{-2}$$

$$A(M) = \begin{cases} 1 & M \leq 30 \text{ gm cm}^{-2} \\ 2.35 \exp(-0.0285\, M) & M > 30 \text{ gm cm}^{-2} \end{cases}$$

M—see Section 8, Figure 8-4,

$G(h)$, $F(h_B)$ = correction factors for altitudes of burst and deposition points—see Figure 2-17.

Energy release times negligible in comparison to transport and deposition times.

Ionization from elastic and inelastic scattering (neglecting transport and deposition times):

$$N_n(h) = \frac{10^{20}\, Wf_n\, \rho(h)\, A(M)\, G(h)\, F(h_B)}{R^2} \text{ ion pairs cm}^{-3} .$$

Transport and deposition times vary from a few microseconds at sea level to a few seconds at 100 km.

Ionization for Wf_n = 0.01 MT—see Figures 2-18, 2-19 and Figures 2-13 through 2-16.

Uncertainty: Neglect of transport and energy deposition times important during energy deposition period. At low altitudes there can be significant deionization during energy deposition. Prediction of total ion pairs formed for a given neutron flux probably within a factor of three.

Ionization from capture reactions:

$$q_{nc}(h,t) = \frac{4 \times 10^{27}\, Wf_n\, D(M)\, \rho(h)\, F(t)\, G(h)\, F(h_B)}{\bar{E}_n R^2}$$

$\bar{E}_n$ = average energy of neutron spectrum (MeV),

$$F(t) = \begin{cases} 1 & t \leq t_c \\ \exp[-(t - t_c)/\tau] & t > t_c \end{cases},$$

$$t_c = \frac{1.33 \times 10^{-6} + 4.44 \times 10^{8} \sqrt{M}}{\rho(h)}$$

$$\tau = \frac{8 \times 10^{-5}}{\rho(h)}$$

D(M)—see Figure 2-20.

Uncertainty: Formulation based on fits to a limited number of detailed calculations. Predictions estimated to be within a factor of two because of uncertainties in the spectrum, cross sections, and exponential atmosphere approximation.

Ionization from neutron decay betas:

$$\frac{q_{n\beta}(h,t)}{N_{n\beta}} = 2 \times 10^{5}\ \rho(h)\ E_1\left(\frac{2.3 \times 10^{-2}\ P(h)}{|\sin \phi|}\right) \text{cm}^{-1} \quad ,$$

$$N_{n\beta} = \frac{3 \times 10^{10}}{R_o^2} W \quad , \quad \frac{t}{R_o} \leq 3 \times 10^{-3} \quad .$$

$$= \frac{3 \times 10^{5}}{t^2} W \quad , \quad \frac{t}{R_o} > 3 \times 10^{-3} \quad .$$

$\frac{q_{n\beta}(h,t)}{N_{n\beta}}$ — see Figure 2-21 .

R_o (dipole field)—see Figures 2-22 through 2-24.

For lines of sight approaching the horizon, the approximate expression overestimates flux ($N_{n\beta}$) and ionization.

Uncertainty: Neutron energy spectrum is variable with weapon; above relations are based on an approximation to integral of beta flux over magnetic field line; uncertainty in ionization varies with time after detonation and location, but is probably less than an order of magnitude for most cases of interest.

DELAYED GAMMA RAYS

Energy release rate—see Figure 2-25:

$$E_\gamma(t) = \frac{1.9}{(1+t)^{1.2}} \left[1 - r_f\left(\frac{9}{15+t}\right)\right] \text{MeV fission}^{-1}\ \text{sec}^{-1} \quad ,$$

$$r_f = \frac{\text{material fissionable by thermal neutrons}}{\text{total fissionable material}} .$$

Spectrum:

$$n_\gamma \approx 1.1e^{-1.1E} \quad \text{photons MeV}^{-1} \text{ photon}^{-1} .$$

Thin-region energy absorption coefficient:

$$\mu_\gamma \approx 0.025 \quad \text{cm}^2 \text{ gm}^{-1}$$

approximately independent of energy and isotopes.

Flux (point source):

$$F_\gamma(h,t) = \frac{1.2 \times 10^{15} E_\gamma(t) W_F A(M)}{R^2} \text{ MeV cm}^{-2} \text{ sec}^{-1} .$$

$$A(M) = \begin{cases} 1 & M \leq 10 \text{ gm cm}^{-2} \\ 1.4e^{-0.034 M} & M > 10 \text{ gm cm}^{-2} \end{cases} .$$

M—see Section 8, Figure 8-4.

Burst region ionization (point source):

$$\frac{q_\gamma(h,t)}{P_\gamma} = \frac{\rho(h) A(M)}{4\pi R^2} \text{ gm cm}^{-3} \text{ km}^{-2} .$$

$$P_\gamma = 4.4 \times 10^{20} W_F E_\gamma(t) \mu_\gamma$$

$$\approx \frac{2 \times 10^{19} W_F}{(1+t)^{1.2}} \text{ ion pairs gm}^{-1} \text{ sec}^{-1} \text{ km}^2 .$$

$\frac{q_\gamma(h,t)}{P_\gamma}$ — see Figures 2-26 through 2-30.

P_γ nomogram—see Figure 2-31.

Uncertainty: Same considerations as for prompt gamma radiation; in addition, the energy release rates at early times are dependent on isotopes.

Burst Region ionization (distributed debris region):

$$\frac{q_\gamma(h,t)}{I_\gamma} \approx 5 \times 10^{11}\, \rho(h) \quad , \quad h > 50 \text{ km} \quad .$$

$$I_\gamma = I'_\gamma C_\gamma \quad \text{watts m}^{-2}$$

$$I'_\gamma = 7 \times 10^{7}\, W_F\, E_\gamma(t)\, \mu_\gamma$$

$$\approx \frac{3.2 \times 10^{6}\, W_F}{(1+t)^{1.2}\, R^2} \quad \text{watts m}^{-2} \quad .$$

I'_γ nomogram—see Figure 2-31.

C_γ—see Figures 2-32A, B, C, D.

I'_γ is the free-space gamma flux, and C_γ is a correction factor to account for transmission loss when the point of interest is above about 50 km. At lower altitudes $I'_\gamma C_\gamma$ may overestimate flux. C_γ is unity for point source and $M < 10$ gm cm^{-2}.

Uncertainty: Production rate predictions for above conditions believed accurate to within a factor of 2. At large ranges where horizon effects are important, this uncertainty refers to variation in range for a given q rather than variation in q for a given range.

Conjugate region ionization (Compton electrons escaping burst region):

$$\frac{q_c(h,t)}{N_c C_c} = \frac{6 \times 10^{4}\, \rho(h)}{|\sin \phi|}\, E_1\left(\frac{2 \times 10^{-3}\, P(h)}{|\sin \phi|}\right) \text{ cm}^{-1} \quad .$$

$\frac{N_c}{I'_\gamma}$ — see Figures 2-33A, B, C, D.

$\frac{q_c(h,t)}{N_c}$ — see Figure 2-34.

C_c—see Figure 2-35.

C_c is a first-order correction factor to account for nonisotropic injection of Compton electrons.

Uncertainty: Formulation involves separate approximations for energy and pitch angle distribution of Compton electrons, the integral of Compton electrons leaving burst region, and deposition of Compton electrons in the conjugate region. Ionization is probably within a factor of 3 for most regions of interest. At large ranges where horizon effects are important, this uncertainty refers to variation in range for a given q rather than variation in q for a given range.

BETA PARTICLES

Beta decay rate—see Figures 2-36 and 2-37.

$$n_\beta(t) \approx \frac{1.2}{(1+t)^{1.15}} \text{ betas fission}^{-1} \text{ sec}^{-1} \quad , \quad t \geq 1 \text{ sec} \quad .$$

Energy spectrum—see Figure 2-38:

For $5 > E(\text{MeV}) > 0.5$,

$$n_{\beta E} \approx \frac{e^{-E/\bar{E}_\beta}}{\bar{E}_\beta} \text{ betas MeV}^{-1} \text{ beta}^{-1} \quad .$$

Energy absorption coefficient—see Figure 2-2:

$$\mu_\beta \approx 2 \text{ MeV cm}^2 \text{ gm}^{-1} \text{ for beta-particle energy} \geq 0.5 \text{ MeV} \quad .$$

Average energy versus time, $\bar{E}_\beta$—see Figure 2-39.

Flux (outside debris region):

$$F_\beta(h,t) = N_\beta \min\left(E_1\left\{\frac{\mu_\beta \Delta P}{\bar{E}_\beta g|\sin\phi|}\right\}, 6\right) \text{ MeV cm}^{-2} \text{ sec}^{-1} \quad .$$

$$N_\beta = \frac{7.35 \times 10^{15} W_F}{A} n_\beta(t) \text{ betas cm}^{-2} \text{ sec}^{-1} \quad .$$

ΔP = pressure difference between debris altitude and altitude h (dynes cm^{-2}).

Ionization (outside debris region):

$$\frac{q_\beta(h,t)}{N_\beta} = \frac{3 \times 10^4 \rho(h)}{|\sin\phi|} \mu_\beta \min\left(E_1\left\{\frac{\mu_\beta \Delta P}{\bar{E}_\beta g|\sin\phi|}\right\}, 6\right) \text{ ion pairs beta}^{-1} \text{ cm}^{-1} \quad .$$

$\frac{q_\beta(h,t)}{N_\beta}$ sin ϕ—see Figure 2-40.

N_β nomogram—see Figure 2-41.

Uncertainty: Calculations assume uniform debris distribution over area A; deposition of beta-particle energy is approximated; energy release rate is dependent on isotopes at early times. Ionization predictions are probably within a factor of 2 when location and distribution of debris are specified.

Beta bremsstrahlung ionization:

The flux and ionization caused by beta bremsstrahlung in the conjugate region are approximately equal to the gamma-ray flux and ionization resulting from a fictitious debris region having the following location and fission yield:

Debris radius = actual debris radius

Debris altitude = 60 km

Fission yield = 2×10^{-2} ε W_F

ε—see Figure 2-42.

Uncertainty: The above is an approximate formulation. Uncertainty in region of interest is estimated to be a factor of 3.

Table 2-1. Distribution of fission energy.

Product	Fission Energy (MeV)
Kinetic energy of fission fragments	165 ± 5
Instantaneous gamma ray energy	7 ± 1
Kinetic energy of fission neutrons	5 ± 0.5
Beta particles from fission products	7 ± 1
Gamma rays from fission products	6 ± 1
Neutrons from fission products	10
Total energy per fission	200 ± 8.5

Table 2-2. Thermonuclear reactions.

Reaction	Energy Release (MeV)
$^{3}T + {}^{2}D = {}^{4}He + n$	17.6 (14.1 carried by n)
$^{2}D + {}^{2}D = {}^{3}T + {}^{1}H$	4.0
$^{2}D + {}^{2}D = {}^{3}He + n$	3.3
$^{3}T + {}^{3}T = {}^{4}He + 2n$	11.3
$^{2}D + {}^{3}He = {}^{4}He + {}^{1}H$	18.3
$^{6}Li + n = {}^{4}He + {}^{3}T$	4.8

Table 2-3. Initial species produced by X-ray bombardment in air of 79-percent N_2 and 21-percent O_2.

Species	Particles Per Ion Pair	
	Ory and Gilmore RDA-TRR-017-1971	Gilmore 1974
N_2^+	0.75	0.64
O_2^+	0.19	0.16
N^+	0.04	0.14
O^+	0.02	0.06
$N_2(A\ ^3\Sigma_u^+)$	0.6	0.5
$O_2(a\ ^1\Delta_g)$	2.	0.4
$N(^4S)$	0.2	0.45
$N(^2D)$	0.3	0.61
$O(^3P) + O(^1D)$	0.3	0.3

Table 2-4. Dissociation and ionization potentials.

E	N_2	O	O_2
Dissociation potential (eV)	3.338	-	3.658
Ionization potential (eV)	15.526	13.62	12.208

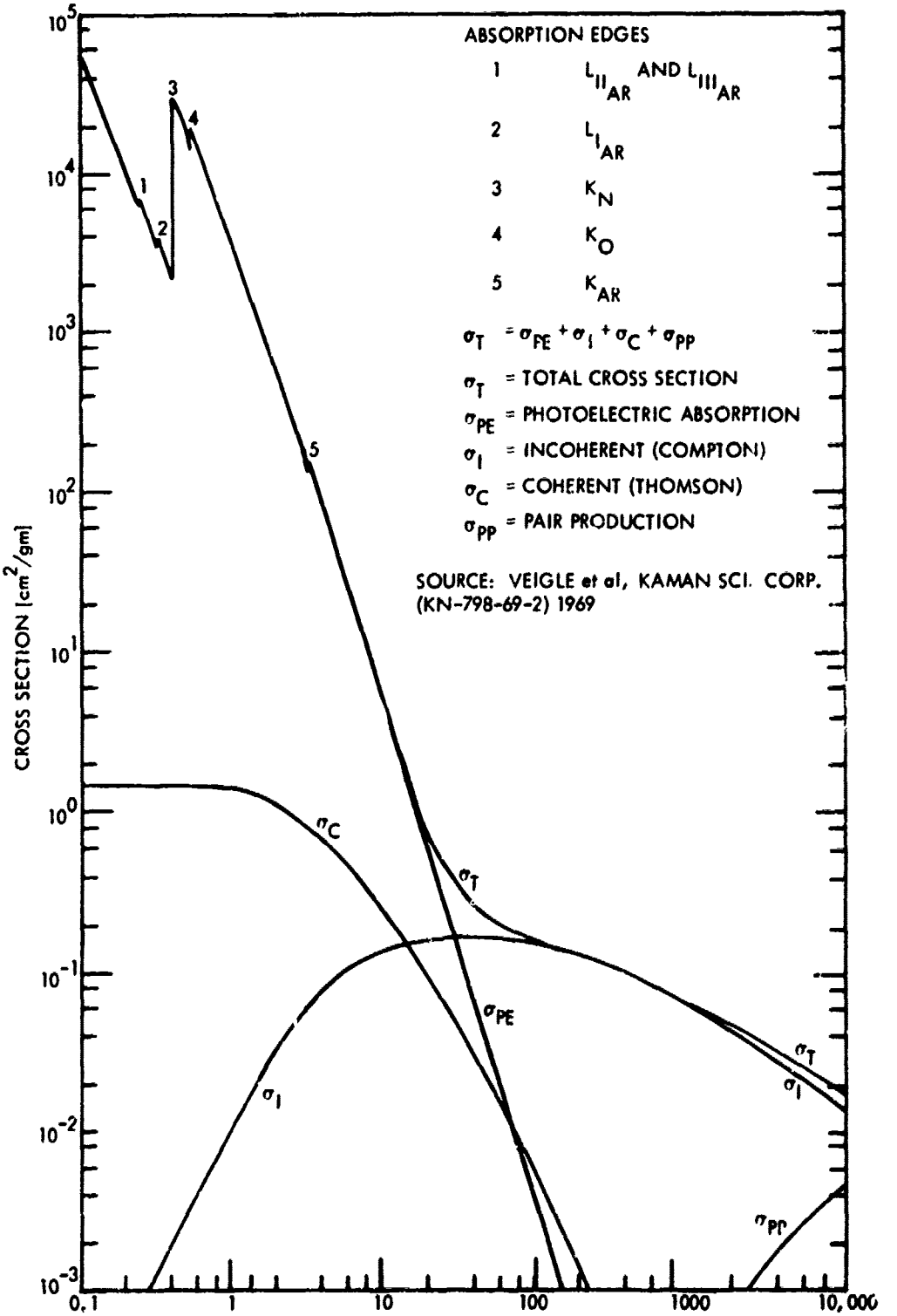

Figure 2-1. Photon cross sections in air.

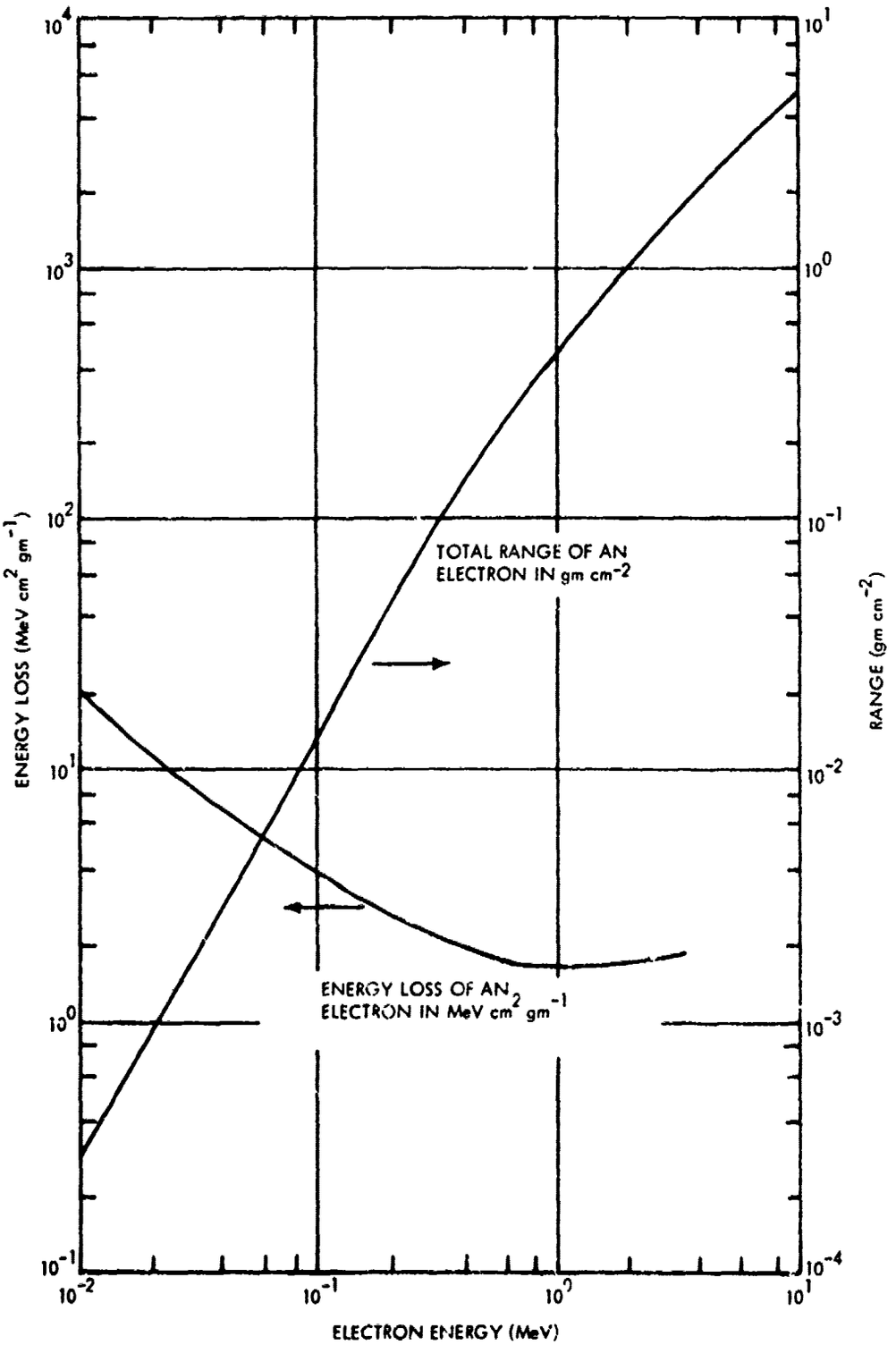

Figure 2-2. Energy loss and total range of an electron in air as a function of its energy.

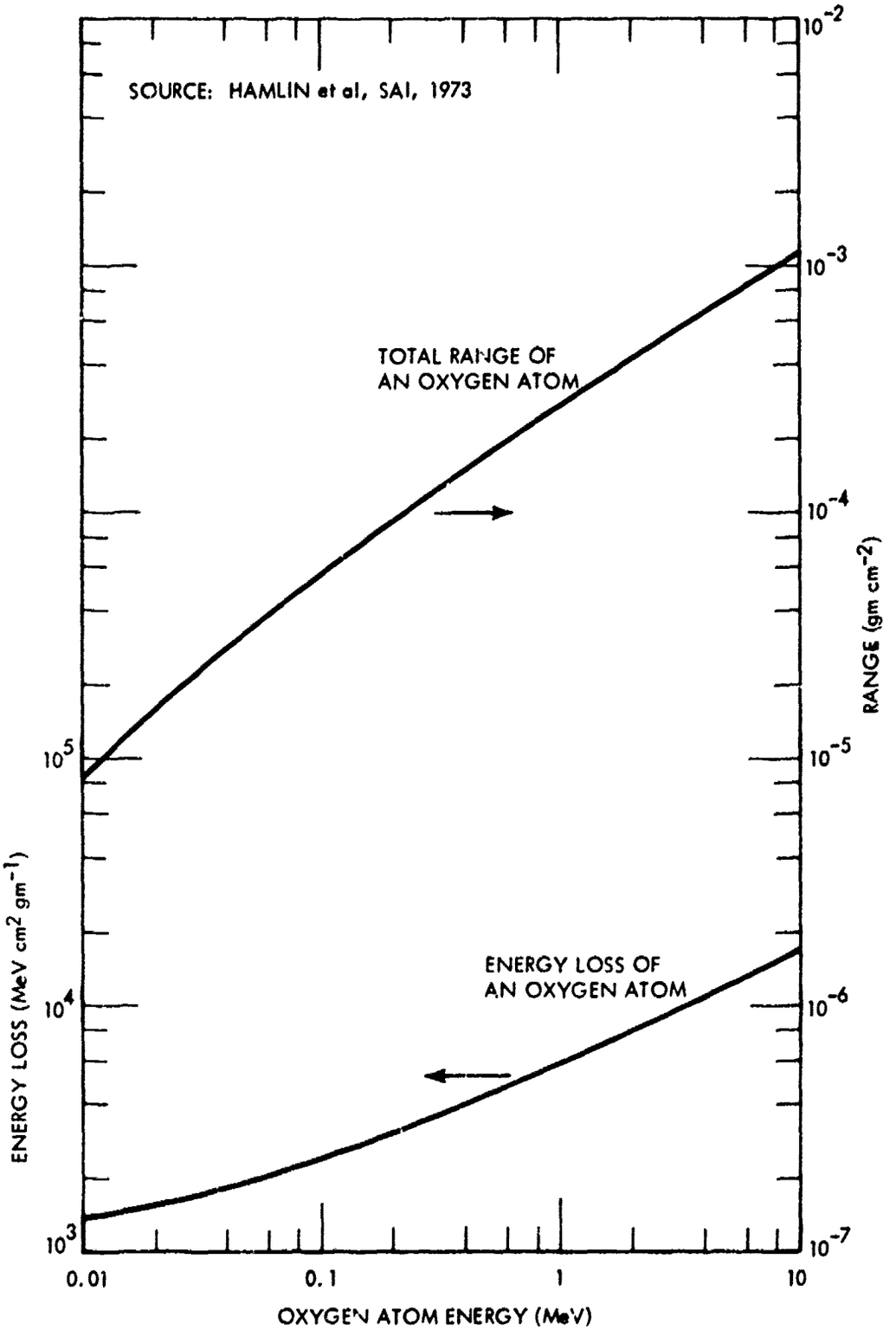

Figure 2-3. Energy loss and total range of atomic oxygen stopping in nitrogen.

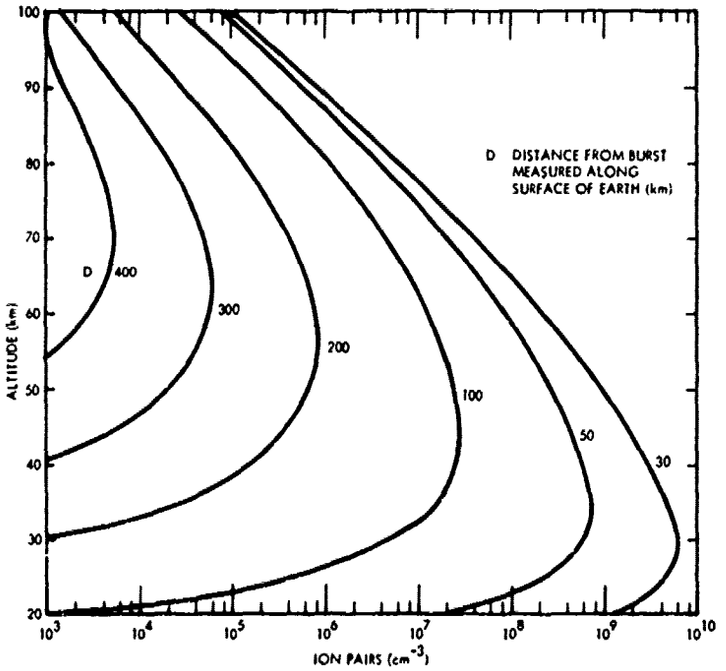

Figure 2-4. Ion-pair density at t = 0 due to 10-KT prompt-gamma source at 30 km.

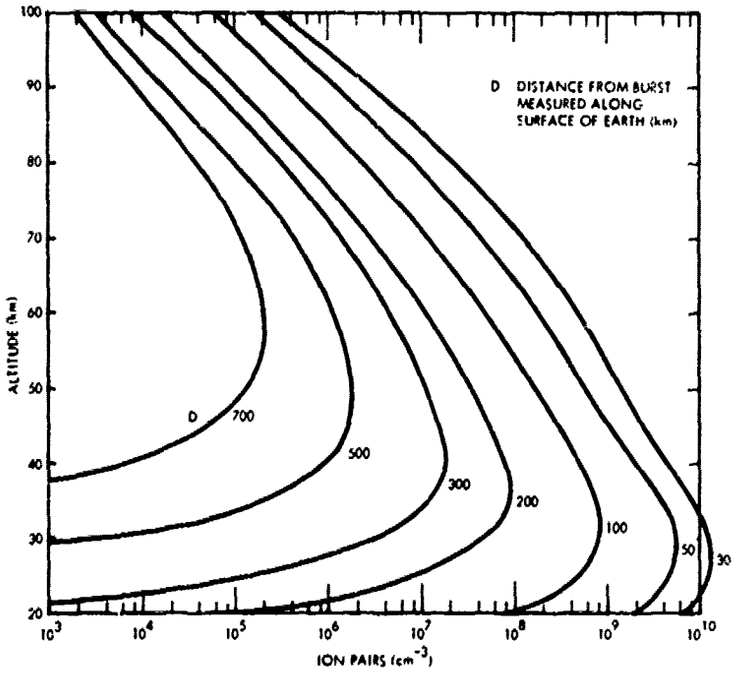

Figure 2-5. Ion-pair density at t = 0 due to 10-KT prompt-gamma source at 60 km.

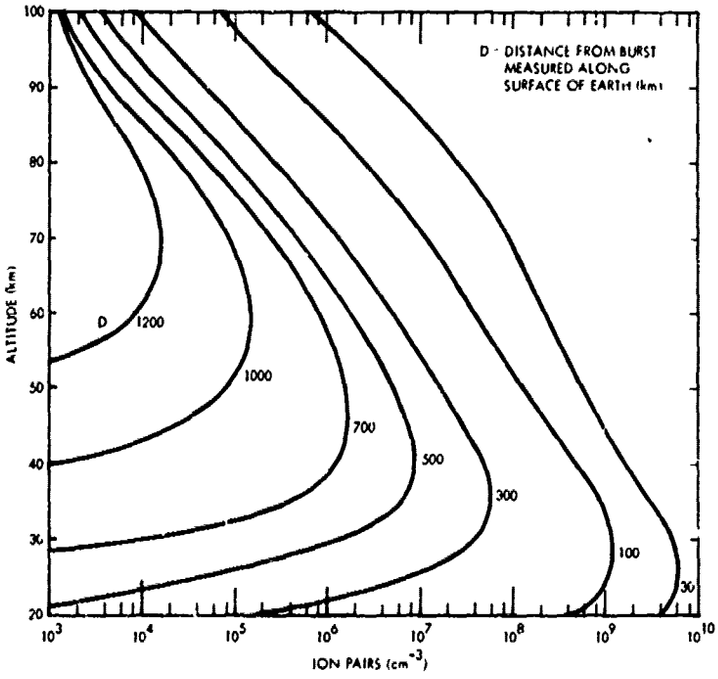

Figure 2-6. Ion-pair density at t = 0 due to 10-KT prompt-gamma source at 90 km.

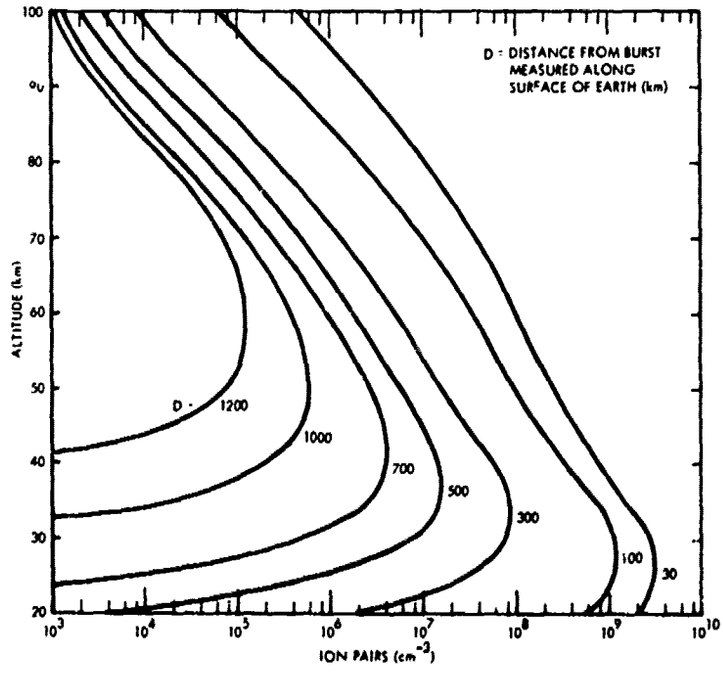

Figure 2-7. Ion-pair density at t = 0 due to 10-KT prompt-gamma source at 120 km.

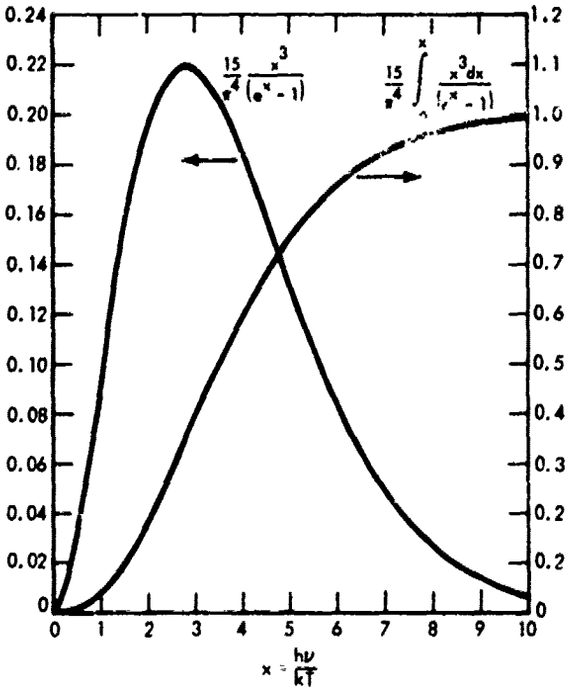

x	$\frac{15}{\pi^4}\frac{x^3}{(e^x-1)}$	$\frac{15}{\pi^4}\int_0^x \frac{x^3dx}{(e^x-1)}$
Small x	$\frac{15}{\pi^4}x^2$	$0.05134\,x^3$
0.01	1.53^{-5}	5.1^{-8}
0.02	6.1^{-5}	4.1^{-5}
0.05	3.75^{-4}	6.3^{-6}
0.07	7.28^{-4}	1.7^{-5}
0.1	1.46^{-3}	4.9^{-5}
0.25	8.47^{-3}	7.3^{-4}
0.5	2.97^{-2}	5.3^{-5}
0.75	5.82^{-2}	1.62^{-7}
1.0	8.96^{-2}	3.46^{-2}
10.0	6.99^{-3}	9.99^{-1}
Large x	$\frac{15}{\pi^4}x^3e^{-x}$	$1-\frac{x^3e^{-x}}{6.5}$

Figure 2-8. Universal Planck curve.

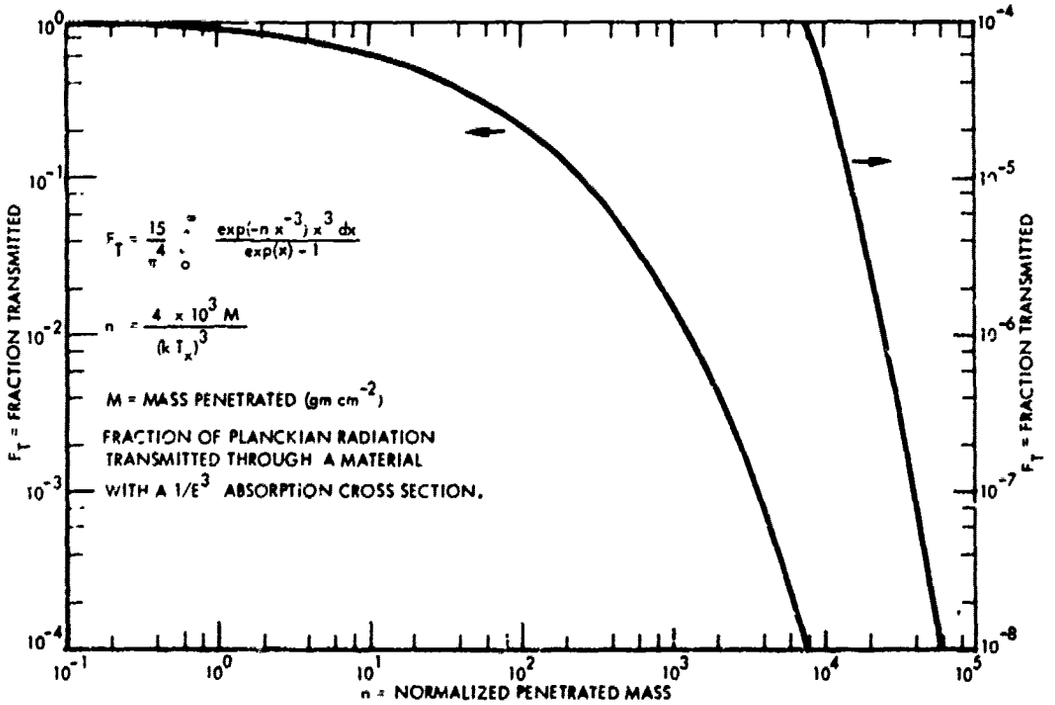

Figure 2-9. X-ray transmission factor.

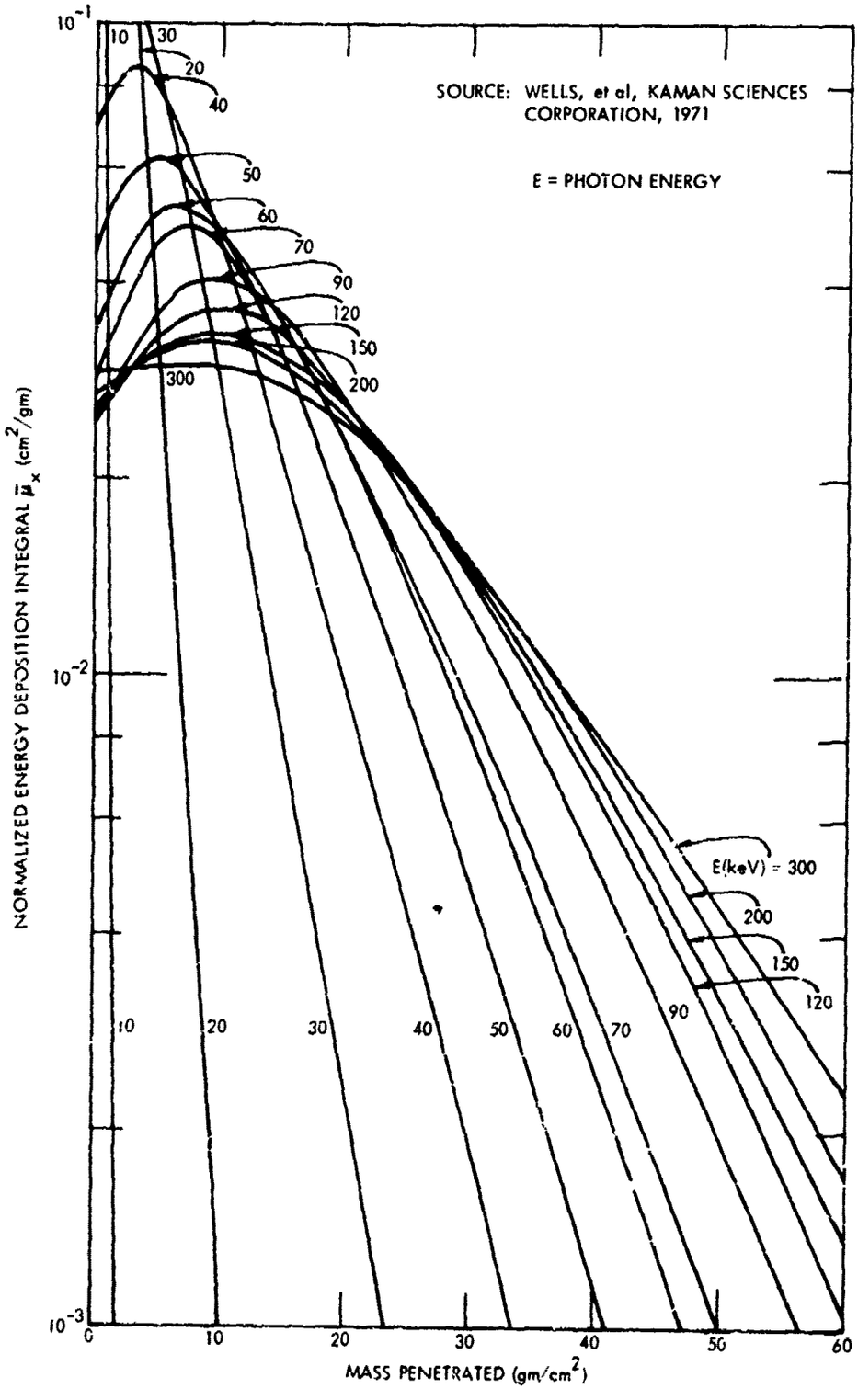

Figure 2-10. X-ray energy deposition integral, monochromatic sources.

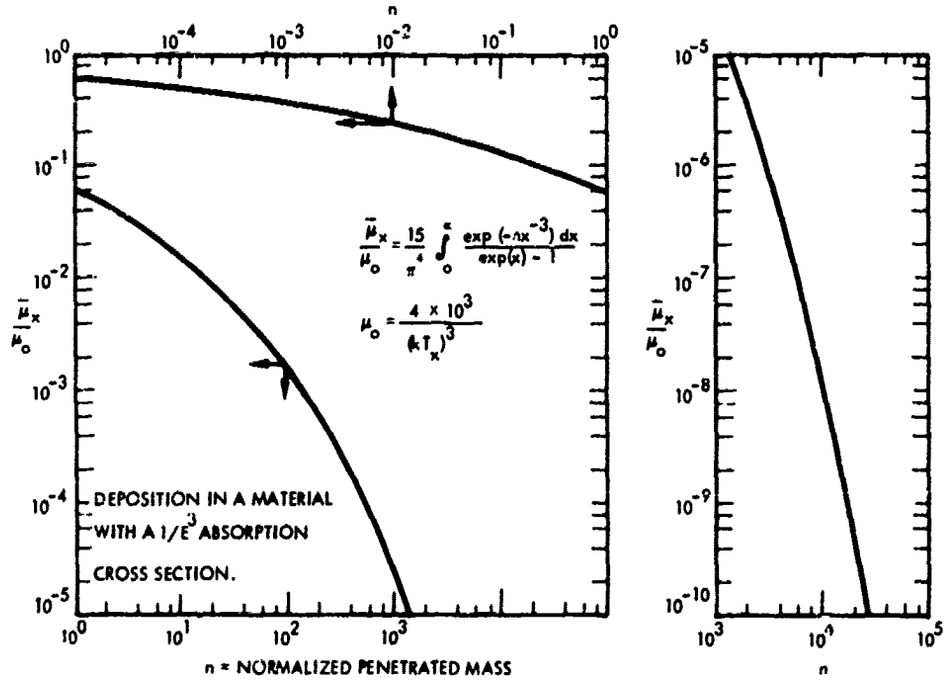

Figure 2-11. X-ray relative energy absorption coefficient.

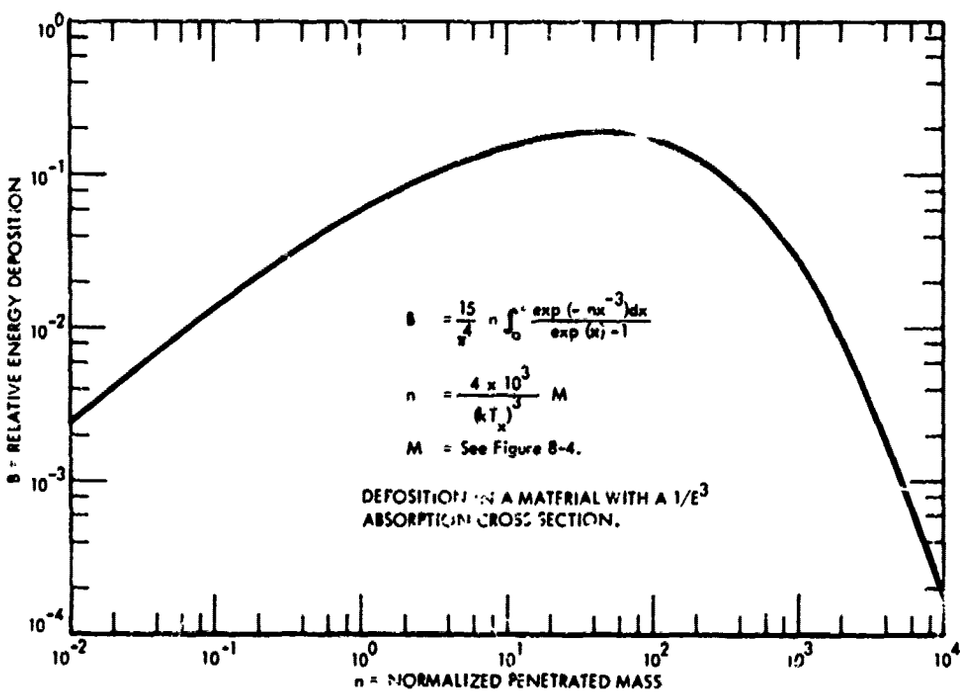

Figure 2-12. X-ray relative energy deposition.

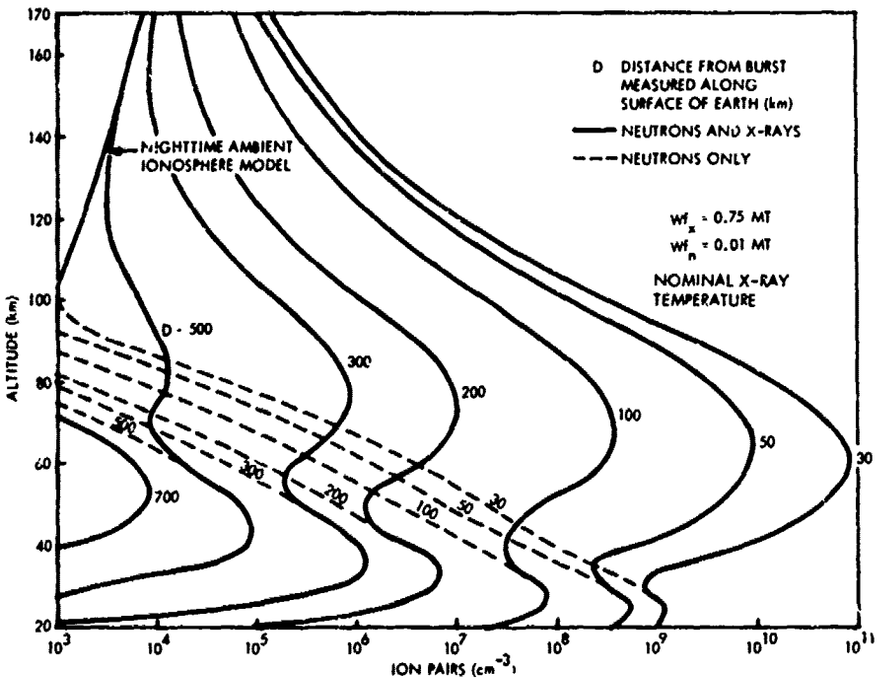

Figure 2-13. Ion-pair density at t = 0 due to X-rays and neutrons, burst at 60 km.

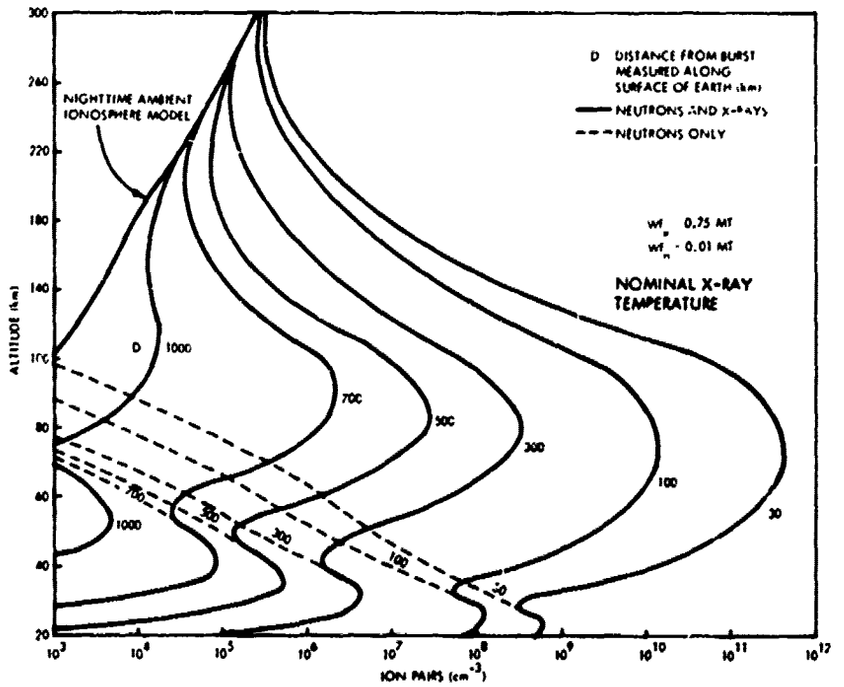

Figure 2-14. Ion-pair density at t = 0 due to X-rays and neutrons, burst at 90 km.

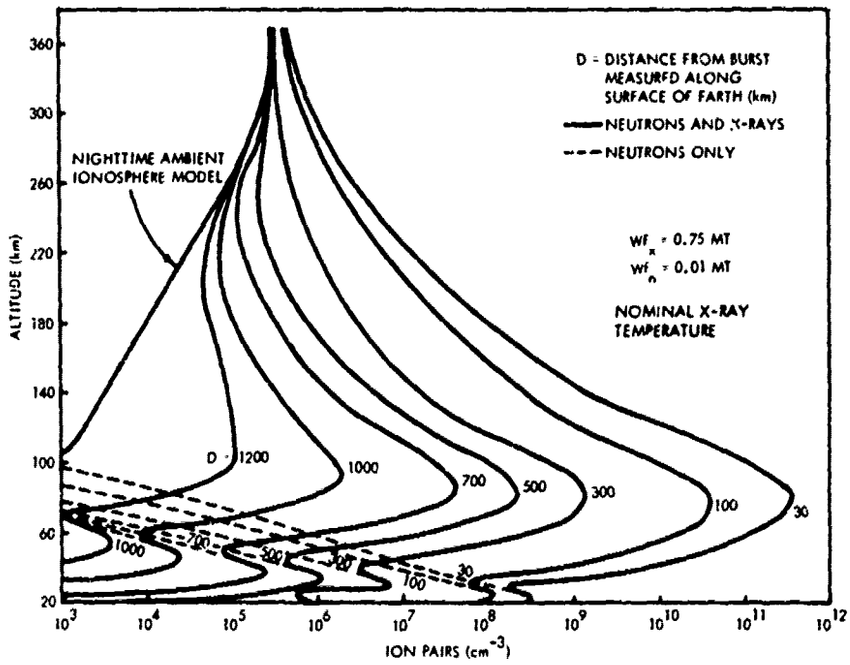

Figure 2-15. Ion-pair density at $t = 0$ due to X-rays and neutrons, burst at 120 km.

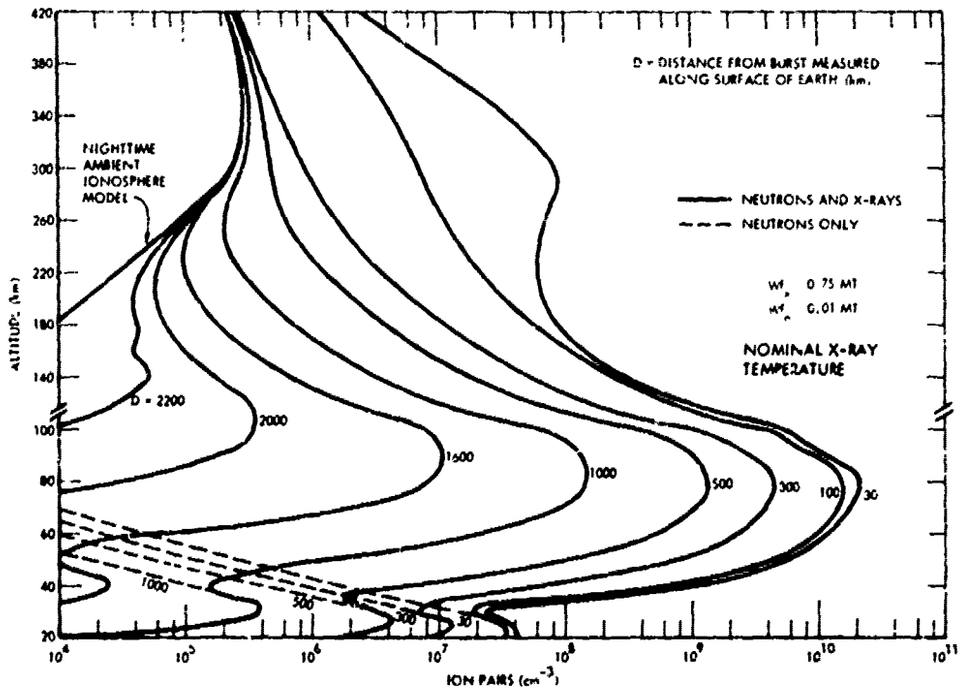

Figure 2-16. Ion-pair density at $t = 0$ due to X-rays and neutrons, burst at 300 km.

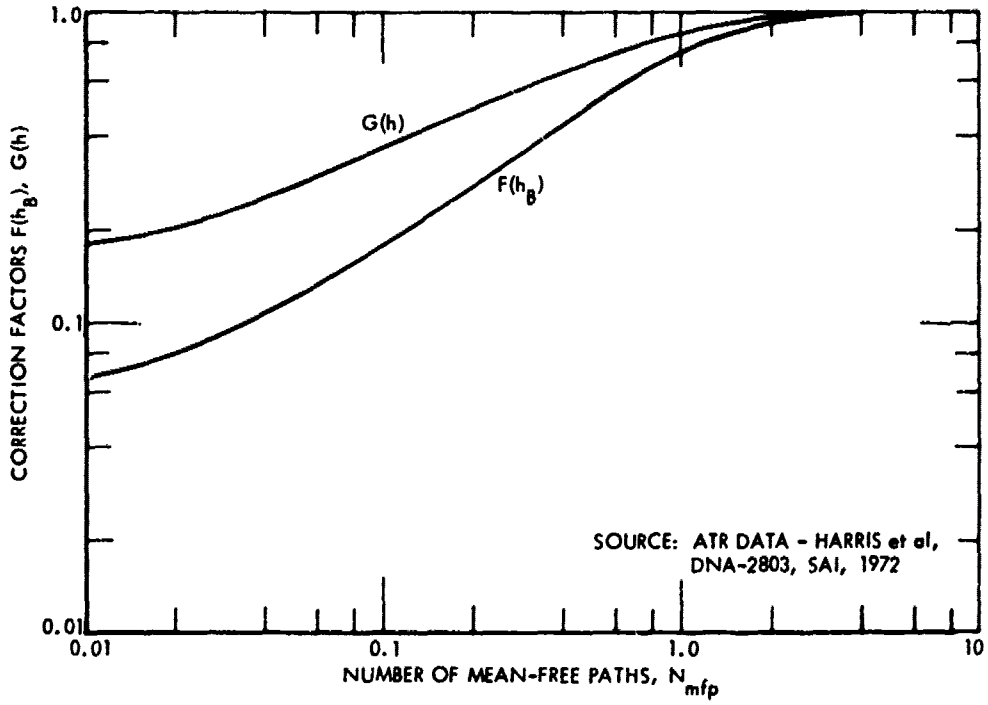

Figure 2-17. Correction factors for altitudes of burst and deposition points.

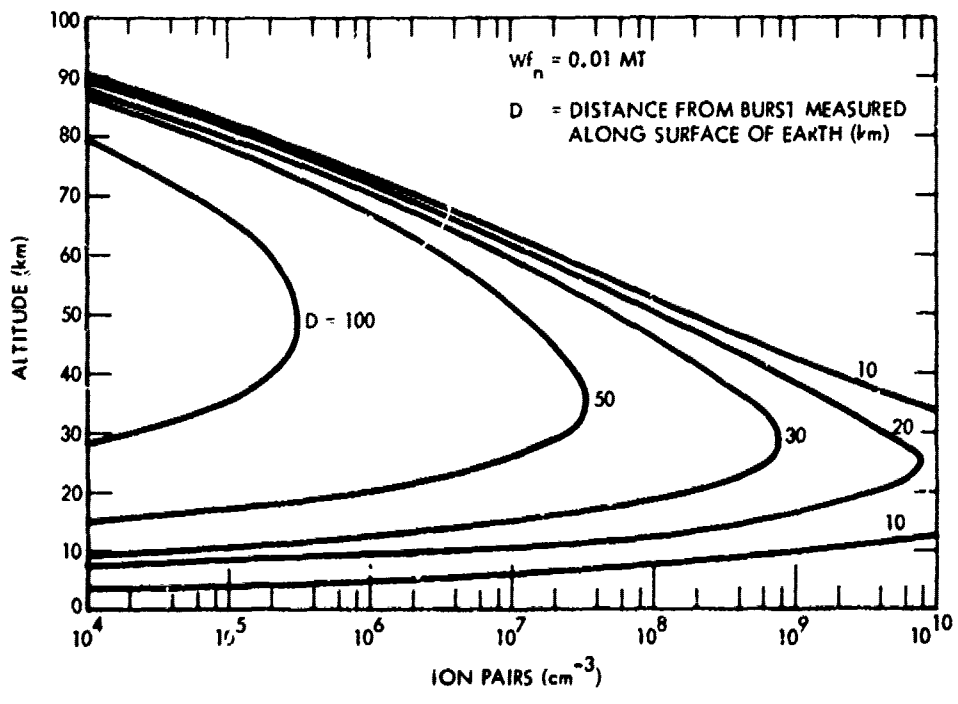

Figure 2-18. Ion-pair density at $t = 0$ due to neutrons, burst at 20 km.

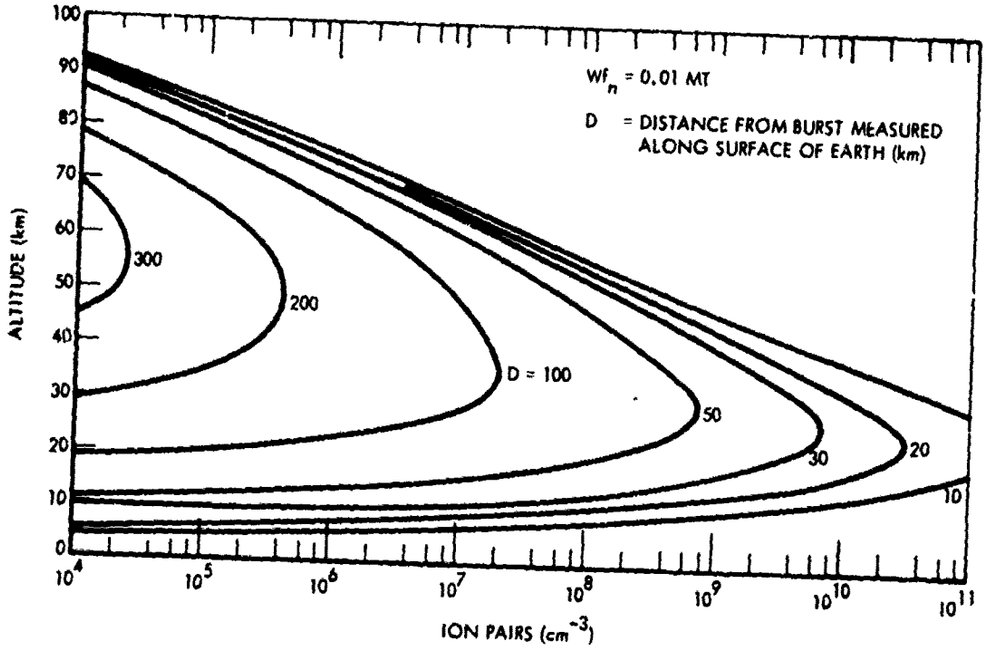

Figure 2-19. Ion-pair density at $t \approx 0$ due to neutrons, burst at 30 km.

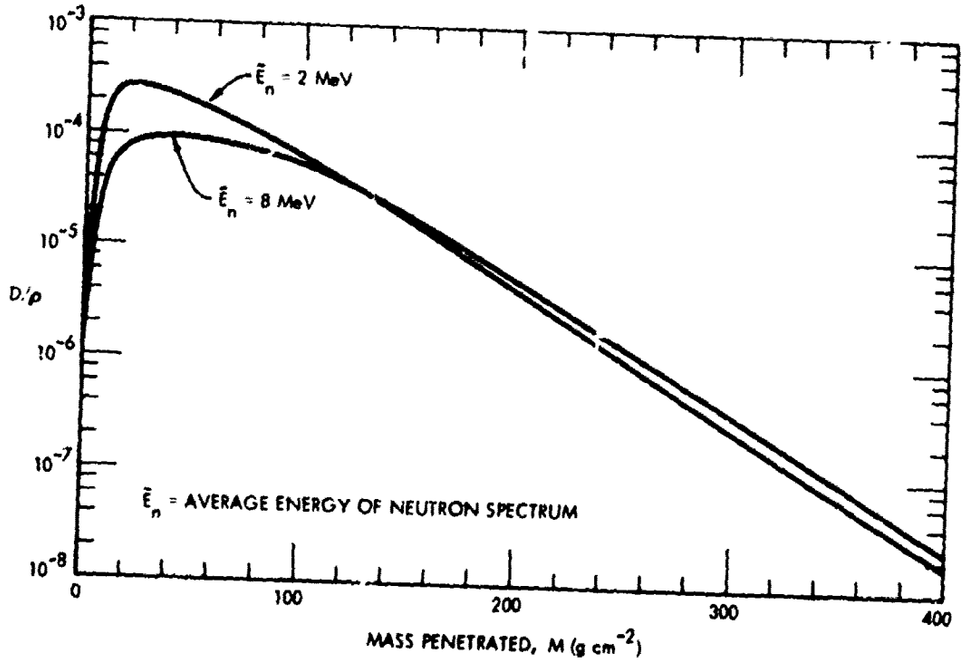

Figure 2-20. Normalized neutron deposition rate.

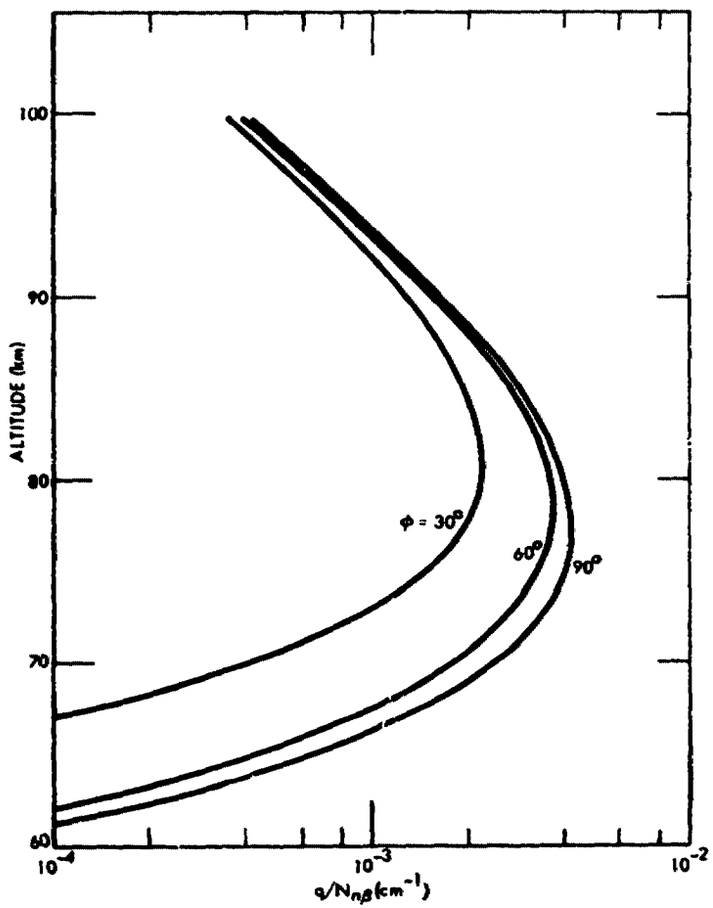

Figure 2-21. Ion-pair production rate due to neutron decay betas.

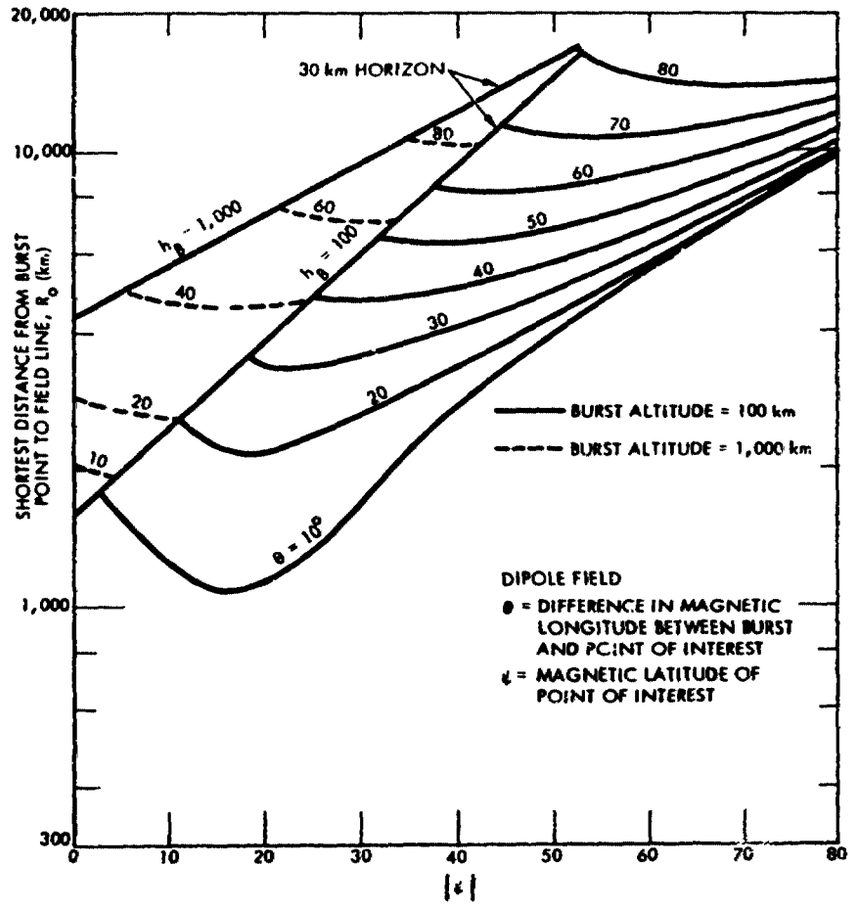

Figure 2-22. Distance R_o burst at ± 15 degrees magnetic latitude.

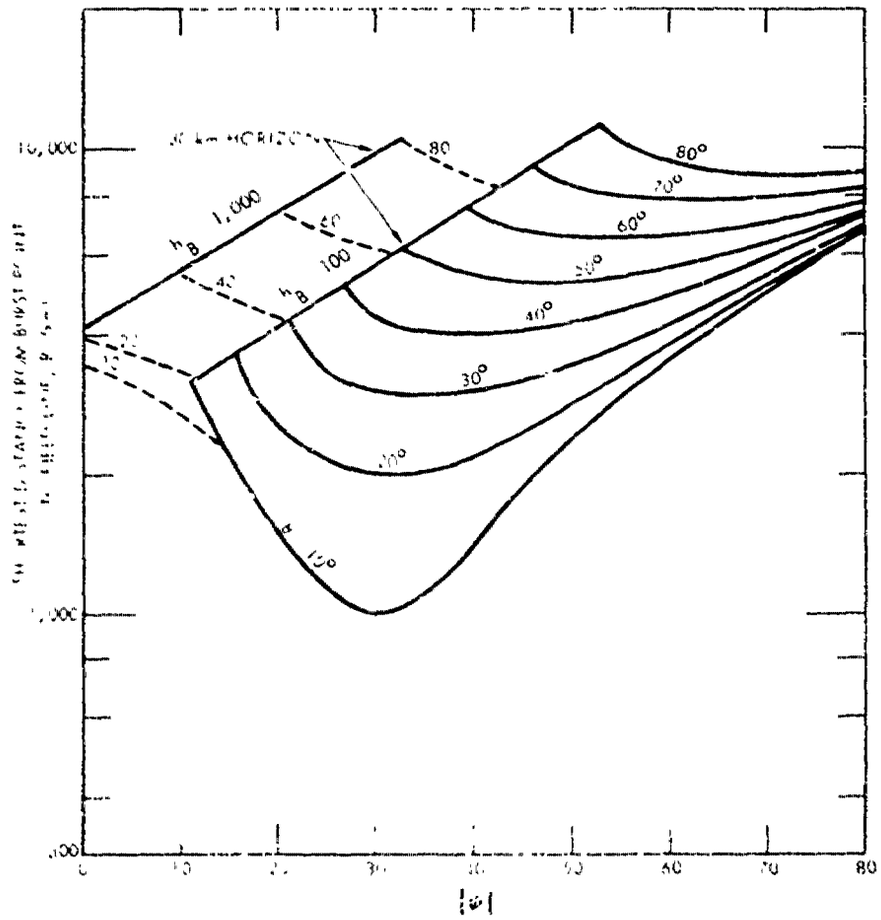

Figure 2-23. Distance R_o for burst at ±30 degrees magnetic latitude.

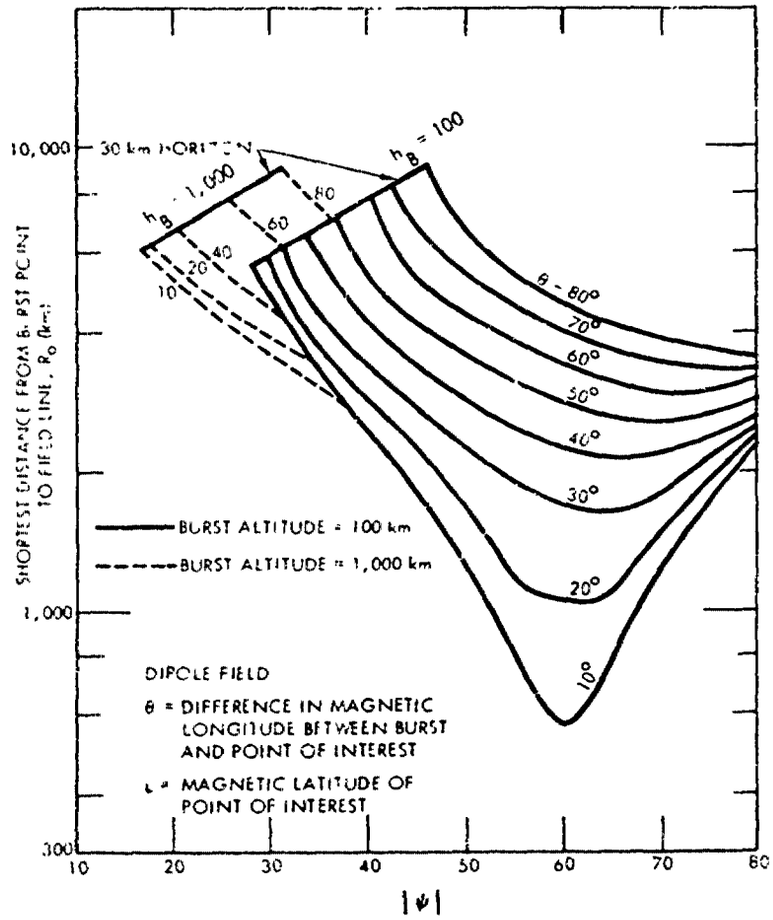

Figure 2-24. Distance R_o for burst at ±60 degrees magnetic latitude.

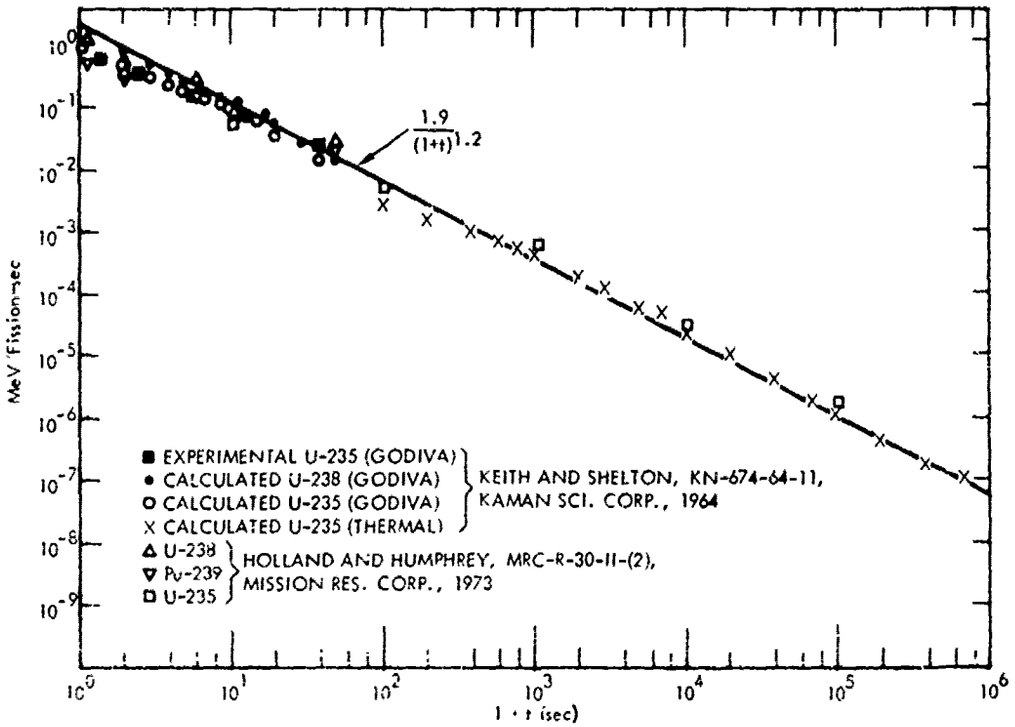

Figure 2-25. Gamma-ray energy release rates.

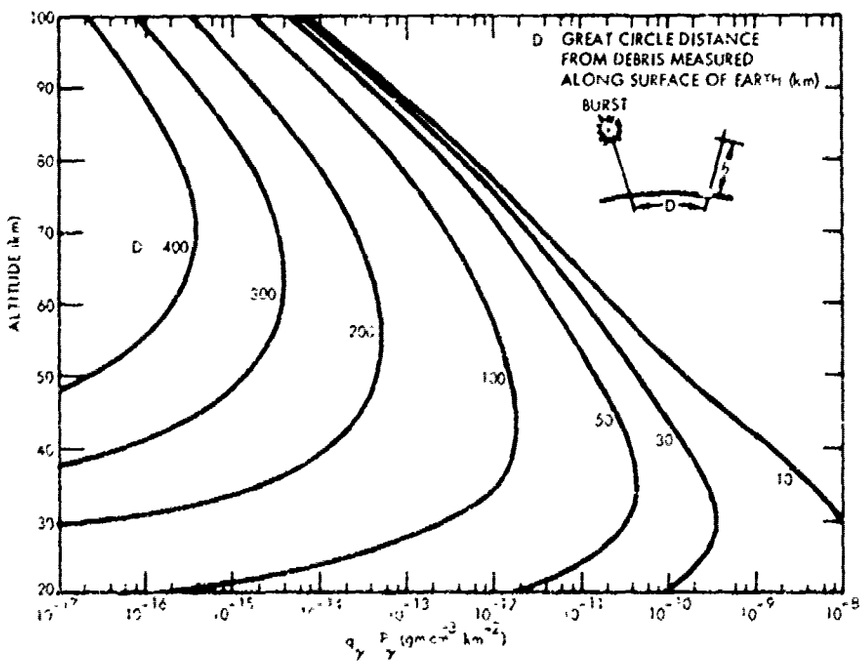

Figure 2-26. Ion-pair production rate, q, due to delayed gamma rays, 30-km point source.

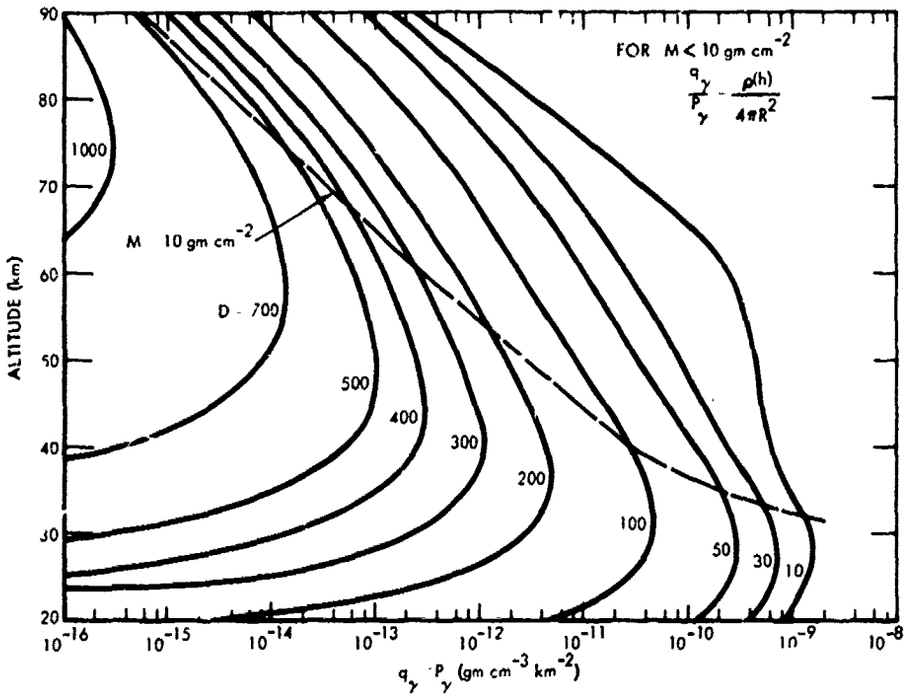

Figure 2-27. Ion-pair production rate, q, due to delayed gamma rays, 60-km point source.

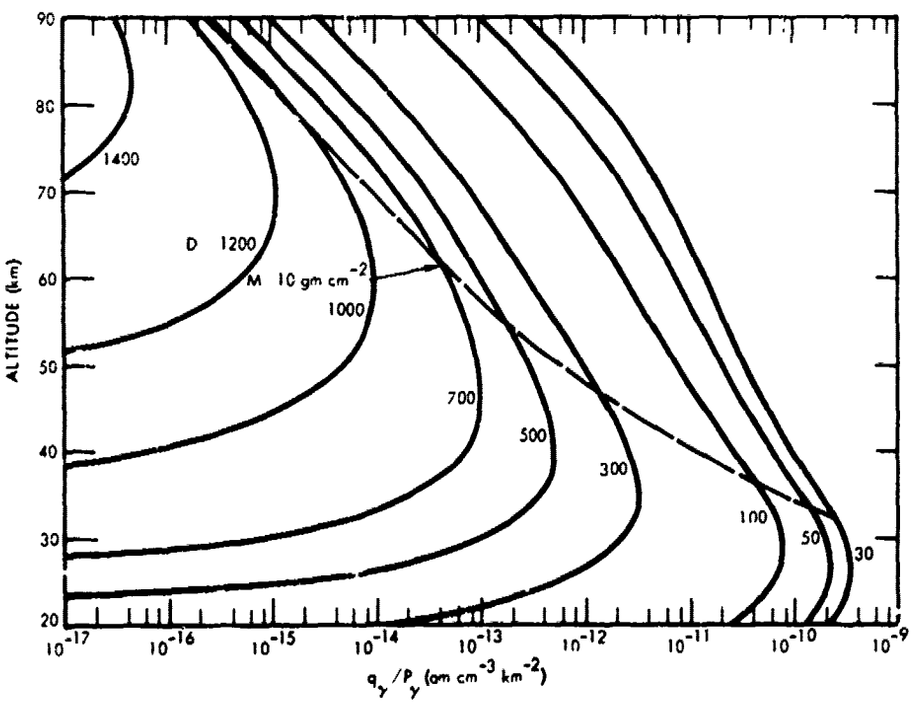

Figure 2-28. Ion-pair production rate, q, due to delayed gamma rays, 90-km point source.

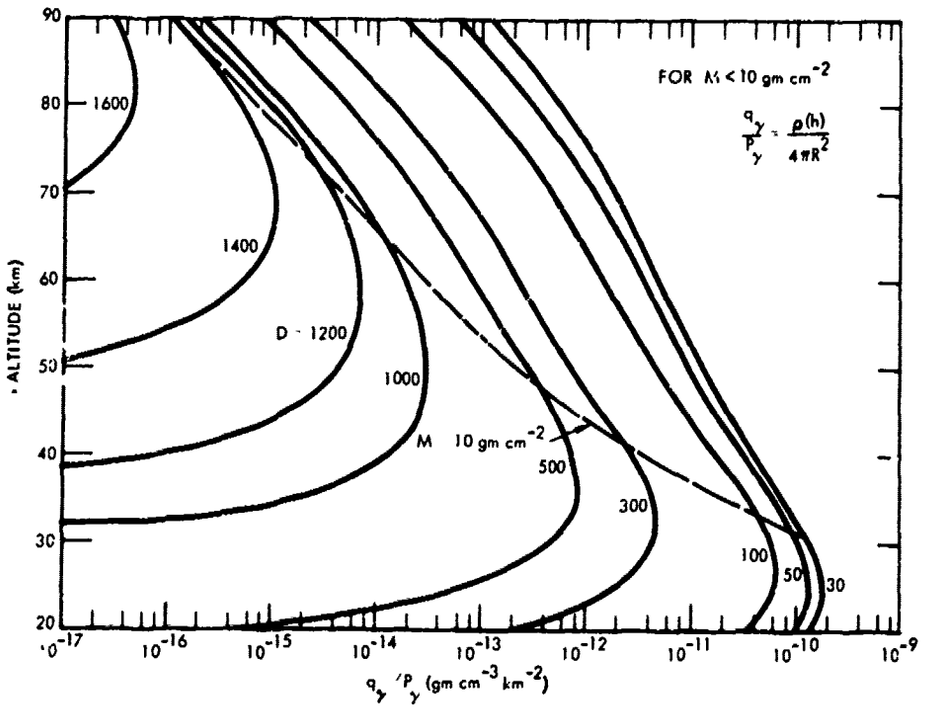

Figure 2-29. Ion-pair production rate, q, due to delayed gamma rays, 120-km point source.

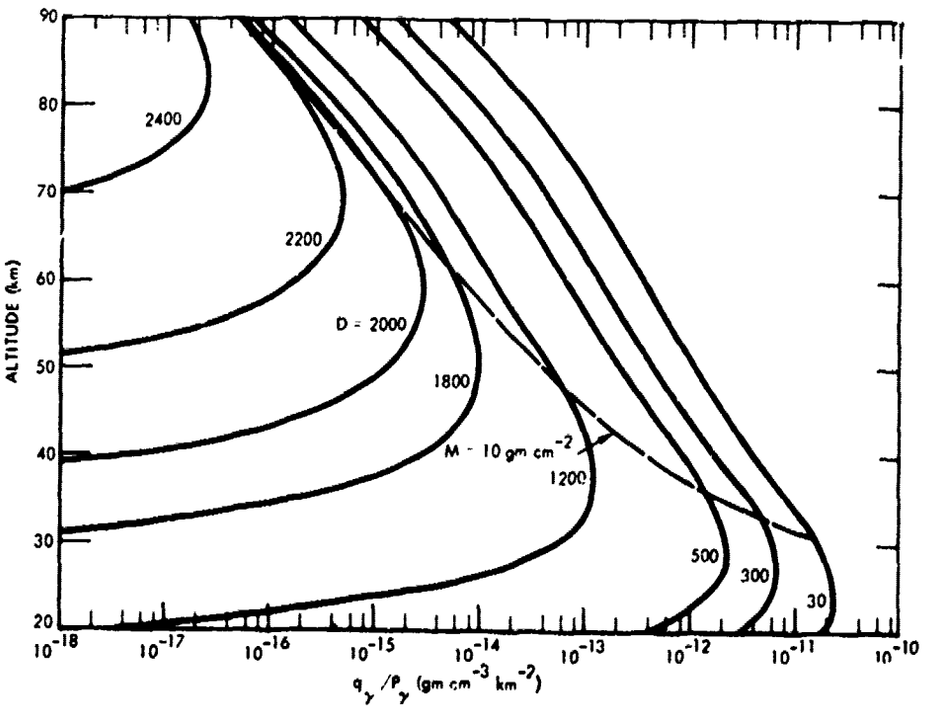

Figure 2-30. Ion-pair production rate, q, due to delayed gamma rays, 300-km point source.

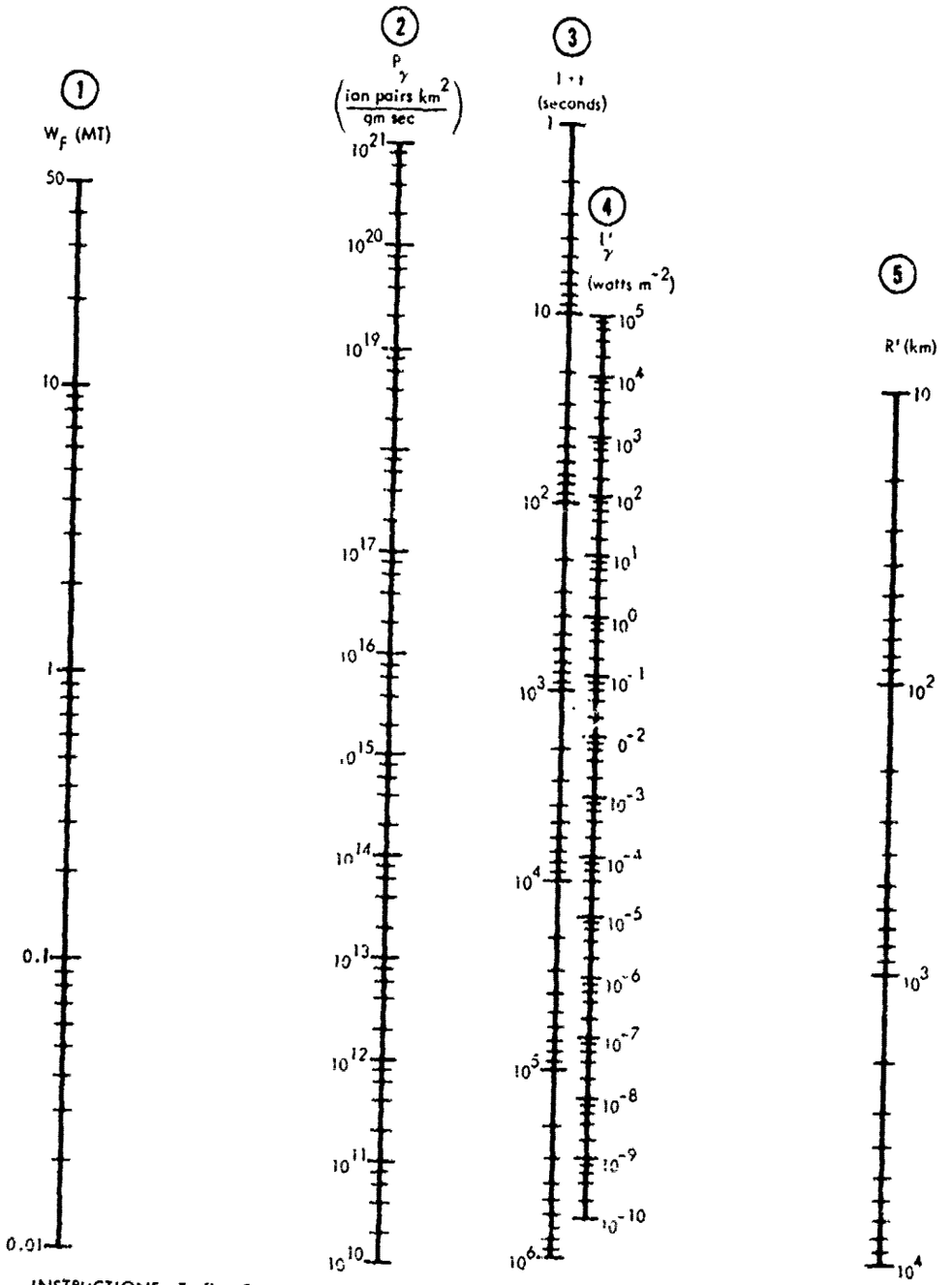

INSTRUCTIONS: To find P_γ connect a straight line from fission yield (Scale 1) to time after detonation on Scale 3 (note this is a 1_{++} scale). The intersection on Scale 2 is P_γ. To find I'_γ connect a straight line from the point determined on Scale 2 to the appropriate distance, R', on Scale 5. The intersection with Scale 4 is I'_γ.

$$R' = \left[D^2 + (h_{DB} - 60)^2\right]^{1/2} \qquad D > R_{DB}$$

$$\left[\left(\frac{R_{DB}}{2}\right)^2 + (h_{DB} - 60)^2\right]^{1/2} \qquad D \leq R_{DB}$$

D = Great circle distance from debris center measured along surface of earth.

Figure 2-31. Gamma radiation intensity nomogram.

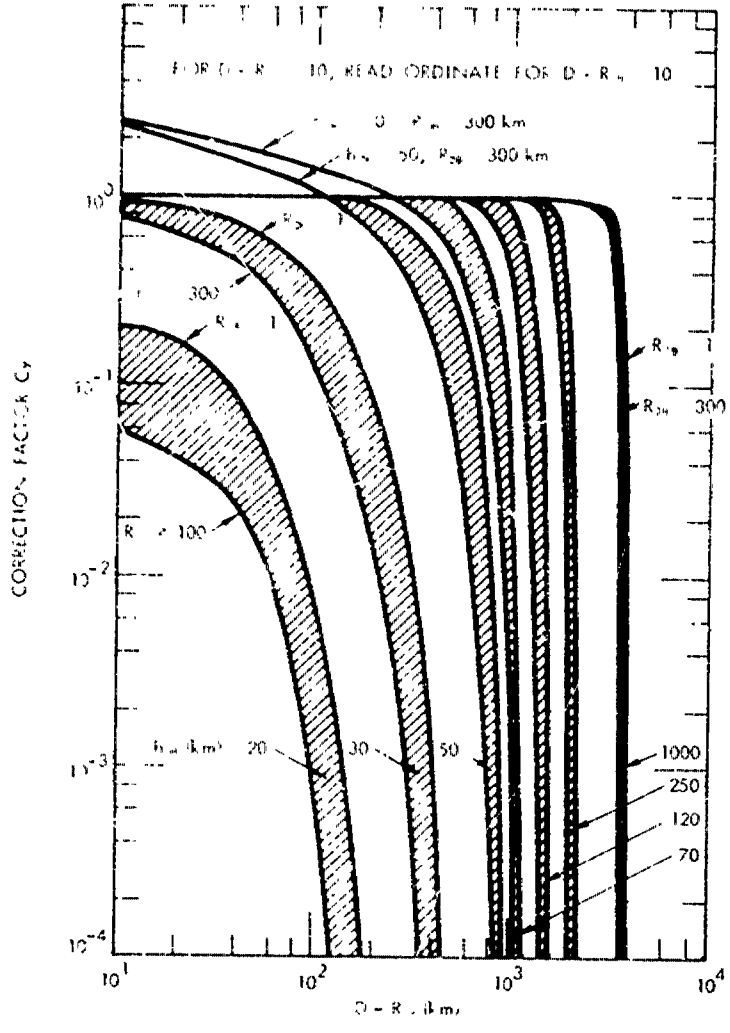

Figure 2-32A. Correction factor for gamma-ray flux, R_{DB} = 1 - 300 km.

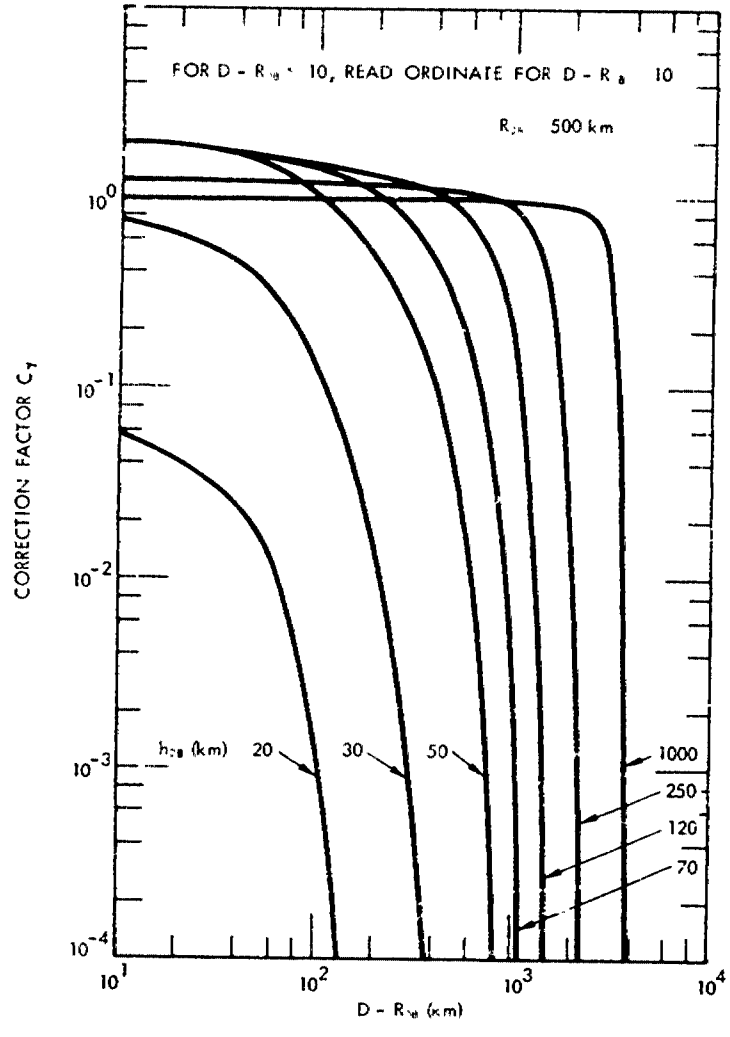

Figure 2-32B. Correction factor for gamma-ray flux, R_{DB} = 500 km.

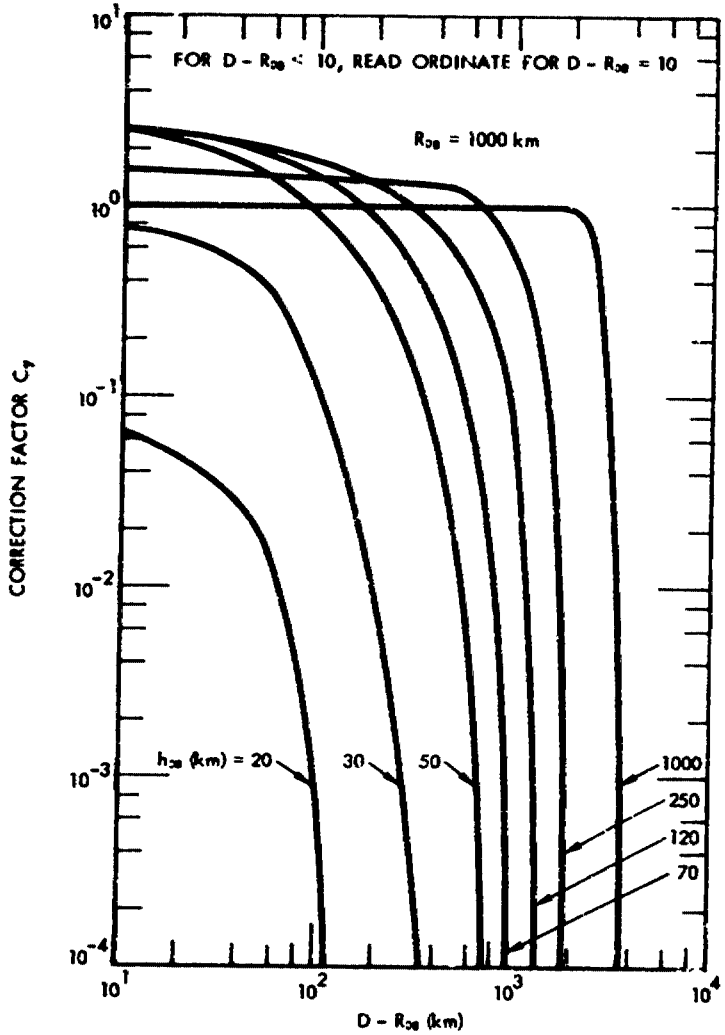

Figure 2-32C. Correction factor for gamma-ray flux, R_{DB} = 1000 km.

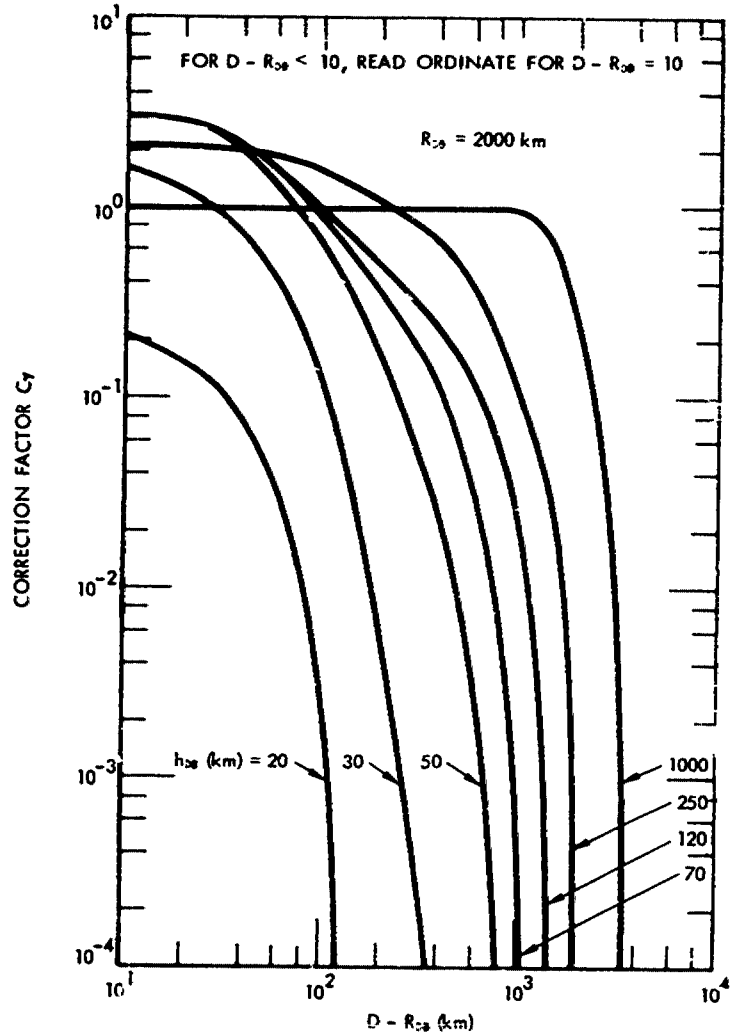

Figure 2-32D. Corrrection factor for gamma-ray flux, R_{DB} = 2000 km.

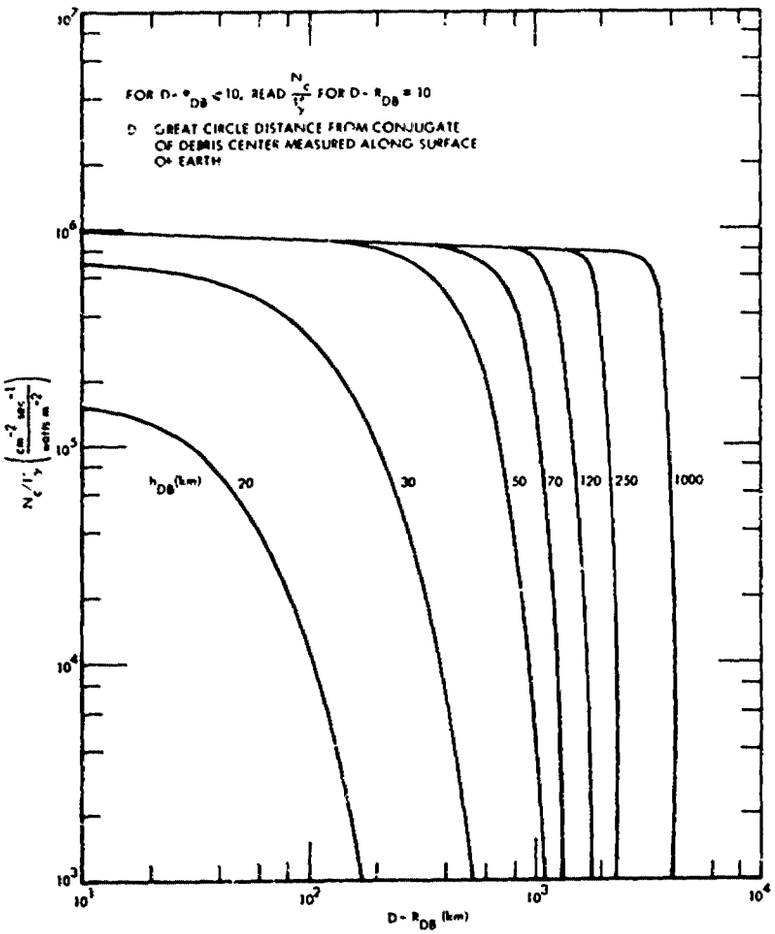

Figure 2-33A. Normalized Compton electron flux, R_{DB} = 1 km.

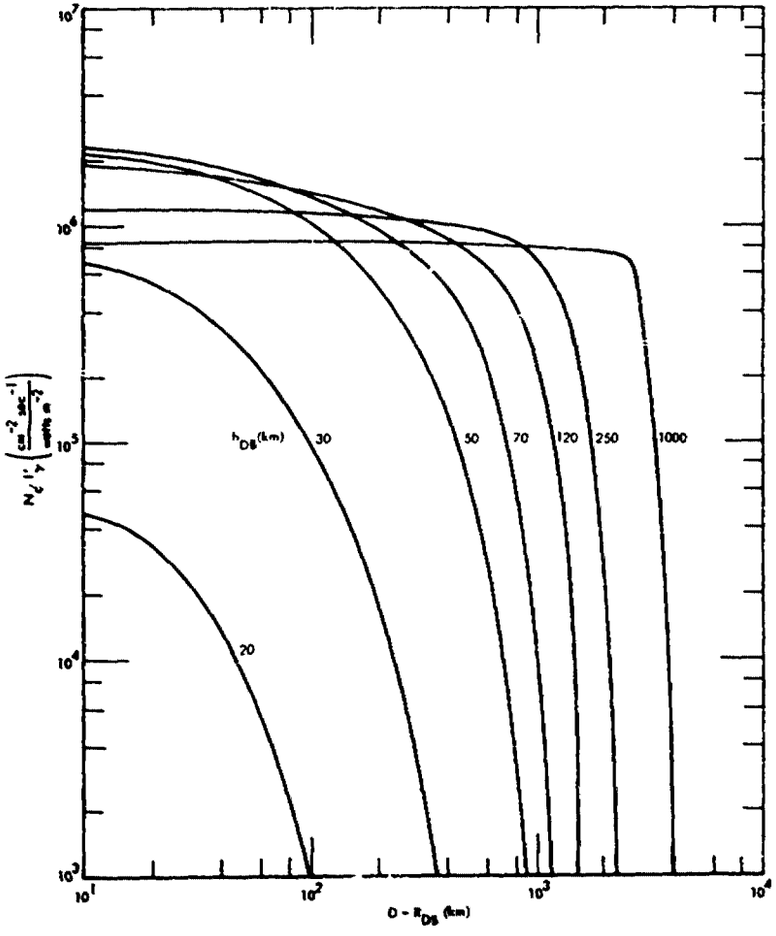

Figure 2-33B. Normalized Compton electron flux, R_{DB} = 500 km.

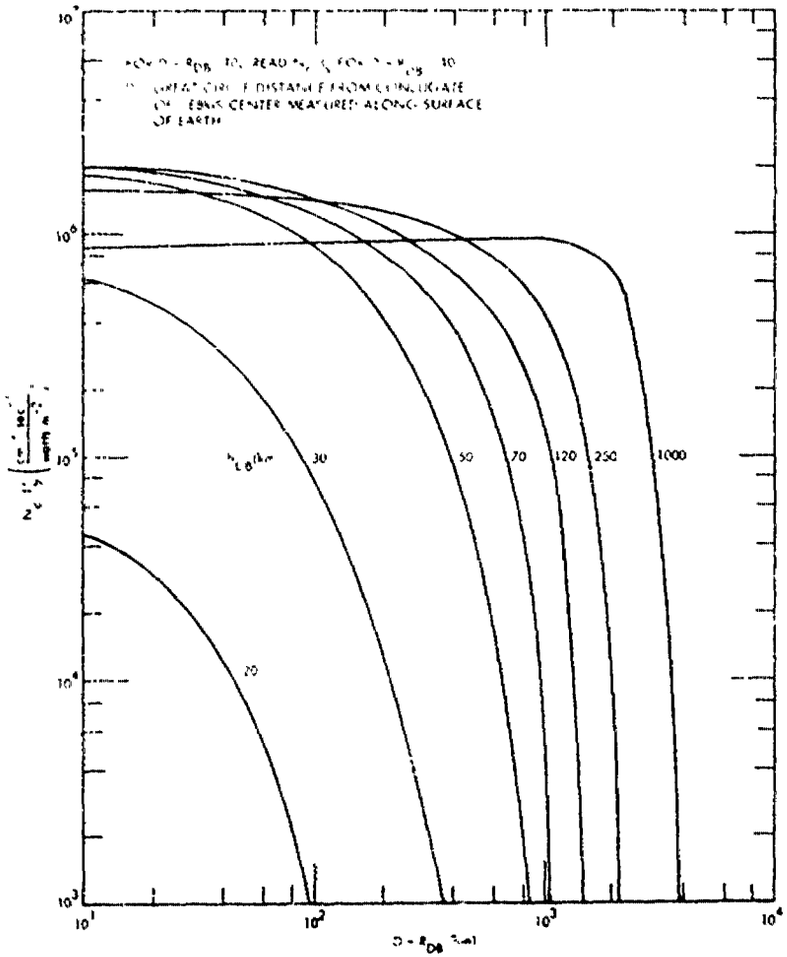

Figure 2-33C. Normalized Compton electron flux, R_{DB} = 1000 km.

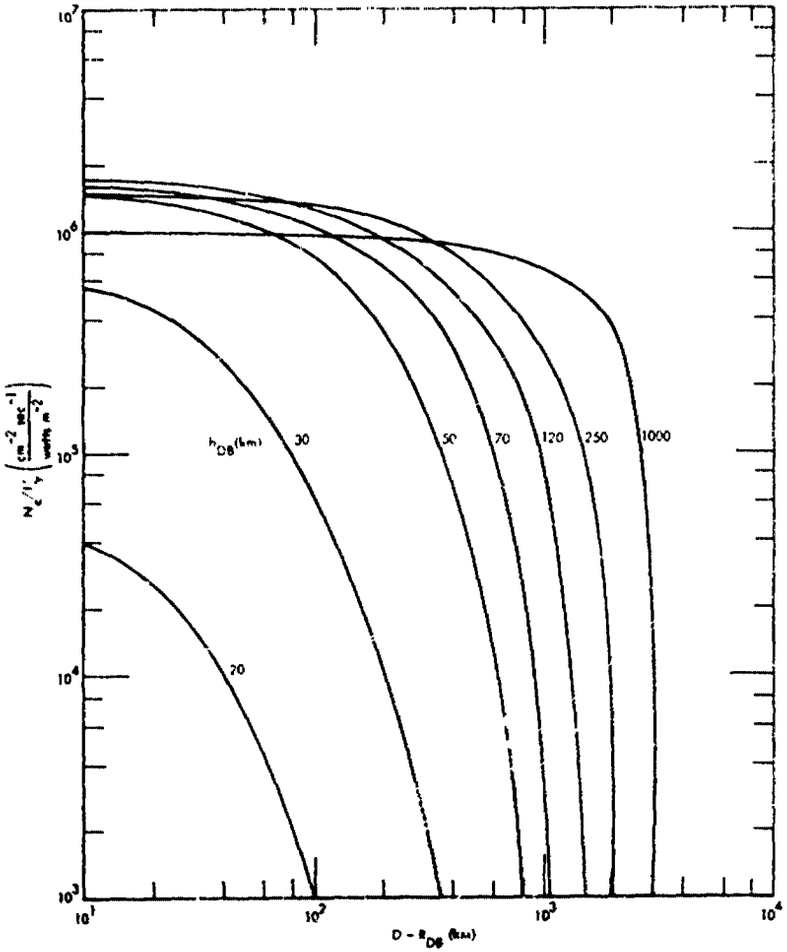

Figure 2-33D. Normalized Compton electron flux, R_{DB} = 2000 km.

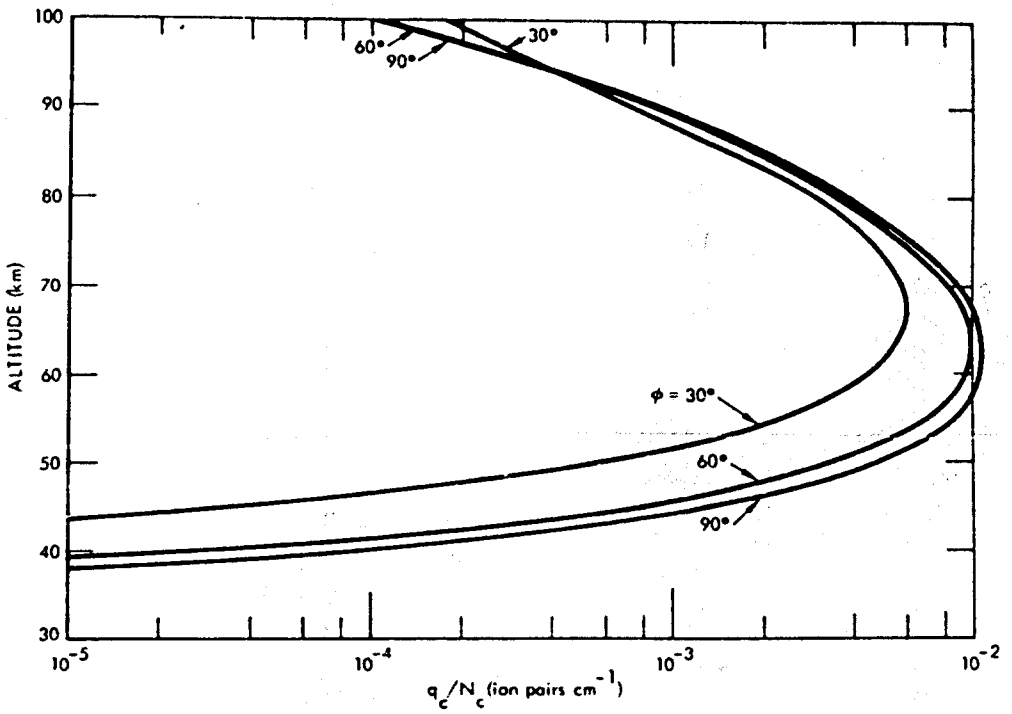

Figure 2-34. Conjugate-region ion-pair production rate due to Compton electrons.

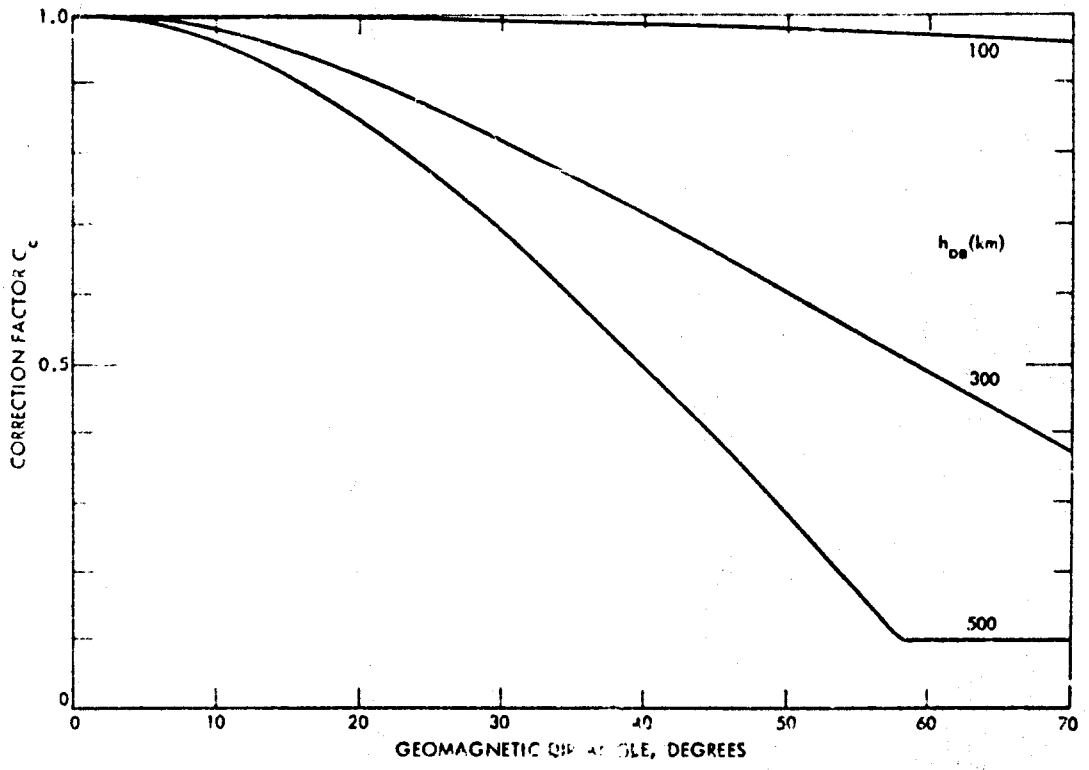

Figure 2-35. Correction factor for Compton-electron ionization.

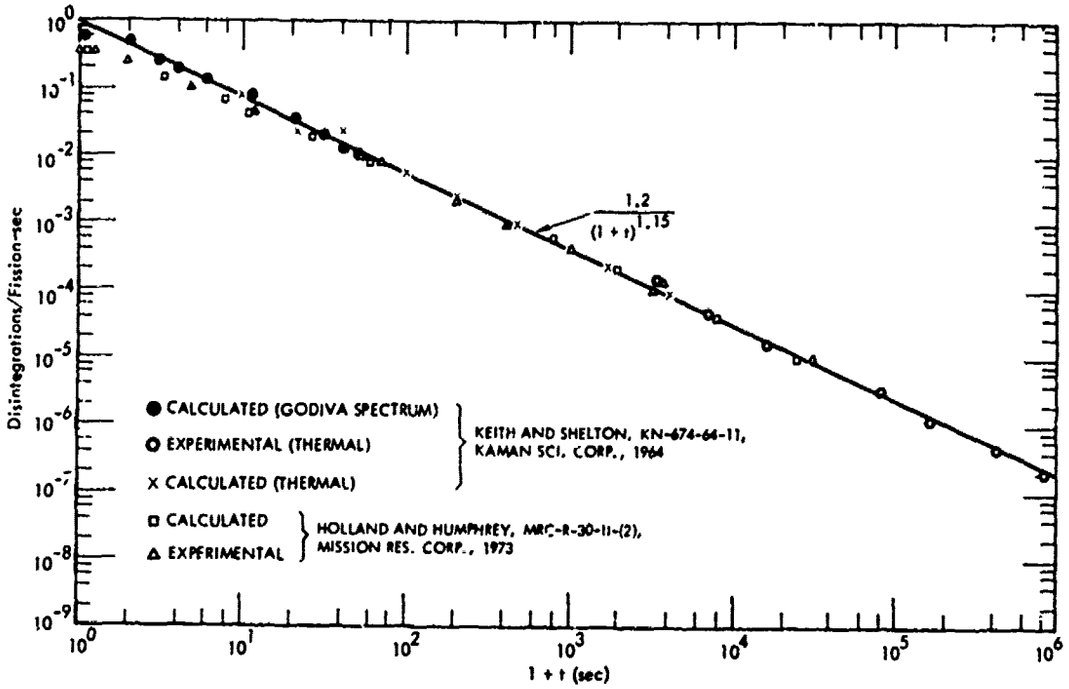

Figure 2-36. U-235 beta decay rate.

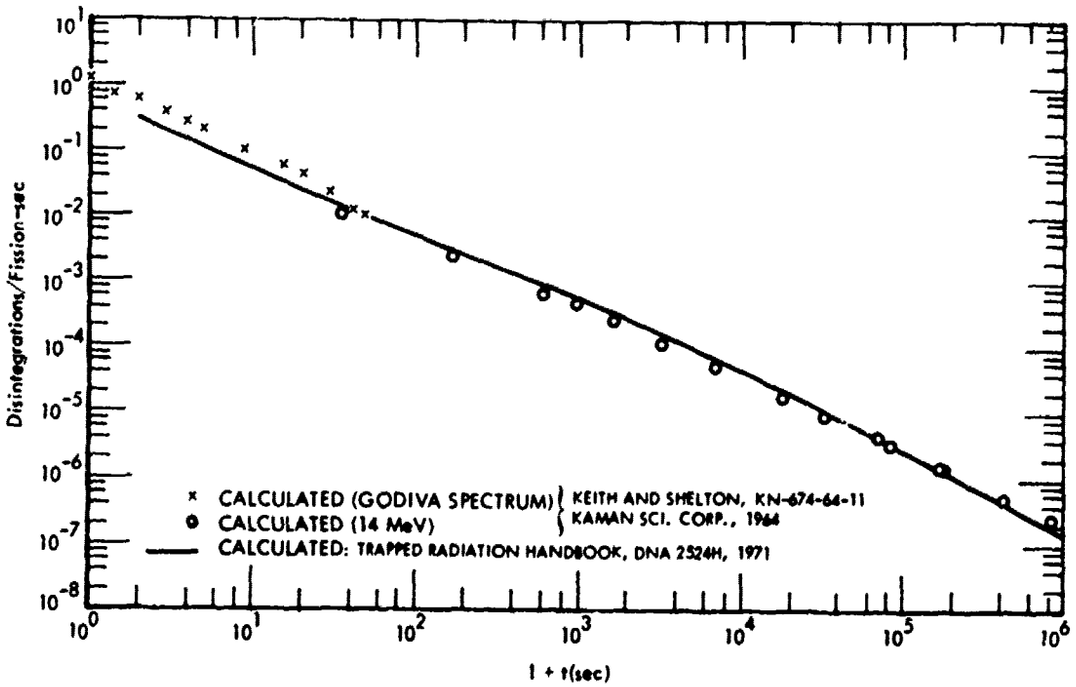

Figure 2-37. U-238 beta decay rate.

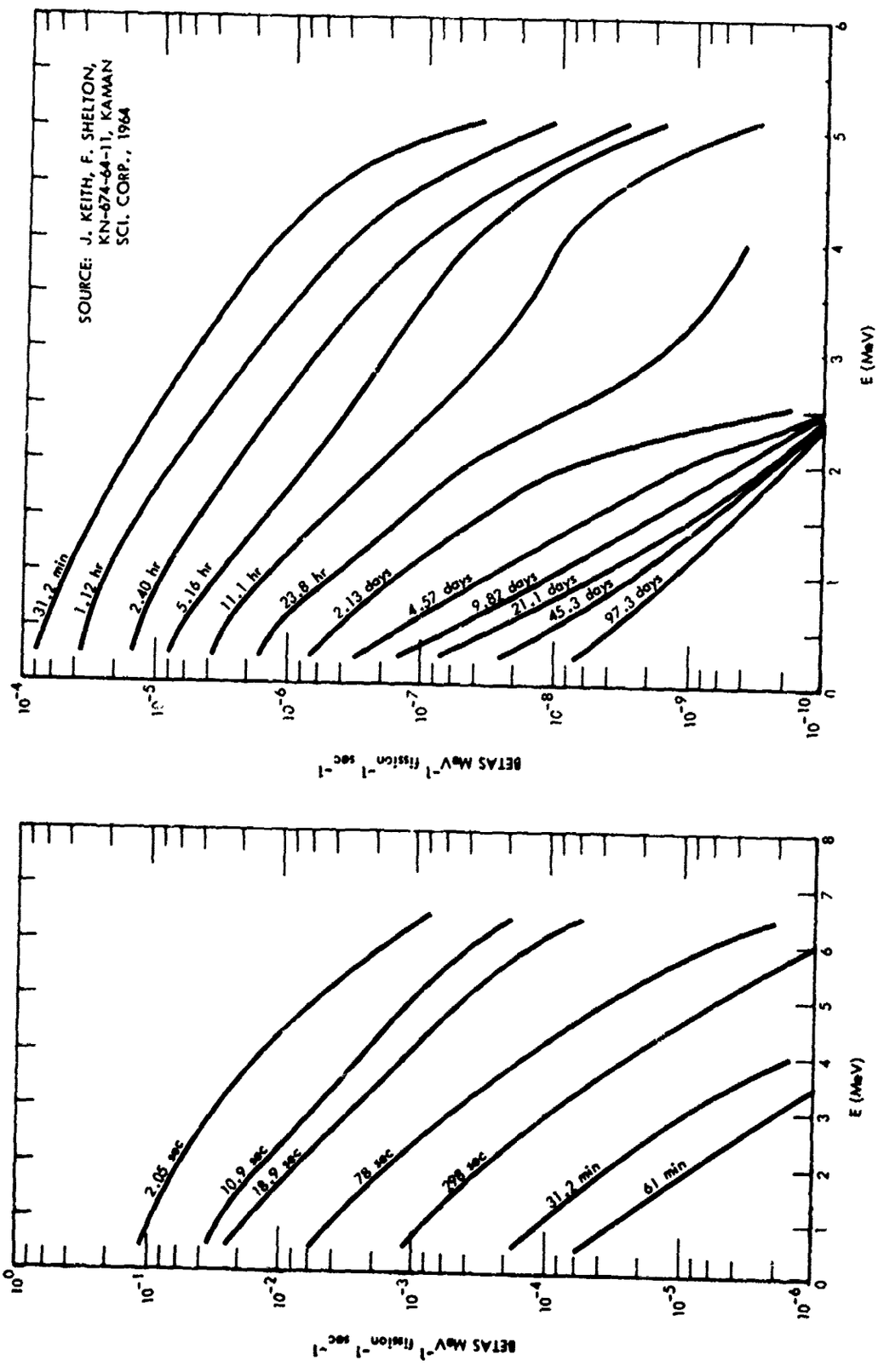

Figure 2-38. Beta spectra for thermal U-235 fissions.

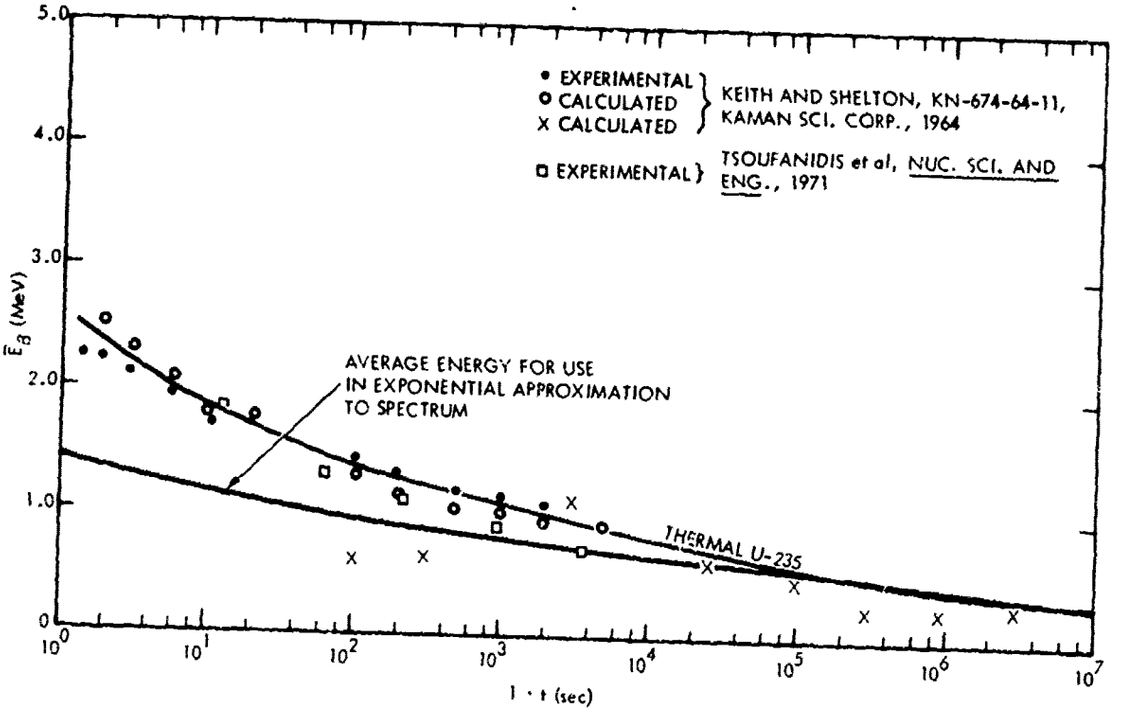

Figure 2-39. Average beta-particle energy.

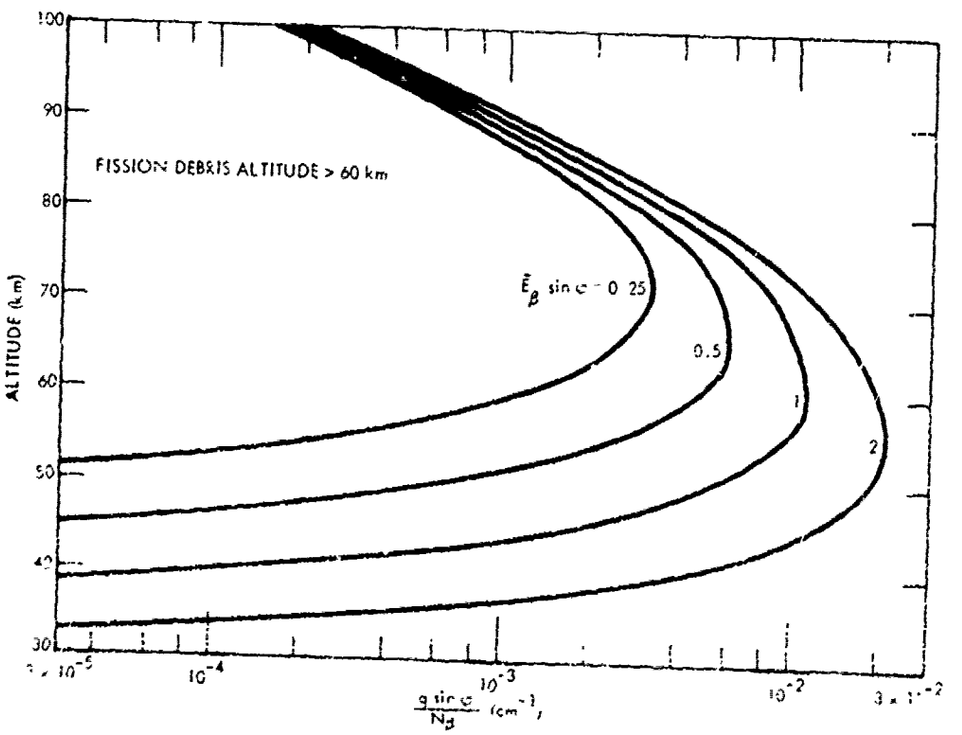

Figure 2-40. Ion-pair production rate due to beta particles.

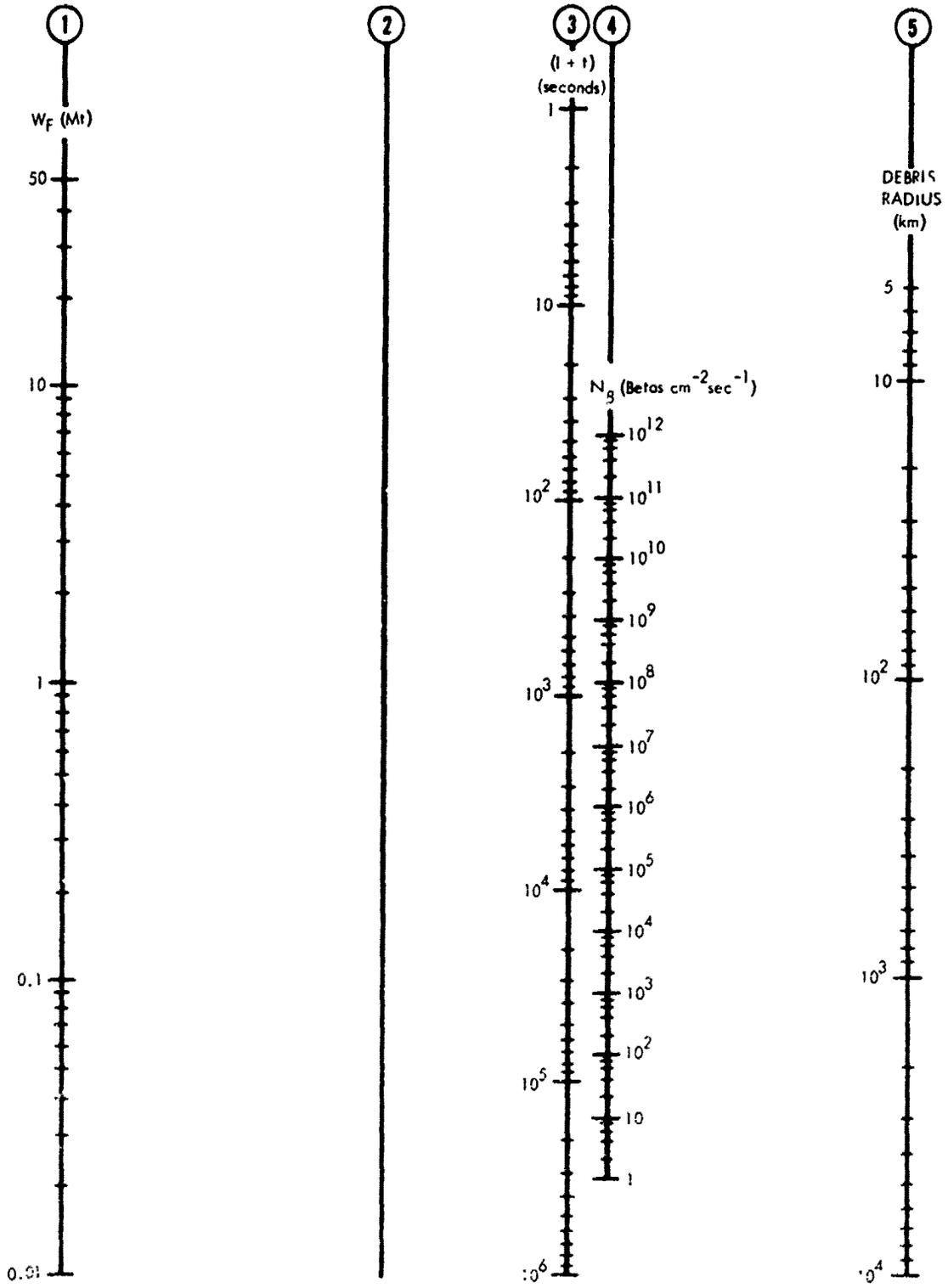

INSTRUCTIONS: To find N_β connect a straight line from fission yield (Scale 1) to time after detonation (Scale 3- this is a 1 + t scale). Mark the point of intersection of this line with Scale 2. Then draw a straight line from this point to the appropriate debris radius on Scale 5. The intersection of the latter line with Scale 4 is N_β

Figure 2-41. Beta radiation intensity nomogram.

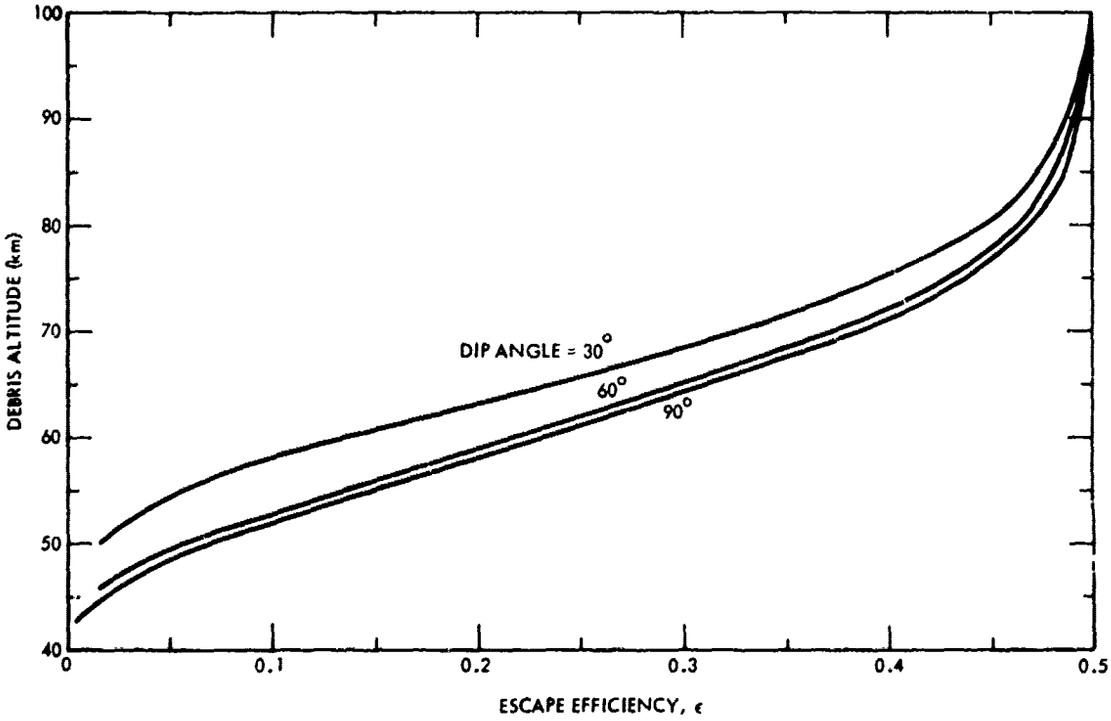

Figure 2-42. Beta radiation escape efficiency to conjugate region.

SECTION 3

PHENOMENOLOGY OF HEATED REGIONS AND THE LOCATION OF FISSION PRODUCTS

HEATED AIR

Internal energy of air—see Figure 3-1.

11 Radiation opacity and mean-free path

$$K = \lambda^{-1} \quad cm^{-1}$$

Planck mean-free path—see Figure 3-2.

$$K_p = \frac{1}{\lambda_p} \equiv \frac{\int_o^\infty d\nu\, \kappa_\nu\, B_\nu}{\int_o^\infty d\nu\, B_\nu} = \frac{\pi}{\sigma T^4} \int_o^\infty \kappa_\nu\, B_\nu\, d\nu \quad cm^{-1} \quad .$$

Rosseland mean-free path—see Figure 3-3.

$$\lambda_R \equiv \frac{1}{K_R} \equiv \frac{\int_o^\infty d\nu \frac{1}{\kappa_\nu} \frac{dB_\nu}{dT}}{\int_o^\infty d\nu \frac{dB_\nu}{dT}} \quad cm \quad .$$

Air opacity to 3.125 eV radiation—see Figure 3-4.

Air opacity versus photon energy—see Figure 3-5.

Ionization produced by energy deposition—see Figure 3-6.

FIREBALL FORMATION

Altitude-yield map showing different fireball phenomenology regions—see Figure 3-7.

Point explosion in uniform atmosphere-spherical shock:

Characteristic radius

$$r_o = 3.5 \times 10^7 \, (W_H/P_a)^{1/3} \quad cm \quad .$$

Characteristic time

$$t_o = 3.5 \times 10^7 \rho_a^{1/2} W_H^{1/3} p_a^{-5/6} \text{ sec} .$$

For $\gamma = 1.4$:

P_s/P_a, t/t_o versus r_s/r_o—see Figure 3-8.

ρ/ρ_s—see Figure 3-9.

P/P_s—see Figure 3-10.

Integrated air density

$$M = \rho_s r_s I \text{ gms cm}^{-2}$$

$$I = \int_0^{r/r_s} (\rho/\rho_s)\, d(r/r_s)$$—see Figure 3-11.

Position of isotherms—see Figure 3-12.

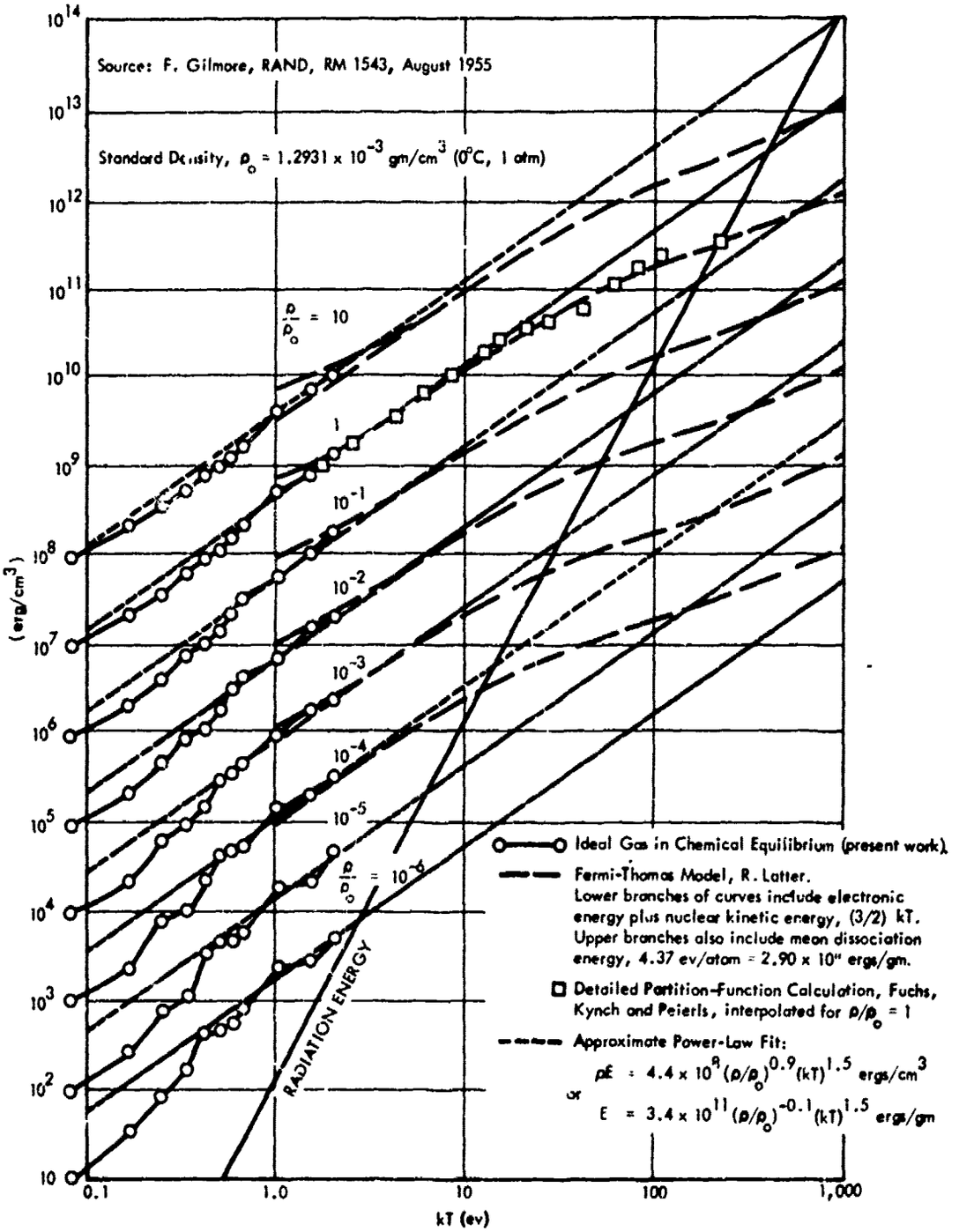

Figure 3-1. Internal energy of air.

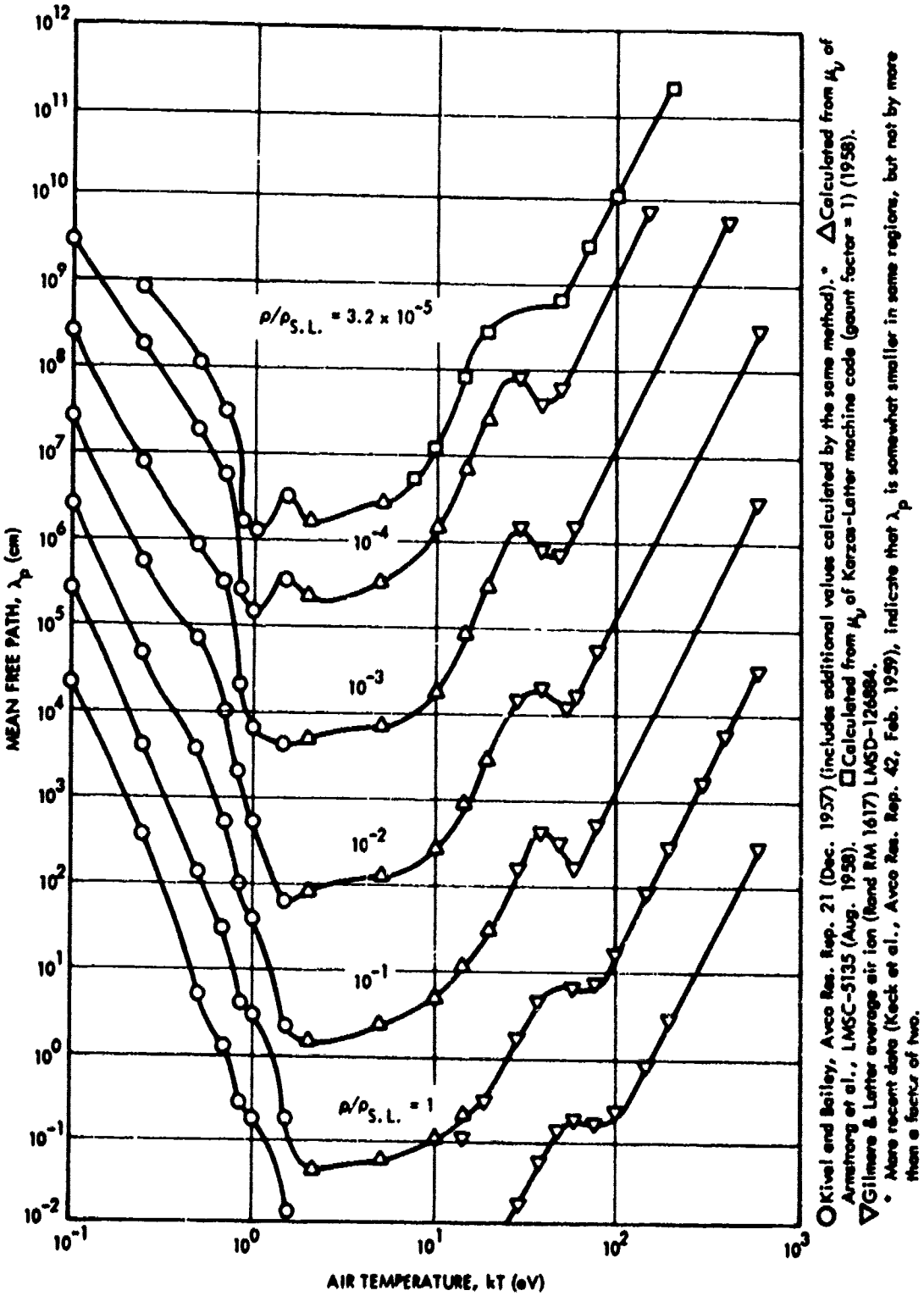

Figure 3-2. Planck mean free path (values shown assume chemical equilibrium, neglecting atomic lines).

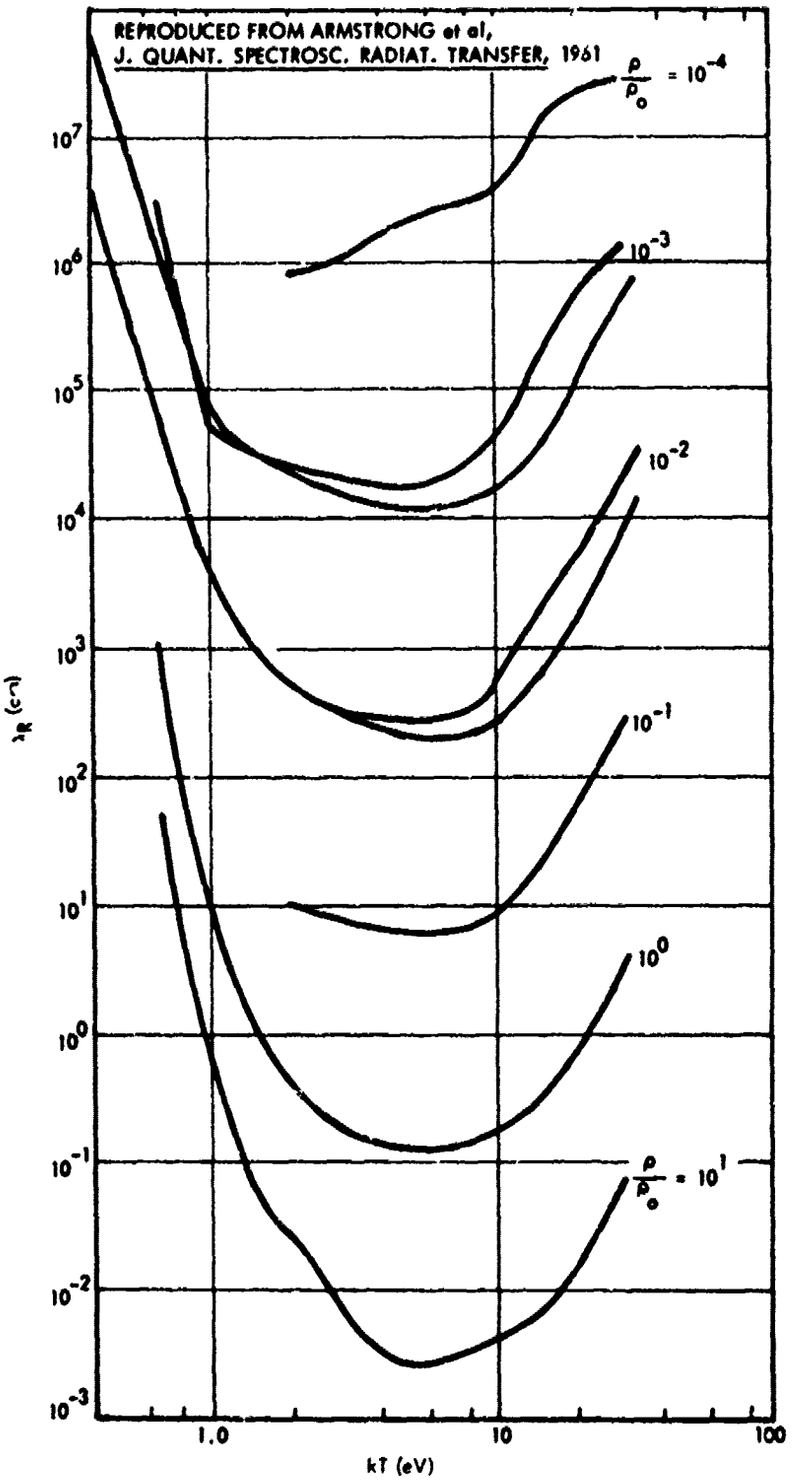

Figure 3-3. Rosseland mean free path λ_R in air.

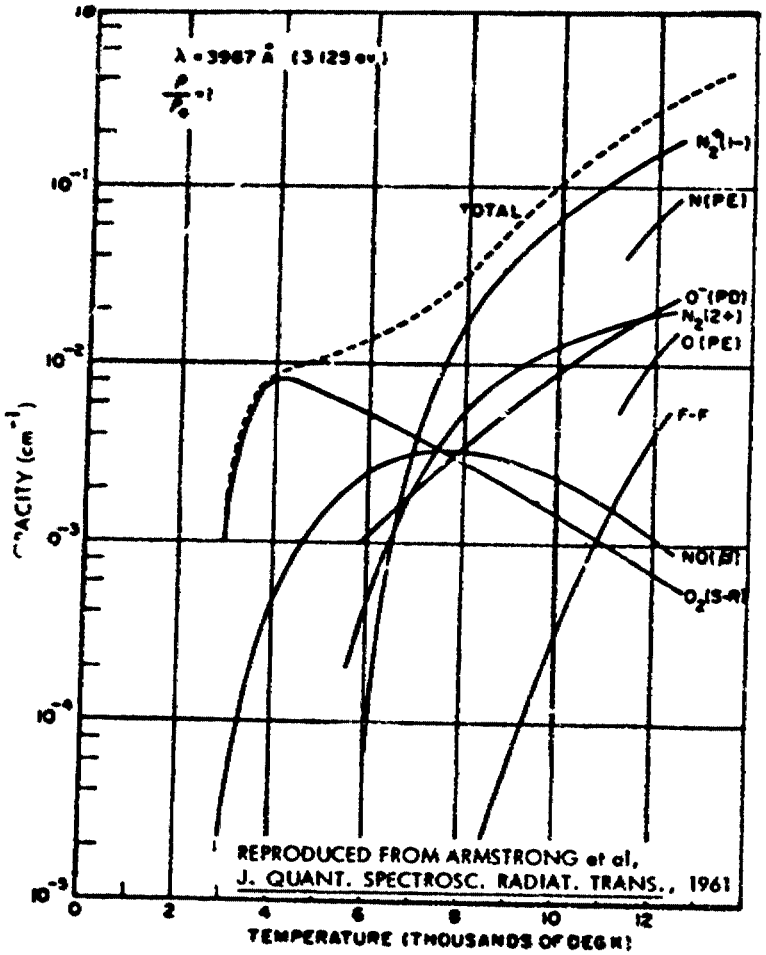

Figure 3-4A. Opacity for λ = 3967Å, ρ/ρ_o = 1.

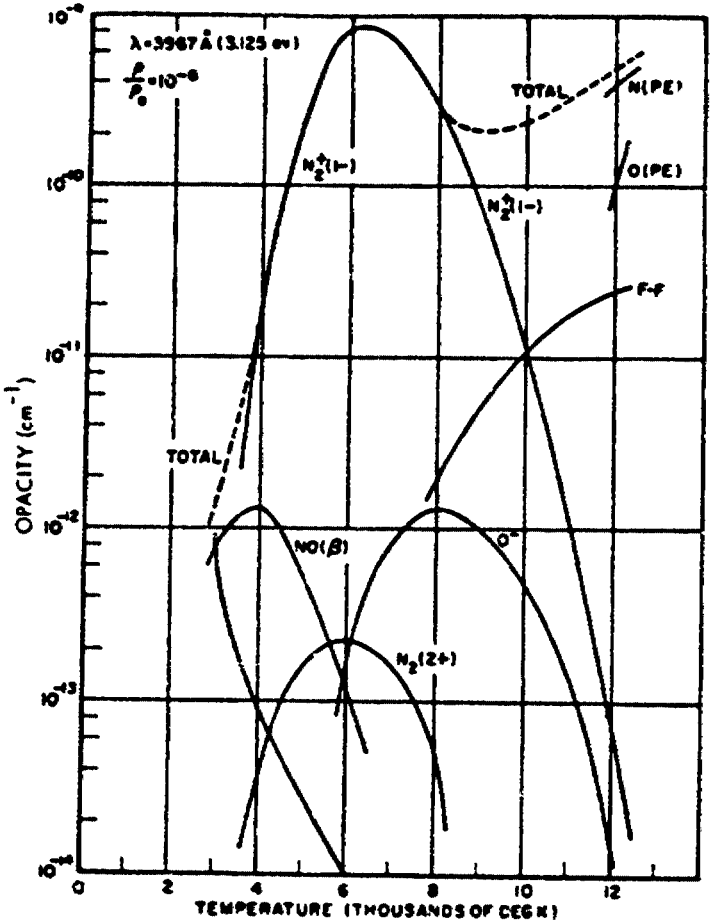

Figure 3-4B. Opacity for λ = 3967Å, $\rho/\rho_o = 10^{-6}$.

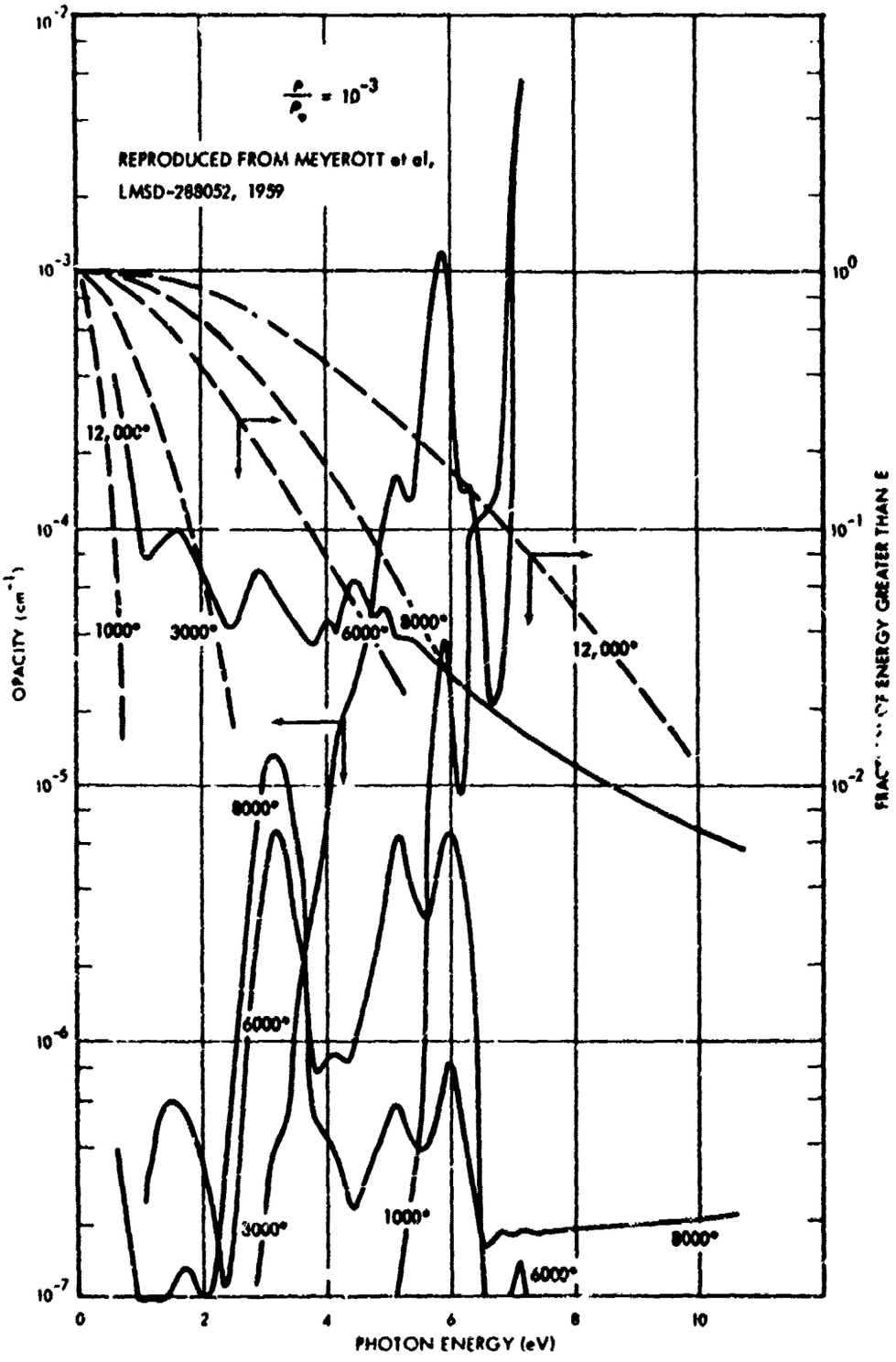

Figure 3-5. Heated air opacity.

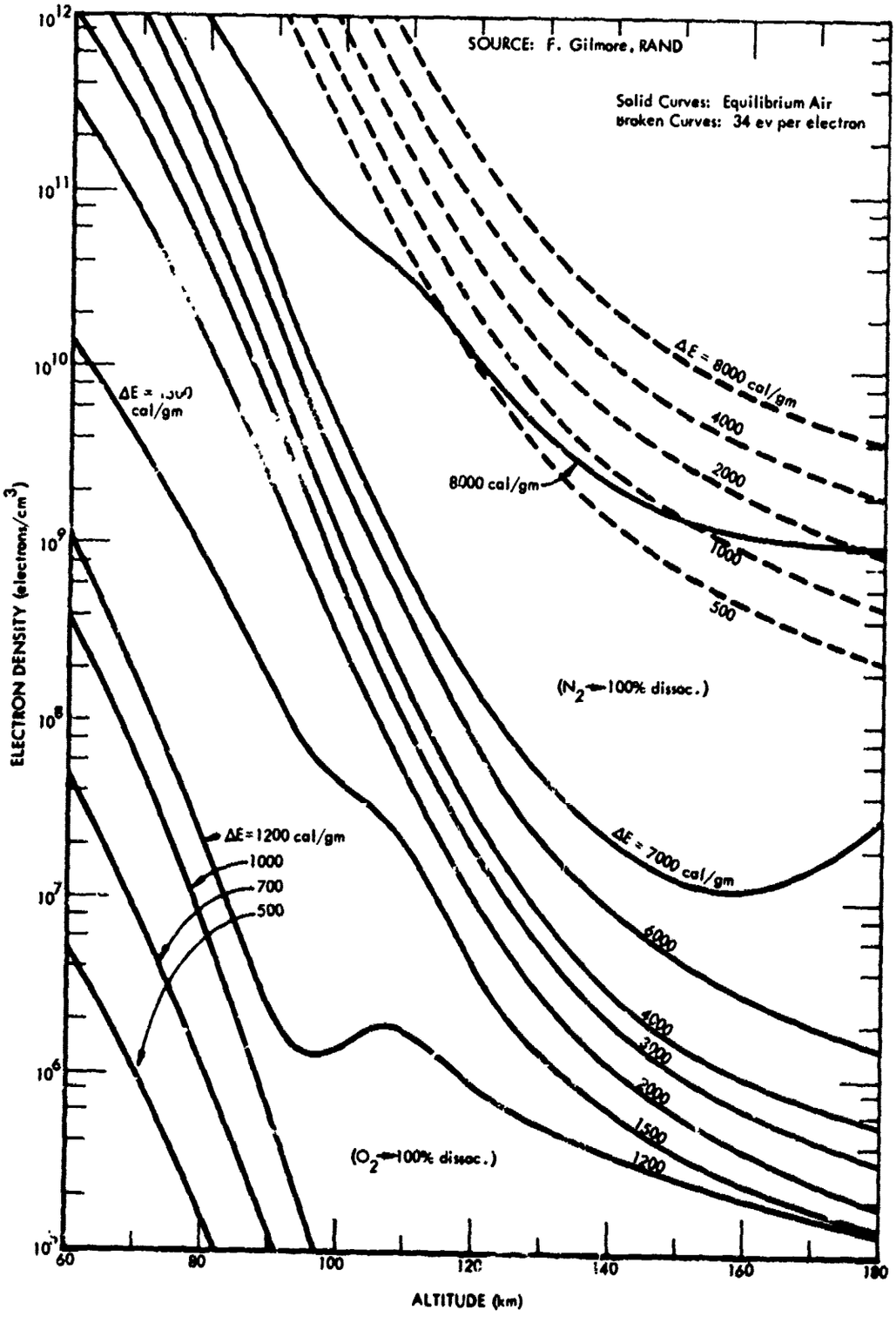

Figure 3-6. Ionization produced by energy deposition, based on U.S. Standard Atmosphere, 1962.

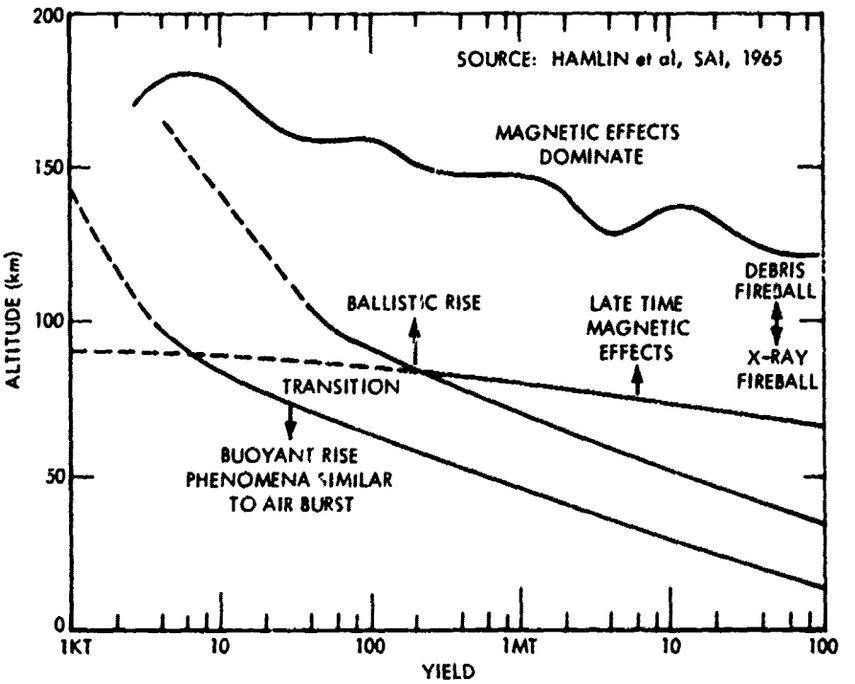

Figure 3-7. Altitude-yield map showing differing regions of phenomenology.

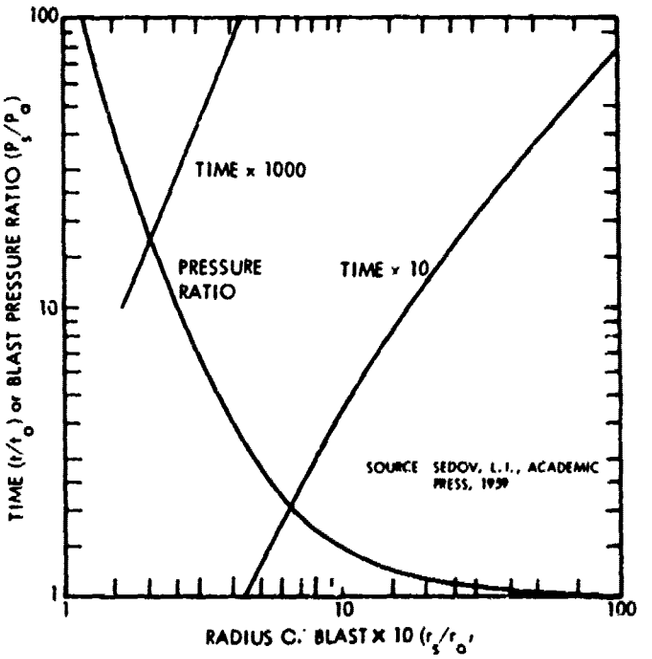

Figure 3-8. Similarity curves for the strength and position of a spherical blast wave.

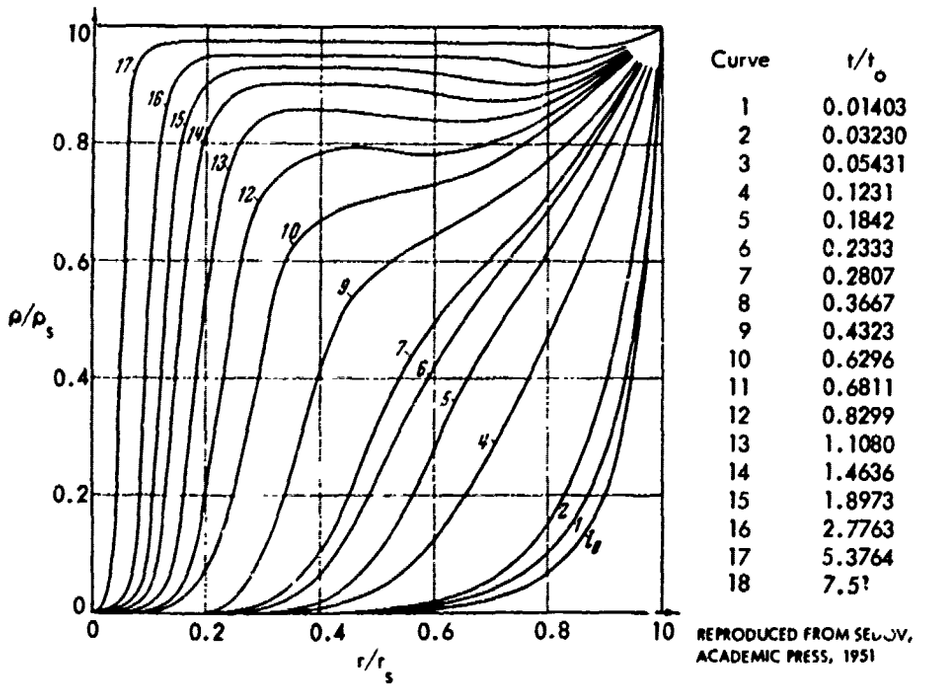

Figure 3-9. Density distribution in a point explosion.

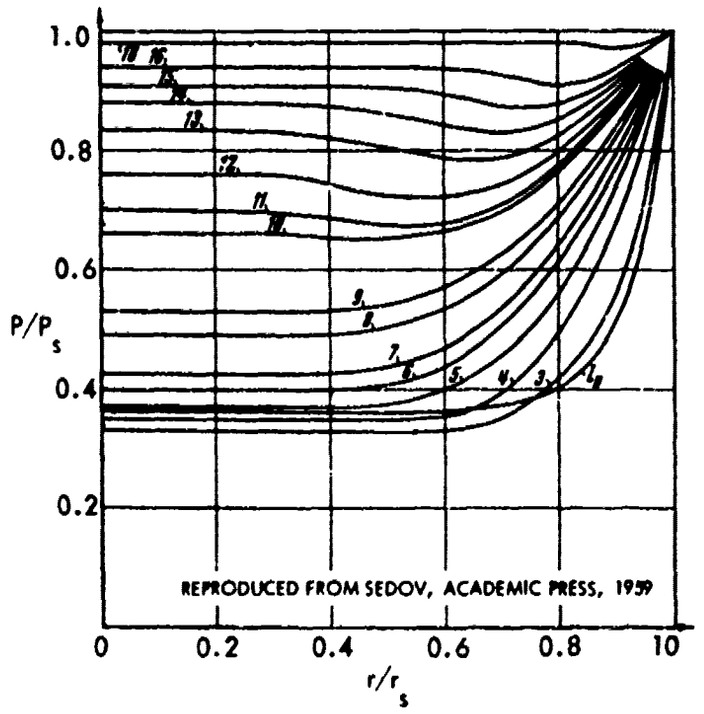

Figure 3-10. Pressure distribution in a point explosion.

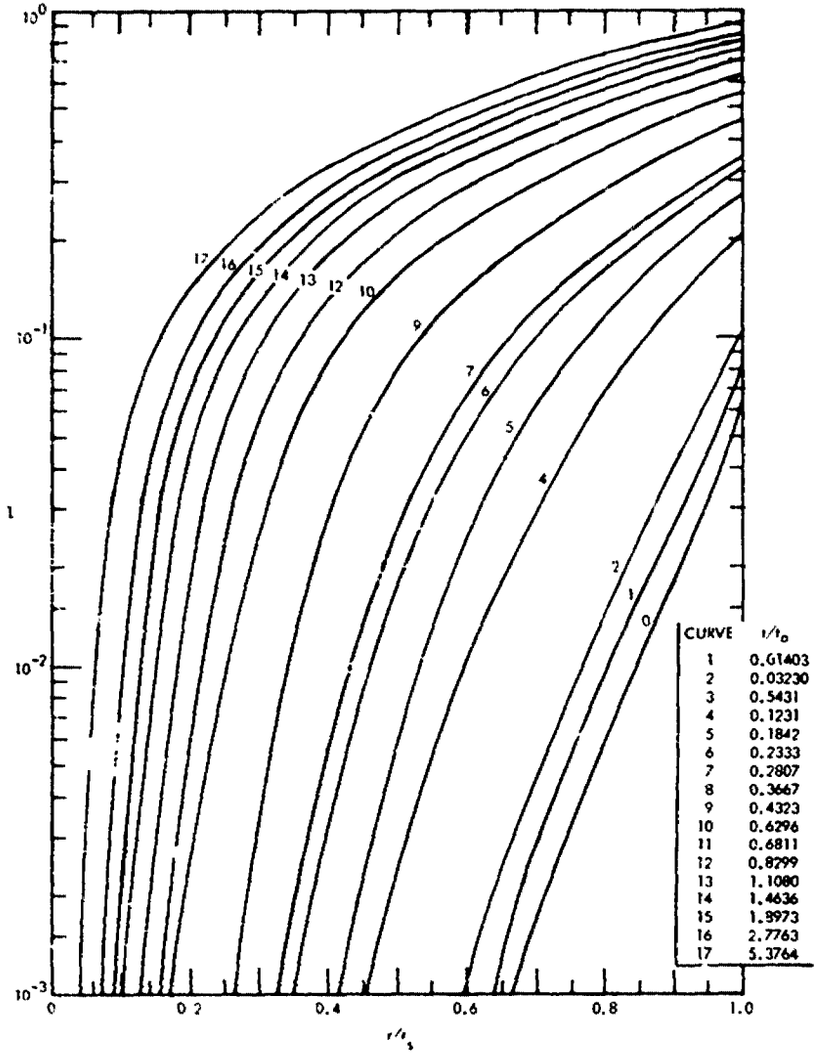

Figure 3-11. Integrated air density in a point explosion.

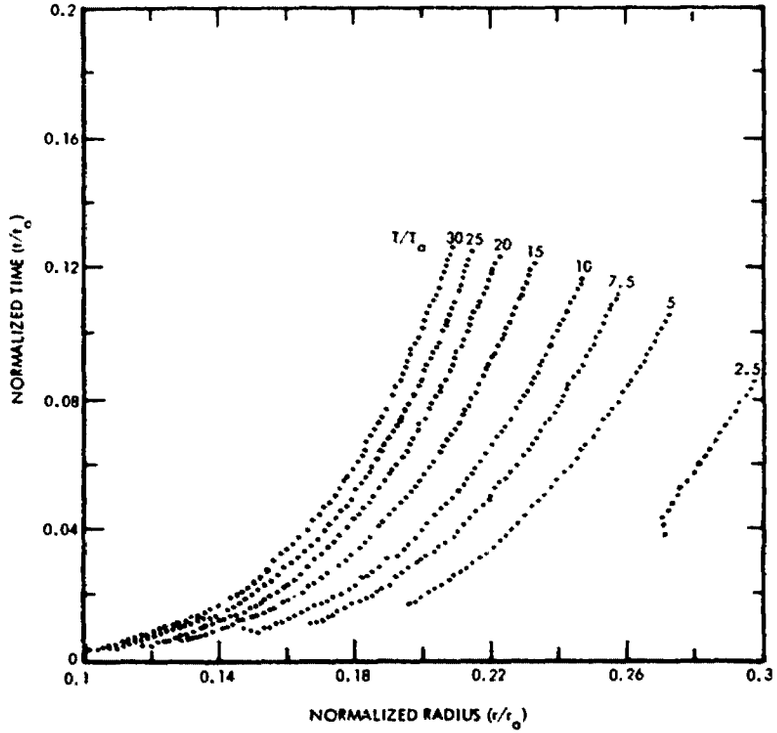

Figure 3-12. Motion of isotherms and fireball surfaces.

SECTION 4
DEIONIZATION

FIREBALL

Equilibrium thermal ionization of air—see Figure 4-1.

Equilibrium thermal ionization of metals:

For single metal atom species where formation of metal oxides can be neglected,

$$N_e = \frac{C}{2}\left(\sqrt{1 + \frac{4MN_o}{wVC}} - 1\right) \quad cm^{-3} \quad ,$$

$$C = \frac{2(2\pi mkT)^{3/2}}{h^3} \frac{B_i(T)}{B_o(T)} e^{-\chi/kT} \quad .$$

B_i, B_o = partition function for metal ions and atoms respectively

w = atomic weight of metal atom

M = weight of metal in region (gm)

V = volume of region (cm^3)

χ = ionization potential (eV).

For $N_a(B_i/B_o = 1/2, \chi = 5.14, w = 22.99)$—see Figure 4-2.

Nonequilibrium thermal ionization of air (electron loss by collisional radiation recombination and volume expansion:

$$N_e(t) \approx \frac{N_e(t_o)\frac{V(t_o)}{V(t)}}{1 + \alpha_r N_e(t_o)\left[\frac{V(t_o)}{V(t)}\right]^{1/3}(t - t_o)} \quad .$$

$N_e(t_o), V(t_o)$ = electron density and volume of region at time when nonequilibrium electron loss processes dominate.

Collisional radiative recombination—see Figure 4-3.

Equilibrium ionization from delayed radiation (beta particles):

$$N_e \approx \begin{cases} \sqrt{q/\alpha_d} & T > T_c \\ q/A & T << T_c \end{cases}$$

T_c depends on negative ion composition. For h > 20 km, $T_c \approx$ 1000°K. At lower altitudes T_c may be as high as 2500°K.

$$\alpha_d \approx \begin{cases} 3 \times 10^{-7} & T \leq 300°K \\ 9 \times 10^{-5}/T \quad , & T > 300°K \end{cases}$$

A—see Figure 4-4.

D-REGION (h < 100 km)

Species affecting air chemistry—see Table 4-1.

Important neutral species chemistry—see Figure 4-5.

Simplified schematic of positive ion evolution —see Figure 4-6.

Simplified schematic of negative ion evolution —see Figure 4-7.

Differential equations for three ion species model:

$$\frac{dN_e}{dt} = q - \alpha_d N_e N_+ - AN_e + DN_-$$

$$\frac{dN_-}{dt} = -\alpha_i N_- N_+ + AN_e - DN_-$$

$$\frac{dN_+}{dt} = q - \alpha_i N_- N_+ - \alpha_d N_e N_+$$

$$N_+ = N_e + N_- \quad .$$

Other Commonly Used Symbols

q	P	P
A	A	β
D	C	σ
α_d	B	α
α_i	E	γ

Reaction rate coefficients for equilibrium conditions (effects of prompt and thermal radiation neglected):

α_d—see Figure 4-8.

α_i—see Figure 4-9.

D—see Figure 4-10.

A—see Figure 4-4.

Solution of deionization equations for $\alpha_d=\alpha_i=\alpha$ and α, A, and D independent of ionization conditions:

$$N_+(t) = \sqrt{\frac{q}{\alpha}}\ \frac{1 + C\, e^{-2\sqrt{q\alpha}t}}{1 - C\, e^{-2\sqrt{q\alpha}t}} \xrightarrow[q \to 0]{} \frac{N_+(0)}{1 + \alpha N_+(0)t}$$

$$N_e(t) = \left(1 - C\, e^{-2\sqrt{q\alpha}t}\right)^{-1}\left\{\left(1 - C\, N_e(0)\ e^{-(A+D+\sqrt{q\alpha})t}\right)\right.$$

$$+ \frac{q + D\sqrt{\frac{q}{\alpha}}}{A + D + \sqrt{q\alpha}}\left[1 - e^{-(A+D+\sqrt{q\alpha})t}\right]$$

$$\left. - C\,\frac{q - D\sqrt{\frac{q}{\alpha}}}{A + D - \sqrt{q\alpha}}\left[e^{-2\sqrt{q\alpha}t} - e^{-(A+D+\sqrt{q\alpha})t}\right]\right\} ,$$

$$\xrightarrow[q \to 0]{} \frac{N_e(0)\ e^{-(A+D)t}}{1 + \alpha N_+(0)t} + \frac{N_+(0)D}{A + D}\left[\frac{1 - e^{-(A+D)t}}{1 + \alpha N_+(0)t}\right]$$

$$C = \frac{N_+(0) - \sqrt{\frac{q}{\alpha}}}{N_+(0) + \sqrt{\frac{q}{\alpha}}} .$$

Solution of deionization equations for $\alpha_d \neq \alpha_i$ and α_d, α_i, A, and D independent of ionization conditions:

$$N_+(h,t) = \frac{N_o}{1 + \alpha N_o t}$$

$$N_e(h,t) \approx \frac{A}{D + A}\ \frac{N_o\, e^{-(A+D)t}}{(1 + \alpha N_o t)^{\frac{\alpha_d}{\alpha}}} + \frac{D}{D + A}\ \frac{N_o}{1 + \alpha N_o t}$$

$$N_e(h,0) = N_+(h,0) = N_o$$

$$\alpha \approx \alpha_d\, e^{-(A+D)t} + \frac{A\alpha_i + D\alpha_d}{A + D}\left(1 - e^{-(A+D)t}\right) .$$

If $\alpha(t)\, N_o t \gg 1$ and $(A + D)t \leq \alpha_d/\alpha$, then the above approximation may underestimate N_e. The approximation can be improved by interpolation.

Equilibrium solution,

$$N_+(h,t) = \sqrt{\frac{q}{\alpha}}$$

$$\alpha \approx \frac{A\alpha_i + D\alpha_d + \alpha_i\alpha_d\sqrt{\frac{q(A+D)}{A\alpha_i + D\alpha_d}}}{A + D + \alpha_i\sqrt{\frac{q(A+D)}{A\alpha_i + D\alpha_d}}} \quad .$$

Graphical solution for α—see Figure 4-11.

$$N_e(h,t) = \frac{q + D\sqrt{\frac{q}{\alpha}}}{A + D + \alpha_d\sqrt{\frac{q}{\alpha}}}$$

$$N_e \approx \begin{cases} \sqrt{\frac{q}{\alpha_d}} & \sqrt{\frac{q}{\alpha_d}} \gg \frac{A+D}{\alpha_i} \\ & \text{or } D \gg A \\ \frac{q}{A} & \sqrt{q\alpha_i} \gg D \\ & \text{and } A \gg D + \alpha_d\sqrt{\frac{q}{\alpha_i}} \\ \frac{D}{D+A}\sqrt{\frac{q}{\alpha}} & D \gg \sqrt{q\alpha} \quad , \\ & \alpha = \frac{A\alpha_i + D\alpha_d}{A + D} \quad . \end{cases}$$

Graphical representation of the above electron density regions—see Figures 4-12 and 4-13.

For small initial ionization, the electron and ion densities build up to equilibrium values with a time constant of the order of

$$\tau \approx \frac{1}{\sqrt{q\alpha}} \text{ sec} \quad .$$

The electron density will reach near-equilibrium conditions faster than indicated by the above time constant when attachment is the dominant electron loss process.

Solution of deionization for α_d, α_i, A, and D dependent on ionization conditions:

Transient solution—see Figures 4-14 through 4-17.

Equilibrium solution (effect of prompt and thermal radiation neglected)—see Figures 4-18 and 4-19.

Effect of changes in neutral species composition caused by prompt radiation on equilibrium reaction rate coefficients and ionization—see Figures 4-20 and 4-21.

Uncertainty: Deionization solutions involve assumptions concerning ambient neutral species, initial neutral and ion species produced by energy deposition, and values for ion and neutral species reaction rate coefficients. It is estimated that the electron and positive ion densities given are accurate to within a factor of two for moderate ionization levels.

13

Electron and ion densities caused by delayed radiation outside of the fireball (equilibrium ionization):

Delayed gamma rays—see Figure 4-22.

Beta particles—see Figure 4-23.

Compton electrons—use Figure 4-23 with N_c instead of N_β.

Uncertainty: Effect of prompt and thermal radiation on equilibrium electron and ion densities neglected. Predictions involve uncertainties in energy transport and deposition in addition to uncertainties in deionization. For gamma rays and beta particles electron and ion densities are believed accurate to within a factor of three for the stated conditions. Uncertainties in the Compton ionization may be larger due to approximations in energy deposition related to the use of the scaling parameter N_c.

E- AND F-REGION

Species affecting air chemistry—see Table 4-2.

Species and reactions considered in simplified numerical solution—see Table 4-3.

Differential equations:

$$\frac{d}{dt}[O^+] = q_1 - \beta_o[O^+] + k_5[O][N^+] - \alpha_r[O^+] \cdot \left([O^+] + [N^+] + [M^+]\right)$$

$$\frac{d}{dt}[N^+] = q_2 - \beta_n[N^+] - k_5[O][N^+] + \alpha_r[N^+] \cdot \left([O^+] + [N^+] + [M^+]\right)$$

$$\frac{d}{dt}[M^+] = q_3 + \beta_o[O^+] + \beta_n[N^+] - \alpha_d[M^+] \cdot \left([O^+] + [N^+] + [M^+]\right)$$

$$\beta_o = k_1[N_2] + k_2[O_2]$$

$$\beta_n = (k_3 + k_4)[O_2] + k_6[NO] \quad .$$

Reaction rate coefficients:

k_1—see Figure 4-24.

$$k_2 = 2 \times 10^{-11} \qquad cm^3\ sec^{-1}$$

$$k_3 = \frac{7}{16}\ (8 \times 10^{-10}) \qquad cm^3\ sec^{-1}$$

$$k_4 = \frac{9}{16}\ (8 \times 10^{-10}) \qquad cm^3\ sec^{-1}$$

$$k_5 = 1 \times 10^{-12} \qquad cm^3\ sec^{-1}$$

$$k_6 = 8 \times 10^{-10} \qquad cm^3\ sec^{-1}$$

$$\alpha_d \approx \begin{cases} 3 \times 10^{-7} & cm^3\ sec^{-1} \quad T_e \leq 300\ k \\ 9 \times 10^{-5}/T_e & cm^3\ sec^{-1} \quad T_e > 300\ K \end{cases}$$

Solution of deionization equations:

Transient solution—see Figure 4-25.

Equilibrium solution—see Figure 4-26.

Uncertainty: Solutions shown applicable for X-ray and beta-particle ionization. Deionization following ionization by UV radiation and heavy particle interaction affected by initial ion species produced. In regions of high energy deposition the production of metastable states and air motion can significantly affect deionization.

Table 4-1. Important species in air chemistry below 100 km.

Neutrals	Neutral Excited States	Negatives	Positives
CH_4	$N(^2D)$	CO_3^-	$H^+(H_2O)_{n=1-5}$
CO	$N_2(A^3\Sigma_u^+)$	$CO_3^-(H_2O)$	$H^+(H_2O)(HO)$
CO_2	$O(^1D)$	CO_4^-	$H^+(H_2O)(N_2)$
H	$O(^1S)$	$CO_4^-(H_2O)$	N^+
HNO_2	$O_2(a^1\Delta_g)$	NO_2^-	NO^+
HNO_3	$O_2(b^1\Sigma_g^+)$	$NO_2^-(H_2O)$	$NO^+(CO_2)$
HO		NO_3^-	$NO^+(H_2O)_{n=1-3}$
HO_2		$NO_3^-(H_2O)_{n=1-5}$	$NO^+(N_2)$
H_2		O^-	NO_2^+
H_2O		O_2^-	N_2^+
H_2O_2		$O_2^-(H_2O)$	O^+
N		O_3^-	O_2^+
NO		O_4^-	$O_2^+(H_2O)$
NO_2		$OONO^-$	O_4^+
NO_3		e	
N_2			
N_2O			
N_2O_5			
O			
O_2			
O_3			

Table 4-2. Some species of importance to E- and F-region multiple species computer codes.

Neutrals[a]	Neutral Excited States	Positive Ions	Positively Charged Excited States
N_2	$N(^2D)$	Me^+	$N^+(^1D)$
O	$N(^2P)$	MeO^+	$N^+(^1S)$
O_2	$N_2(A^3\Sigma_u^+)$	N^+	$O^+(^2D)$
N	$O(^1D)$	NO^+	$O^+(^2P)$
NO	$O(^1S)$	N_2^+	$O_2^+(a^4\pi_u)$
Me[b]	$O_2(a^1\Delta_g)$	O^+	
MeO[c]	$O_2(b^1\Sigma_g^+)$	O_2^+	

Notes:

[a]Minor species such as CO_2, A, etc, also may be included.

[b]Me denotes a metallic atom, viz, U, Fe, Al, Li, Na, or Si.

[c]MeO denotes a metallic oxide.

Table 4-3. Species and reactions considered in simplified numerical solutions.

Species Considered:

Neutrals N_2, O_2, NO, O, N, $N(^2D)$, $O(^1D)$

Ions O_2^+, NO^+, O^+, N^+

Reactions Considered:

Reaction	Coefficient
$NO^+ + e \rightarrow N + O$	α_d
$O_2^+ + e \rightarrow O + O$	α_d
$O^+ + e \rightarrow O + h\nu$	α_r
$N^+ + e \rightarrow N + h\nu$	α_r
$O^+ + N_2(v) \rightarrow NO^+ + N$	k_1
$O^+ + O_2 \rightarrow O + O_2^+$	k_2
$N^+ + O_2 \rightarrow O_2^+ + N$	k_3
$N^+ + O_2 \rightarrow NO^+ + O$	k_4
$N^+ + O \rightarrow N + O^+$	k_5
$N^+ + NO \rightarrow N + NO^+$	k_6
$O_2^+ + N \rightarrow NO^+ + O$	k_7
$N(^2D) + O_2 \rightarrow NO + O$	k_8
$O + N_2 \rightarrow NO + N$	k_9
$N + O_2 \rightarrow NO + O$	k_{10}

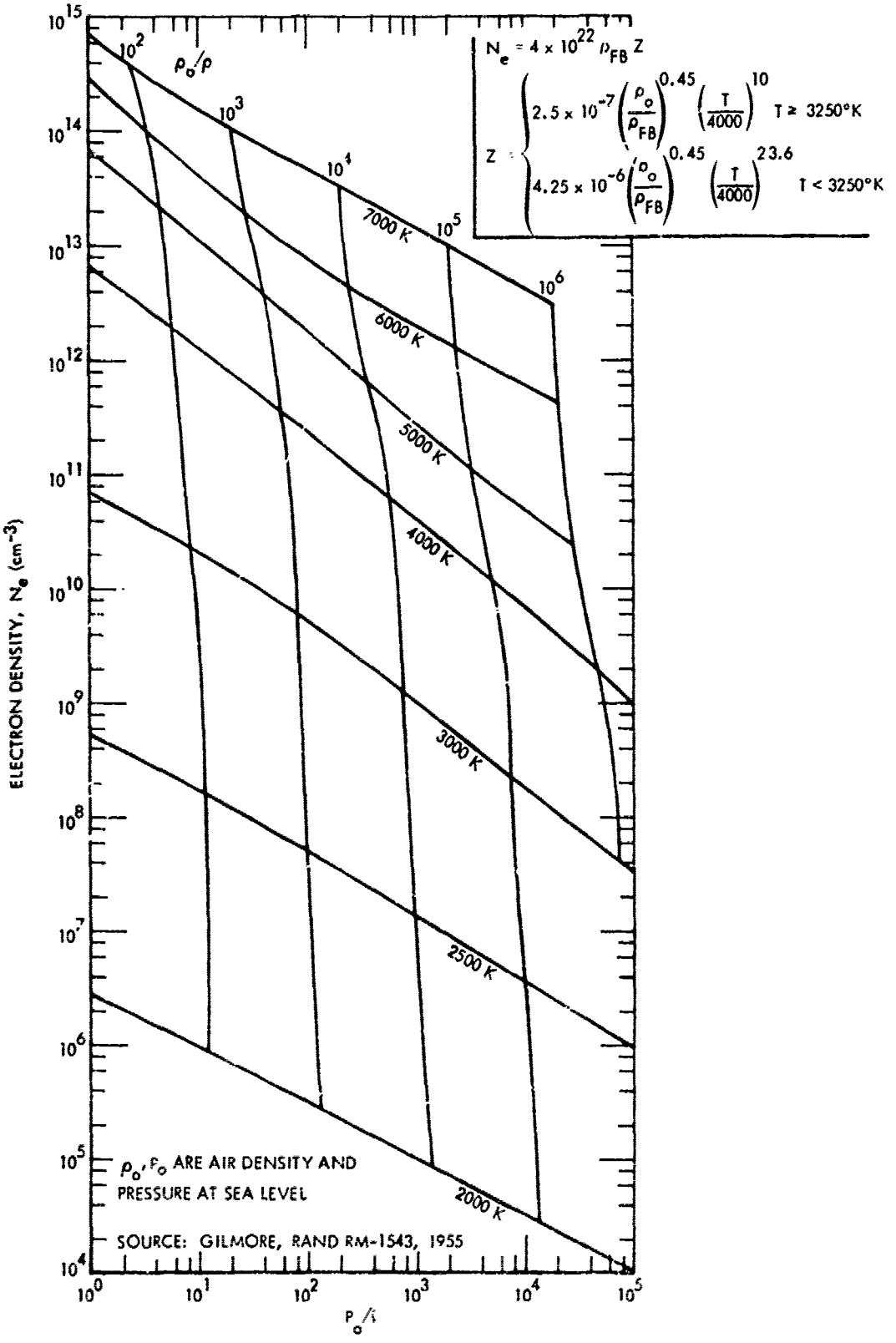

Figure 4-1. Electron density due to thermal ionization.

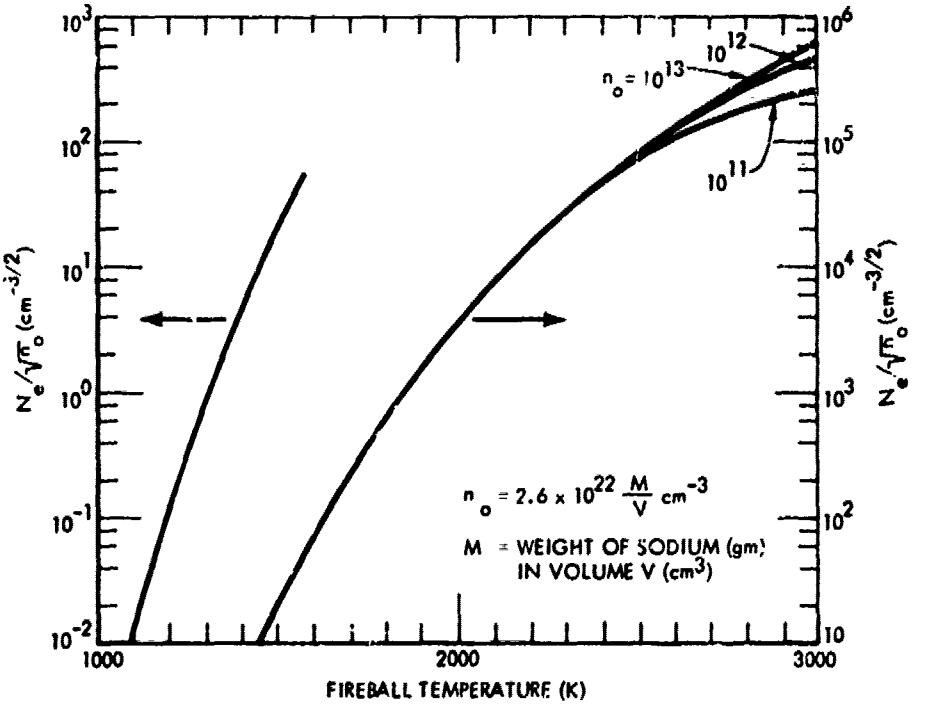

Figure 4-2. Equilibrium thermal ionization of sodium atoms.

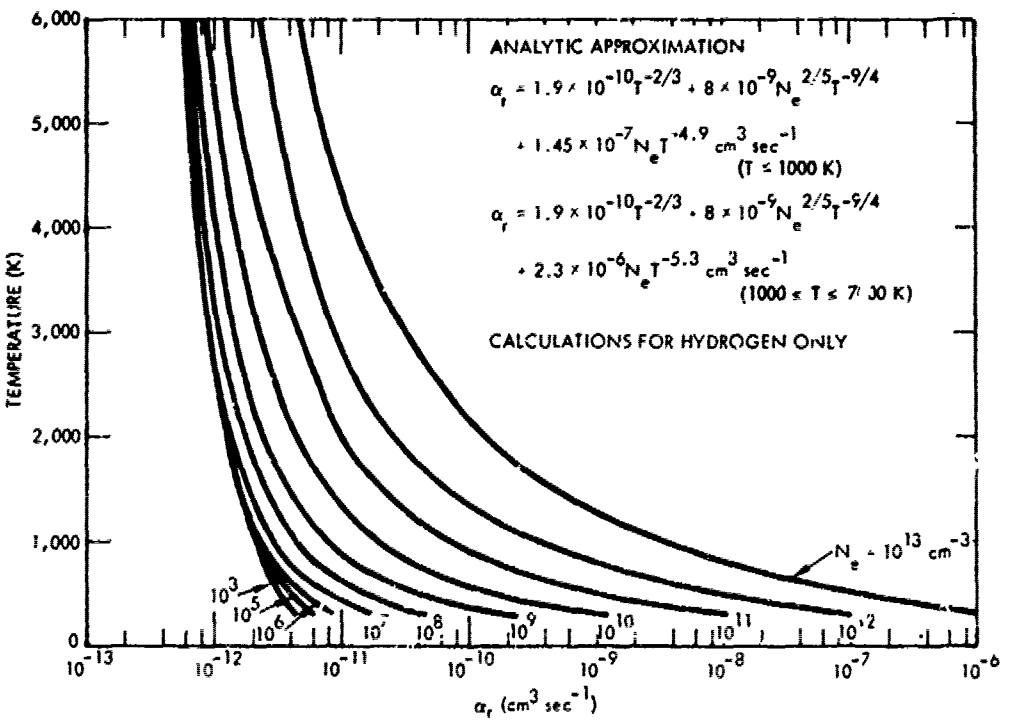

Figure 4-3. Collisional radiative recombination coefficient for H^+.

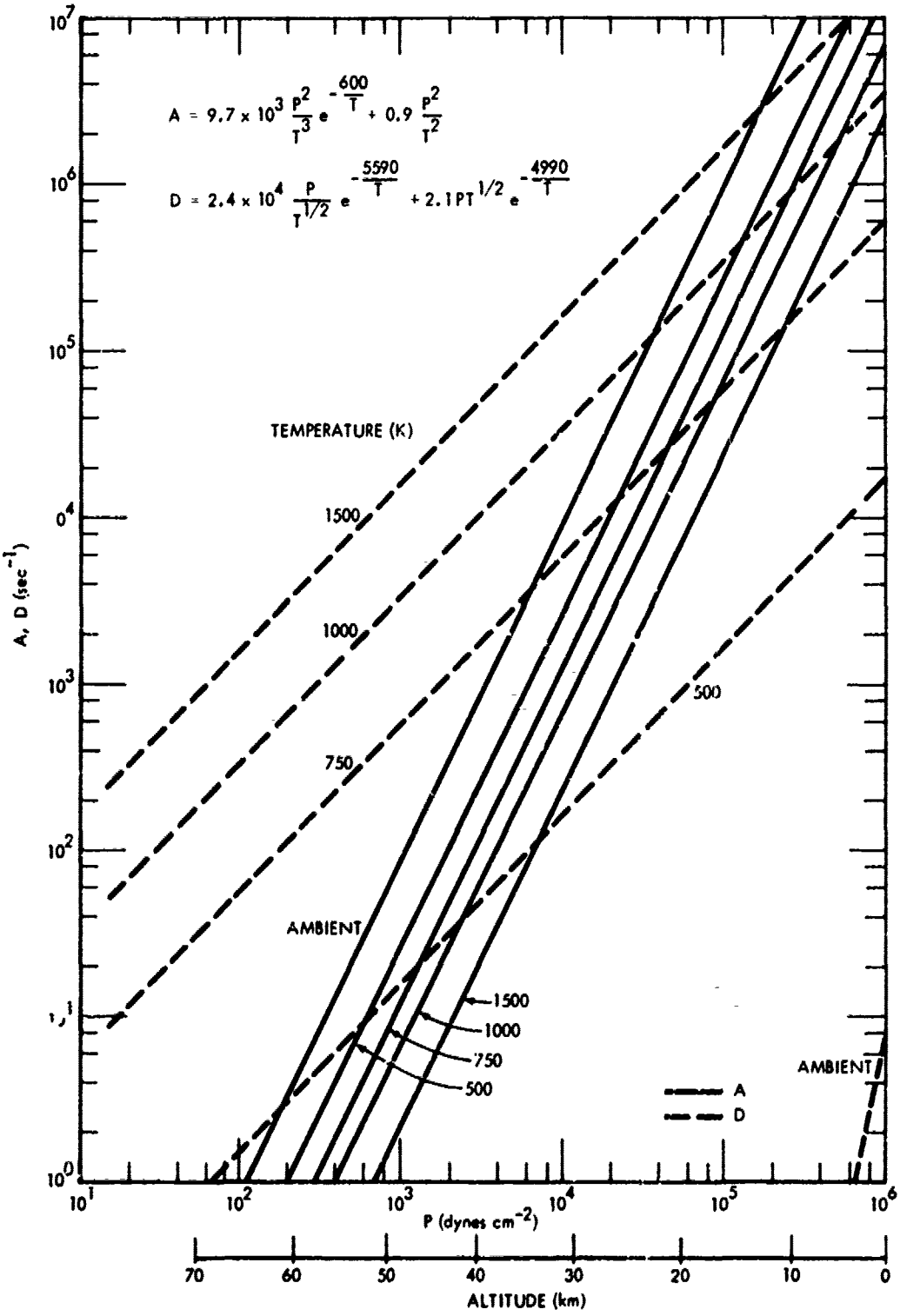

Figure 4-4. Three-body attachment to O_2 and collisional detachment from O_2^-, pressure equilibrium conditions.

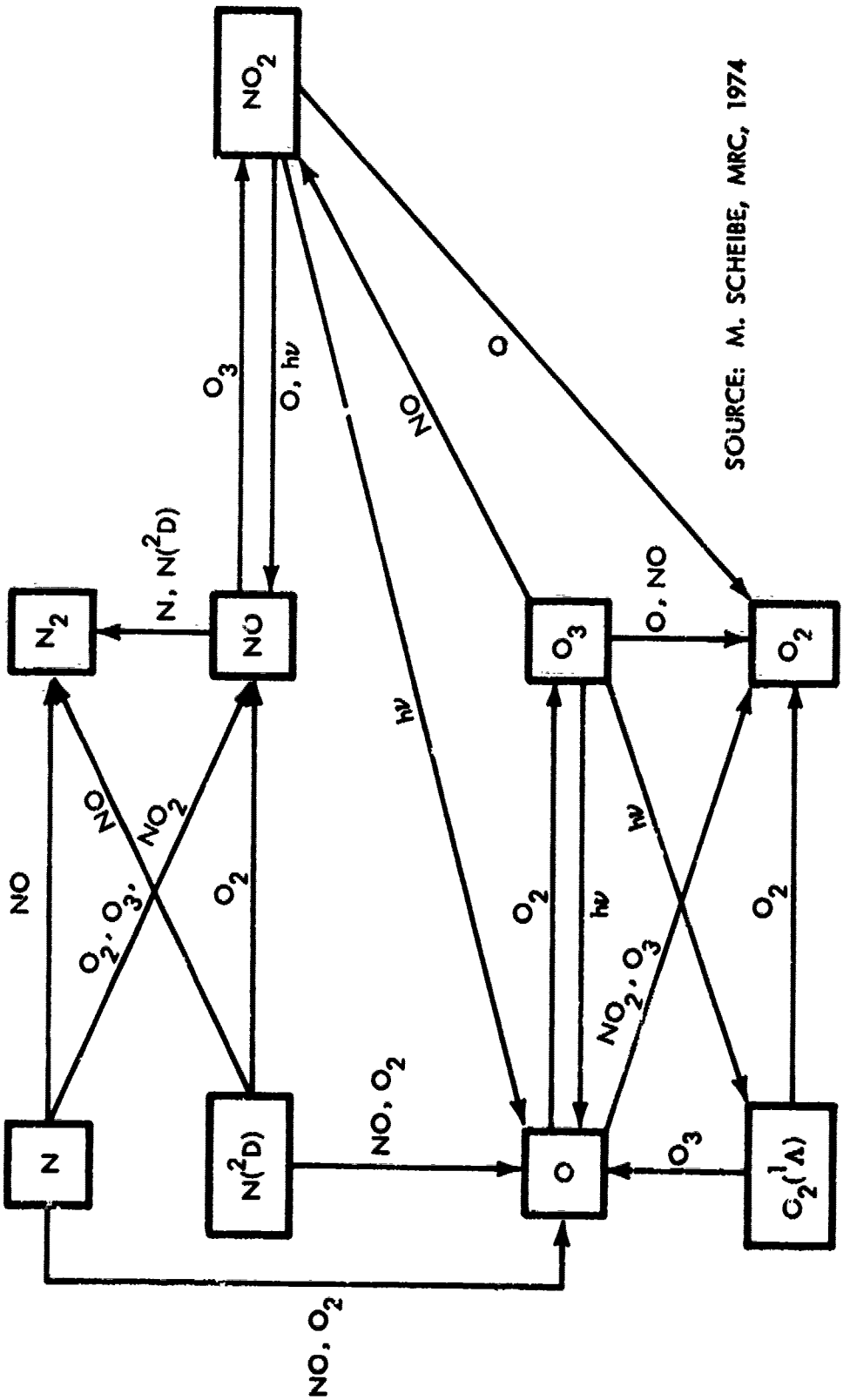

Figure 4-5. Important neutral chemistry.

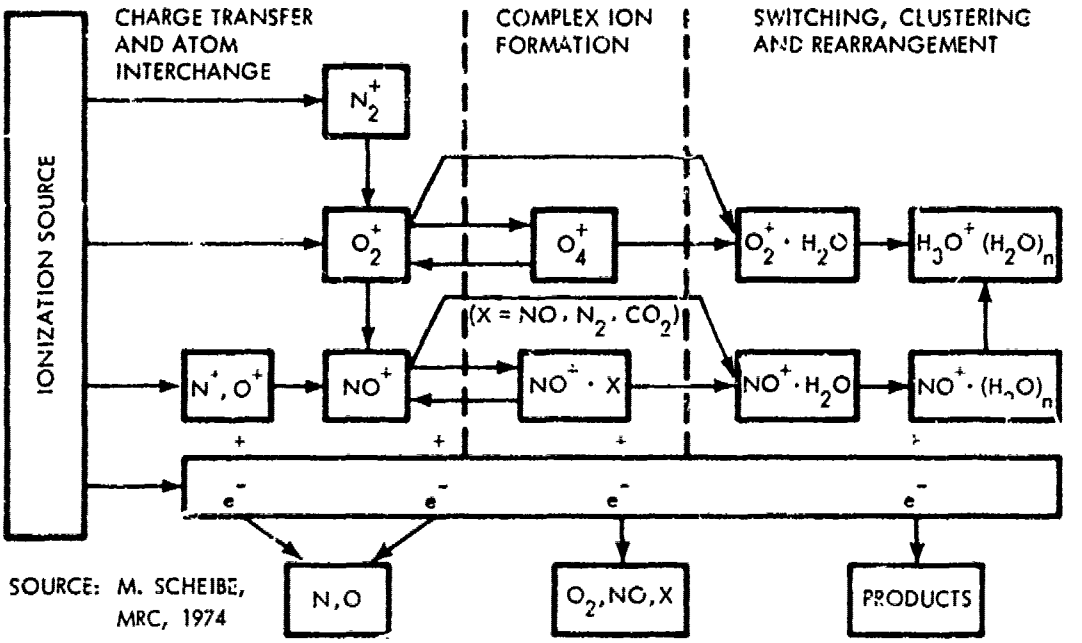

Figure 4-6. Simplified schematic of positive ion evolution.

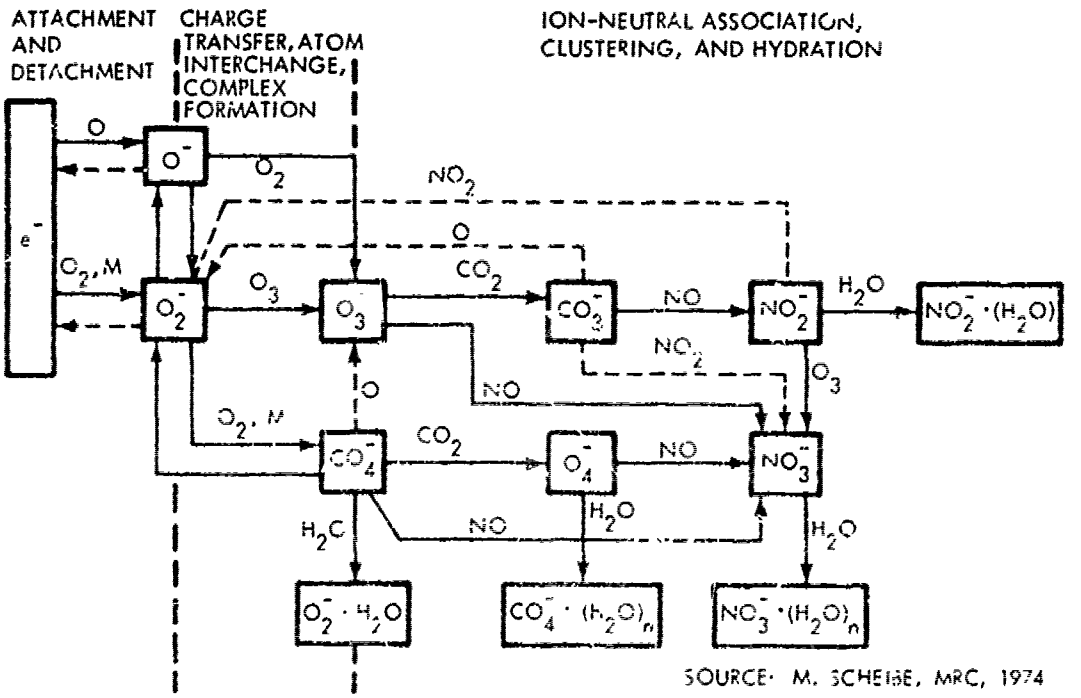

Figure 4-7. Attachment, detachment and negative ion reactions (dashed arrows indicate paths most affected by changes in photodetachment conditions).

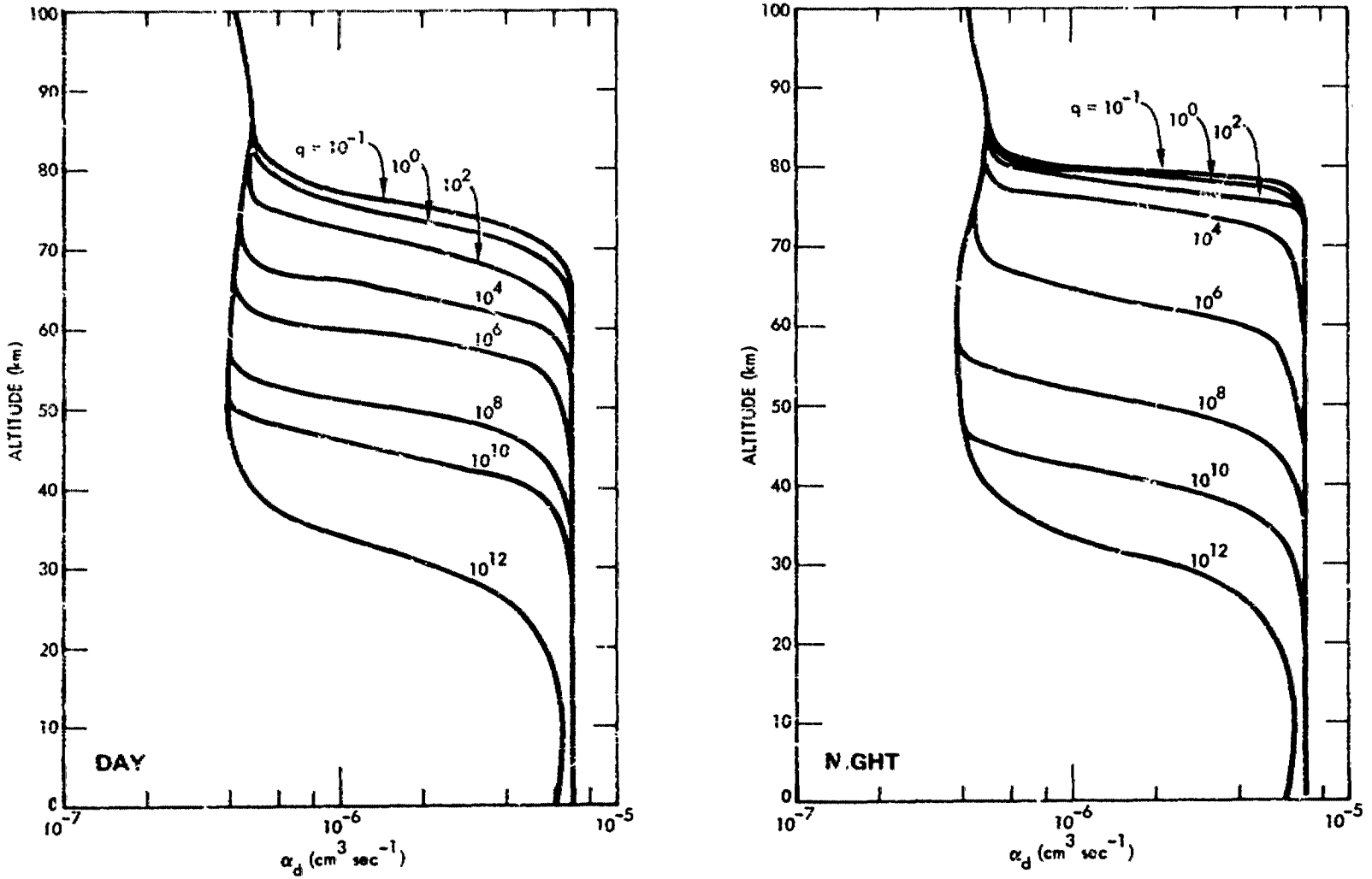

Figure 4-8. Effective values for dissociative recombination coefficient for equilibrium ionization conditions.

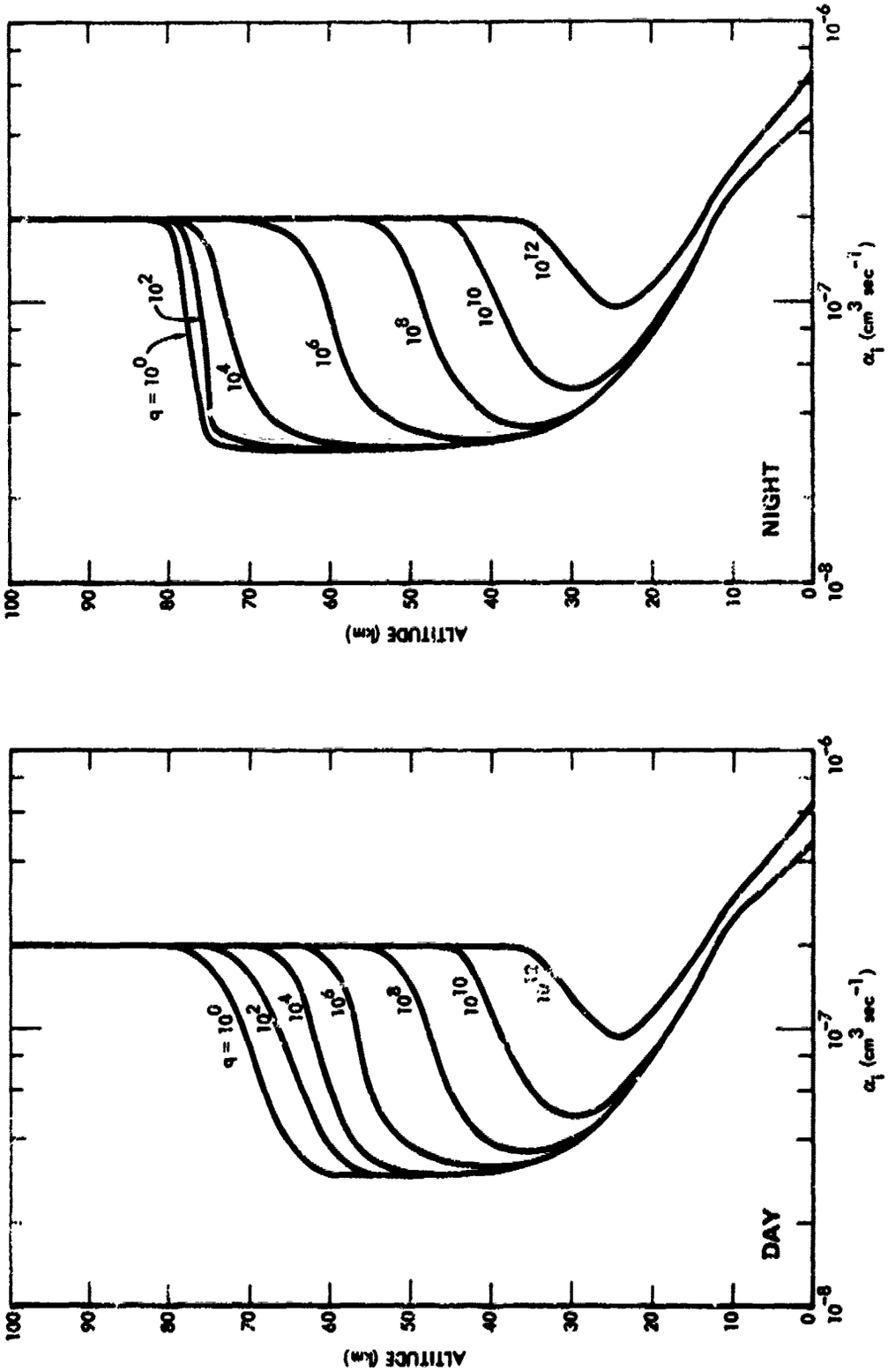

Figure 4-9. Effective values for ion-ion recombination coefficient for equilibrium conditions.

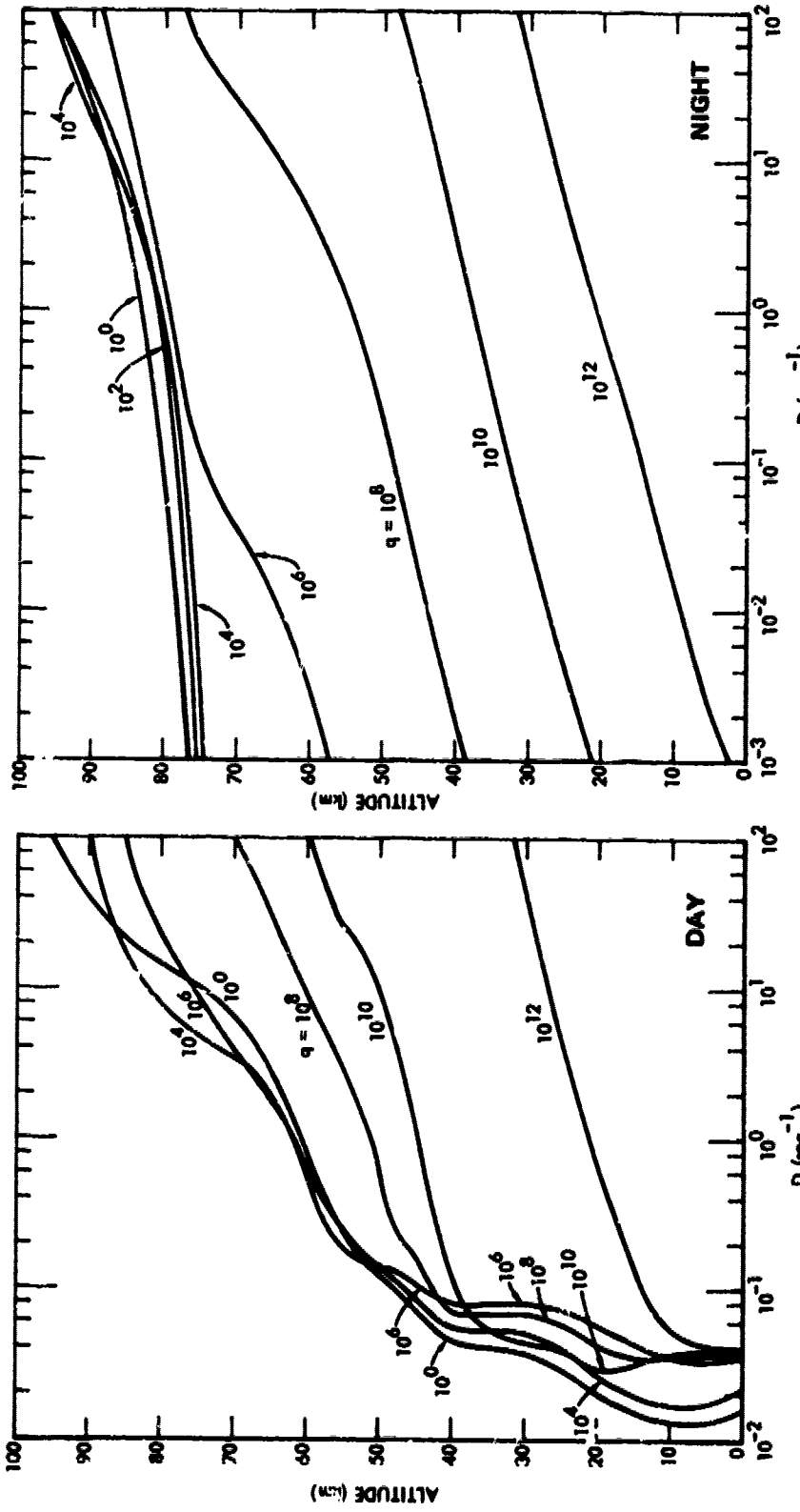

Figure 4-10. Effective values for detachment rate for equilibrium conditions.

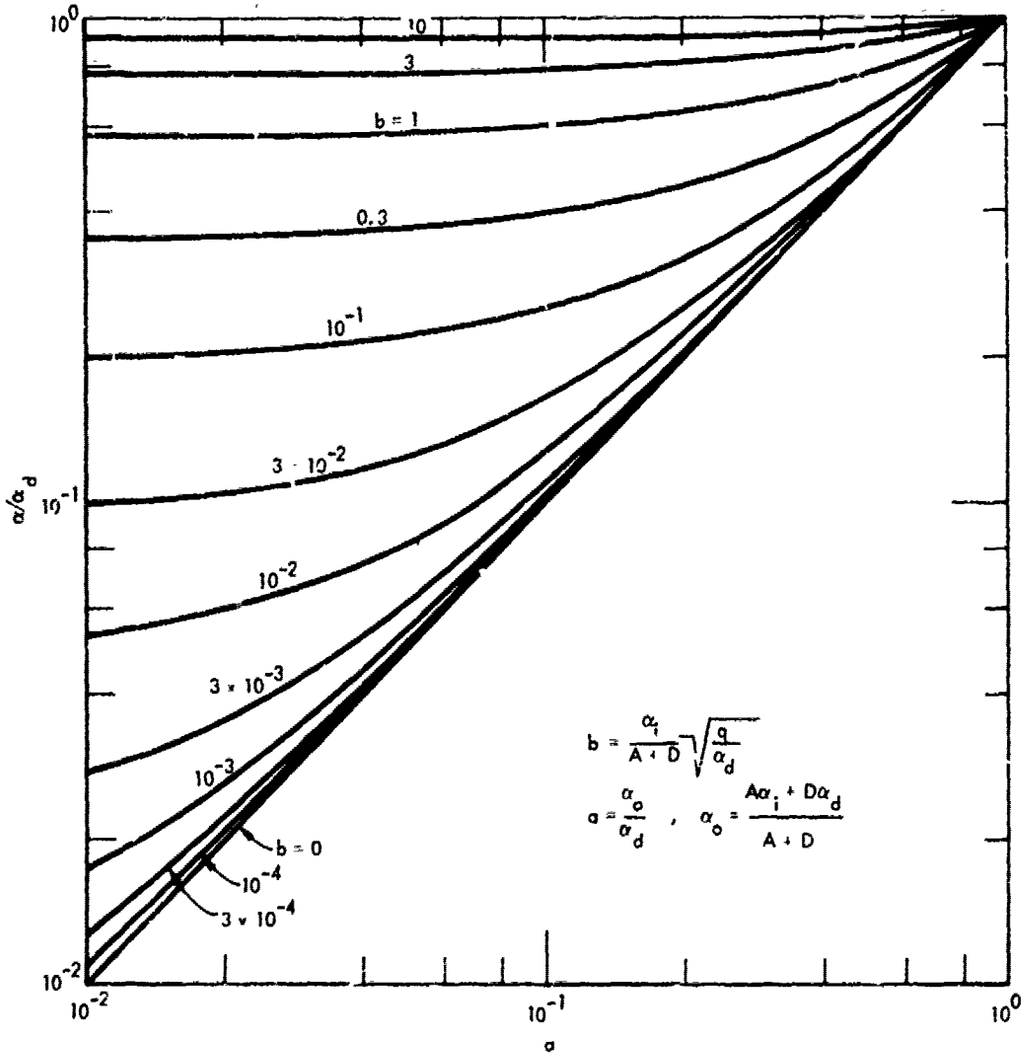

Figure 4-11. Graphical solution for effective recombination rate coefficient, equilibrium conditions.

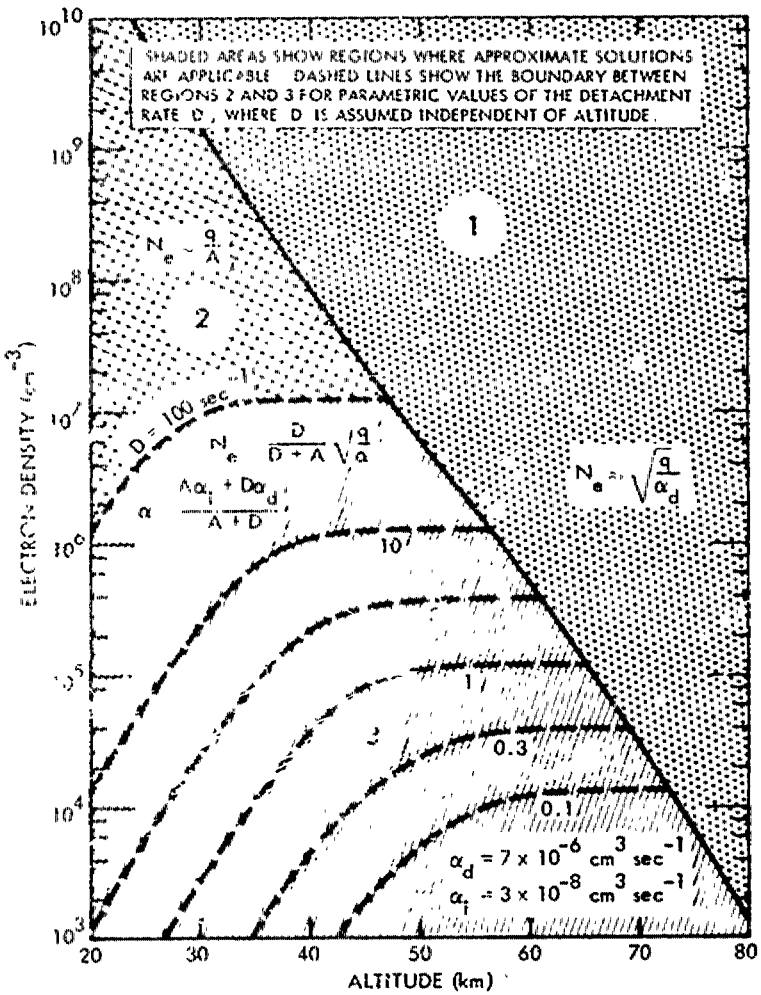

Figure 4-12. Approximate equilibrium electron density solutions, cluster ions.

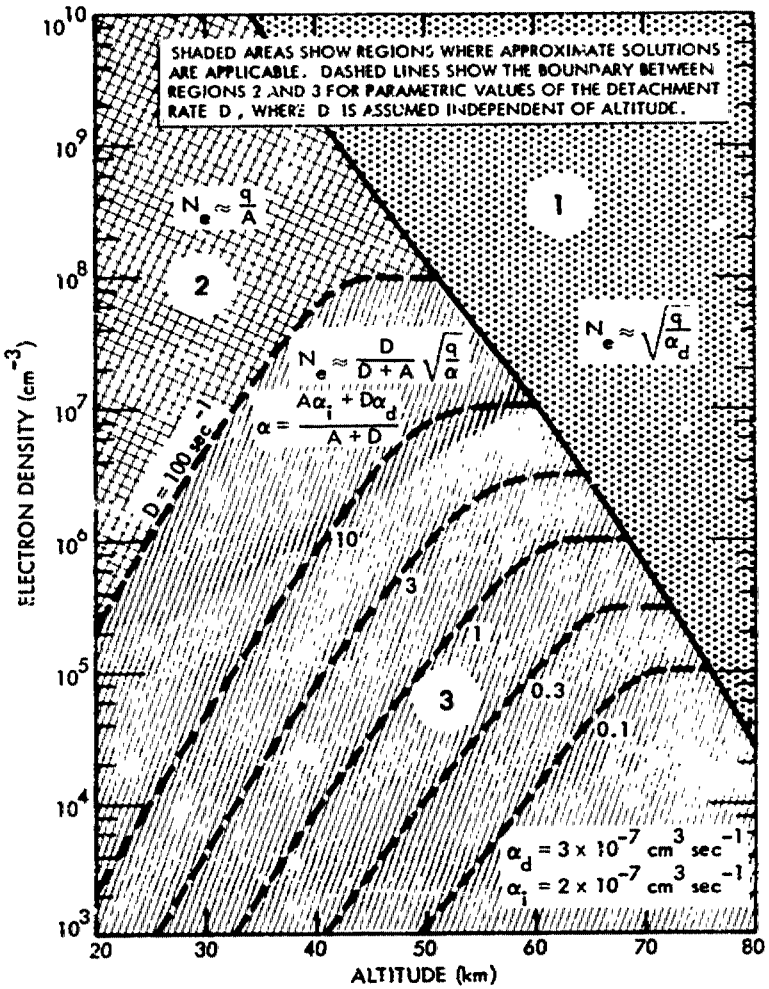

Figure 4-13. Approximate equilibrium electron density solutions, diatomic ions.

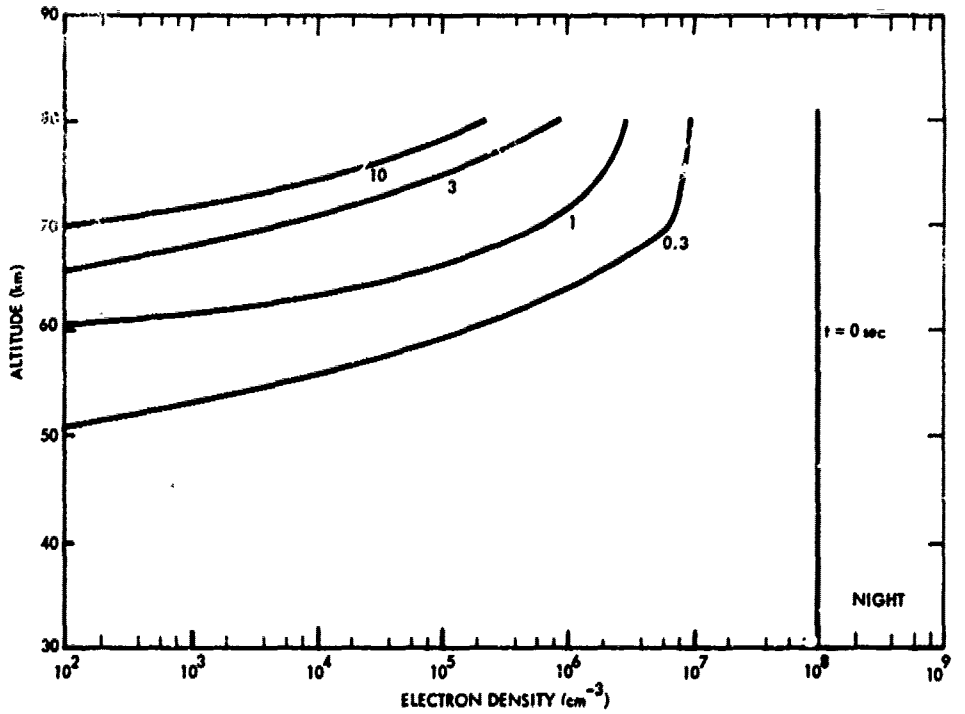

Figure 4-14. Decay of ionization impulse of 10^8 cm^{-3}, nighttime.

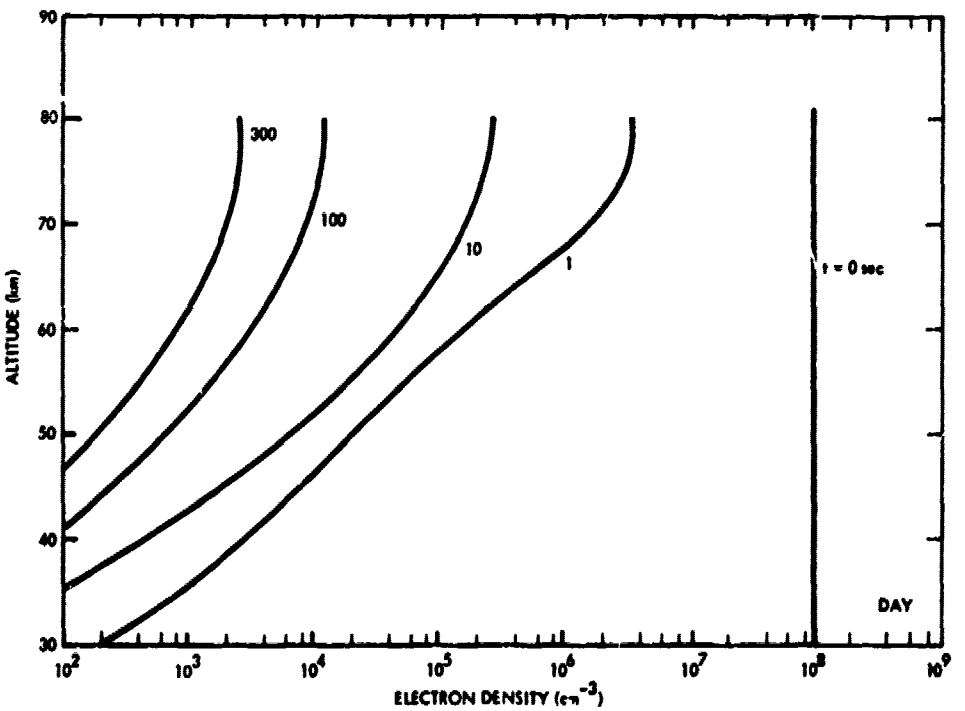

Figure 4-15. Decay of ionization impulse of 10^8 cm^{-3}, daytime.

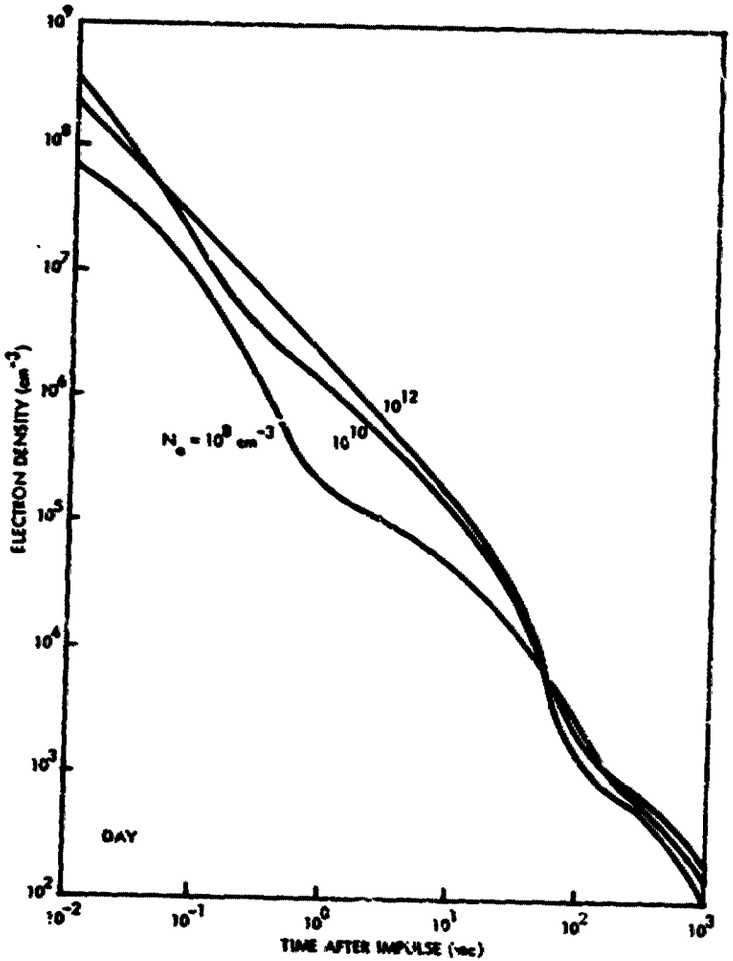

Figure 4-16. Decay of prompt ionization impulse at 60 km, daytime.

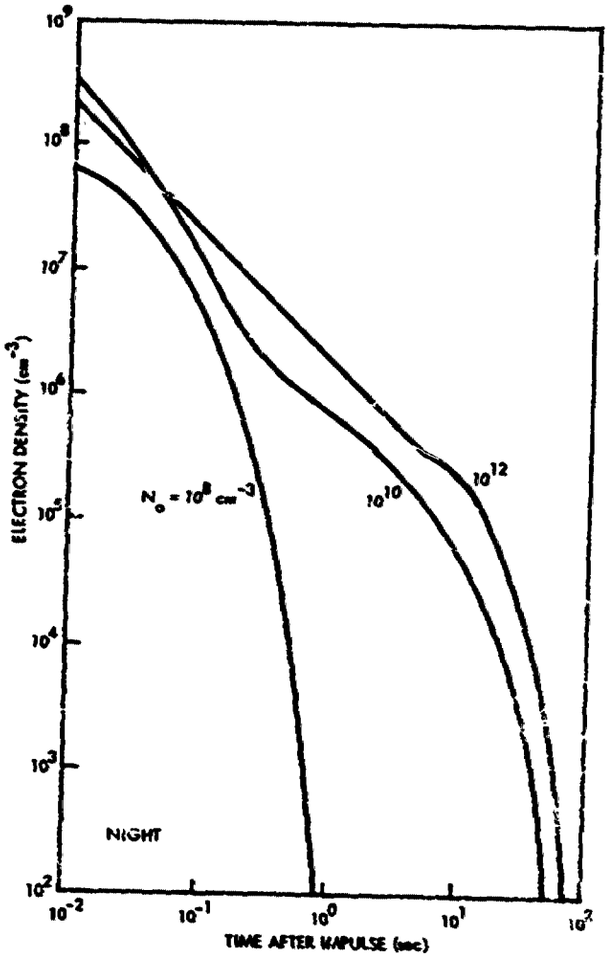

Figure 4-17. Decay of prompt ionization impulse at 60 km, nighttime.

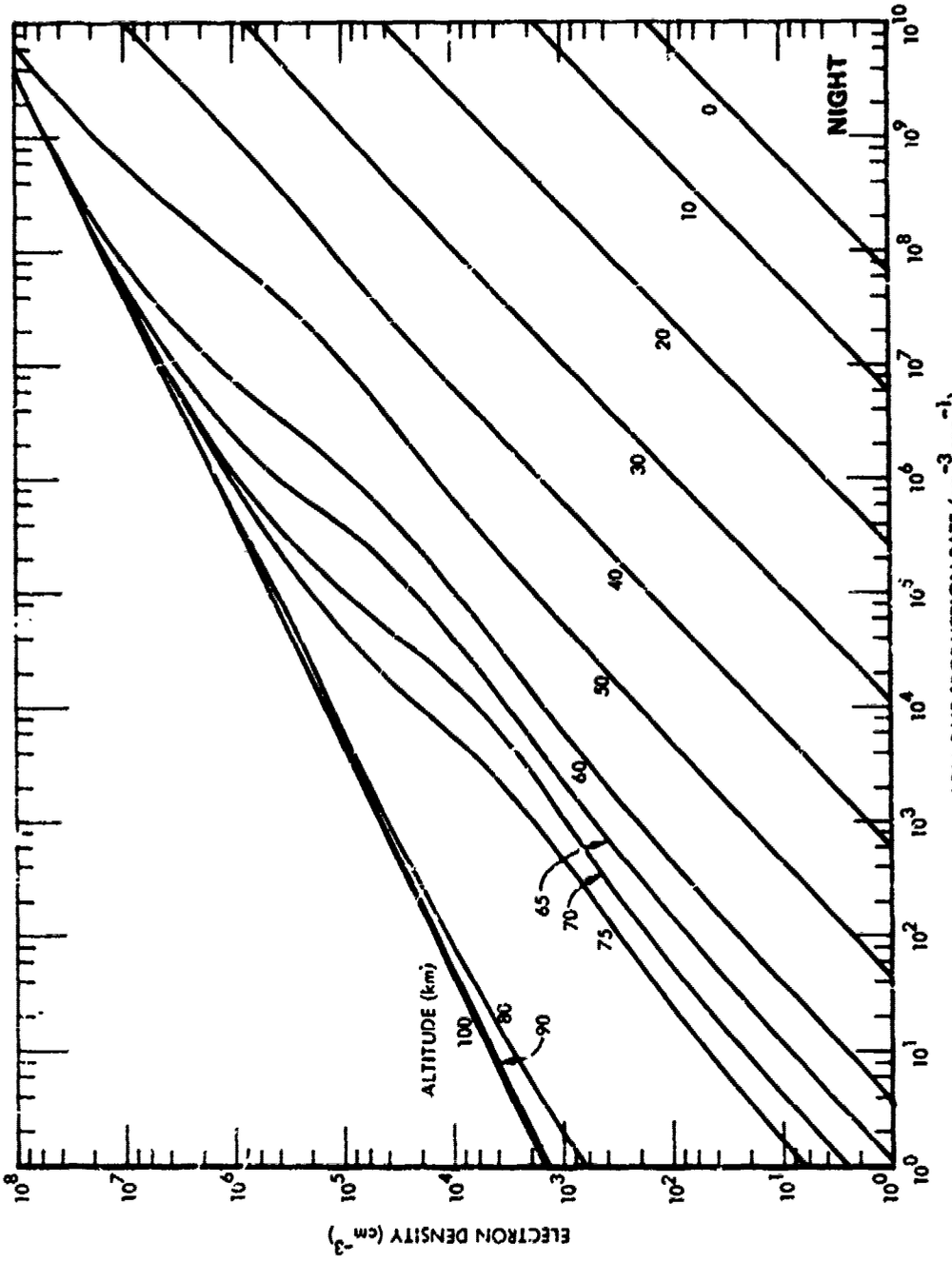

Figure 4-18. Equilibrium electron density versus ion-pair production rate, nighttime.

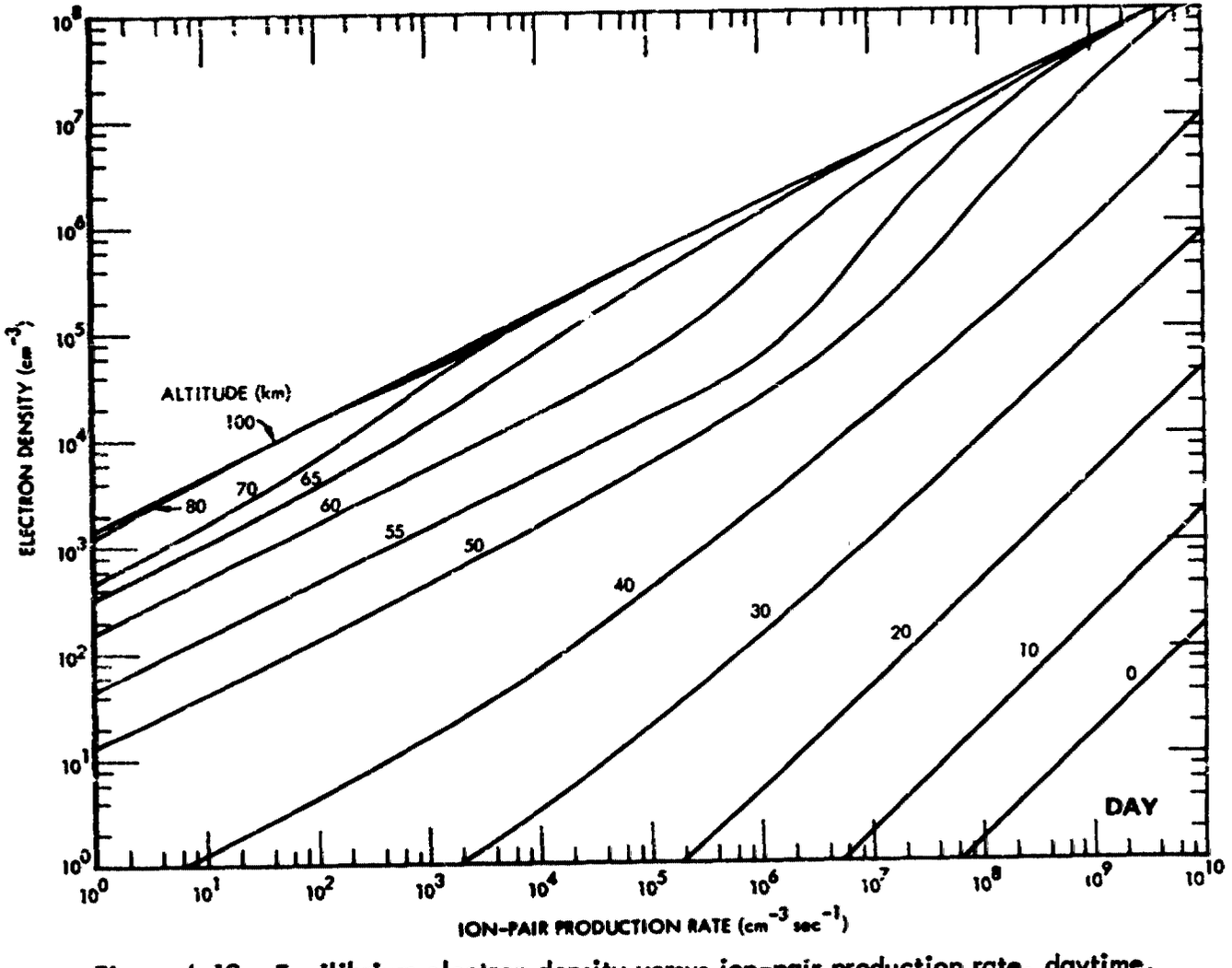

Figure 4-19. Equilibrium electron density versus ion-pair production rate, daytime.

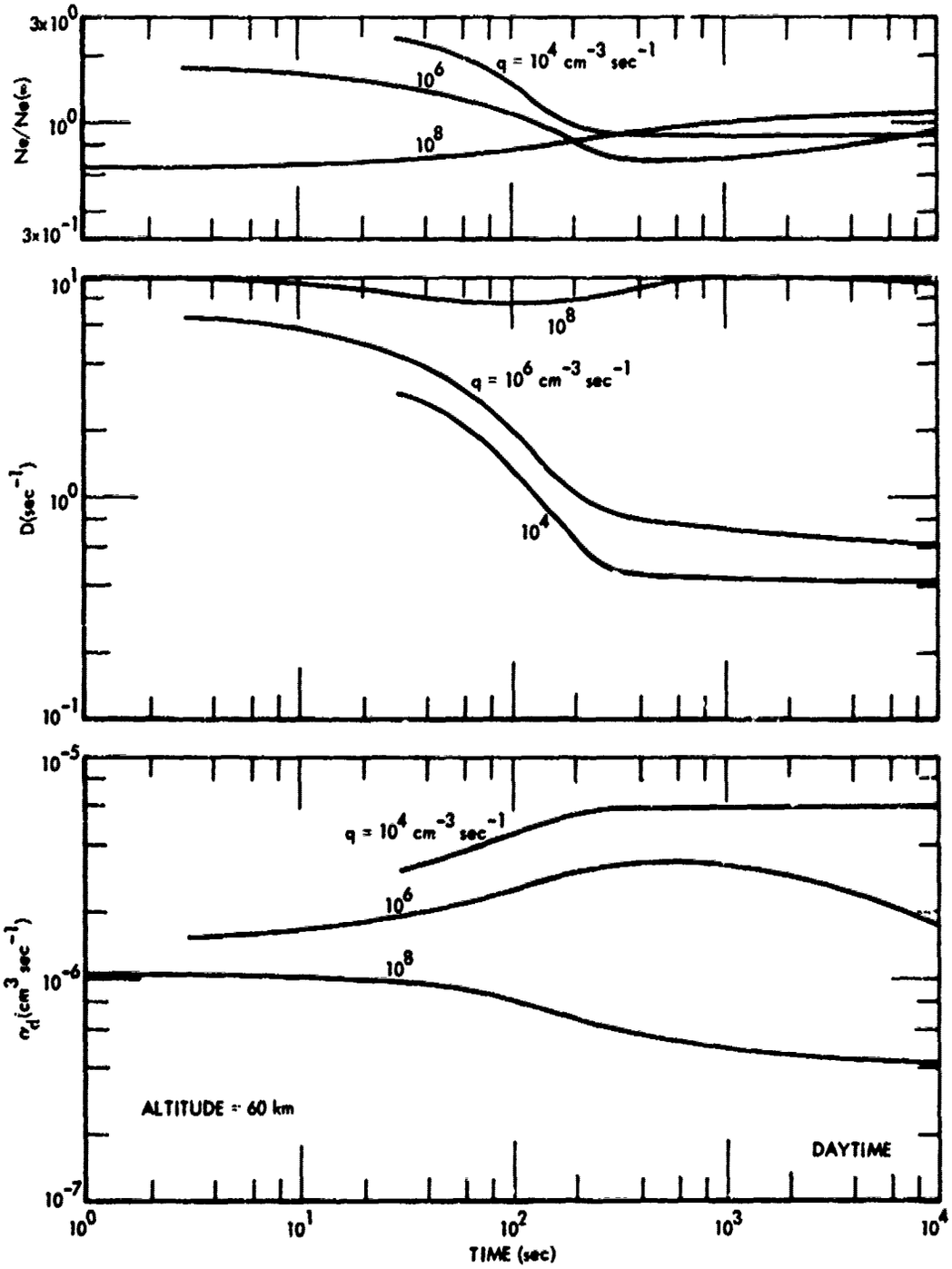

Figure 4-20. Effect of prompt radiation on effective reaction rate coefficients and electron density caused by delayed radiation, $N_o = 10^{10}$ cm^{-3}.

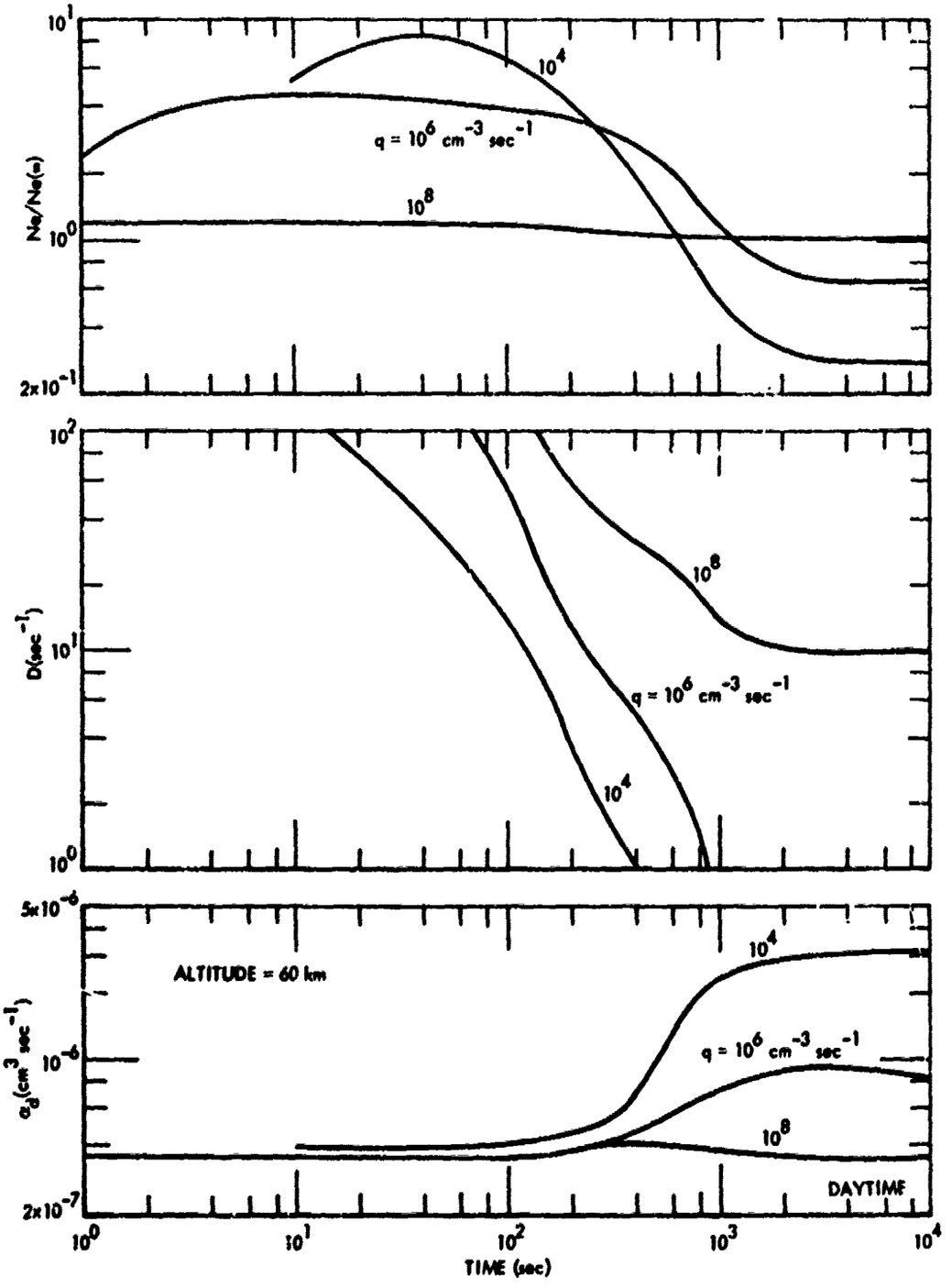

Figure 4-21. Effect of prompt radiation on effective reaction rate coefficients and electron density caused by delayed radiation, $N_o = 10^{12}$ cm^{-3}.

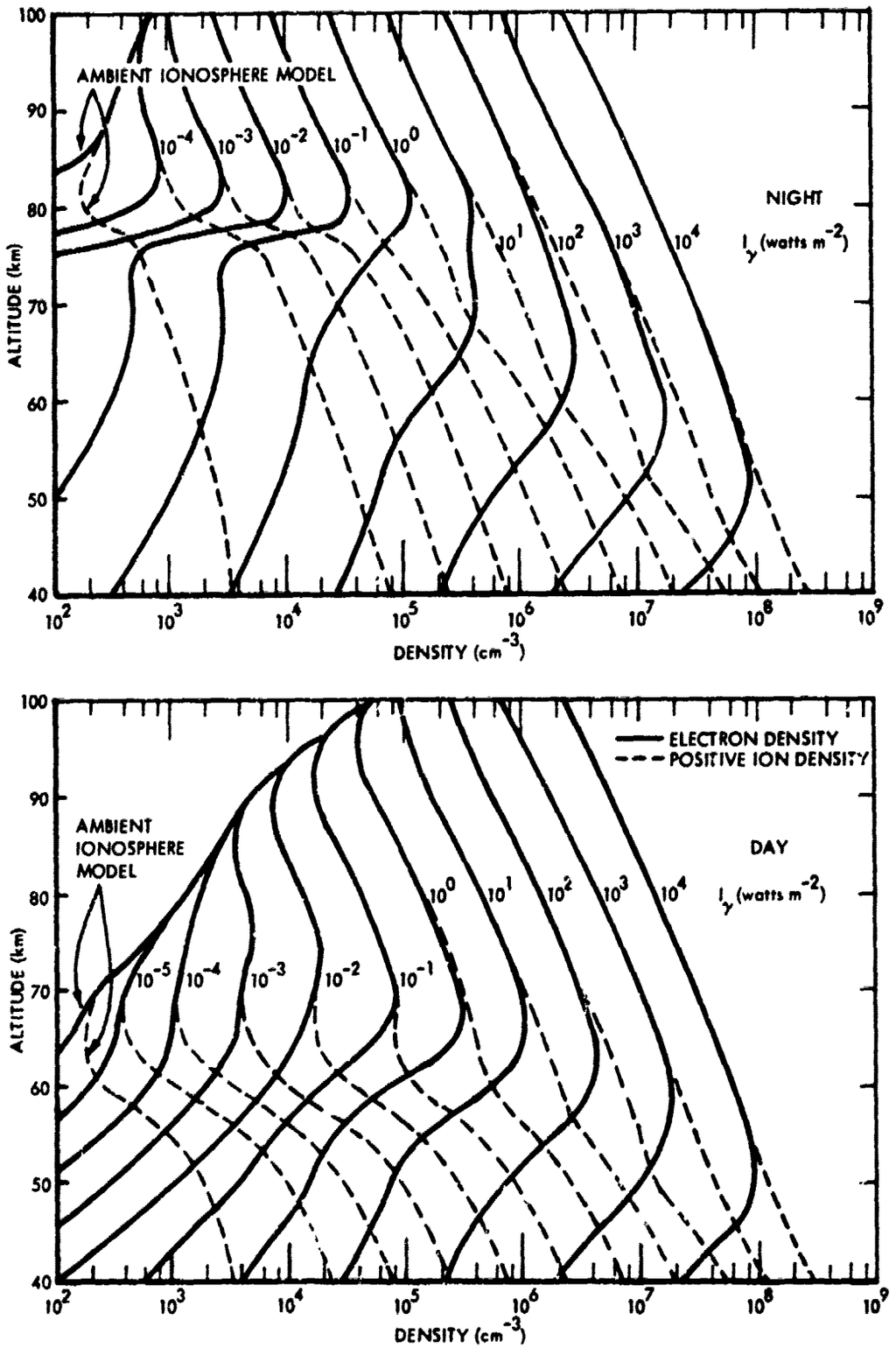

Figure 4-22. Equilibrium electron and positive ion density due to delayed gamma rays.

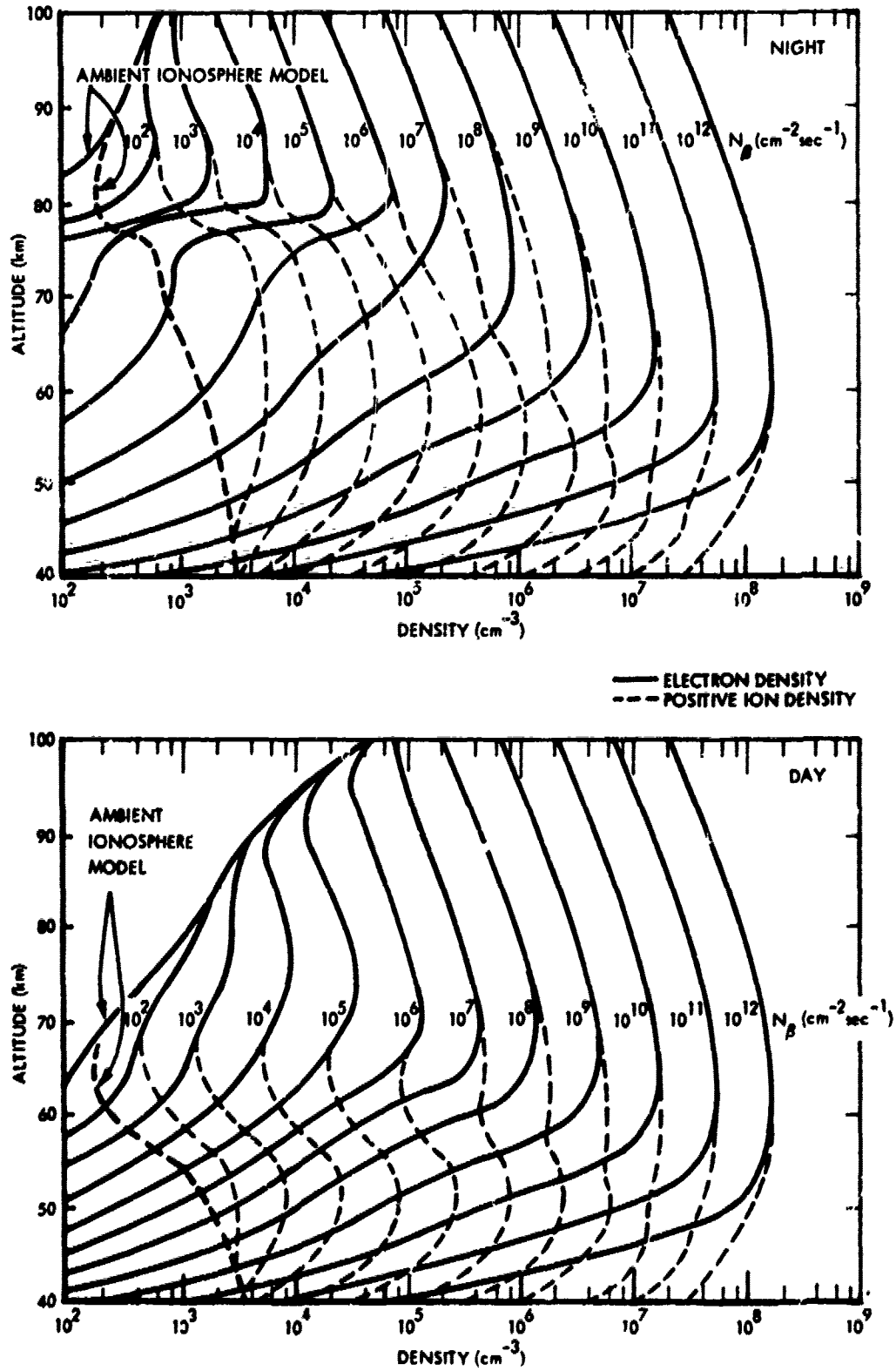

Figure 4-23. Equilibrium electron and positive ion density due to beta particles, 60-degree magnetic dip angle.

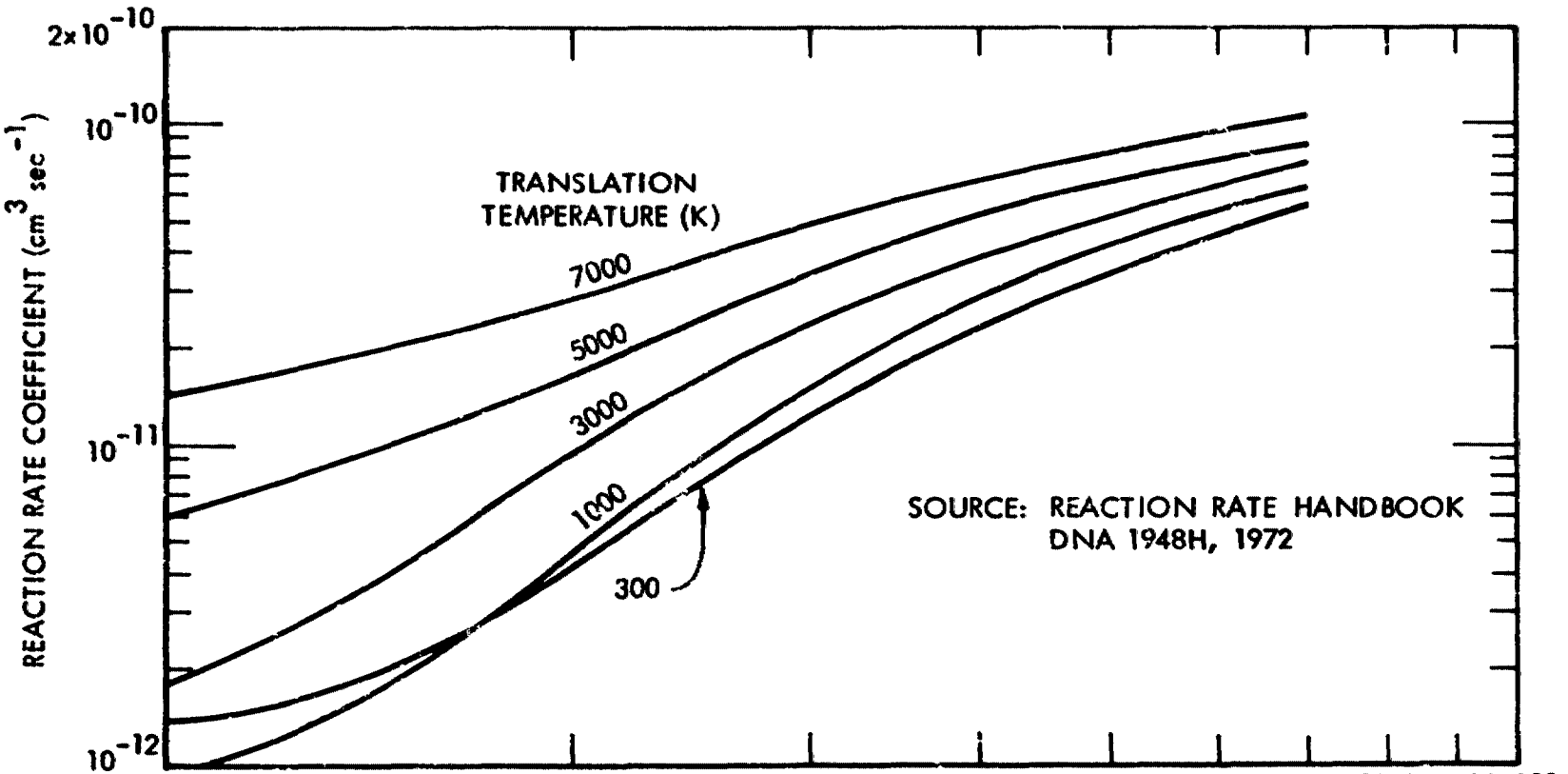

Figure 4-24. Reaction rate coefficient for the reaction $N_2 + O^+ \rightarrow NO^+ + N$ for a range of vibrarional and translational temperature.

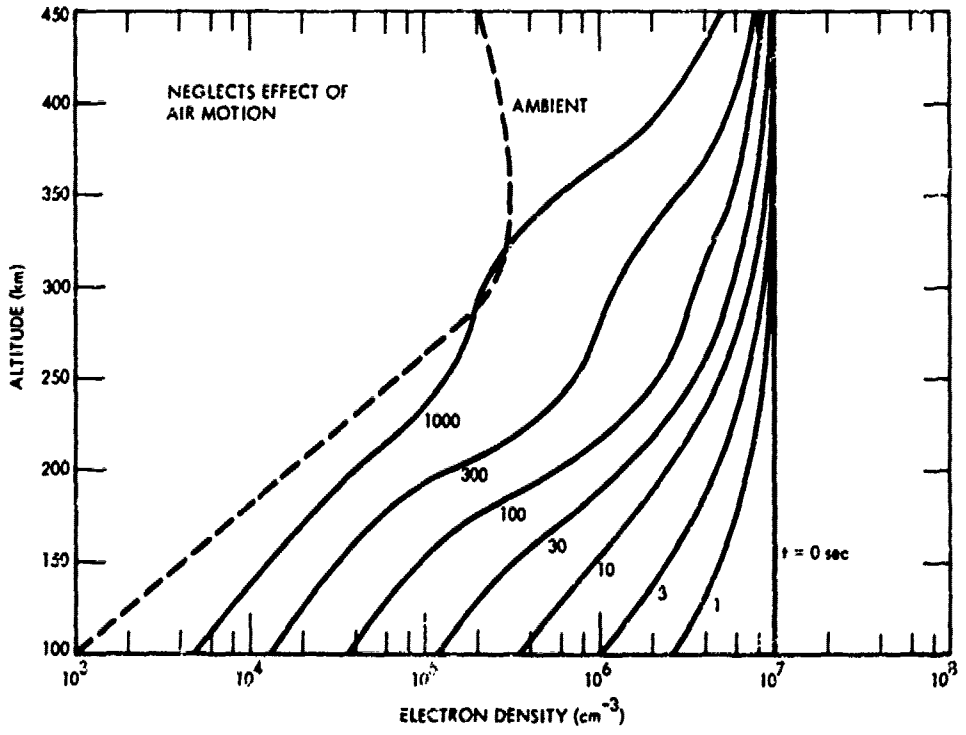

Figure 4-25. Decay of ionization impulse of 10^7 cm^{-3} above 100 km, nighttime.

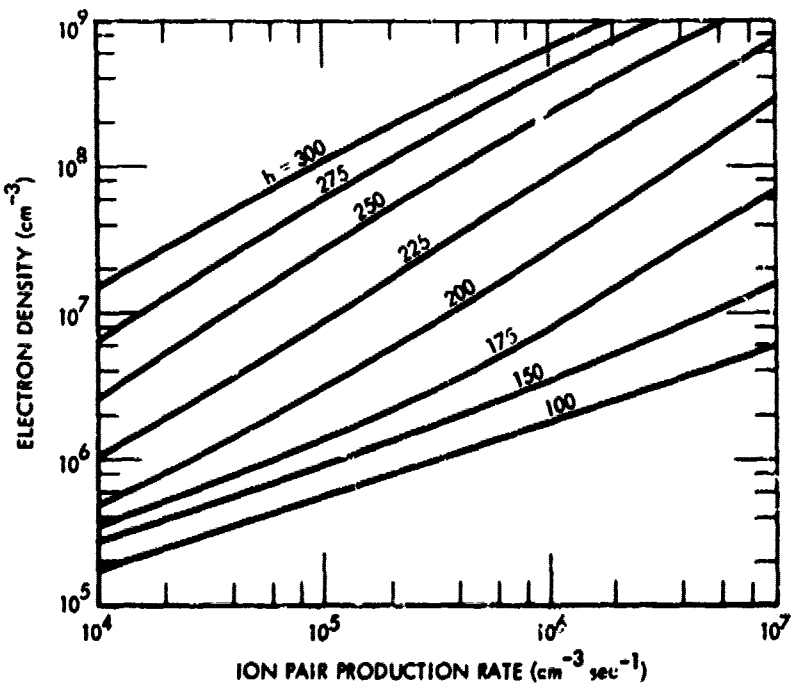

Figure 4-26. Equilibrium electron density versus ion-pair production rate above 100 km.

SECTION 5
ABSORPTION

COLLISION FREQUENCY*
(Shkarofsky's definition)

Electron-neutral—see Figure 5-1:

$$\bar{\nu}_{em} = 2.0 \times 10^{-11}\ nT \approx 1.7 \times 10^{5} p \quad sec^{-1} \quad .$$

Ion-neutral:

$$\frac{\bar{\nu}_{em}}{10} \leq \bar{\nu}_{im} \leq \frac{\bar{\nu}_{em}}{40}$$

$$\bar{\nu}_{im} = \frac{\bar{\nu}_{em}}{40}$$ for calculations in this document unless otherwise stated

Electron-ion—see Figure 5-2:

$$\bar{\nu}_{ei} = 1.8\ N_e T^{-3/2}\ \ell n\left(1.54 \times 10^{8} \frac{T^3}{N_e} \frac{f_p^2}{f^2}\right)$$

$$f_p^2 = 8.1 \times 10^{7} N_e$$

f = wave frequency (Hz) .

---

*Assumed momentum-transfer cross sections (cm^2):

Electron-nitrogen molecules	$3.1 \times 10^{-23}\ v$
Electron-oxygen molecules	$1.3 \times 10^{-23}\ v$
Electron-oxygen atoms	5.6×10^{-16}
Electron-ion	$\frac{8.05 \times 10^{17}}{v^4} \ell n\left(1.24 \times 10^{4} \frac{T^{3/2}}{N_e^{1/2}} \frac{f_p}{f}\right)$

$N_e (cm^{-3})$, $v (cm\ sec^{-1})$

NONDEVIATIVE ABSORPTION

Electron-neutral—see Figures 5-3, 5-4, and 5-5:

$$a = \frac{4.6 \times 10^4 N_e \bar{\nu}_{em}\, g}{(\bar{\nu}_{em}\, g)^2 + (\omega h)^2} \text{ dB km}^{-1}$$

g and h are correction factors to account for the velocity dependence of electron collisions—see Figure 5-6:

$g = h = 1$ for $\omega \gg \bar{\nu}$

$g \to 3/5$, $h \to 3$ } ror $\omega \ll \bar{\nu}$.

Ion-neutral—see Figures 5-3 and 5-4:

$$a = \frac{0.79 N_i \bar{\nu}_{im}}{(\bar{\nu}_{im})^2 + \omega^2} \text{ dB km}^{-1} .$$

Electron-ion:

$$a = \frac{4.6 \times 10^4 N_e \bar{\nu}_{ei}}{(\bar{\nu}_{ei})^2 + \omega^2} \text{ dB km}^{-1} .$$

DEVIATIVE ABSORPTION

a(deviative) = C_a a(nondeviative)

C_a—see Figure 5-7.

ATMOSPHERIC OXYGEN AND WATER VAPOR ABSORPTION

Total atmospheric absorption—see Figure 5-8.

Model data (Straiton, 1964)—see Figure 5-9.

ABSORPTION CAUSED BY NUCLEAR EXPLOSIONS*

Fireball/debris region:

*Path absorptions presented are one-way vertical unless otherwise indicated. An estimate of path absorption for oblique paths can be obtained by multiplying one-way vertical absorption by secant of the angle of incidence—see Figure 5-29.

Absorption due to thermal ionization—see Figure 5-10.

Absorption due to beta-particle ionization within a cylindrical debris region (vertical thickness = 8 km, radius = R_{DB})—see Figure 5-11.

Absorption due to prompt radiation outside fireball:

Saturation impulse [$N_e(h,0) \leq 10^8, N_e(h,0)\alpha >> 1$]—see Figure 5-12.

Approximate relation for absorption in dB (frequency in gigahertz):

$$A \approx \frac{0.3}{f^2 t} \qquad \text{(daytime)}$$

$$A \approx \left\{ \begin{array}{ll} \dfrac{0.055}{f^2 t^{1.6}} & t < 10 \text{ sec} \\ \\ \dfrac{0.011}{f^2 t^{0.9}} & t > 30 \text{ sec} \end{array} \right\} \text{(nighttime)} \quad .$$

Effect of changes in neutral species composition caused by large ionization impulses— see Figure 5-13.

Uncertainty: Figure 5-12 and the approximate solutions neglect effects of changes in the neutral species from prompt and thermal radiation and the effect of the fireball photodissociation and photodetachment of negative ions. For conditions where $N_e(0) \leq 10^8$ cm^3 near 60 km (see Section 2) and $N_e(0)\alpha t >> 1$, the duration of absorption obtained from Figure 5-11 or the approximate relations is believed to be within a factor of three.

Absorption from beta particle ionization outside the fireball.

Offset of beta particle absorption region from fission debris (no geomagnetic field distortion)—see Figure 5-14.

Absorption from equilibrium ionization (effect of prompt and thermal radiation neglected)—see Figures 5-15 through 5-18.

Approximate expressions for one-way vertical absorption in dB (frequency in gigahertz):

$$A \approx \begin{cases} \dfrac{0.4}{f^2}\left(\dfrac{N_\beta}{10^8}\right)^{0.68} & N_\beta \geq 10^8 \\ \dfrac{0.31}{f^2}\left(\dfrac{N_\beta}{10^8}\right)^{0.55} & N_\beta < 10^8 \end{cases} \text{(Daytime)}$$

$$A \approx \begin{cases} \dfrac{0.26}{f^2}\left(\dfrac{N_\beta}{10^8}\right)^{0.75} & N_\beta > 10^9 \\ \dfrac{0.17}{f^2}\left(\dfrac{N_\beta}{10^8}\right)^{0.91} & 10^6 < N_\beta \leq 10^9 \\ \dfrac{0.07}{f^2}\left(\dfrac{N_\beta}{10^8}\right)^{0.71} & N_\beta \leq 10^6 \end{cases} \text{(Nighttime)}$$

Beta particle absorption has been calculated using an average beta particle energy of 1 MeV. For the effect on absorption caused by changing the average energy—see Figures 5-19A and B.

Uncertainty: The effect of prompt and thermal radiation on the equilibrium electron density and resultant absorption have been neglected in Figures 5-15 through 5-18 and in the approximate relations. For the effect on beta particle absorption produced by changes in the neutral species composition from prompt radiation, see Figure 5-20. For moderate ionization levels the predicted absorption is believed to be within a factor of two to three.

Absorption from Compton electron ionization in the conjugate region.

Use Figures 5-15 through 5-18 with N_β replaced by N_c. Approximate expressions for one-way vertical absorption in dB (frequency in megahertz):

$$A \approx \frac{6000}{f^2}\left(\frac{N_c}{10^5}\right)^{0.57} \quad \text{(Daytime)}$$

$$A = \frac{510}{f^2}\left(\frac{N_c}{10^5}\right)^{0.64} \quad \text{(Nighttime)} \quad .$$

Uncertainty: For moderate ionization levels the predicted absorption is believed to be within a factor of two to three.

Absorption due to gamma radiation along propagation paths close to debris regions:

This procedure is for debris regions that are below 120 km and for which d < 200 km (see Figure 5-21 for geometry). For higher debris regions or paths farther from the debris region, use the procedure for paths far from the debris region.

The absorption calculated is the one-way path absorption (not the vertical absorption).

f is in megahertz in the calculations.

Restrictions:

- Negligible photodetachment due to fireball radiance.
- Ionization calculated using equilibrium solution.
- Negligible changes in neutral species composition from prompt and thermal radiation.
- Ambient atmospheric temperature and composition.
- Fission debris a point source of gamma radiation.

Choose from Figures 5-22A, B, C, D, and E the figure with the angle of approach closest to θ. From this figure obtain $A(f_1)$, the absorption at 1000 MHz, 10 sec after burst.

Calculate A_γ:

$$A_\gamma = A(f_1) \left(\frac{10^6}{f^2}\right)\left(\frac{11}{1+t}\right) \quad .$$

For the effect of prompt and thermal fireball radiation on one-way absorption (θ = 0 degrees)—see Figures 5-23A, B, and C. Only the effect of prompt radiation on neutral species composition is included.

Absorption due to gamma radiation along propagation paths far from debris regions:

Debris altitude above about 120 km or calculation points located farther than 200 km from debris edge.

Restrictions:

- Equilibrium values for neutral and ionized species.
- Effects of prompt and fireball radiation on the effective deionization reaction rate coefficients can be neglected.

Incremental absorption versus I_γ for f = 30, 300, and 1000 MHz—see Figures 5-24 through 5-26.

One-way vertical absorption versus I_γ—see Figure 5-27.

Approximate expression for one-way vertical absorption (frequency in gigahertz):

$$A \approx \begin{cases} \dfrac{0.068 I_\gamma^{0.52}}{f^2} & 10^{-4} < I_\gamma \leq 10^{-2} \\ \dfrac{0.12 I_\gamma^{0.62}}{f^2} & 10^{-2} < I_\gamma \leq 10^{0} \\ \dfrac{0.11 I_\gamma^{0.86}}{f^2} & I_\gamma > 10^{0} \end{cases} \text{Daytime}$$

$$A \approx \dfrac{0.068 I_\gamma^{0.52}}{f^2} \qquad I_\gamma > 10^{0} \quad \text{Nighttime} \quad .$$

The approximate expressions restricted to frequencies greater than 100 MHz at night and 10 MHz during the daytime. At lower frequencies f^{-2} scaling breaks down because the electron-neutral collision frequency becomes comparable to the wave frequency in the region of maximum absorption.

Uncertainty: The predicted absorption is believed to be within a factor of 3 for moderate ionization levels.

Comparison of absorption due to gamma and beta radiation--see Figure 5-28.

ATTENUATION OF VLF AND LF SIGNALS CAUSED BY NUCLEAR EXPLOSIONS

rms electric field strength (1-kW radiated power):

$$\bar{E}(D) = \bar{E}(4000) \exp\left[-\frac{\bar{\alpha}(D - 4000)}{8700}\right] \text{ V/m}$$

D = ground range between transmitter and receiver (km)

$\bar{E}(D)$ = rms mode (VLF) or rms sky-wave sum (LF)

$\bar{\alpha}$ = effective attenuation rate (dB/1000 km) .

$\bar{E}(4000)$ and $\bar{\alpha}$ for spread-debris environment—see Figures 5-30, 5-31, 5-32, and 5-33.

Figures 5-30 through 5-33 show attenuation rates and field strengths for beta-particle and gamma-ray ionization from a uniform distribution of fission debris over the entire propagation path. The debris is assumed to be at several hundred kilometers altitude.

$\bar{E}(4000)$ and $\bar{\alpha}$ for prompt-radiation environment—see Figures 5-34, 5-35, 5-36, and 5-37.

Figures 5-34 through 5-37 show attenuation rates and field strengths for ionization due to prompt radiation from a 1-MT burst detonated at 1-earth-radius altitude above the center of the propagation path.

Uncertainty: Attenuation rates and field strengths are obtained by fitting field-strength calculations for circuit path lengths between 2000 and 8000 km. Predicted attenuation is sensitive to assumed values for the ion-neutral collision frequency and ion-ion recombination coefficient. An ion-neutral collision frequency one-fortieth of the electron-neutral collision frequency was used in the VLF and LF calculations. Larger ion-neutral collision frequencies would reduce the predicted attenuation rates. The calculated signal strength is the rms mode (VLF) or rms sky-wave sum (LF); it does not predict variations in signal strength with circuit path length due to interference between modes or sky waves. In addition to attenuation, nuclear explosions can cause large, rapid phase changes.

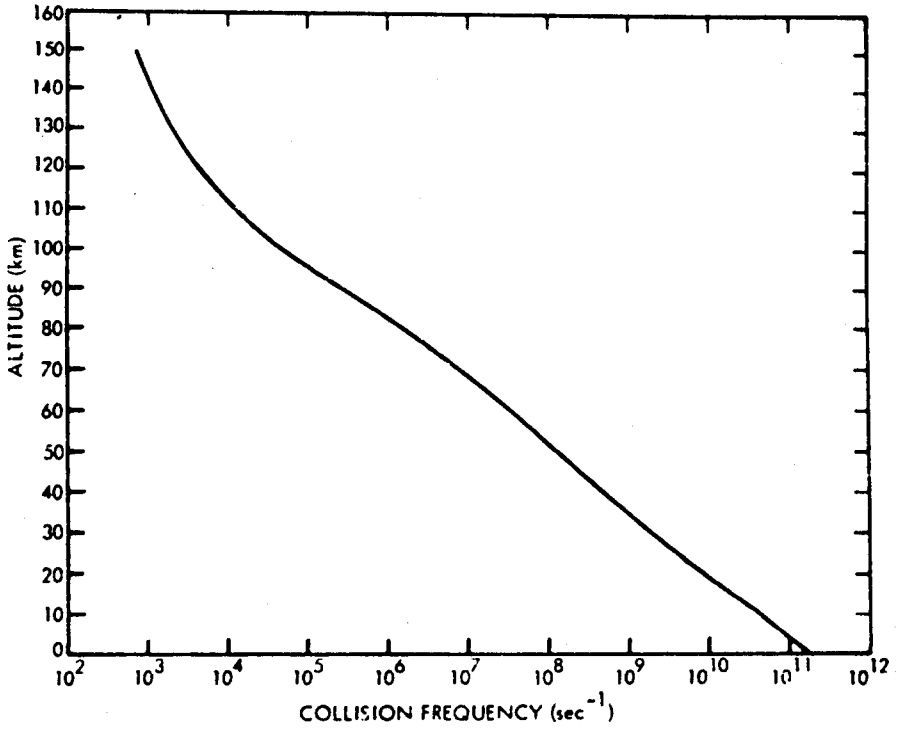

Figure 5-1. Electron-neutral collision frequency for the normal atmosphere.

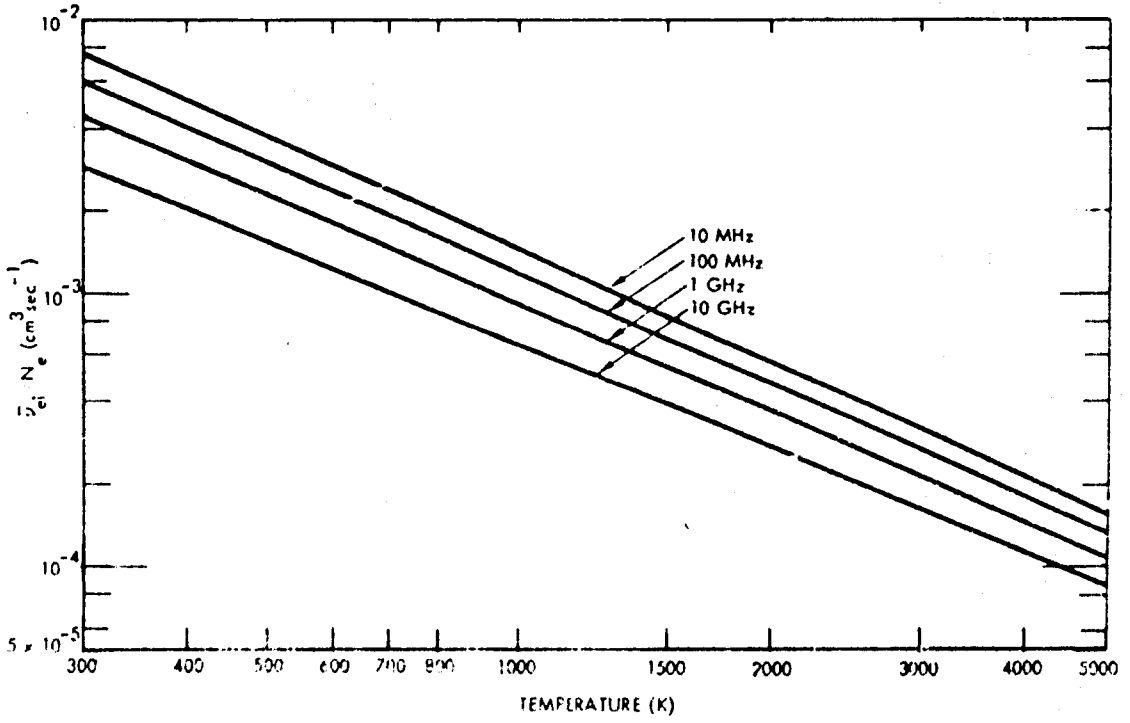

Figure 5-2. Electron-ion collision frequency.

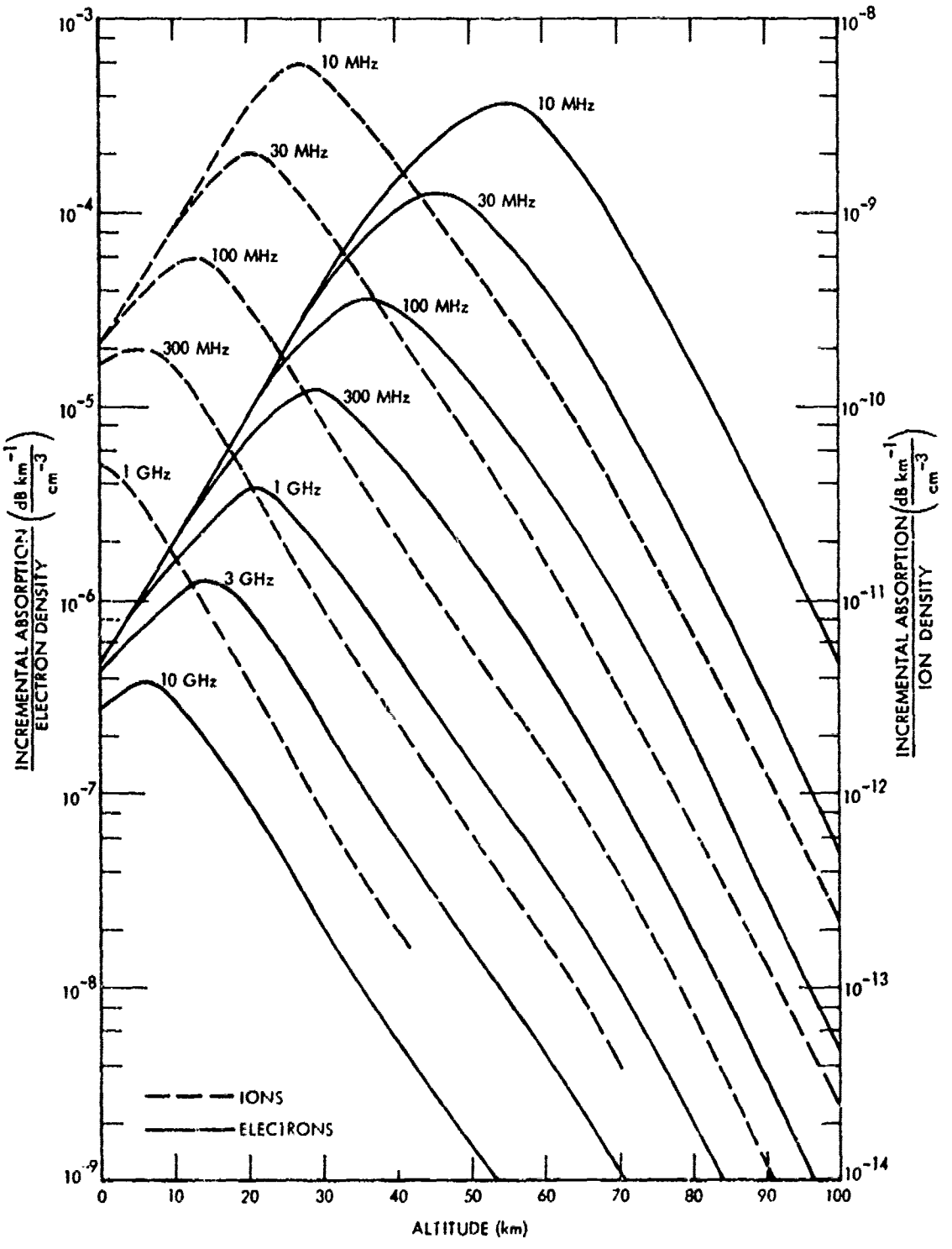

Figure 5-3. Incremental absorption caused by electron-neutral and ion-neutral collisions (ambient atmosphere).

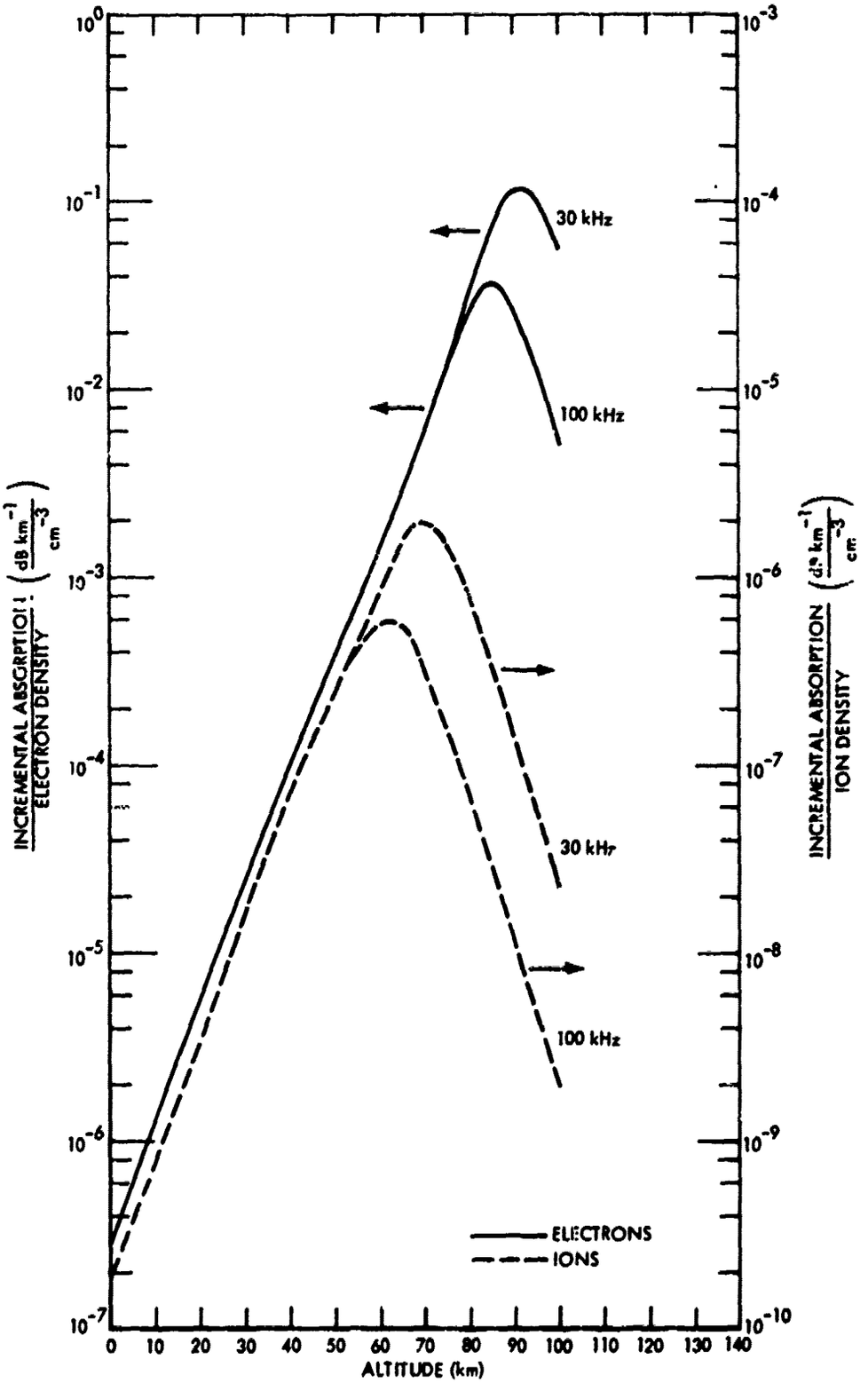

Figure 5-4. Incremental absorption caused by electron-neutral and ion-neutral collisions (ambient atmosphere) for 30 and 100 kHz.

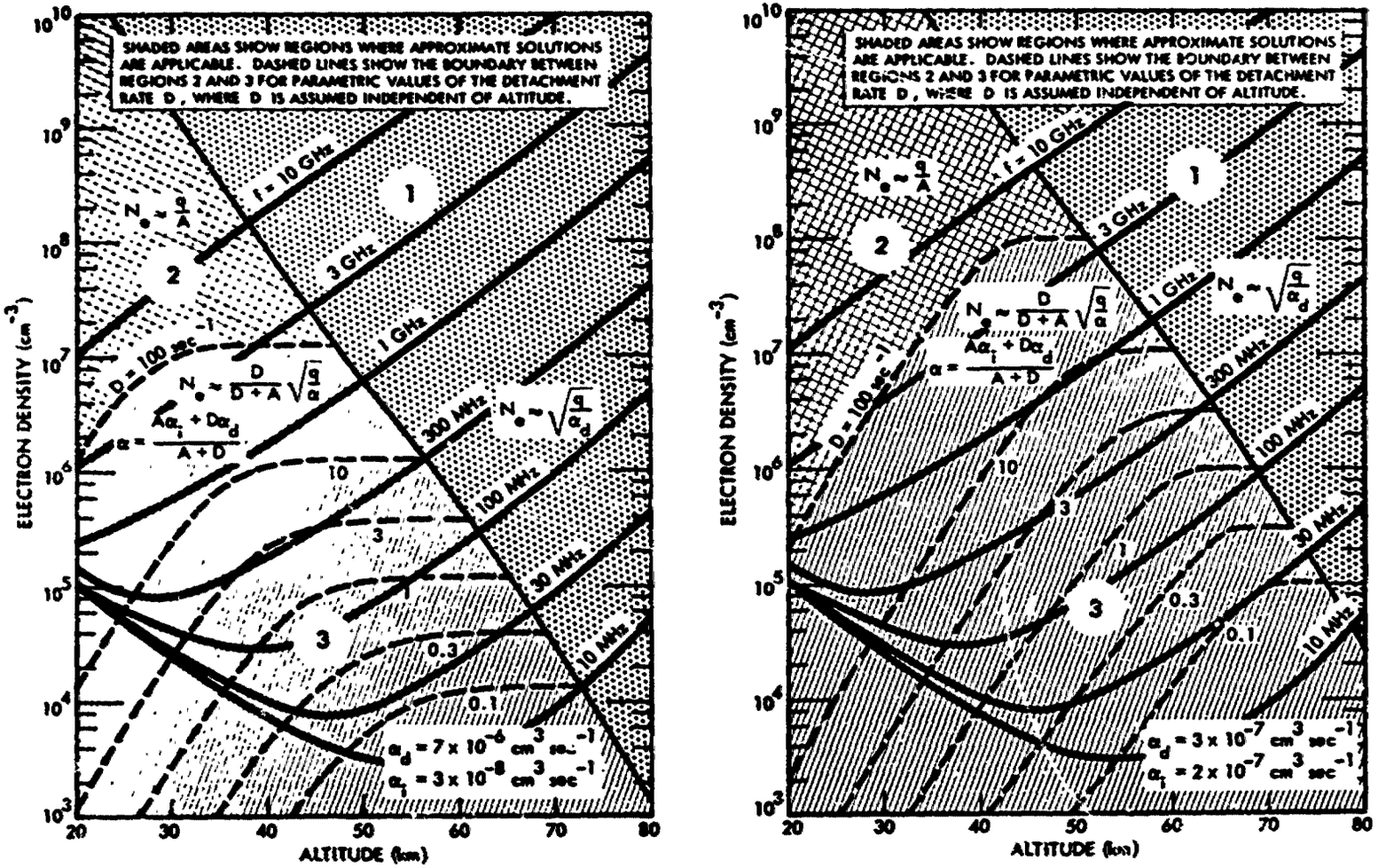

Figure 5-5. Replot of Figures 4-12 and 4-13 showing electron density required to produce 1-dB/km incremental absorption.

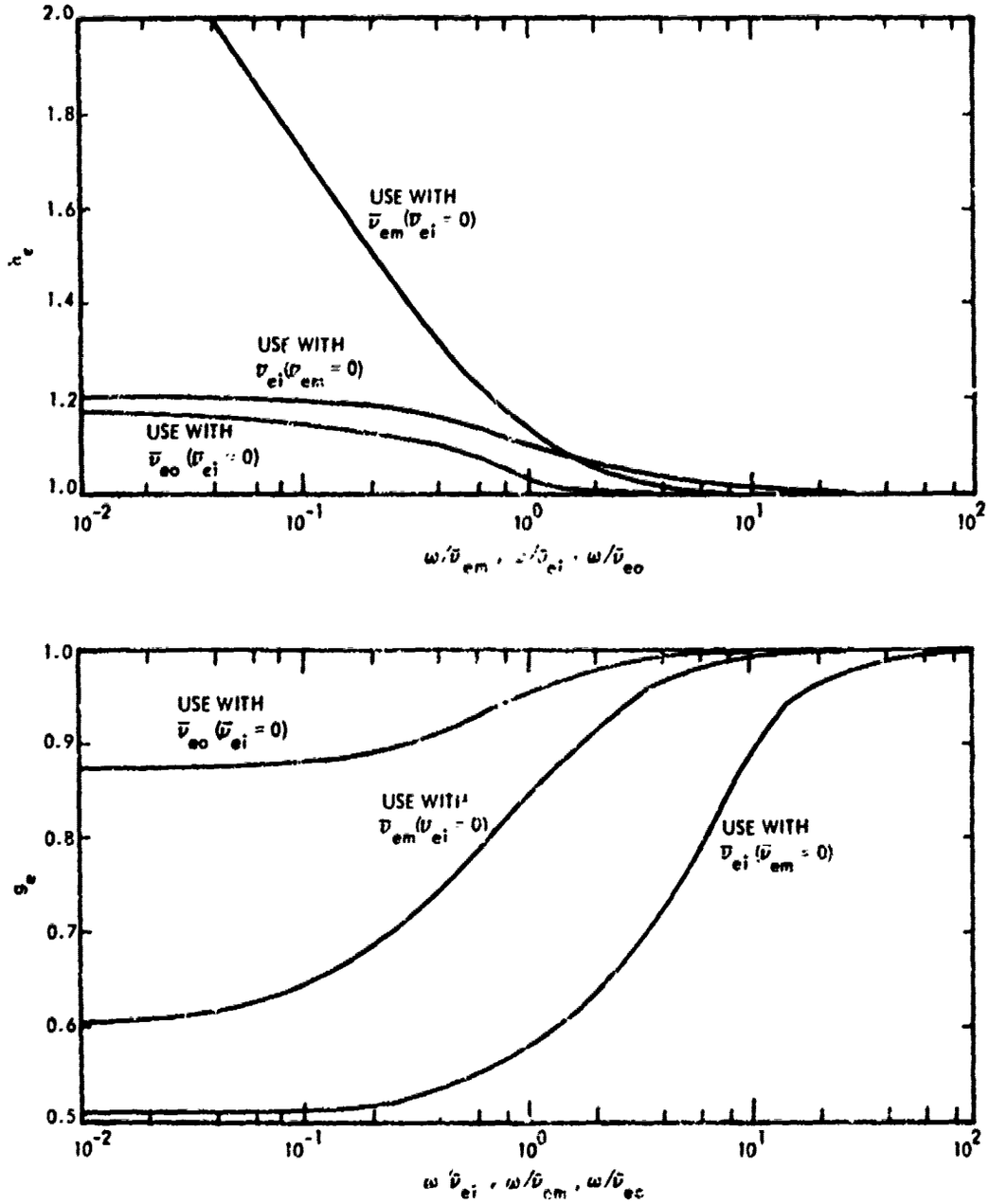

Figure 5-6. Collision frequency correction factors.

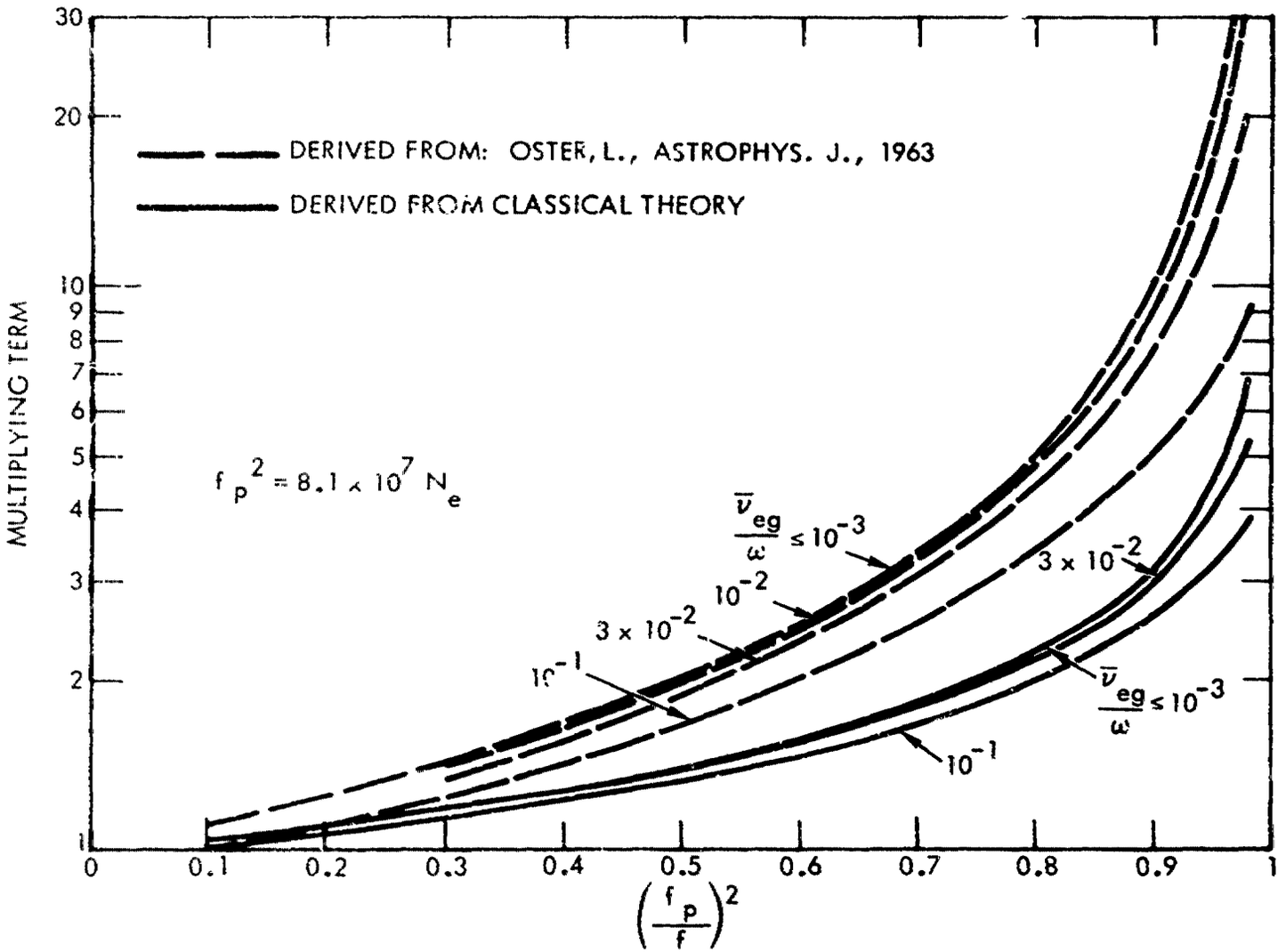

Figure 5-7. Multiplying term for correction of nondeviative absorption near plasma frequency.

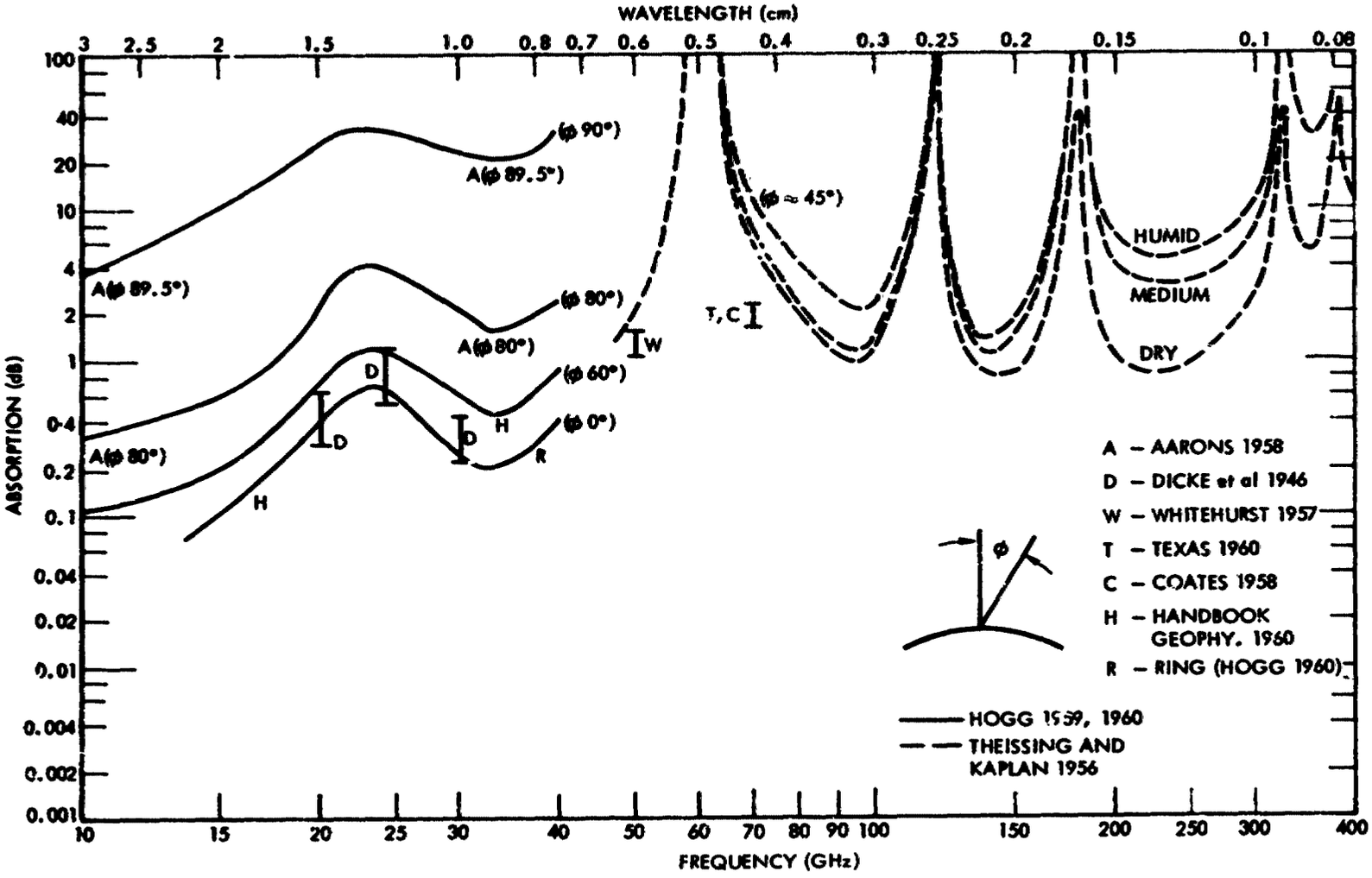

Figure 5-8. Total integrated absorption through the atmosphere.

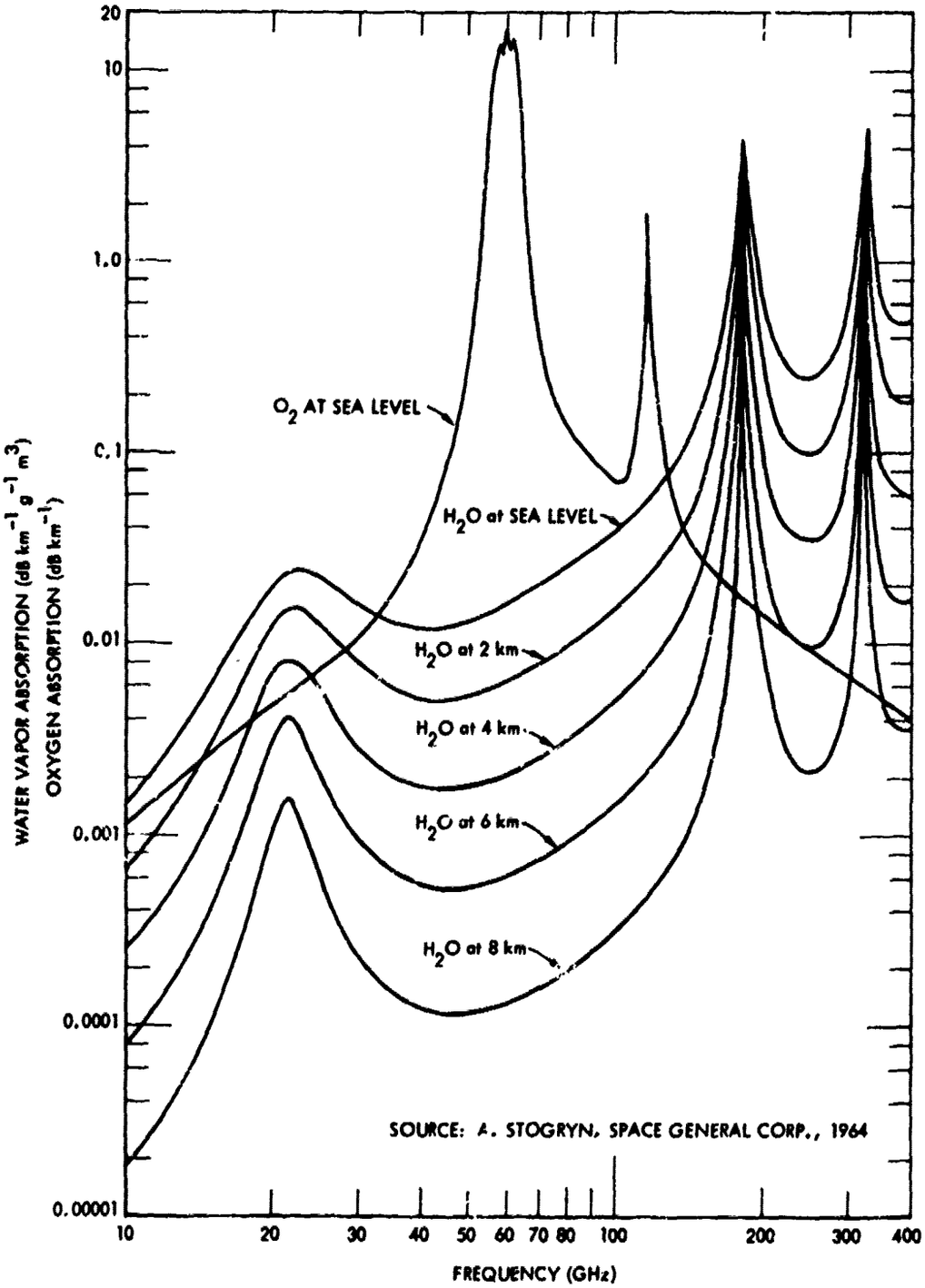

Figure 5-9. Water vapor absorption at various altitudes and oxygen absorption at sea level.

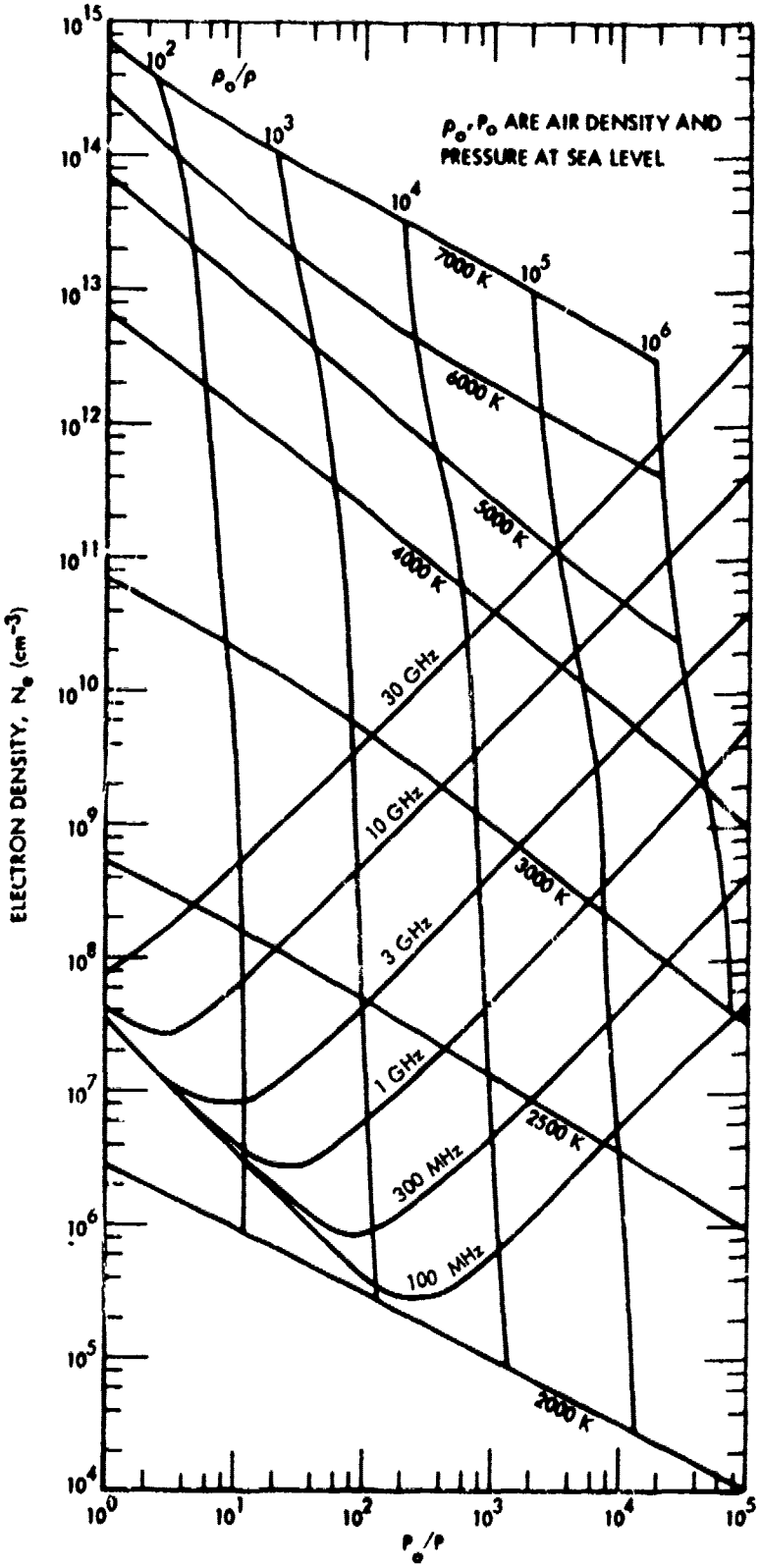

Figure 5-10. Replot of Figure 4-1 showing electron density required to produce 10 dB/km incremental absorption.

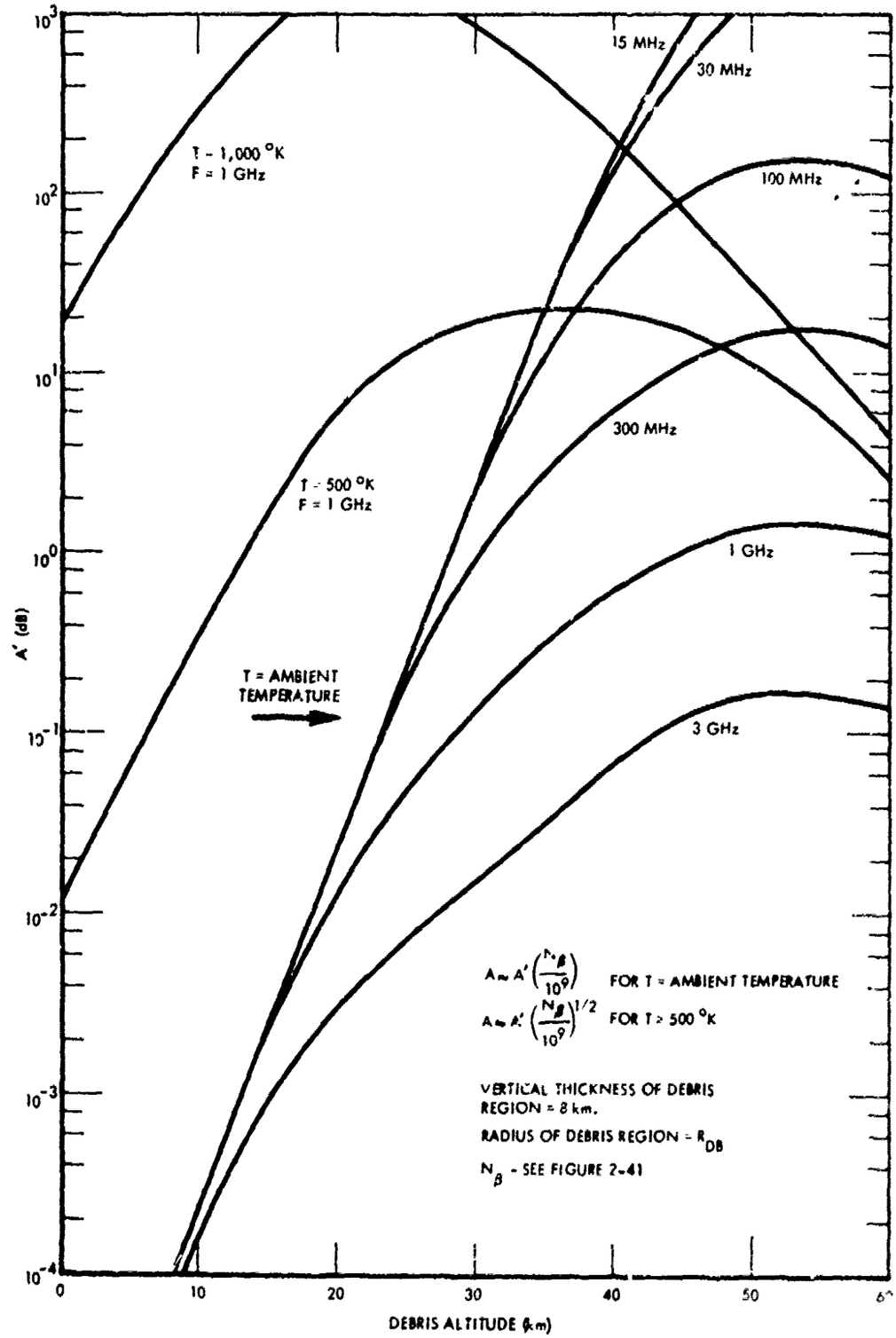

Figure 5-11. One-way absorption through cylindrical debris region due to beta particles.

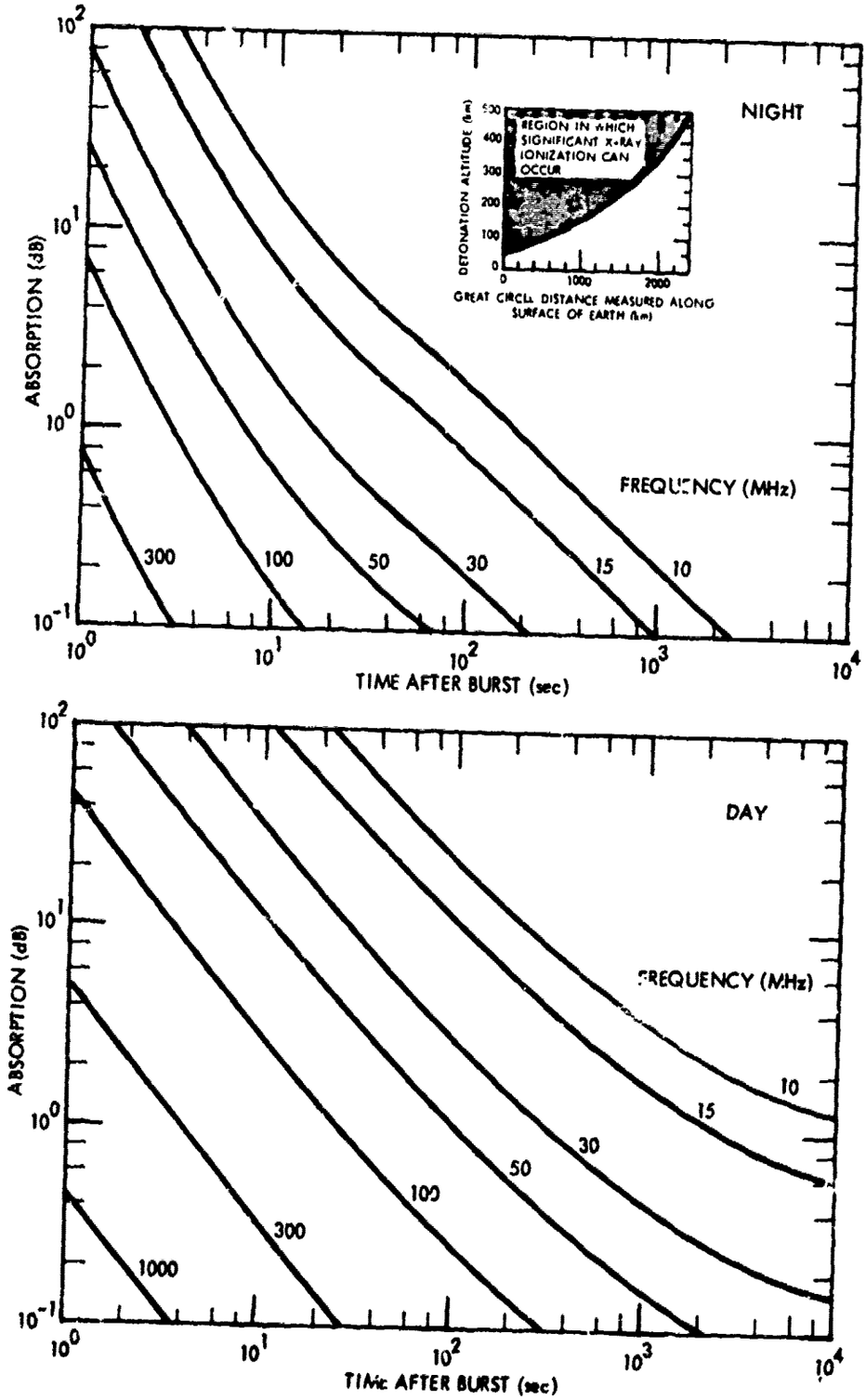

Figure 5-12. One-way, vertical absorption due to saturation impulse of ionization neglection changes in neutral species composition.

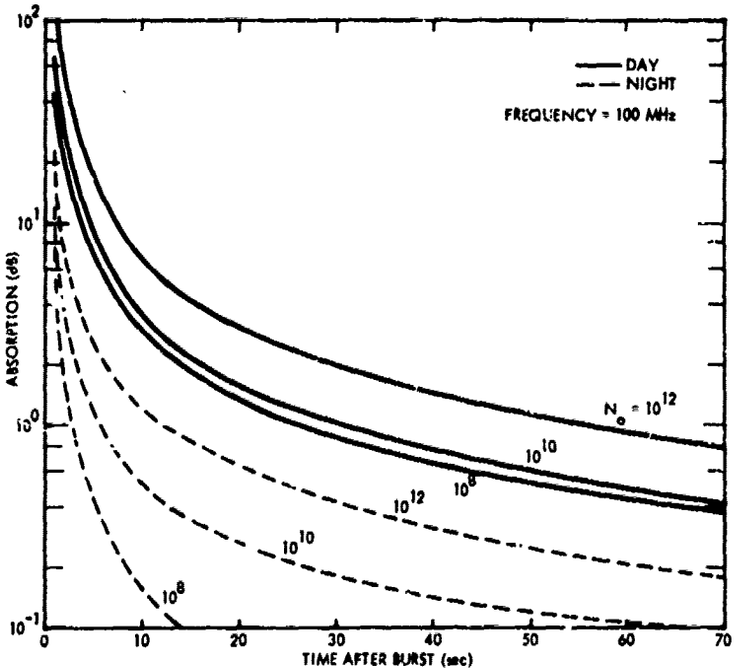

Figure 5-13. One-way vertical absorption due to prompt radiation including effects of changes in neutral species composition.

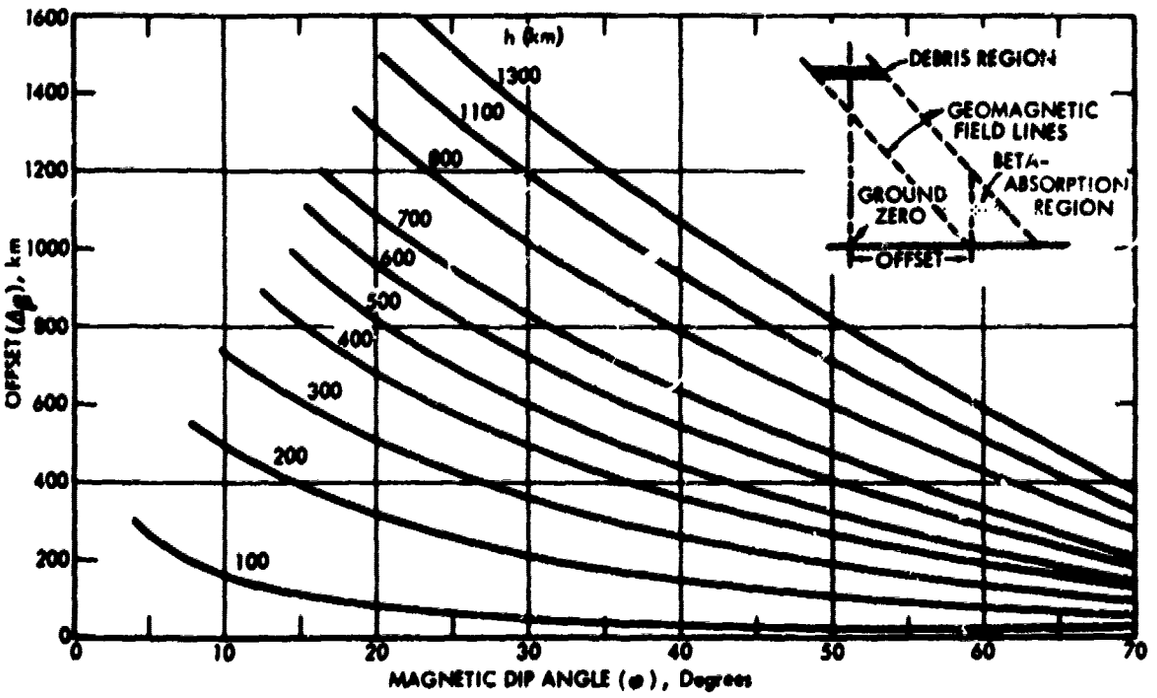

Figure 5-14. Offset of beta-absorption region.

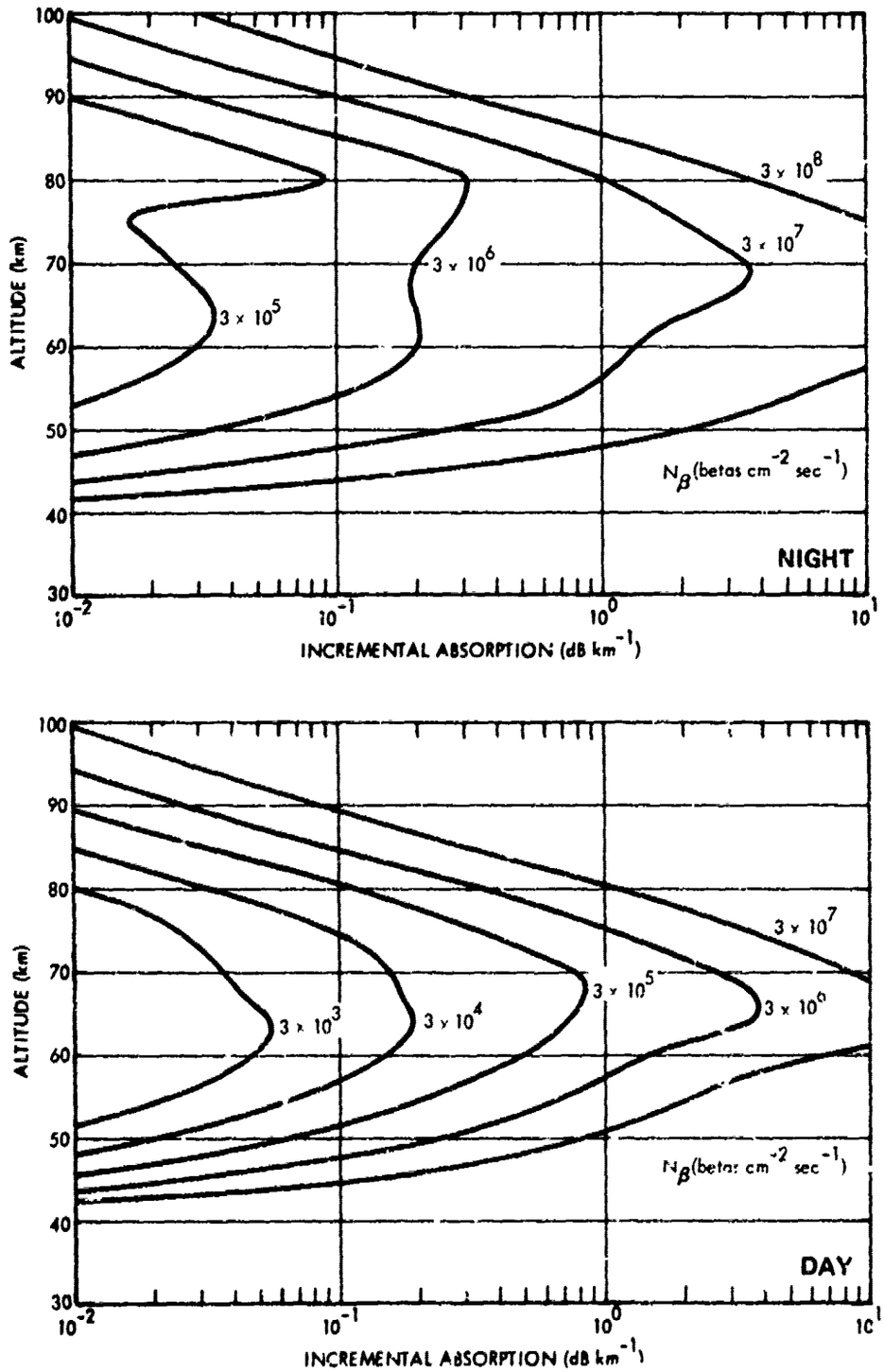

Figure 5-15. Incremental absorption due to beta particles for a magnetic dip angle of 60 degrees, f = 30 MHz.

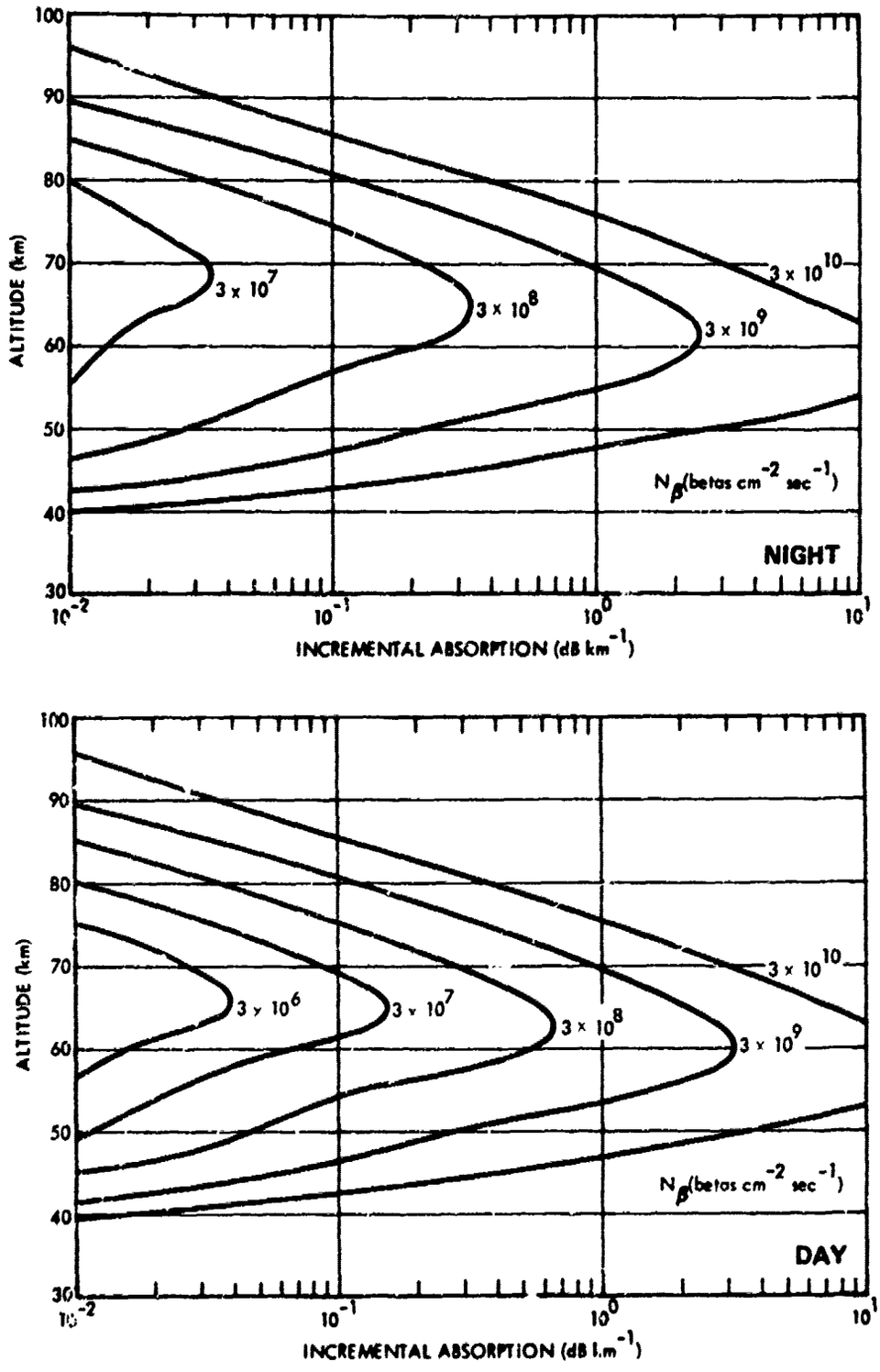

Figure 5-16. Incremental absorption due to beta particles for a magnetic dip angle of 60 degrees, f = 300 MHz.

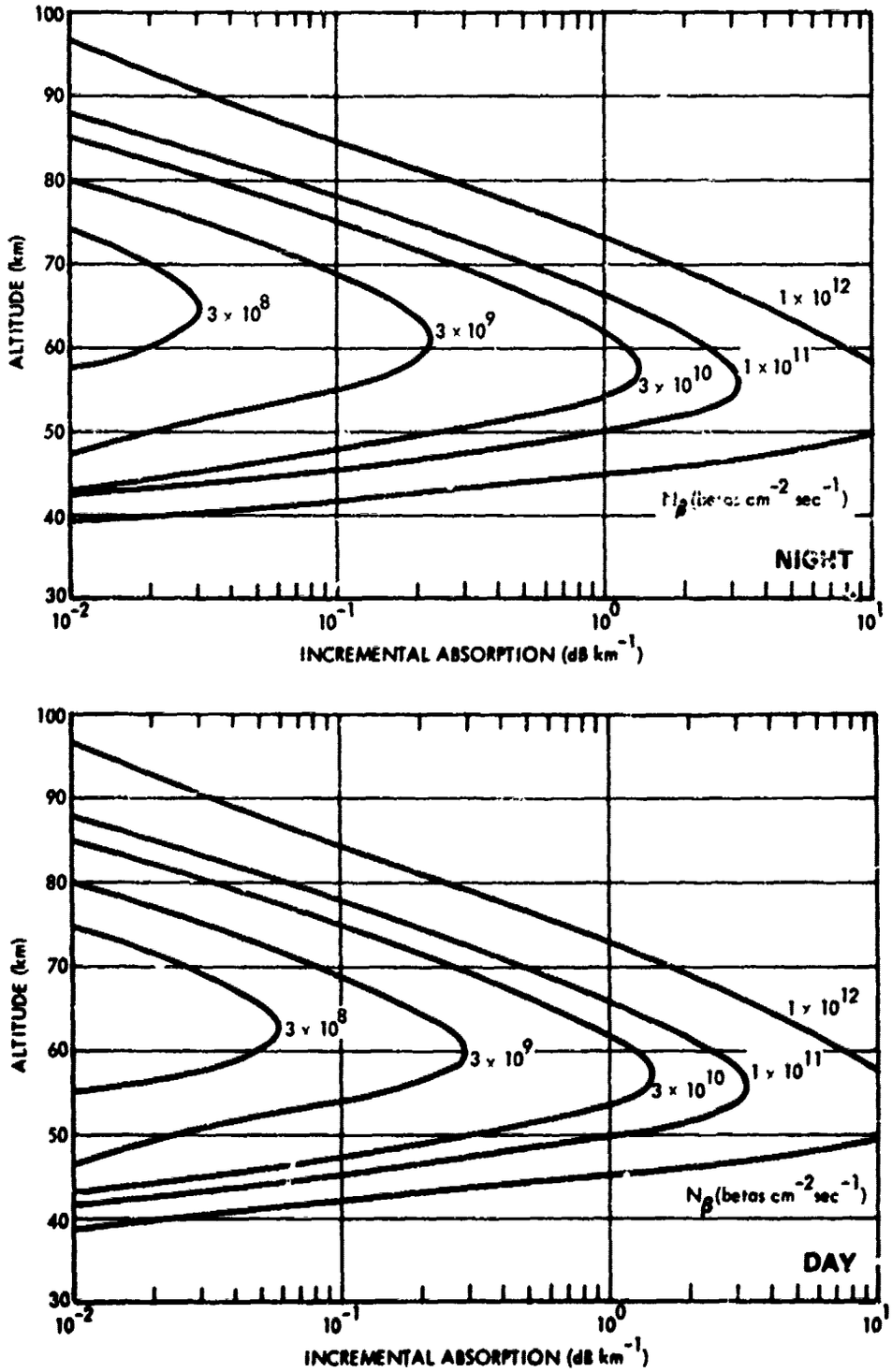

Figure 5-17. Incremental absorption due to beta particles for a magnetic dip angle of 60 degrees, f = 1 GHz.

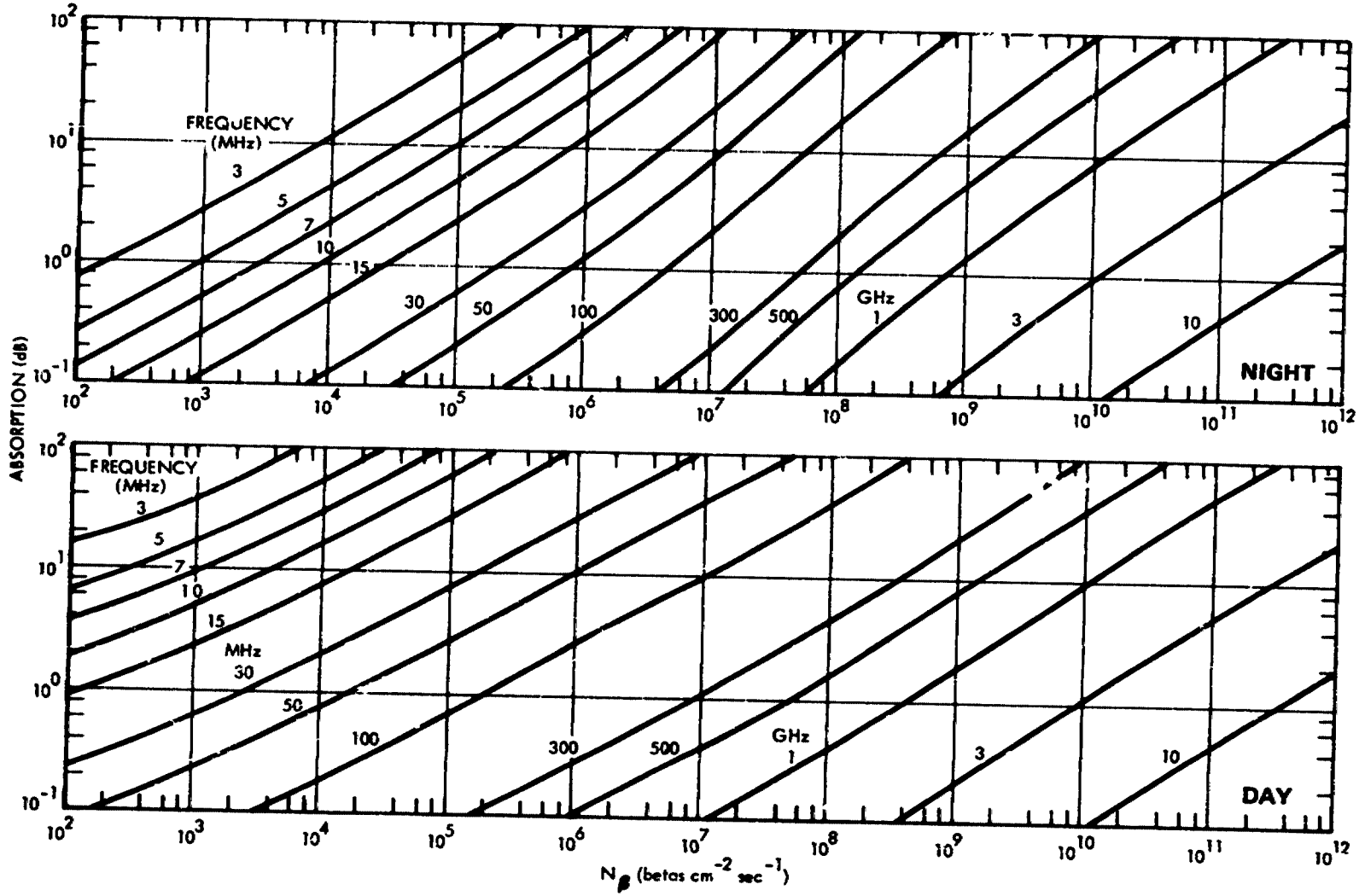

Figure 5-18. One-way vertical absorption due to beta particles, debris altitude above 60 km.

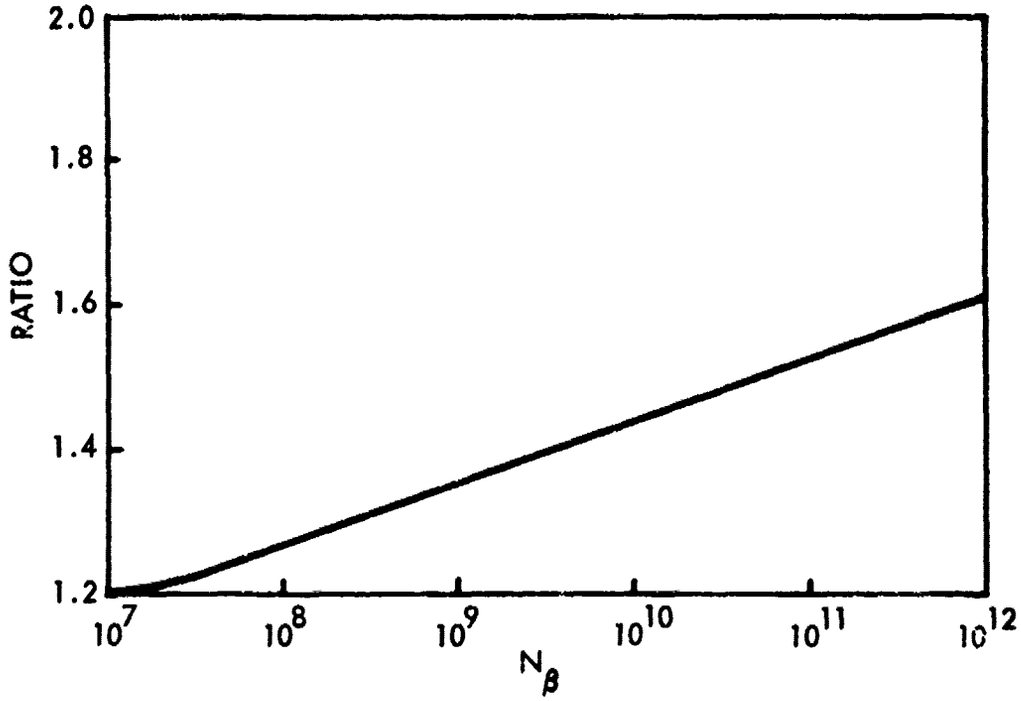

Figure 5-19A. Ratio of beta particle absorption obtained with average beta particle energy of 1.5 MeV to that obtained with average energy of 1 MeV.

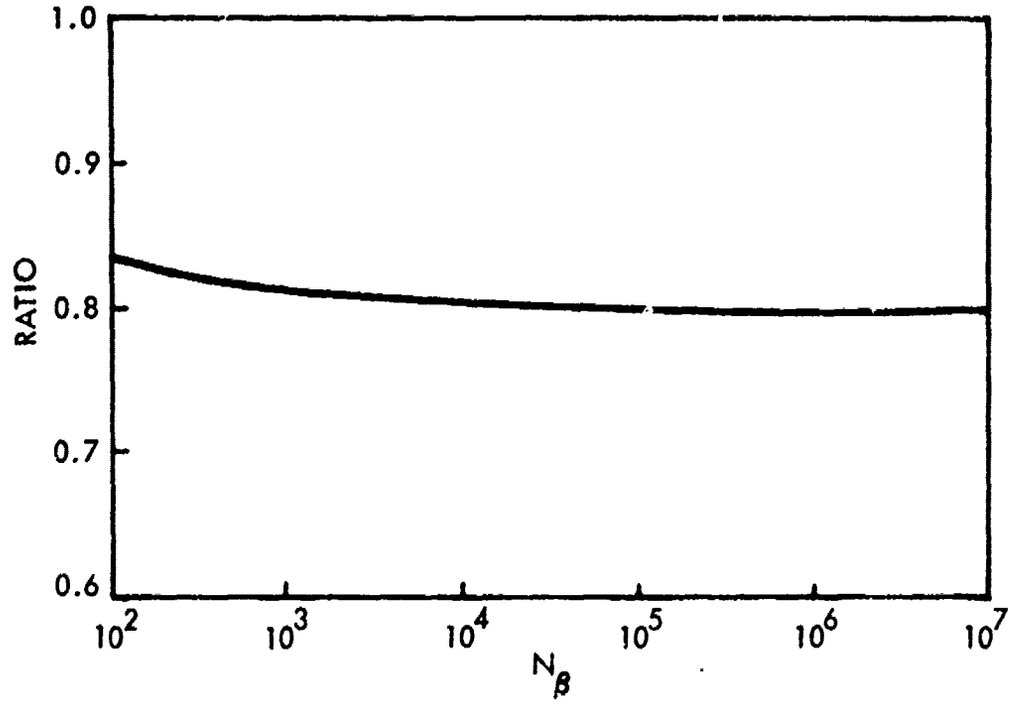

Figure 5-19B. Ratio of beta particle absorption obtained with average beta particle energy of 0.7 MeV to that obtained with average energy of 1 MeV.

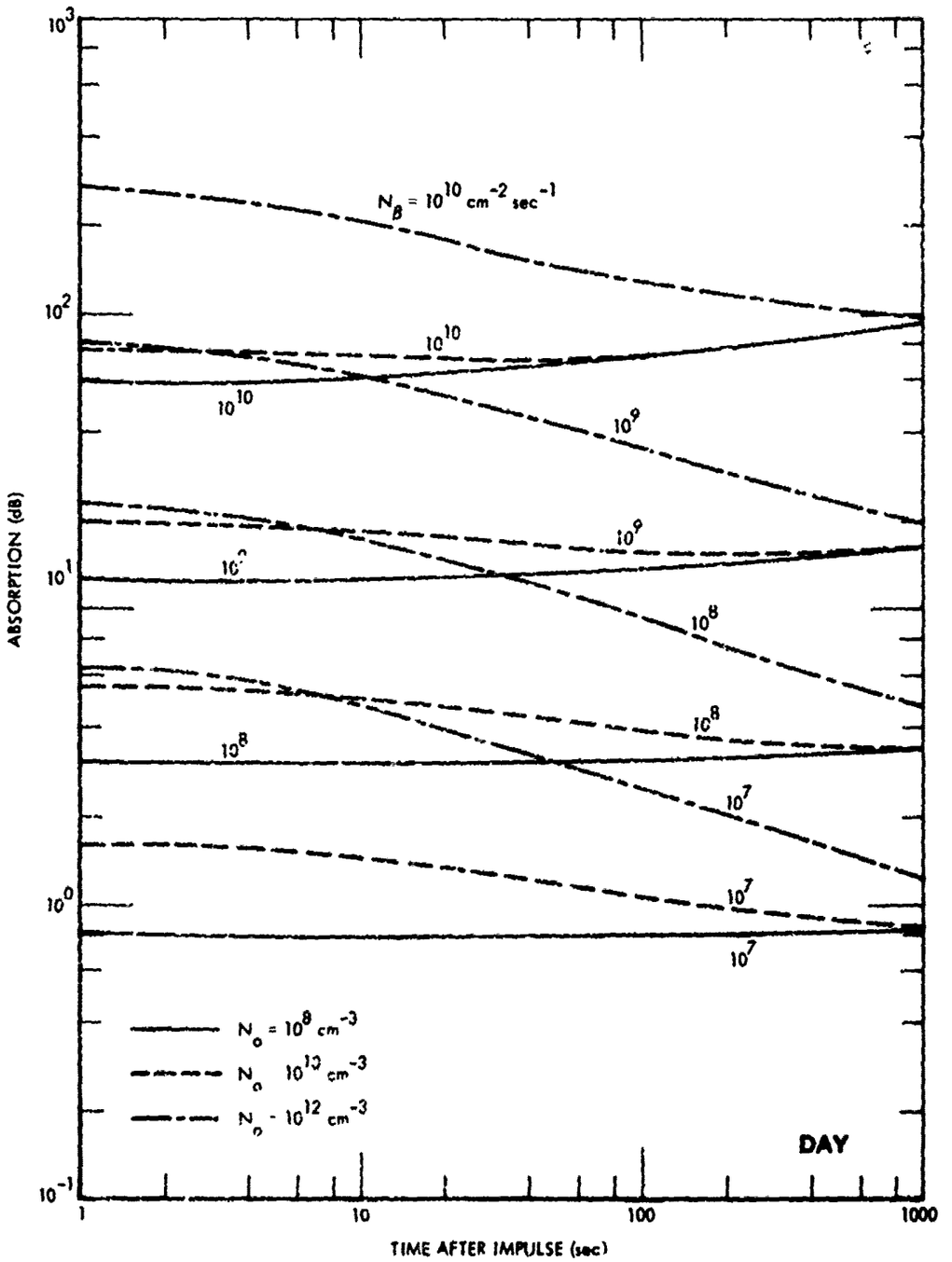

Figure 5-20. Effect of prompt radiation on the one-way vertical absorption caused by beta particles.

EQUATIONS DEFINING d AND θ

$$d = R \sin \xi$$

where R is the slant range to the fireball center, and

$$\cos \xi = \cos \epsilon_{fb} \cos \epsilon_{ray} \cos \alpha + \sin \epsilon_{fb} \sin \epsilon_{ray}$$

where

ϵ_{fb} = elevation angle of fireball center,

ϵ_{ray} = elevation angle of ray path, and

α = azimuth separation between fireball center and ray path.

Neglecting the curvature of the earth, the angle θ may be computed as

$$\sin \theta = \frac{R}{d} (\cos \xi \sin \epsilon_{ray} - \sin \epsilon_{fb})$$

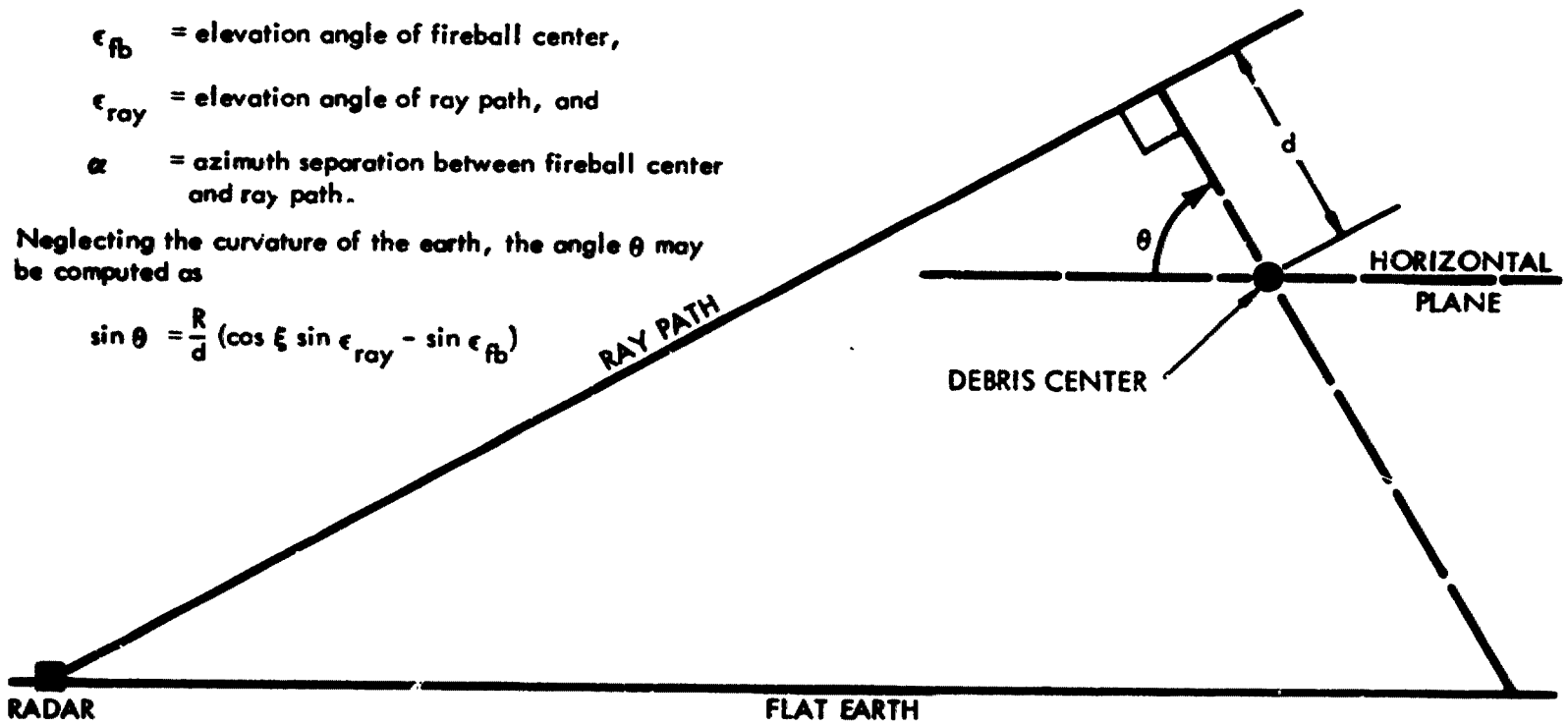

Figure 5-21. Geometry for gamma ray absorption calculations.

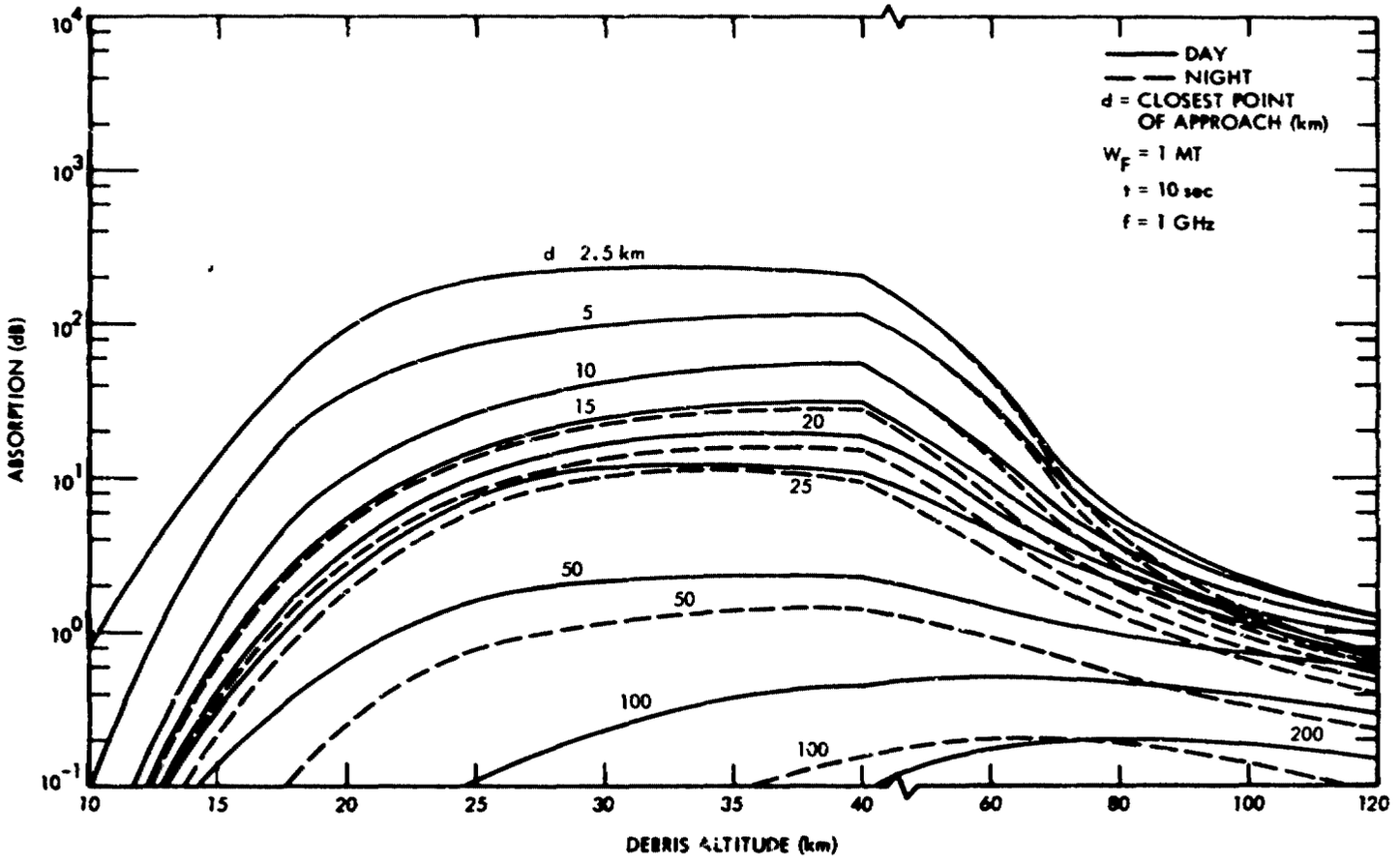

Figure 5-22A. One-way absorption due to gamma rays, θ = +60 degrees.

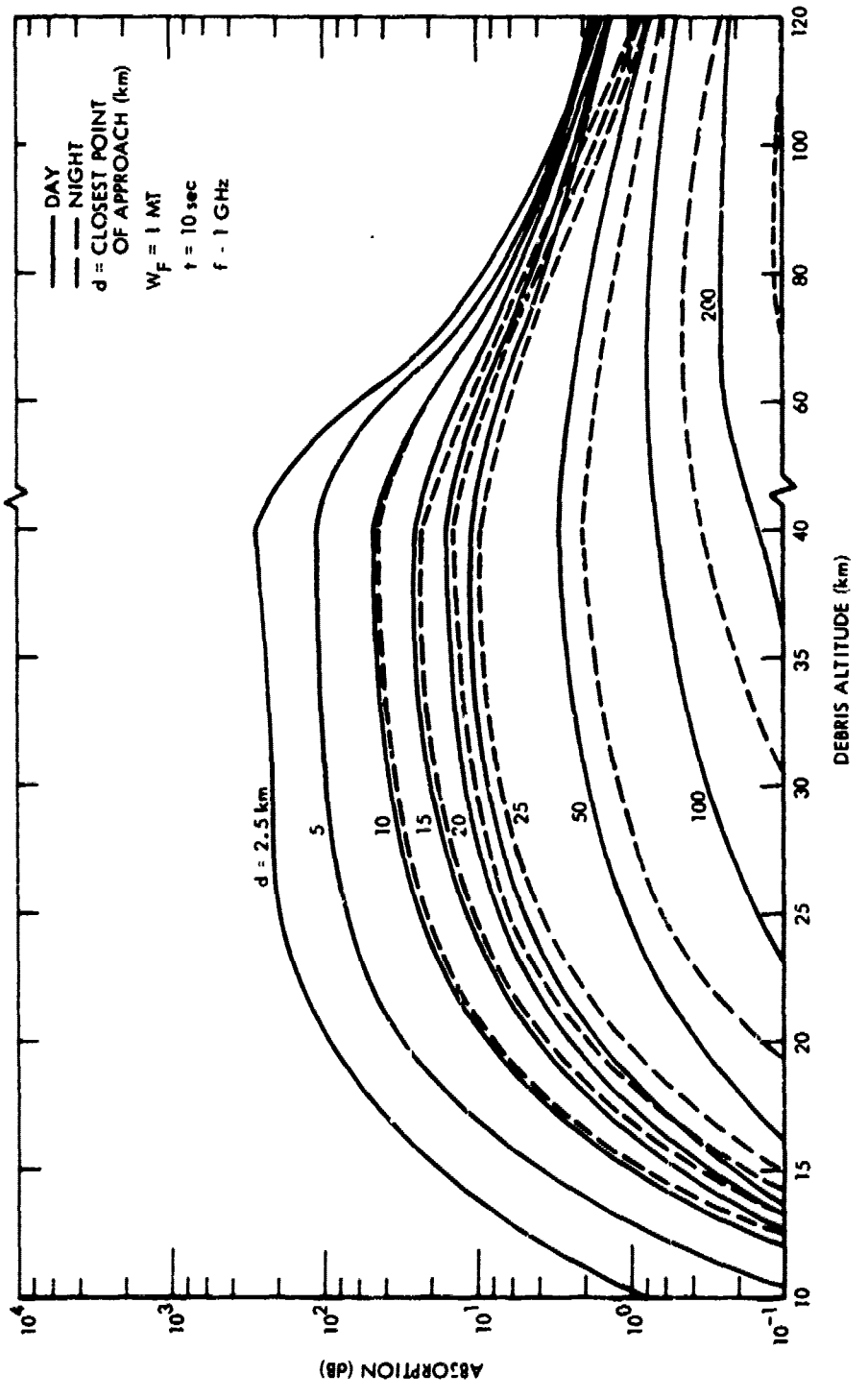

Figure 5-22B. One-way absorption due to gamma rays, θ = +30 degrees.

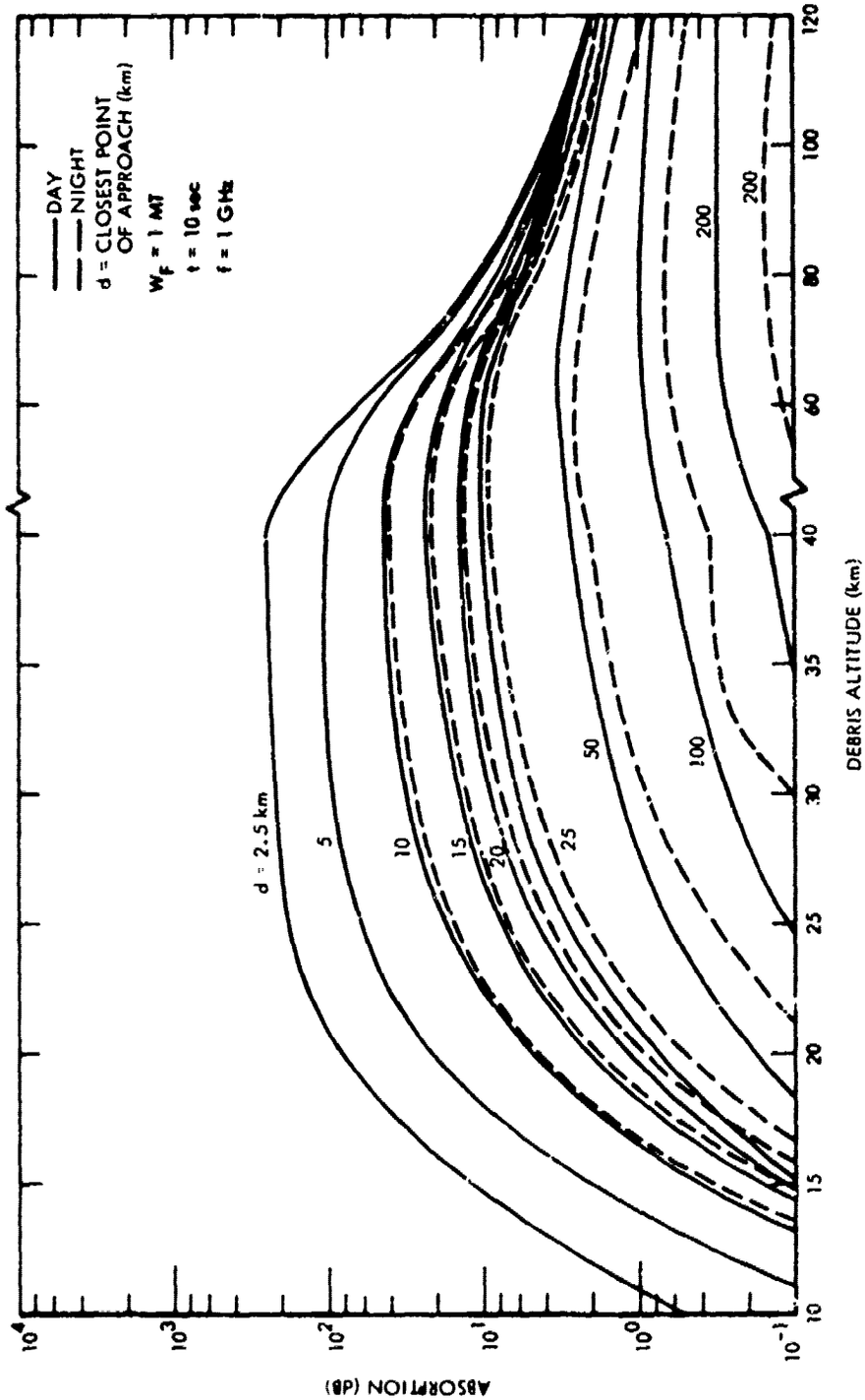

Figure 5-22C. One-way absorption due to gamma rays, $\theta = 0$ degrees.

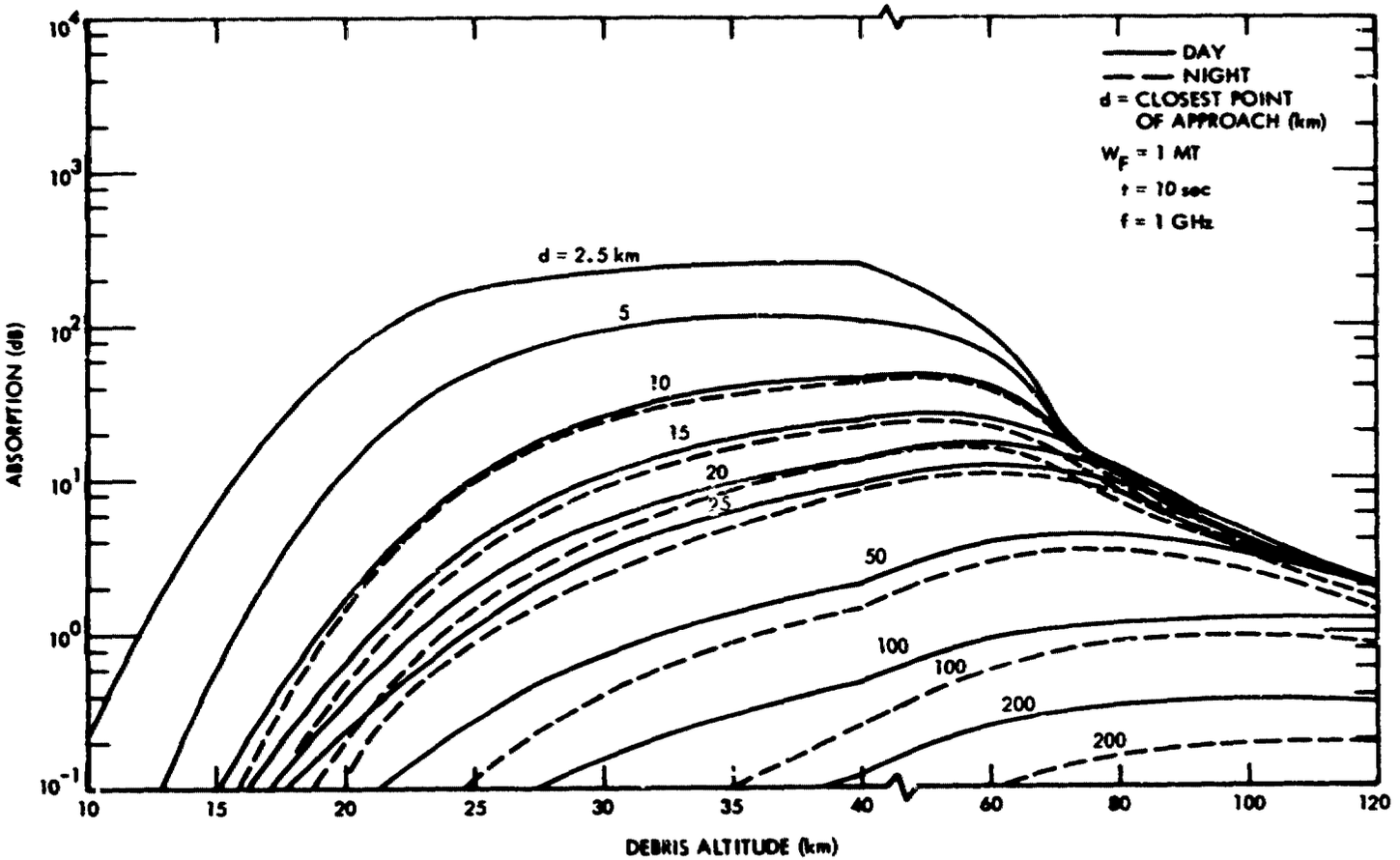

Figure 5-22D. One-way absorption due to gamma rays, θ = - 30 degrees.

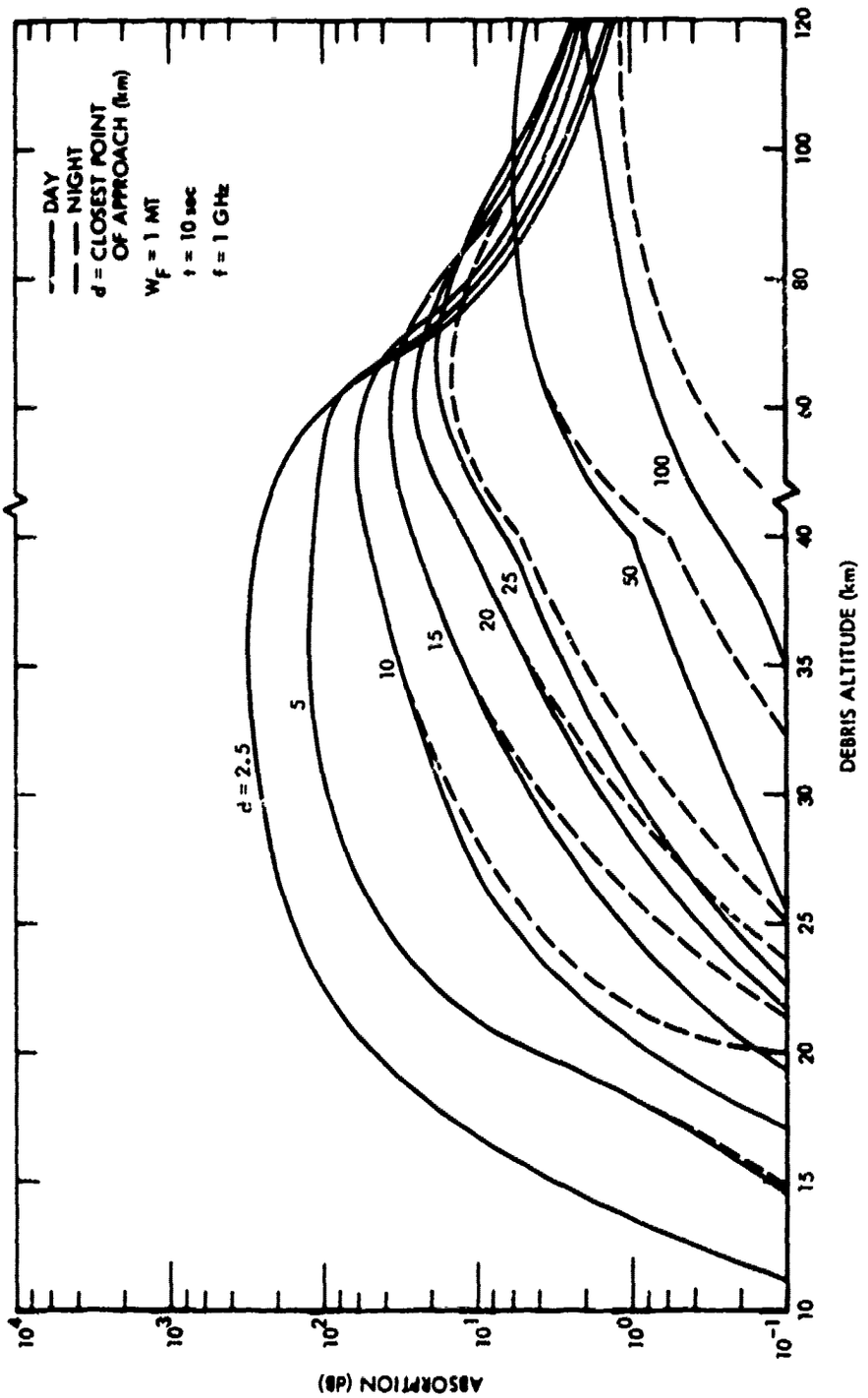

Figure 5-22E. One-way absorption due to gamma rays, $\theta = -60$ degrees.

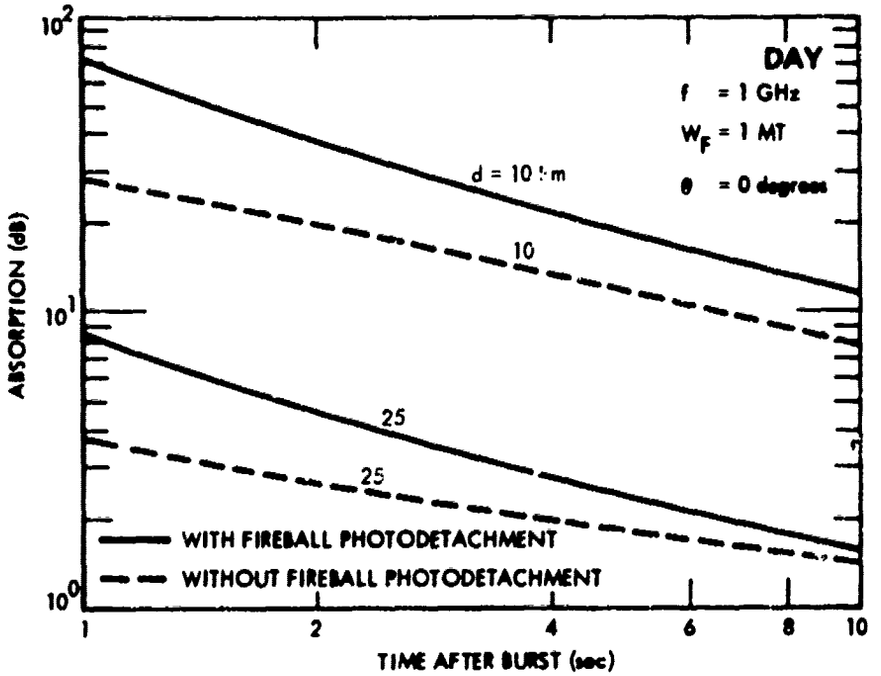

Figure 5-23A. One-way absorption due to gamma rays, 1-MT burst at 20 km.

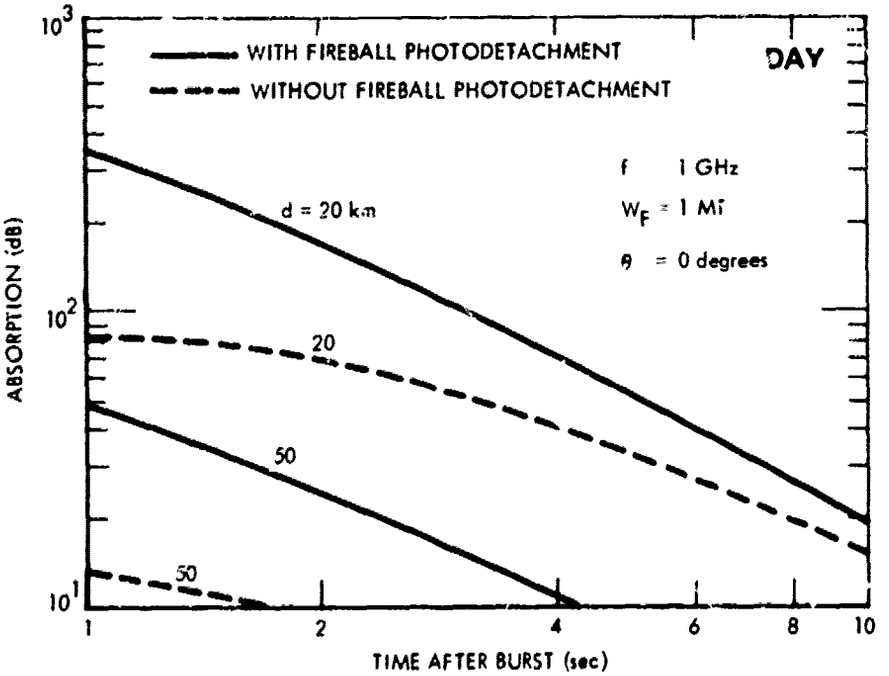

Figure 5-23B. One-way absorption due to gamma rays, 1-MT burst at 40 km.

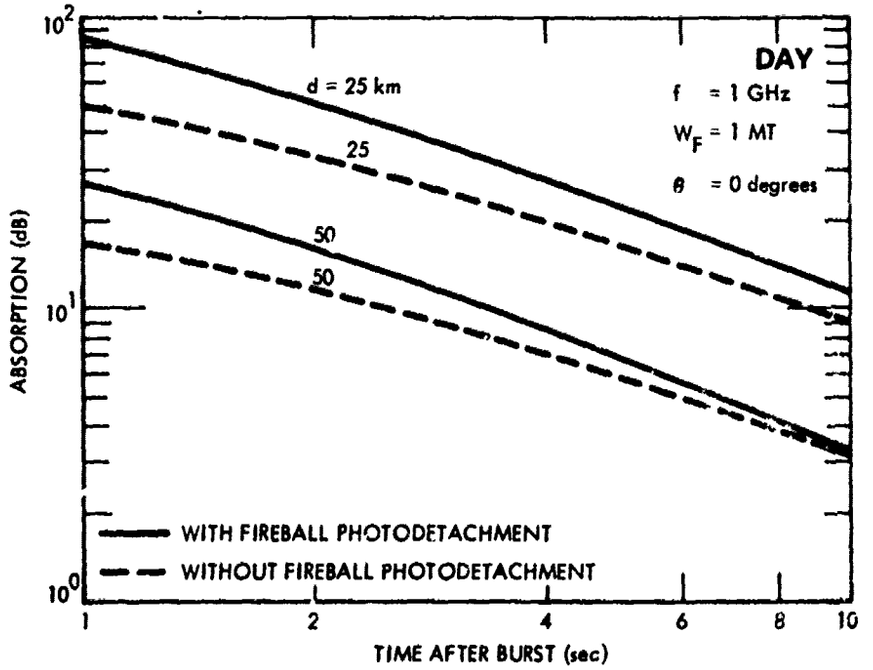

Figure 5-23C. One-way absorption due to gamma rays, 1-MT burst at 60 km.

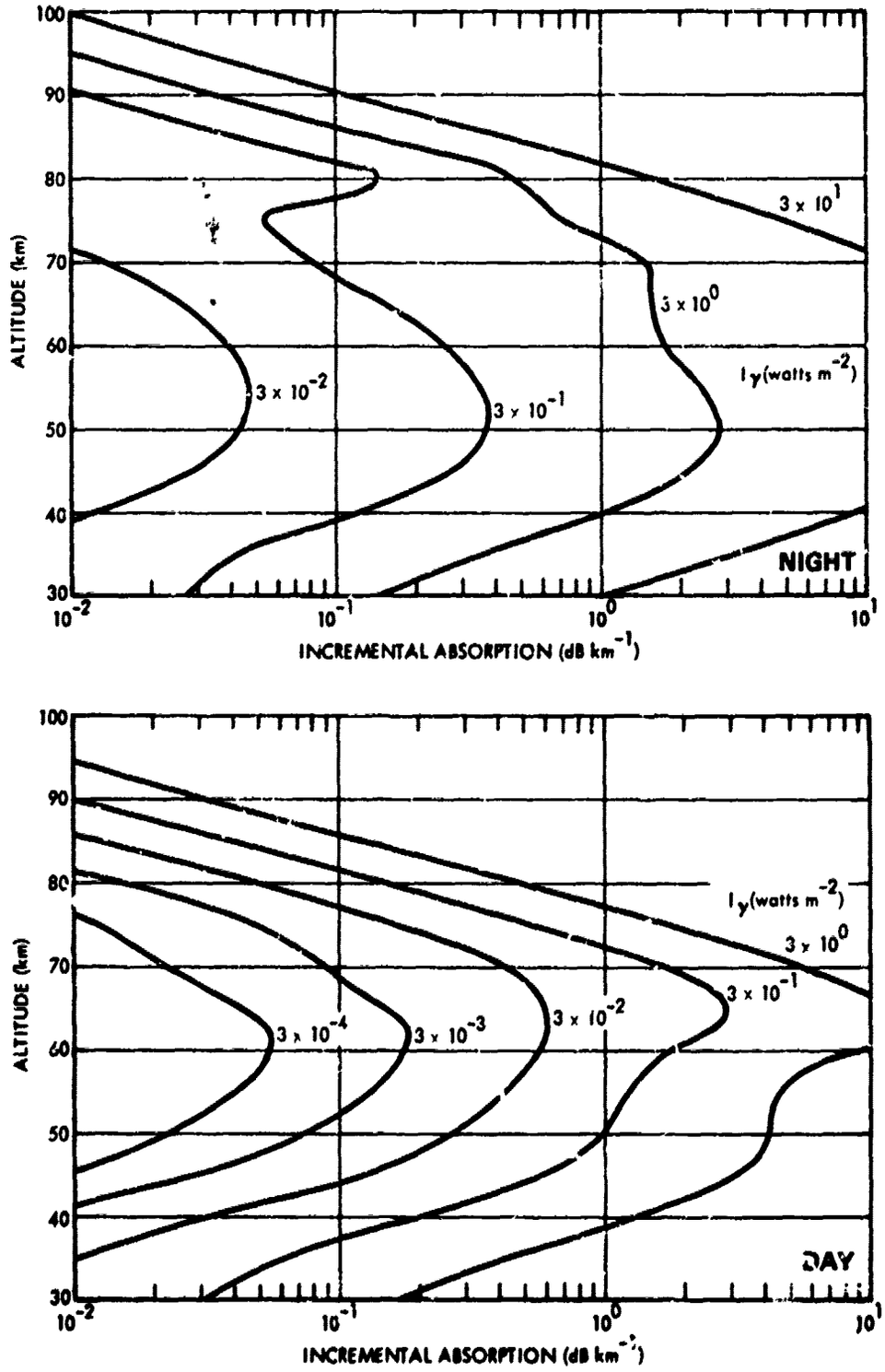

Figure 5-24. Incremental absorption due to gamma rays, f = 30 MHz.

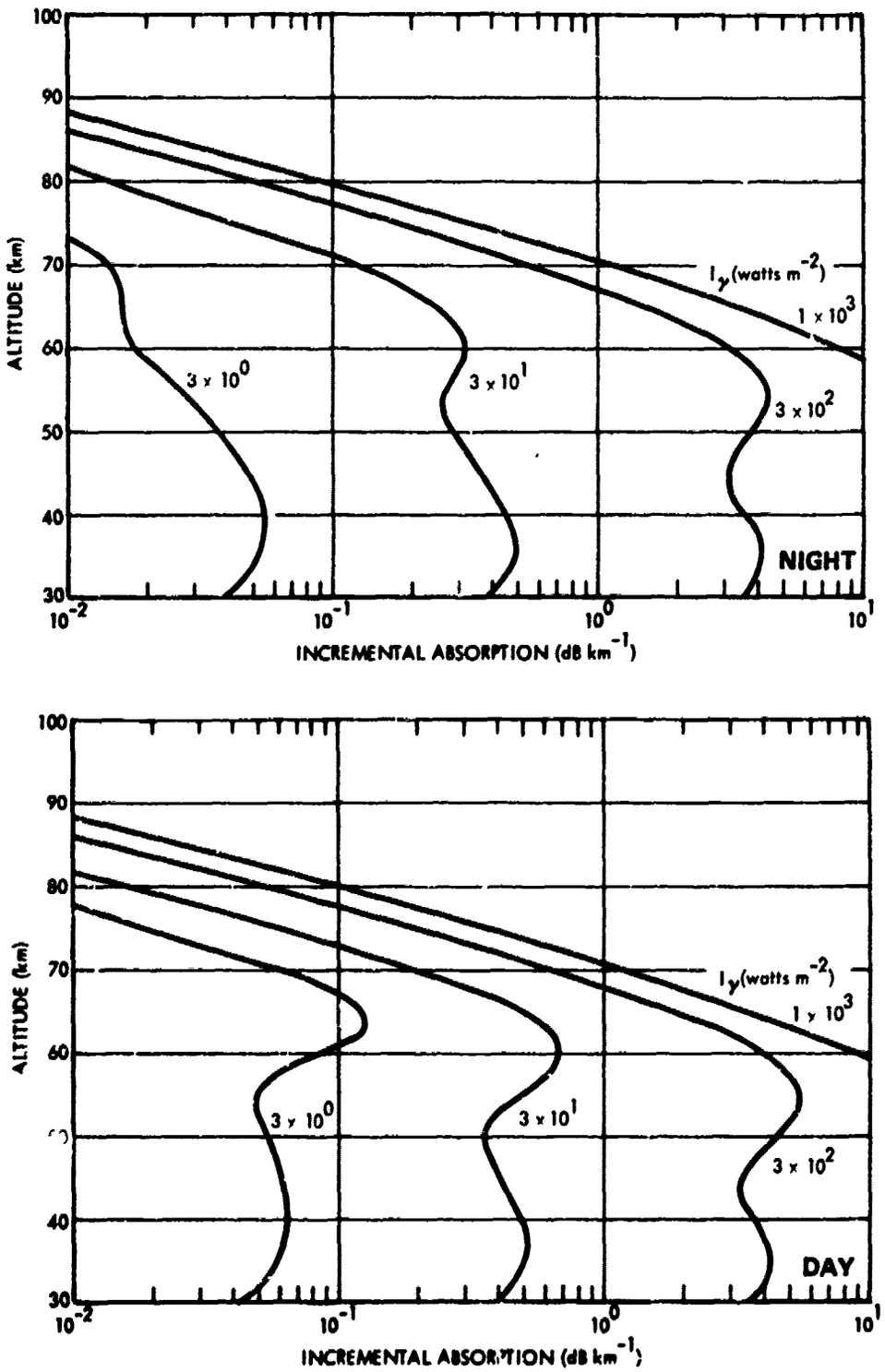

Figure 5-25. Incremental absorption due to gamma rays, f = 300 MHz.

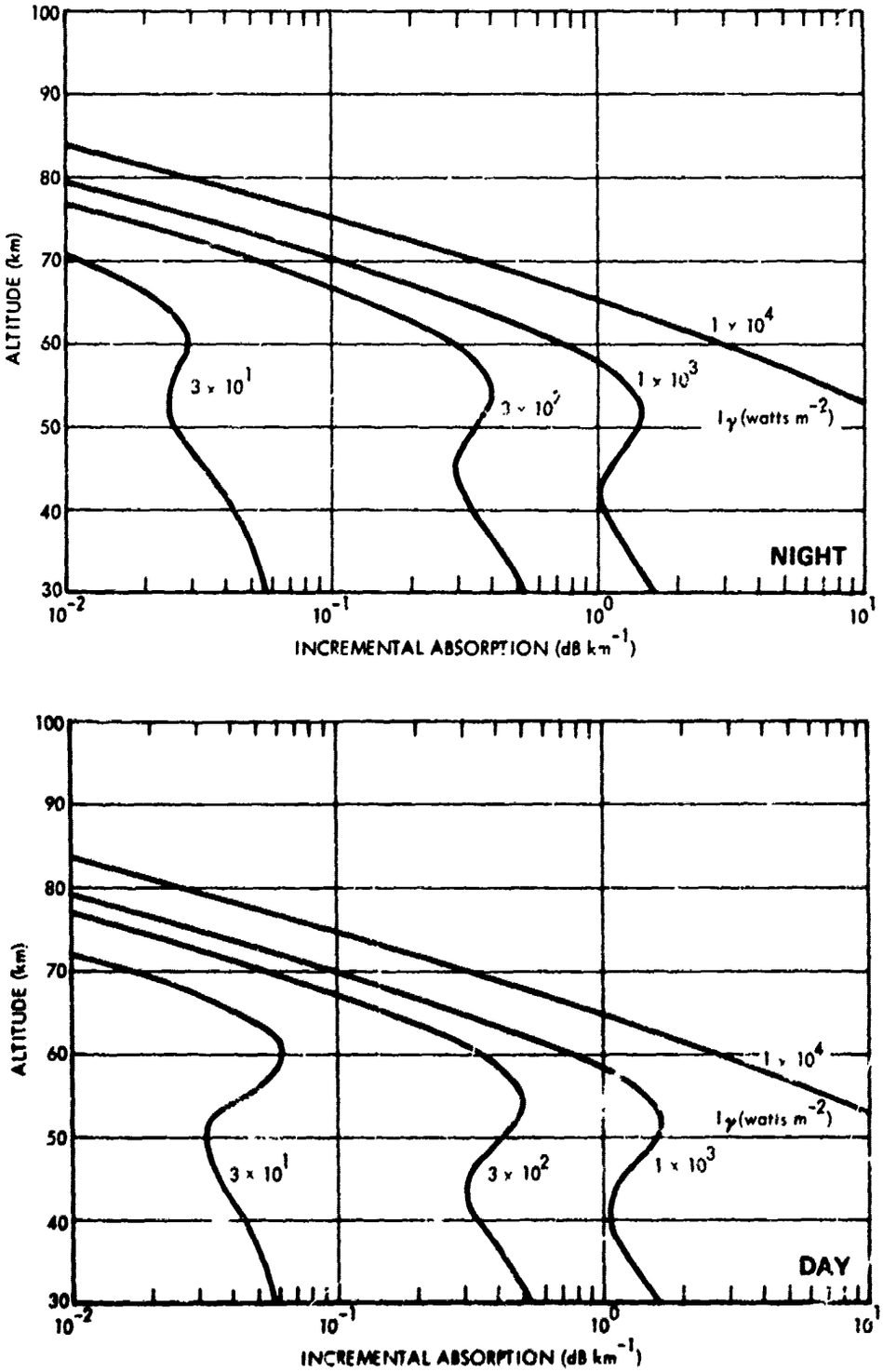

Figure 5-26. Incremental absorption due to gamma rays, f = 1 GHz.

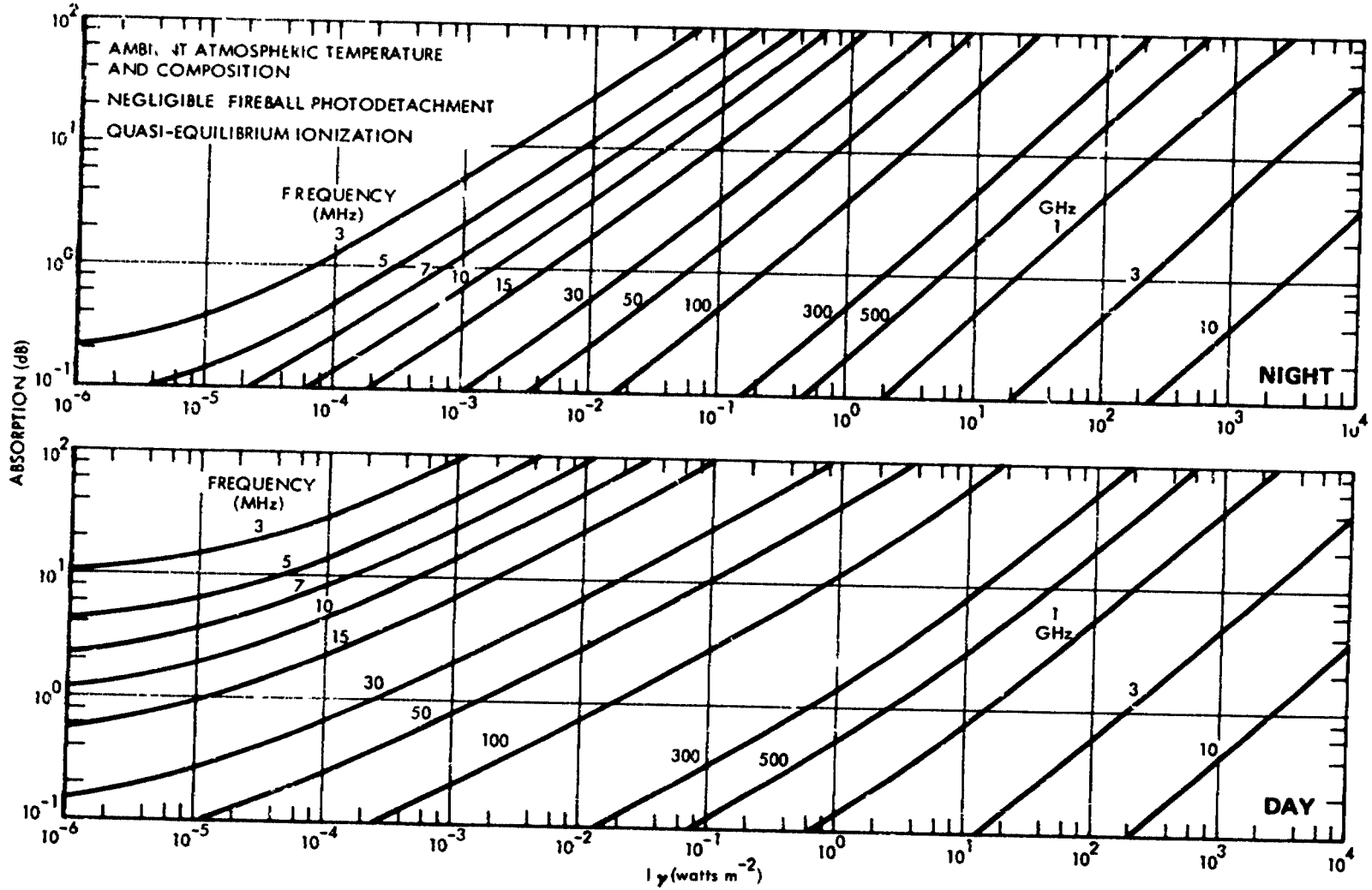

Figure 5-27. One-way vertical absorption due to gamma rays.

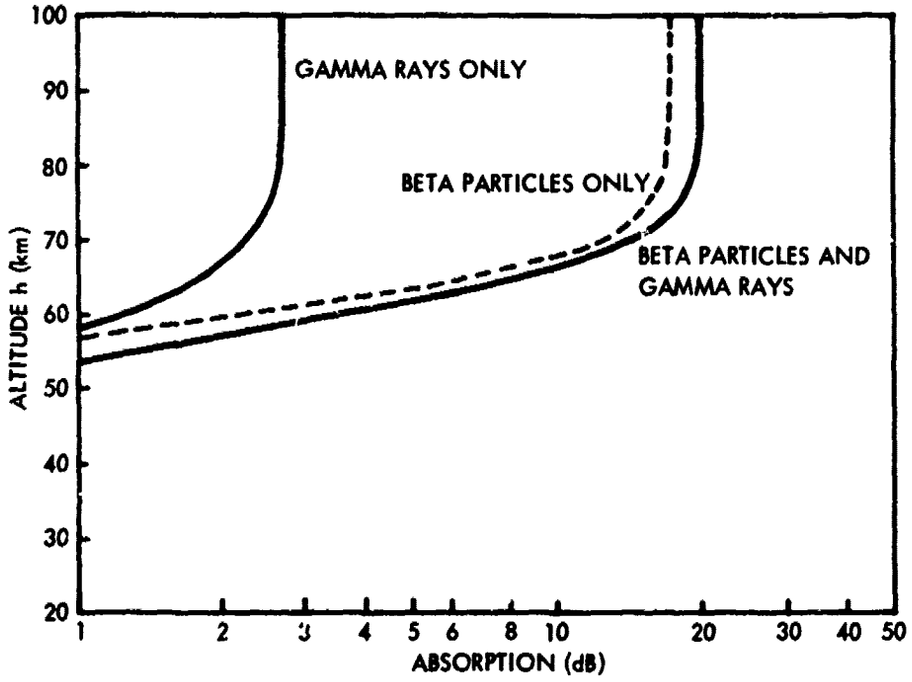

Figure 5-28. Comparison of integrated absorption up to altitude h due to beta and gamma radiation.

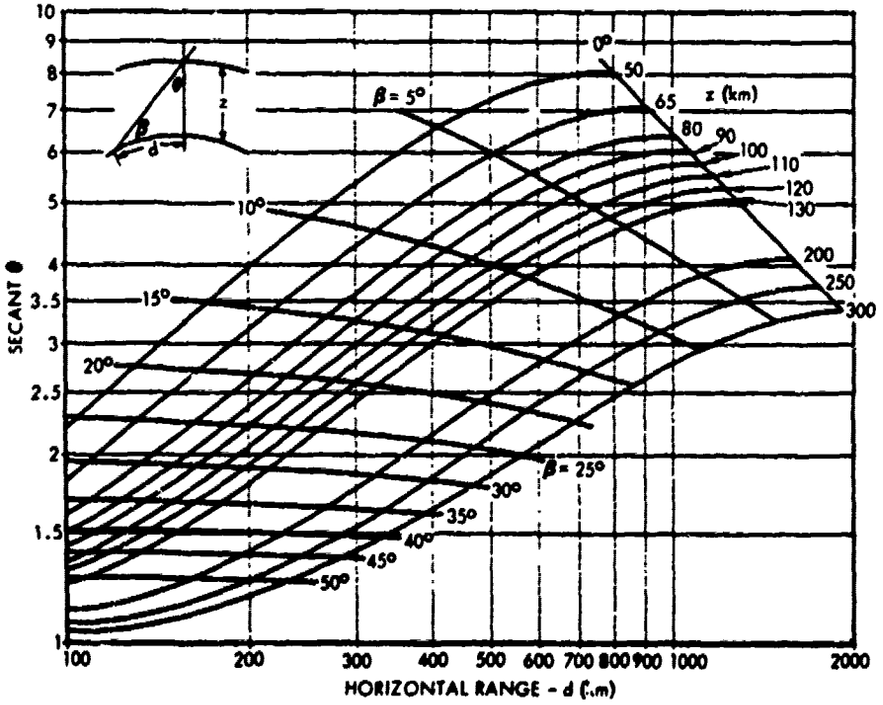

Figure 5-29. Secant θ chart.

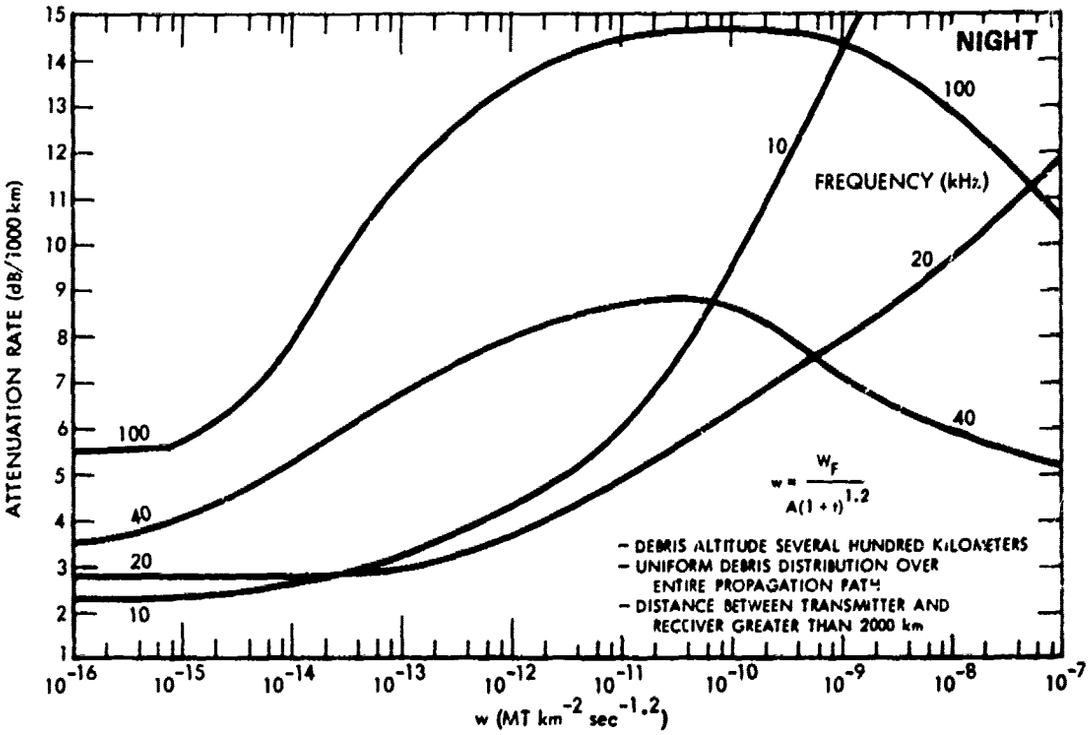

Figure 5-30. VLF and LF attenuation rate due to delayed radiation from high-altitude spread debris, nighttime.

21

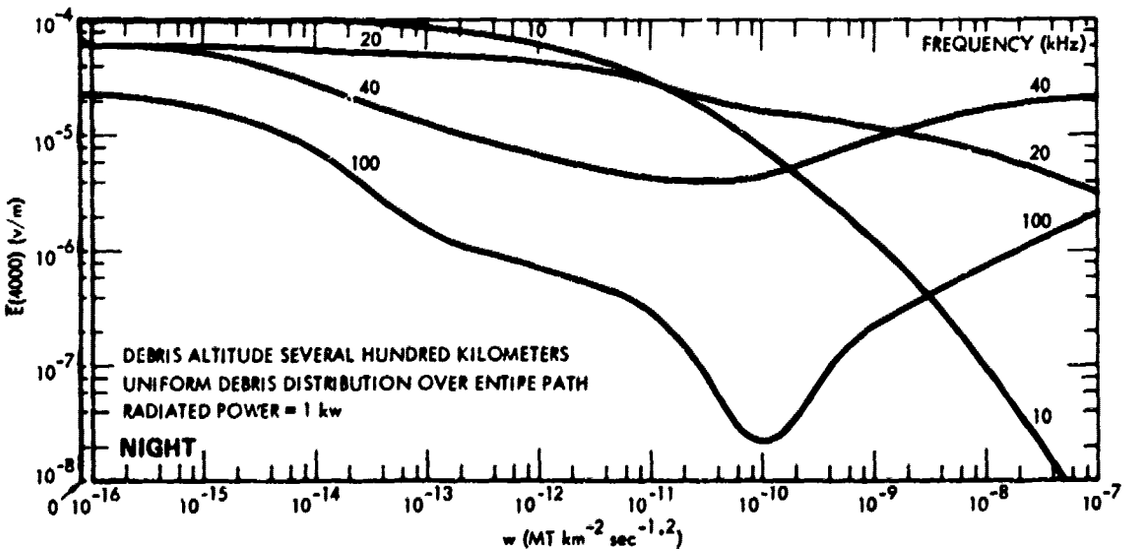

Figure 5-31. VLF and LF RMS electric field strength for 4000-km path, nighttime high-altitude spread-debris environment.

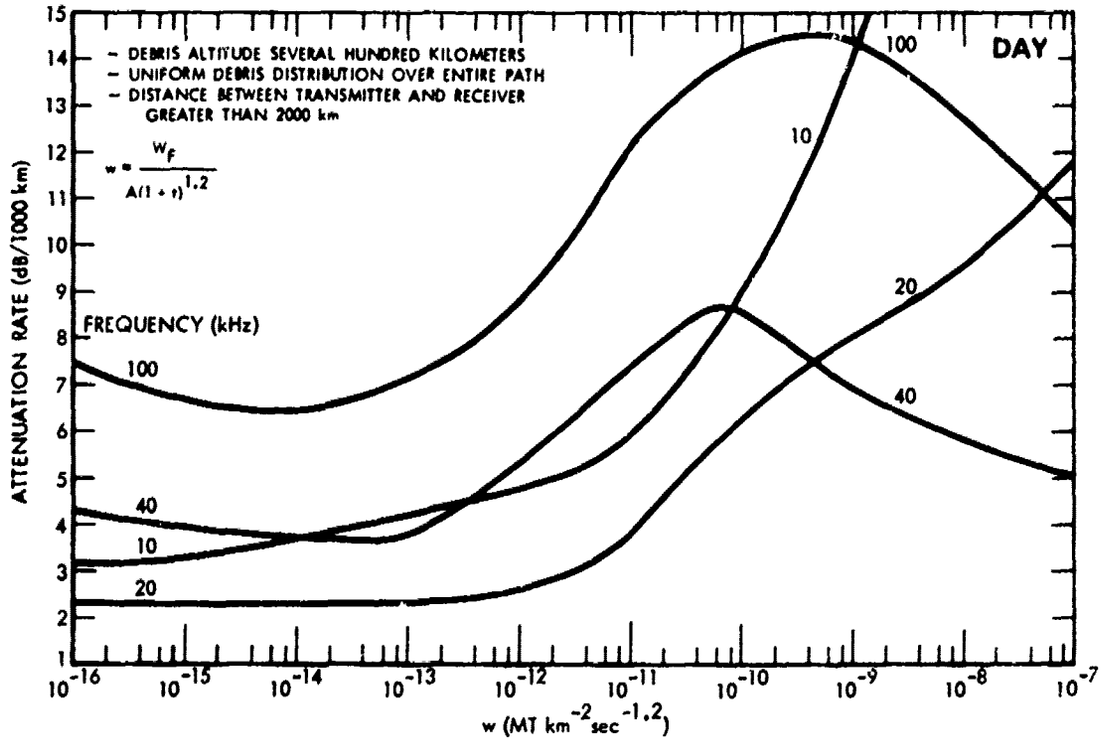

Figure 5-32. VLF and LF attenuation rate due to delayed radiation from high-altitude spread debris, daytime.

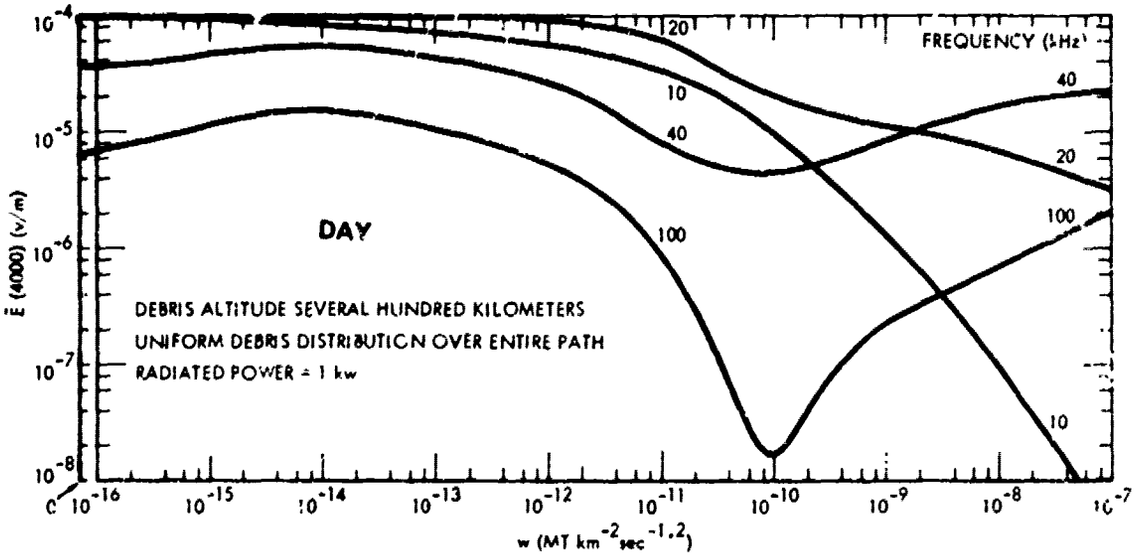

Figure 5-33. VLF and LF electric field strength for 4000-km path, daytime high-altitude spread-debris environment.

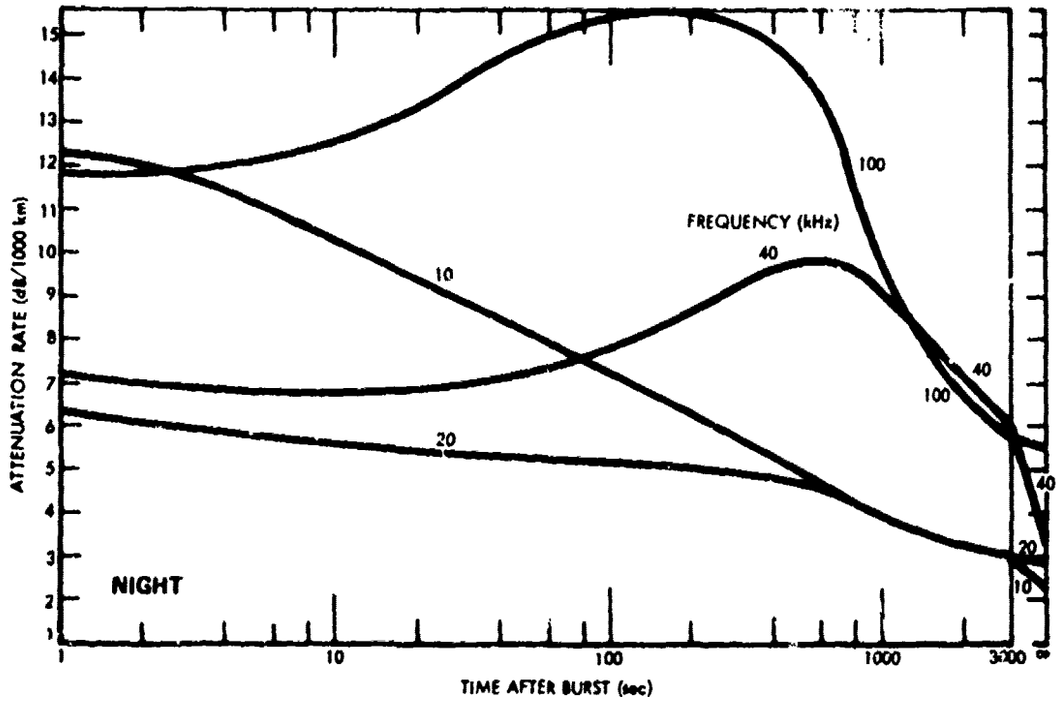

Figure 5-34. VLF and LF attenuation rate due to prompt radiation from a 1-MT burst detonated at 1-earth-radius altitude, nighttime.

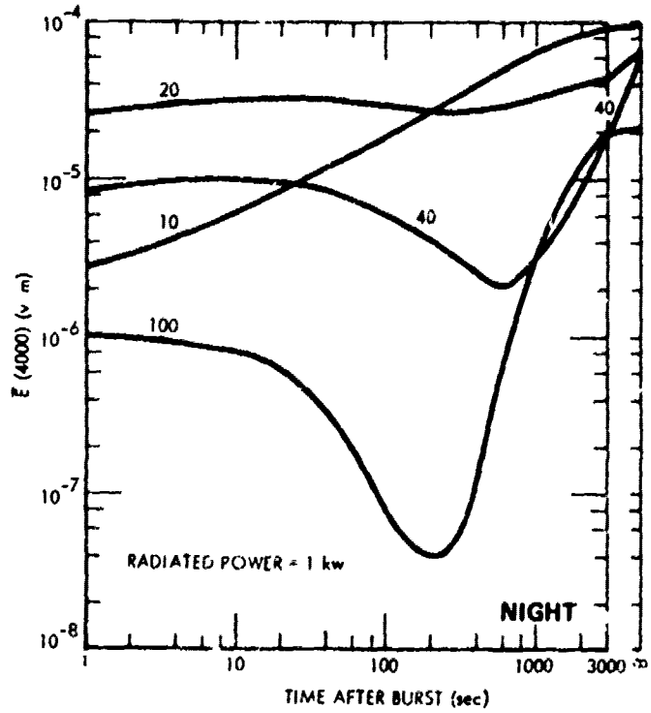

Figure 5-35. VLF and LF electric field strength for 4000-km path, nighttime prompt radiation environment.

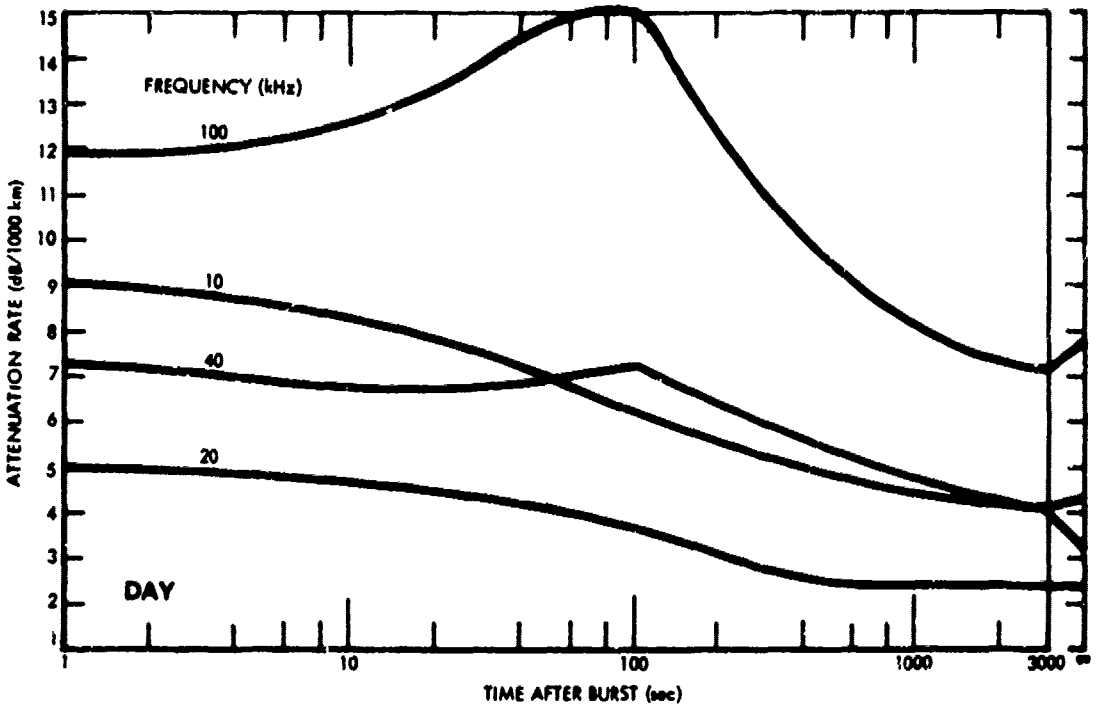

Figure 5-36. VLF and LF attenuation rate due to prompt radiation for 1-MT burst detonated at 1-earth-radius altitude, daytime.

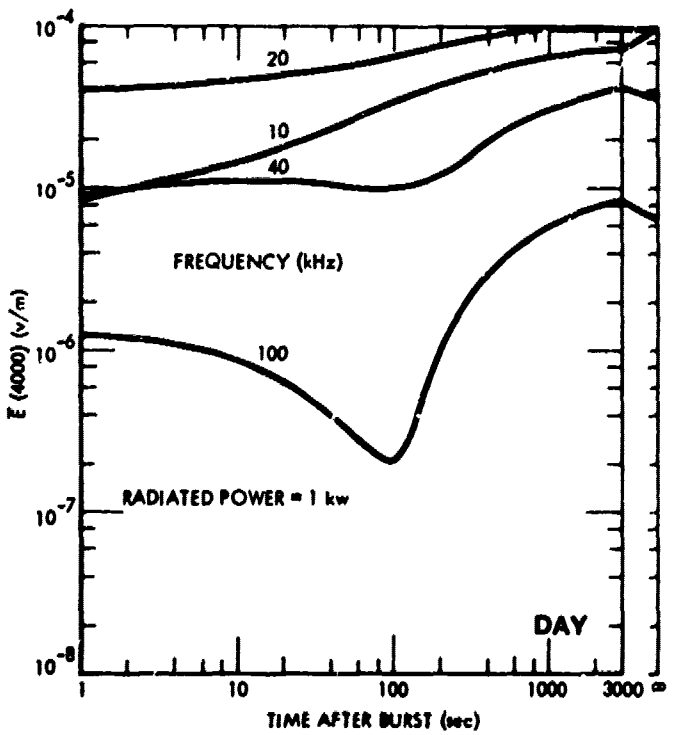

Figure 5-37. VLF and LF electric field strength for 4000-km path, daytime prompt radiation environment.

SECTION 6
PHASE EFFECTS

INDEX OF REFRACTION

$$\eta = \mu - \frac{ick}{\omega}$$

$$2\mu^2 = [(1 - A)^2 + B^2]^{1/2} + (1 - A)$$

$$2\left(\frac{ck}{\omega}\right)^2 = [(1 - A)^2 + B^2]^{1/2} - (1 - A)$$

$$A = \frac{\omega_p^2}{(\bar{\nu}_{em})^2 + \omega^2}$$

$$B = \frac{\bar{\nu}_{em}}{\omega} A$$

Electron-ion and ion-neutral collisions and collision-frequency correction factors neglected.

$$\omega_p^2 = (2\pi)^2 (9 \times 10^3)^2 N_e \quad \sec^{-2} \quad .$$

For lossless medium ($\bar{\nu}_{em} = 0$):

$$\eta = \mu$$

$$\mu^2 = 1 - \left(\frac{\omega_p}{\omega}\right)^2 = 1 - \left(\frac{9 \times 10^3}{f}\right)^2 N_e \quad .$$

PHASE AND GROUP VELOCITY

$$v_p = \frac{c}{\mu}$$

$$v_g = \frac{c}{\mu'}$$

$$\mu' = \mu + \omega \frac{d\mu}{d\omega} \quad .$$

For lossless medium ($\bar{\nu}_{em} = 0$):

$$\mu' = \frac{1}{\mu}$$

$$v_g = \mu c$$

$$v_g v_p = c^2 \quad .$$

REFLECTION

Reflection coefficient for normal incidence on sharp boundary separating region 1 (vacuum) and region 2 (plasma):

$$R = \frac{(1 - \mu_2)^2 + \left(\frac{ck_2}{\omega}\right)^2}{(1 + \mu_2)^2 + \left(\frac{ck_2}{\omega}\right)^2} \quad .$$

R versus ν/ω—see Figure 6-1.

Reflection coefficient for normal incidence with

$$N_e(z) = \frac{N_o}{1 + e^{-z/z_o}} \quad .$$

$$R = \left|\frac{1 - \eta_2}{1 + \eta_2}\right|^2 P \quad ,$$

where

$$P = \left|\frac{\Gamma\left[1 + \frac{2\pi i z_o}{\lambda}(\eta_2 + 1)\right]}{\Gamma\left[1 + \frac{2\pi i z_o}{\lambda}(\eta_2 - 1)\right]}\right|^4$$

η_2 evaluated with $N_e = N_o$ (ie, $z = +\infty$). R versus z_o/λ—see Figures 6-3 through 6-5.

REFRACTION (INCREMENTAL BENDING OF RAY PATH)

$$d\Psi(\vec{r}) = \frac{1}{\mu(\vec{r})} \frac{\partial \mu(\vec{r})}{\partial \rho} ds \quad \text{radians}$$

$\vec{r}$ = position along path

ρ, s = orthogonal coordinates, s in direction of ray path, ρ normal to ray path

$d\Psi(\vec{r})$ = change in ray direction at position $\vec{r}$.

For lossless medium ($\bar{\nu}_{em} = 0$):

$$d\Psi(\vec{r}) = \left[\frac{1}{1 - \left(\frac{9 \times 10^3}{f}\right)^2 N_e}\right] \frac{(9 \times 10^3)^2}{2f^2} \frac{\partial N_e(\vec{r})}{\partial \rho} ds \quad .$$

RANGE ERRORS

Resulting from change in propagation velocity (neglects errors due to change in path length caused by refraction):

$$\Delta R = \int_o^S \left(\frac{1}{\mu} - 1\right) ds \quad .$$

For $\bar{\nu}_{em} = 0$ and $\omega_p << \omega$.

$$\Delta R \approx \frac{(9 \times 10^3)^2}{2f^2} \int_o^S N_e ds \quad \text{cm} \quad .$$

DOPPLER SHIFT

$$D = \frac{f}{c} \frac{d}{dt} \int_o^S (\mu - 1) ds \quad \text{Hz} \quad .$$

for $\bar{\nu}_{em} = 0$ and $\omega_p << \omega$:

$$D \approx \frac{(9 \times 10^3)^2}{2cf} \frac{d}{dt} \int_o^S N_e ds \quad \text{Hz} \quad .$$

FARADAY ROTATION

$$d\Omega = \frac{1}{2} \frac{\omega}{c} (\mu_o - \mu_x) ds \quad \text{radians}$$

$d\Omega$ = incremental polarization rotation

μ_o, μ_x = real part of index of refraction of ordinary and extraordinary waves, respectively.

For $\bar{\nu}_{em} = 0$, $\omega_p << \omega$, and quasi-longitudinal propagation (f > 40 MHz and propagation not perpendicular to magnetic field):

$$\Omega = \frac{(9 \times 10^3)^2}{2} \frac{\omega_b \cos\theta}{cf^2} \int_o^S N_e \, ds \quad \text{radians}$$

$$\omega_b = \frac{eB}{m} \quad \text{sec}^{-1}$$

B = magnitude of d-c magnetic field (for $e = 1.6 \times 10^{-20}$ and $m = 9 \times 10^{-28}$, B is in gauss)

θ = angle between direction of propagation and magnetic field.

ELECTRON DENSITY INTEGRALS AND RELATED ABSORPTION

Prompt radiation—see Figure 6-5.

Delayed gamma rays—see Figure 6-6.

Beta particles—see Figure 6-7.

Fireball region above 100 km (electron density and temperature assumed uniform) losses from electron-ion collisions—see Figure 6-8.

BEARING AND RANGE ERRORS FOR PLANE STRATIFICATION

Geometry—see Figure 6-9.

Ray path equation:

$$\frac{dx}{dh} = \frac{\sin\theta_o}{\sqrt{\mu^2(h) - \sin^2(\theta_o)}}$$

Reflection condition ($\bar{\nu}_{em} = 0$):

$$N_e = \left(\frac{\cos\theta_o \, f}{9 \times 10^3}\right)^2 \quad \text{cm}^{-3} \; .$$

Bearing error—see Figure 6-10.

$$\Delta\theta \approx \frac{\tan \theta_o}{2\omega^2 h_T} (9 \times 10^3)^2 \int_o^{h_T} N_e \, dh \quad \text{radians} \quad .$$

This equation neglects second-order terms; the error is less than 25 percent for

$$\omega \geq \frac{2\omega_p}{\cos \theta_o} \quad .$$

Range error—see Figure 6-10:

$$\Delta R \approx R_T \cos \theta_o \, \Delta\theta \quad .$$

Bearing and range errors as function of absorption:

$$\Delta\theta \approx \frac{3 \times 10^6 \tan \theta_o}{\bar{\nu}_{em} \cos \theta_o} \frac{A}{h_T} \quad \text{degrees}$$

$$\Delta R \approx \frac{5 \times 10^4 \, A}{\bar{\nu}_{em} \cos^2 \theta_o} \quad \text{km}$$

$\bar{\nu}_{em}$ = electron-neutral collision frequency at center of electron density integral

A = one-way absorption (dB)

h_T = target altitude (km).

BEARING AND RANGE ERRORS FOR SPHERICAL STRATIFICATION

Geometry—see Figure 6-11.

Ray path equation:

$$\frac{d\beta}{dr} = \pm \frac{K}{r\sqrt{\mu^2 r^2 - K^2}} \quad .$$

$K = \mu(r) \, r \sin \phi =$ constant.

ϕ = angle between ray path and radius vector $\vec{r}$.

Bearing error:

$$\Delta\theta = \Psi - \sin^{-1}\frac{R_o}{R_T}\left[\sin(\Psi + \phi_o) - \sin\phi_o\right] \quad .$$

For Ψ and $\Delta\theta$ less than about 10 degrees:

$$\Delta\theta = \Psi\left(1 - \frac{R_o}{R_T}\right) \quad .$$

Ψ—see Figures 6-12 and 6-13.

Range errors—see Figures 6-12 and 6-13.

Bearing and range errors as functions of absorption for n = 10—see Figure 6-12:

$$\Psi \approx \frac{10^7 A}{\bar{\nu}_{em} r_o} \text{ degrees}$$

$$\Delta R \approx \frac{2 \times 10^4 A}{\bar{\nu}_{em}} \text{ km}$$

$\bar{\nu}_{em}$ = electron-neutral collision frequency in absorption region

A = one-way path absorption (dB)

r_o = closest point of approach (km).

DISPERSION AND PULSE DISTORTION

For a gaussian pulse initially given by

$$f(t) = A_o \exp\left[-\frac{t^2}{2\sigma^2} + i\omega t\right] \quad .$$

After propagating through an ionized medium for which $(\omega/\omega_p)^2 >> 1$.

A_D/A_o—see Figure 6-14.

σ_D/σ_o—see Figure 6-14.

Note: $\Delta f = 1/4\sigma$ is bandwidth of transmitted signals.

SCATTERING-RADAR EQUATION

Neglecting multiple scattering the radar equation can be written as

$$P_R = \int_{\phi=0}^{2\pi}\int_{\theta=0}^{\pi}\int_{s=0}^{\infty}\left[\frac{P_T G_T(\theta,\phi)}{4\pi s^2} e^{-\int_0^s \alpha_T(r,\theta,\phi)\, dr}\right]$$

$$\cdot\left[\sigma_v(s,\theta,\phi)s^2 \sin\theta\, d\theta\, d\phi\, ds\right]\left[\frac{e^{\int_s^0 \alpha_T'(r,\theta,\phi)\, dr}}{4\pi s^2}\right]\left[\frac{\lambda^2 G_R(\theta,\phi)}{4\pi}\right]$$

where s, θ and ϕ are spherical coordinates with the origin at the radar. When the distance to the scattering region, d, is much greater than the spatial extent of the scatterer, Δd,

$$P_R \approx \frac{\lambda^2 P_T}{(4\pi)^3 d^2}\int_0^{2\pi}\int_0^{\pi} G_T(\theta,\phi)G_R(\theta,\phi)e^{-2L(\theta,\phi)}\sigma_s(\theta,\phi) \sin\theta\, d\theta\, d\phi$$

$$L(\theta,\phi) = \int_0^d \alpha_T(r,\theta,\phi)\, dr$$

$$\sigma_s(\theta,\phi) = \int_d^{d+\Delta d} \sigma_v(s,\theta,\phi)e^{-2\int_d^s \alpha_T(r,\theta,\phi)\, dr}\, ds \quad m^2/m^2 \quad .$$

For L independent of θ and ϕ and for a system with pulse compression F,

$$P_R = \frac{P_T\lambda^2 F}{(4\pi d)^2}\sigma_E 10^{-\Lambda_p/5}\int\int_{\Omega}\frac{G_T(\theta,\phi)G_R(\theta,\phi)}{4\pi}\sin\theta\, d\theta\, d\phi$$

$$\sigma_E = \frac{\int_0^{2\pi}\int_0^{\pi} G_T G_R e^{-2L}\sigma_s(\theta,\phi) \sin\theta\, d\theta\, d\phi}{\int\int_{\Omega} G_T G_R \sin\theta\, d\theta\, d\phi} \quad ,$$

where Ω is the solid angle subtended by the scattering region when viewed from the radar.

Normalized backscatter coefficient for a spherical particle versus normalized circumference—see Figure 6-15.

Surface scattering is important for large electron density gradients and overdense plasmas. Both surface and volume scattering may become aspect sensitive at high altitudes because of magnetic field interaction.

Uncertainty: Surface scattering coefficient models do not generally include the effect of homogeneities and are a sensitive function of the assumed electron gradient scale length, especially when the scale length and radio wavelength are comparable.

SCINTILLATION FROM STRIATIONS

Striations cylindrical, aligned with ambient magnetic field and contained in a planar region (see Figure 6-16 for geometry). The electron density is given by

$$N_e(\rho) = N_o \exp[-\rho^2/\sigma_o^2] - \bar{N}_{eb} \quad .$$

RMS phase fluctuation for a wave passing through striated region:

$$\Delta\phi_{rms} = \left(\frac{\sqrt{2}\pi}{3}\right)^{1/2} \left(\frac{\pi N_o \sigma_o}{\lambda N_c}\right) \sqrt{2\sigma_o DN_A \csc\alpha} \text{ radians}$$

$$N_c = \left(\frac{9 \times 10^3}{f}\right)^2 \text{ cm}^{-3}$$

Range of $\Delta\phi_{rms}$—see Figure 6-17.

Angular fluctuation at phase screen:

$$\Delta\theta_{rms} = \frac{\lambda}{2.62\pi\sigma_o} \Delta\phi_{rms} \quad .$$

Angular fluctuation at receiver,

$$\Delta\psi_{rms} = \frac{S_T - S_S}{S_T} \Delta\theta_{rms} \quad .$$

Range error,

$$\Delta R_{rms} = \frac{\lambda}{2\pi} \Delta\phi_{rms} + \frac{1}{2} S_S \Delta\theta_{rms} \Delta\psi_{rms}$$

the amplitude fluctuations,

$$\overline{\left(\frac{\Delta A}{A}\right)^2} = \min(1, \Delta\phi_{rms}^2) \begin{cases} 1 & Z, Z_f' \gg Z_f' \\ \dfrac{\left(\dfrac{ZZ'}{Z+Z'}\right)^2}{Z_f'^2} & Z \text{ or } Z' \ll Z_f' \end{cases}$$

$$Z = S_S \quad ,$$

$$Z' = S_T - S_S \quad ,$$

$$Z_f' = \frac{\ell_\theta^2}{\lambda \max(1, (\Delta\phi_{rms})^2)} \quad .$$

Doppler fluctuation

$$\Delta\phi_{rms} = \frac{1}{2\pi} V_\perp \frac{\Delta\phi_{rms}}{\sigma_o} \quad .$$

Beam spread loss

$$\frac{I'}{I_o} \approx \frac{\gamma}{2\Delta\Psi_{rms}}$$

SCINTILLATION EFFECTS ON BINARY PSK COMMUNICATION SYSTEM

Probability of bit error versus energy (signal) to noise ratio—see Figures 6-18 and 6-19.

Demodulation signal loss for binary PSK versus T_D/T_S—see Figure 6-20.

Uncertainty: The prediction for the phase and amplitude are a sensitive function of the model used for calculating the inhomogeneities associated with the striated medium. The bit error probabilities and the demodulation signal loss predictions are further dependent on the type and parameters of the signal processing technique. The latter can be seen in the differences between Figures 6-18 and 6-19.

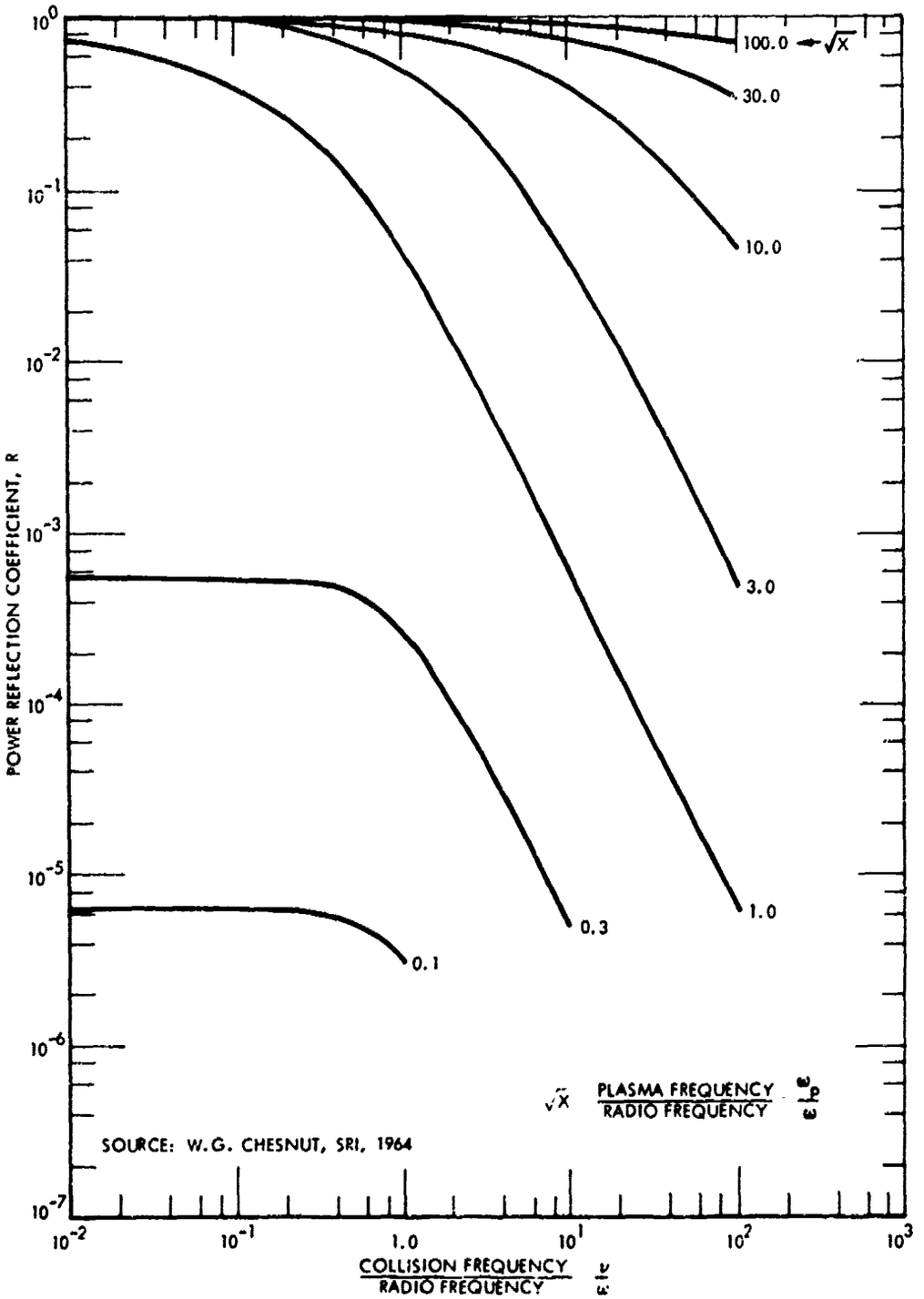

Figure 6-1. Power reflection coefficient versus collision frequency for various plasma electron densities at a vacuum-plasma interface, Appleton-Hartree theory used, with no magnetic field.

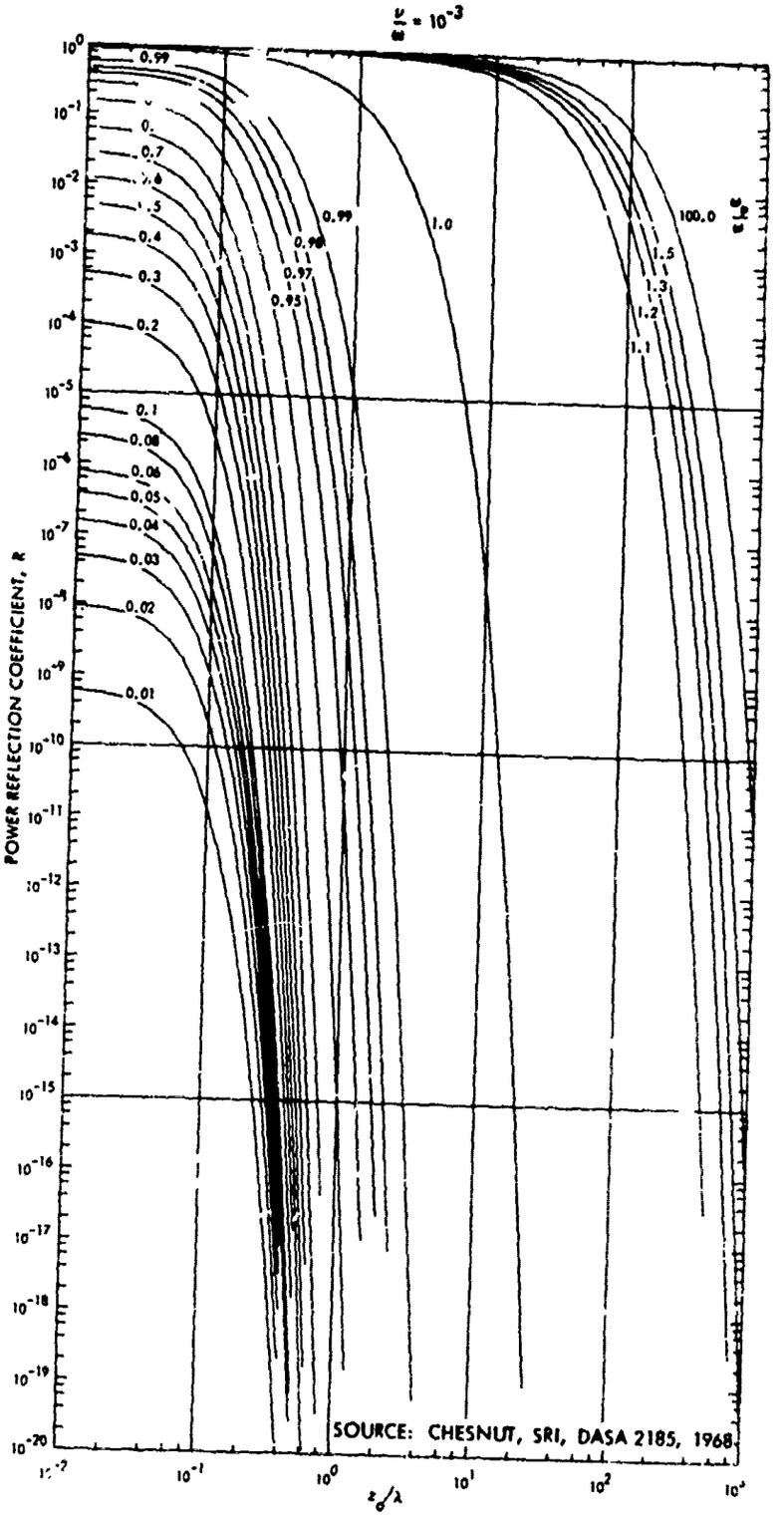

Figure 6-2. Power reflection coefficient versus the ratio z_o/λ for $\frac{\nu}{\omega} = 10^{-3}$.

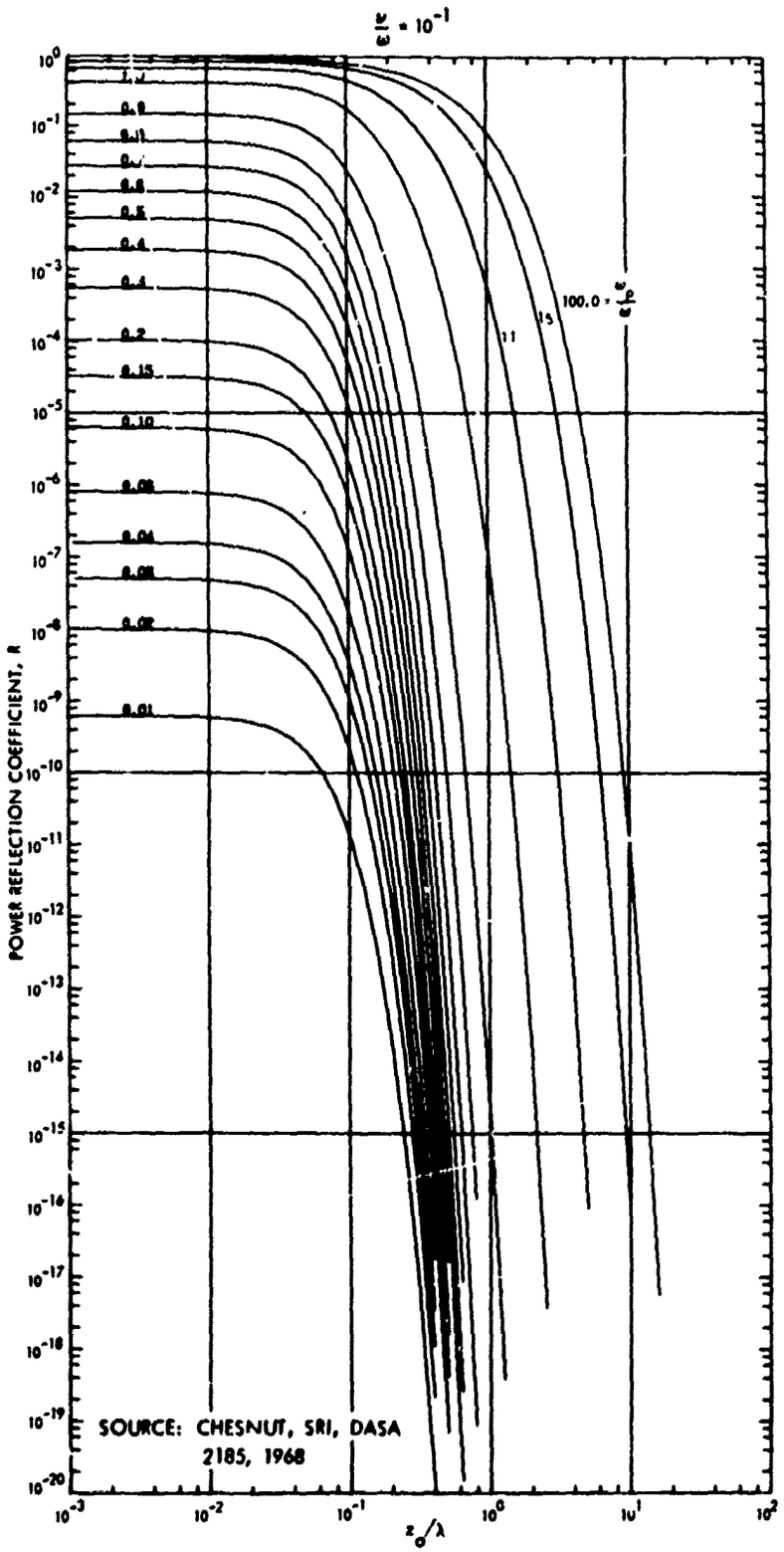

Figure 6-3. Power reflection coefficient versus the ratio z_o/λ for $\frac{\nu}{\omega} = 10^{-1}$.

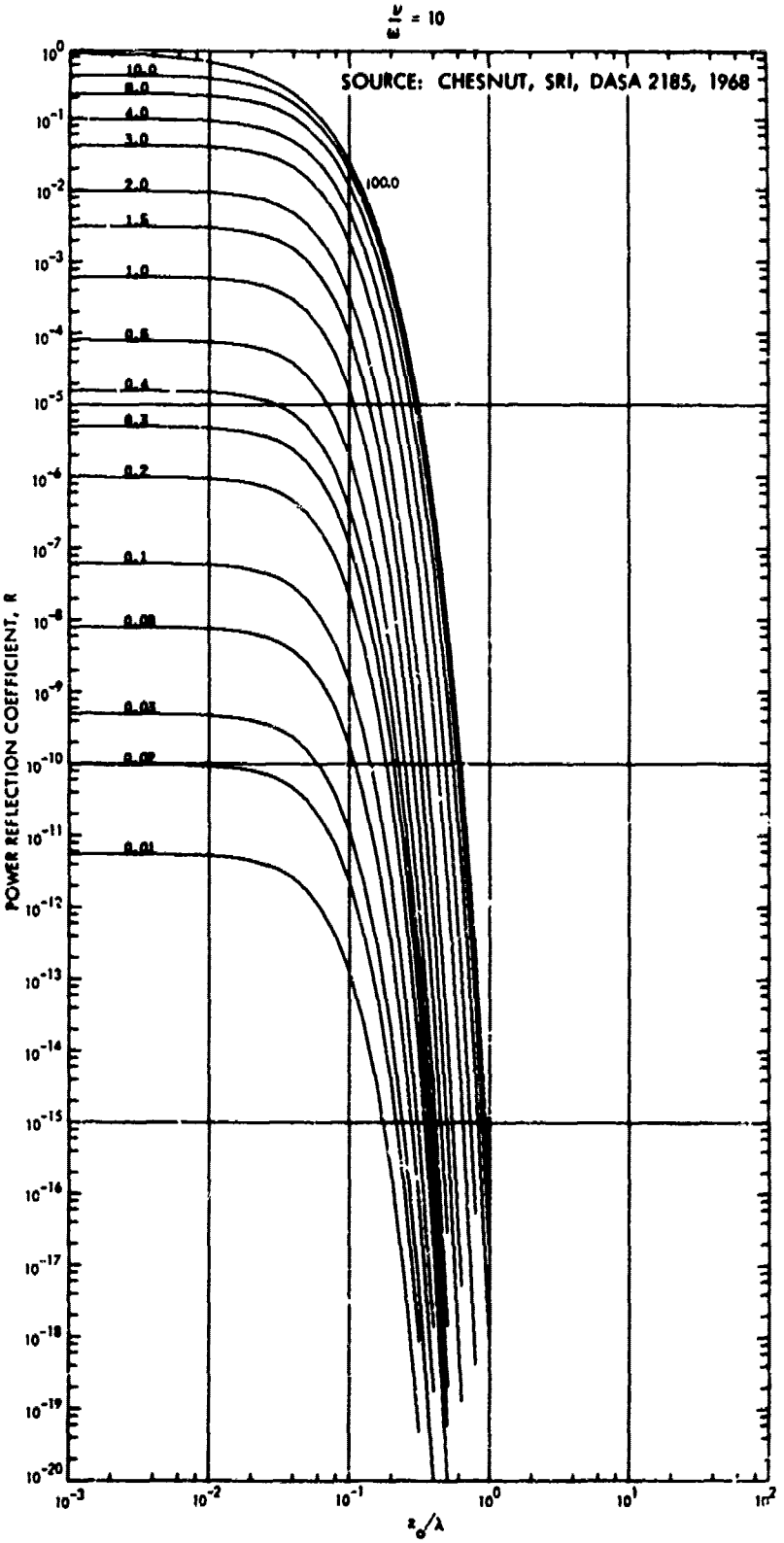

Figure 6-4. Power reflection coefficient versus the ratio z_o/λ for $\frac{\nu}{\omega} = 10$.

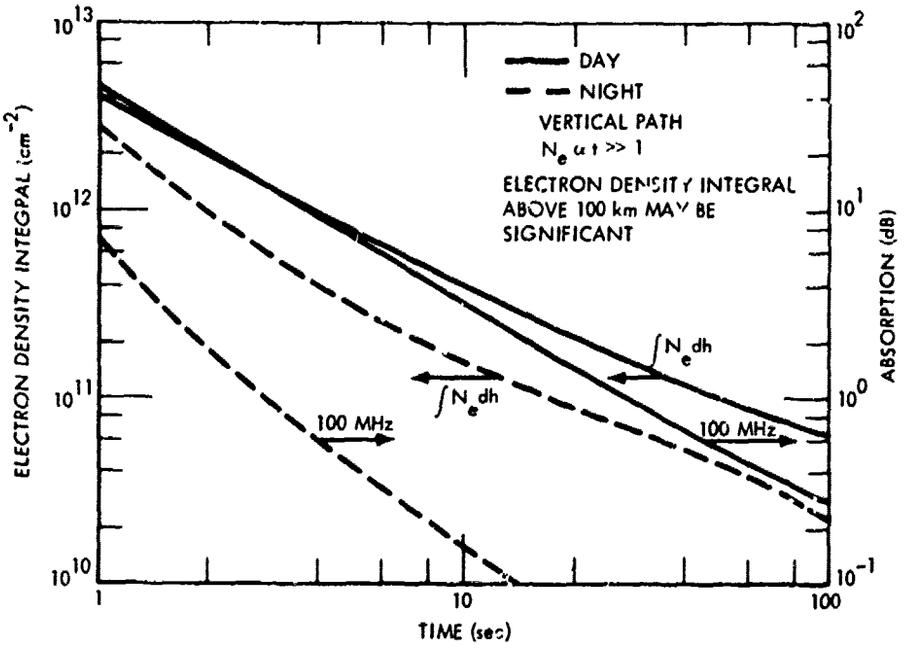

Figure 6-5. Integral of electron density and absorption up to 100 km altitude following an ionization impulse of 10^8 cm^{-3}.

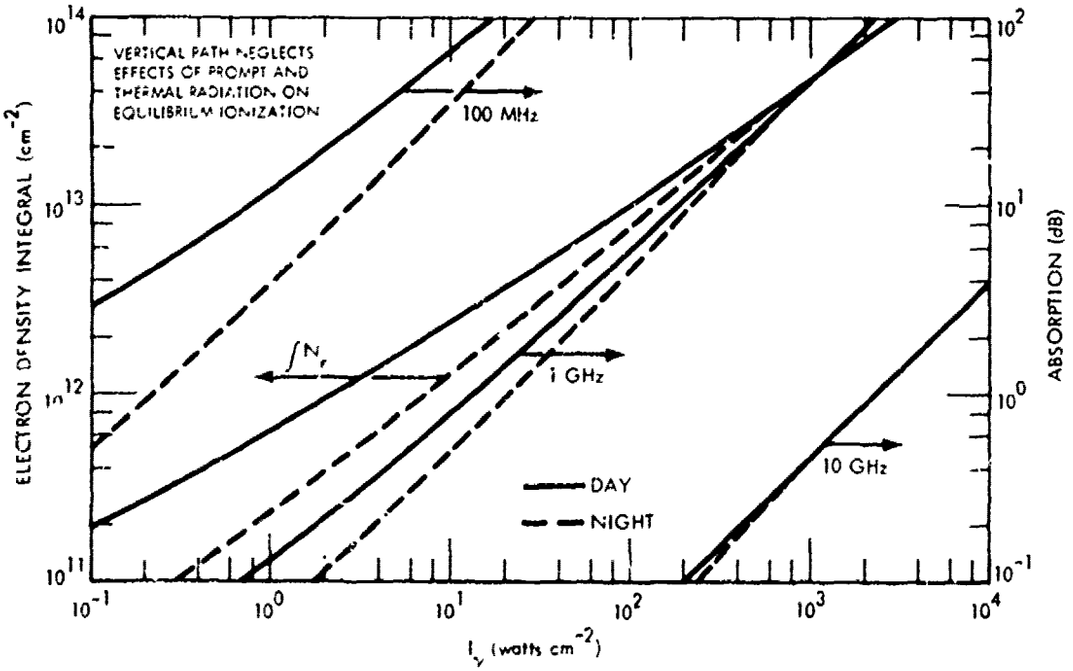

Figure 6-6. Integral of equilibrium electron density and absorption due to delayed gamma rays up to 100 km.

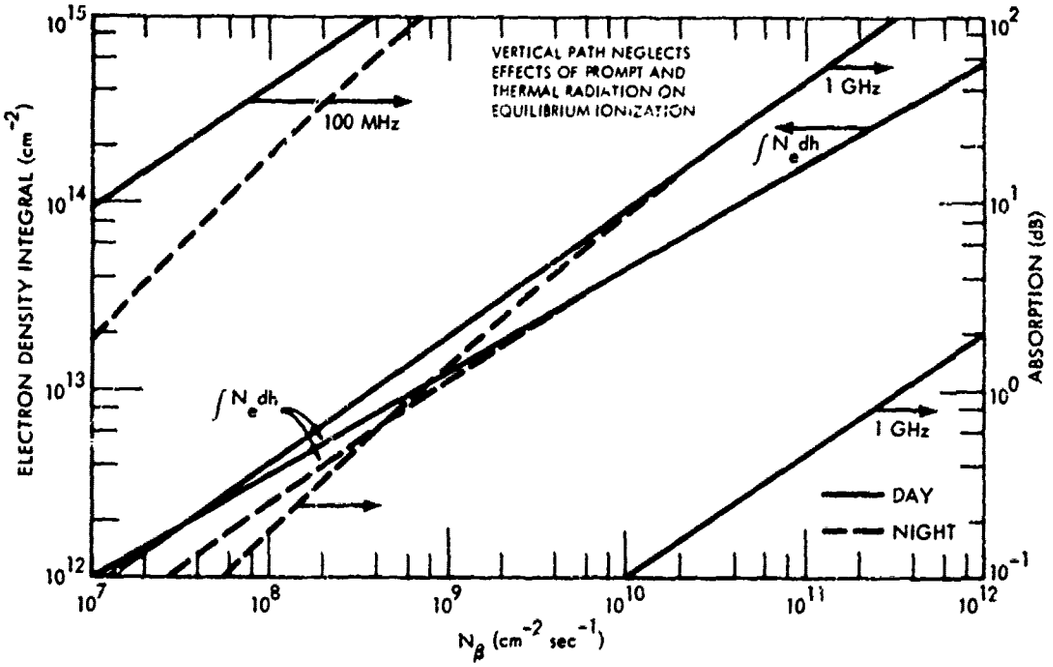

Figure 6-7. Integral of equilibrium electron density and absorption due to beta particles up to 100 km.

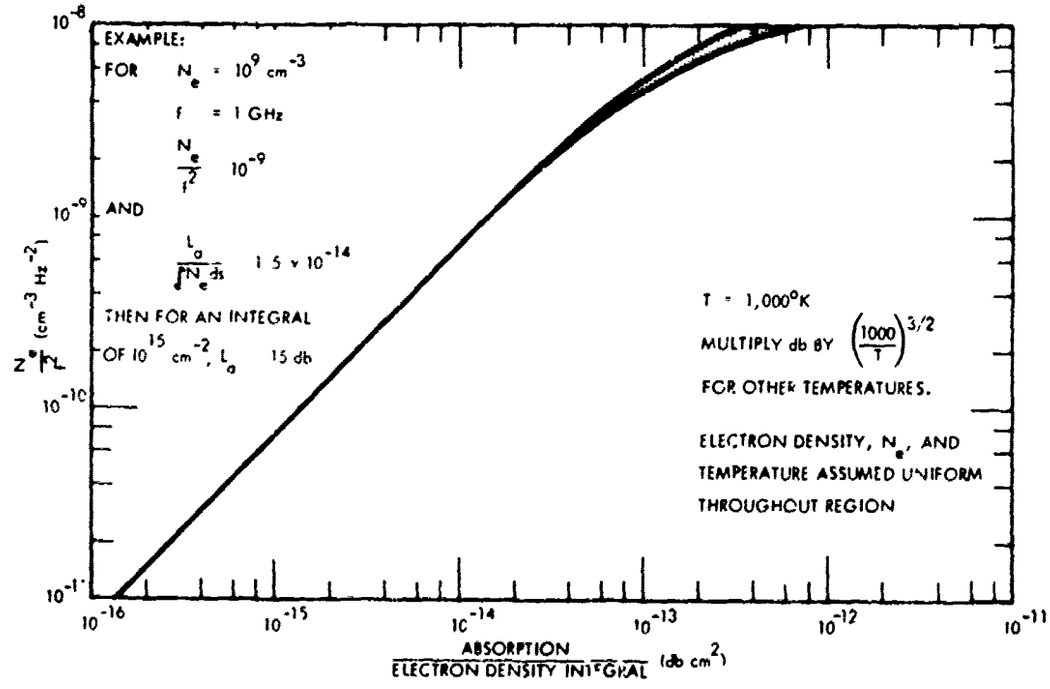

Figure 6-8. Integral of electron density and absorption in high-altitude plasma.

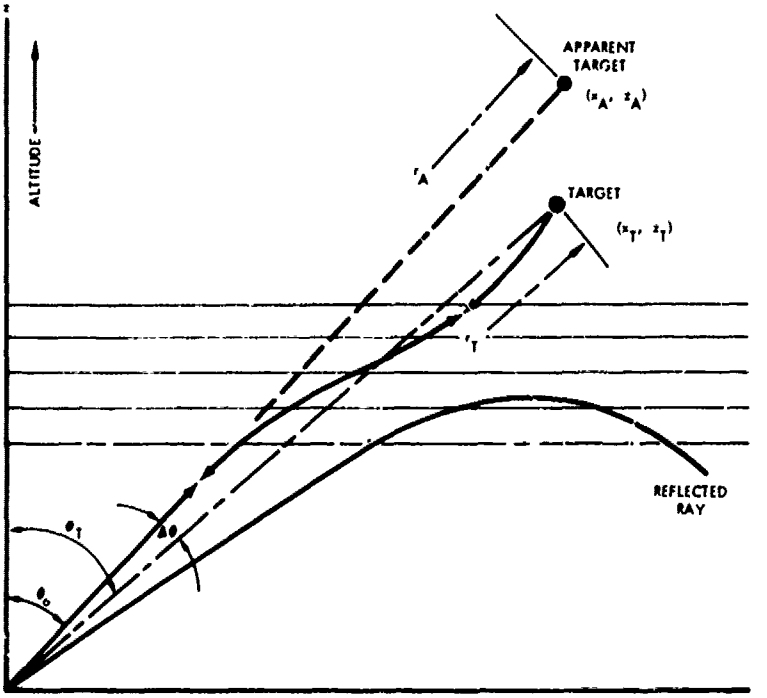

Figure 6-9. Geometry for refraction in horizontally stratified medium.

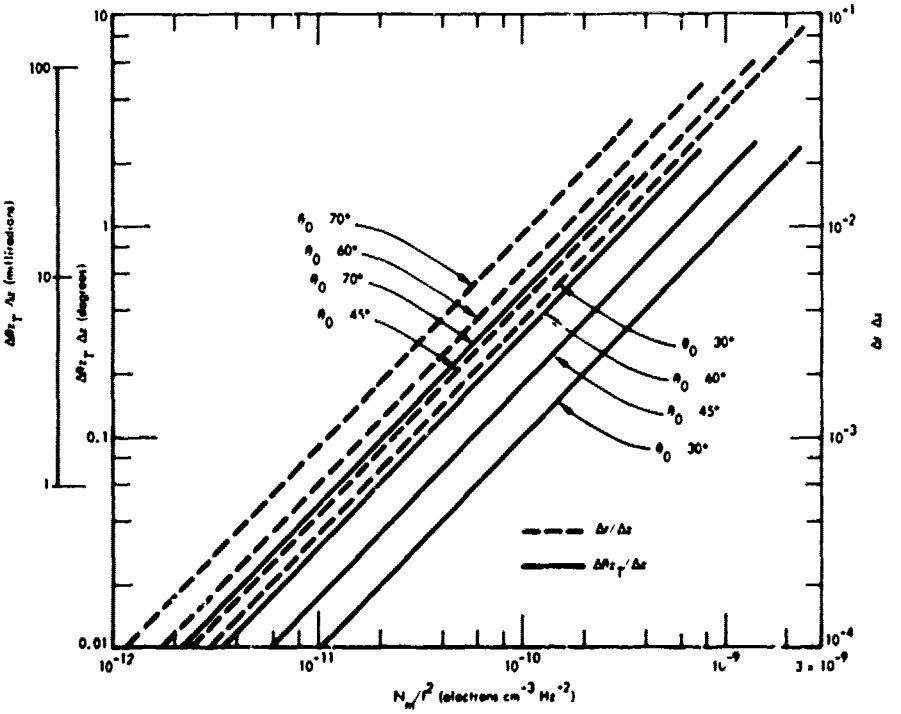

Figure 6-10. Approximate bearing and range errors in horizontally stratified medium.

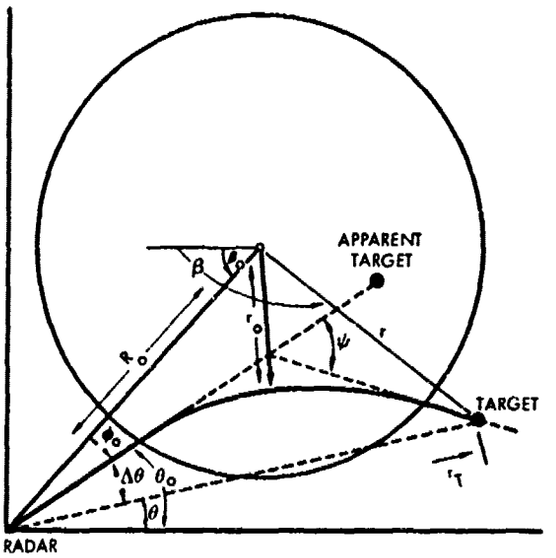

Figure 6-11. Geometry for refraction by spherically stratified region.

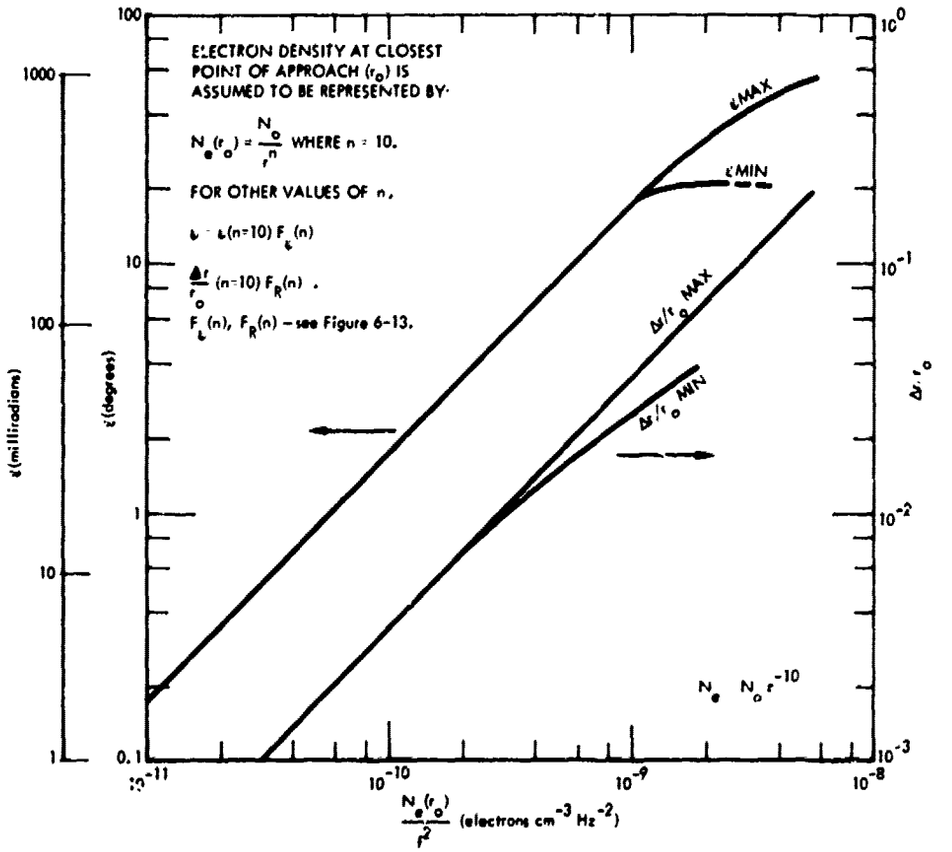

Figure 6-12. Refraction and range errors in spherically stratified medium.

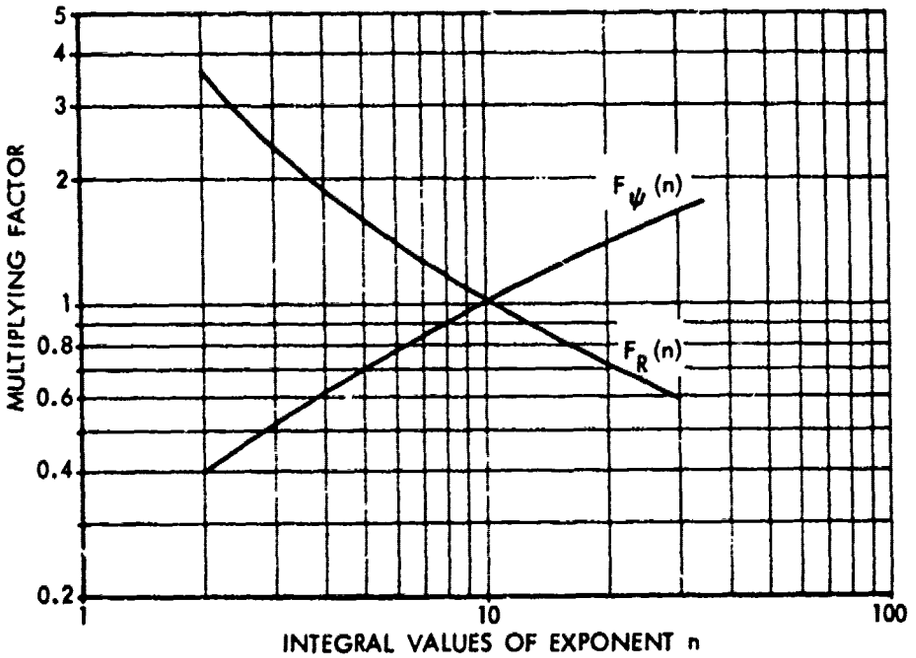

Figure 6-13. Multiplying factors for refraction and range errors in a spherically stratified region.

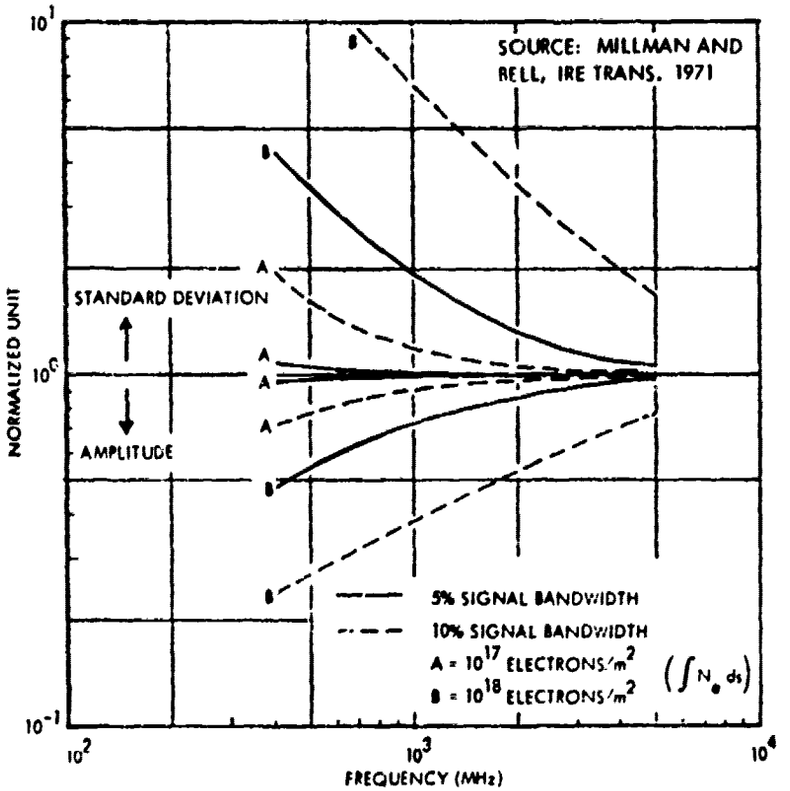

Figure 6-14. Amplitude and pulse-length modification of compressed pulse traversing ionosphere.

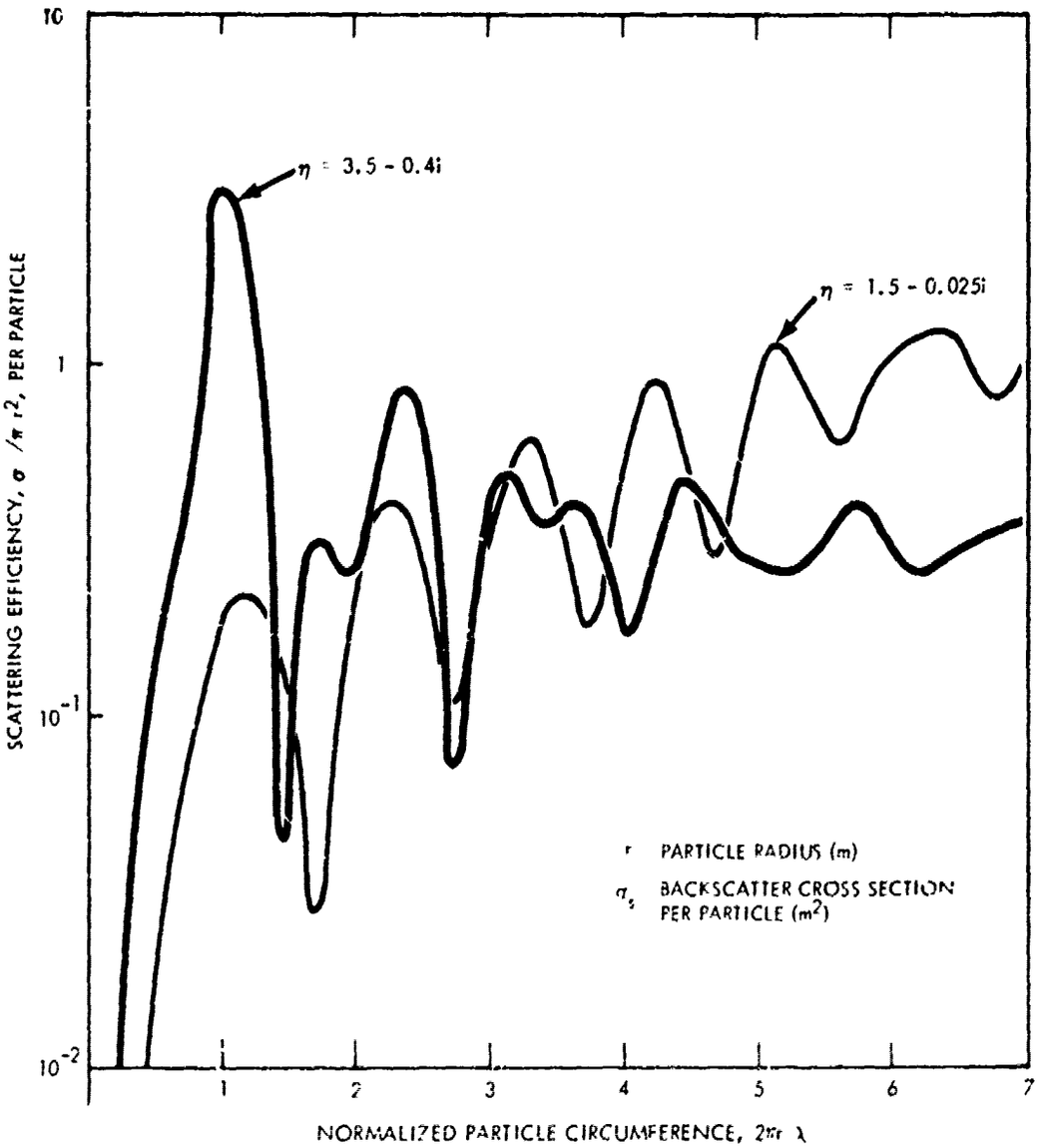

Figure 6-15. Backscatter efficiency as a function of normalized particle radius for wet clay and dry sand.

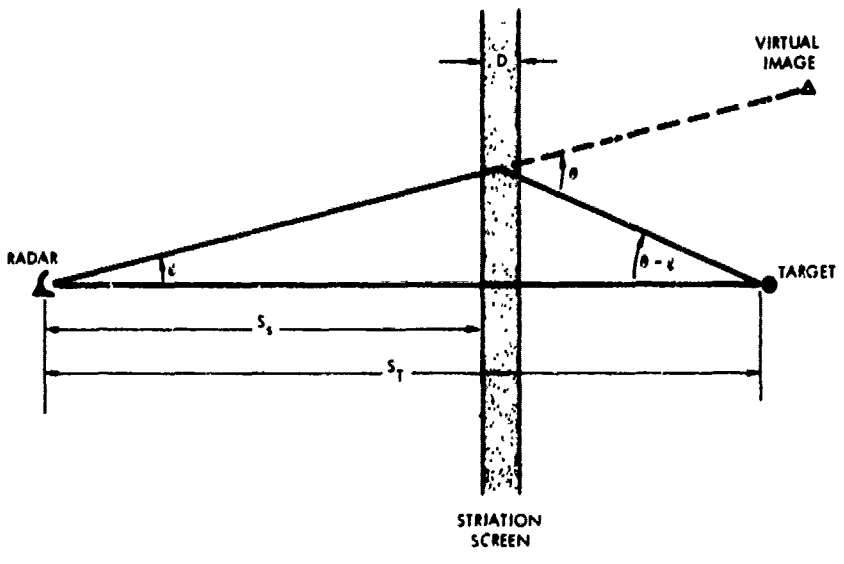

Figure 6-16. Scattering geometry.

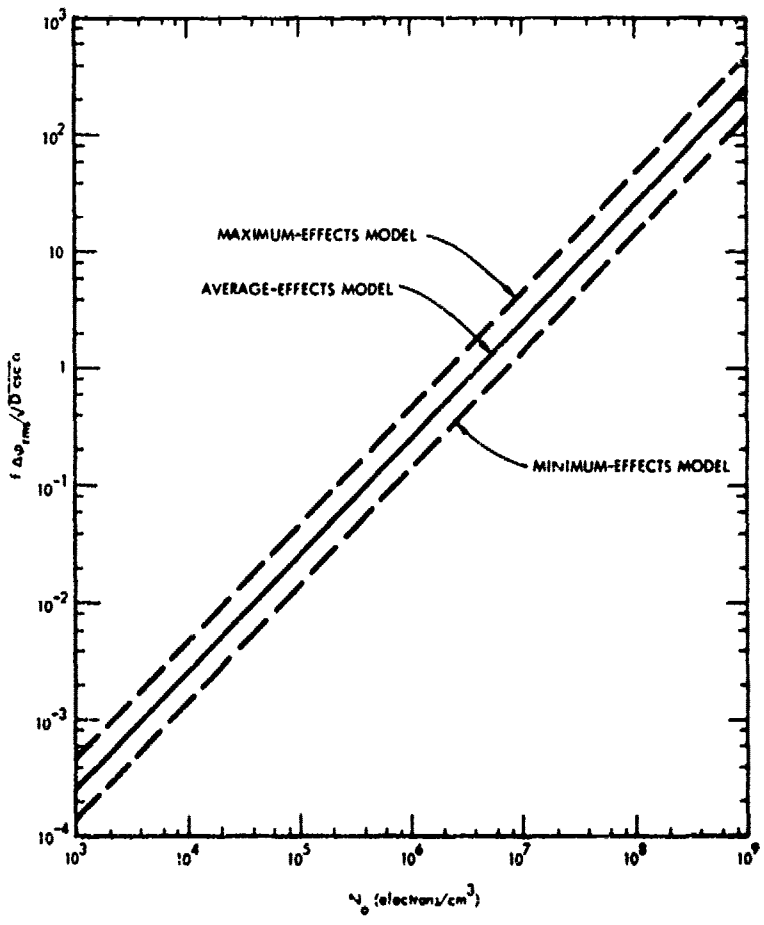

Figure 6-17. Magnitude of striation effects as calculated by three models.

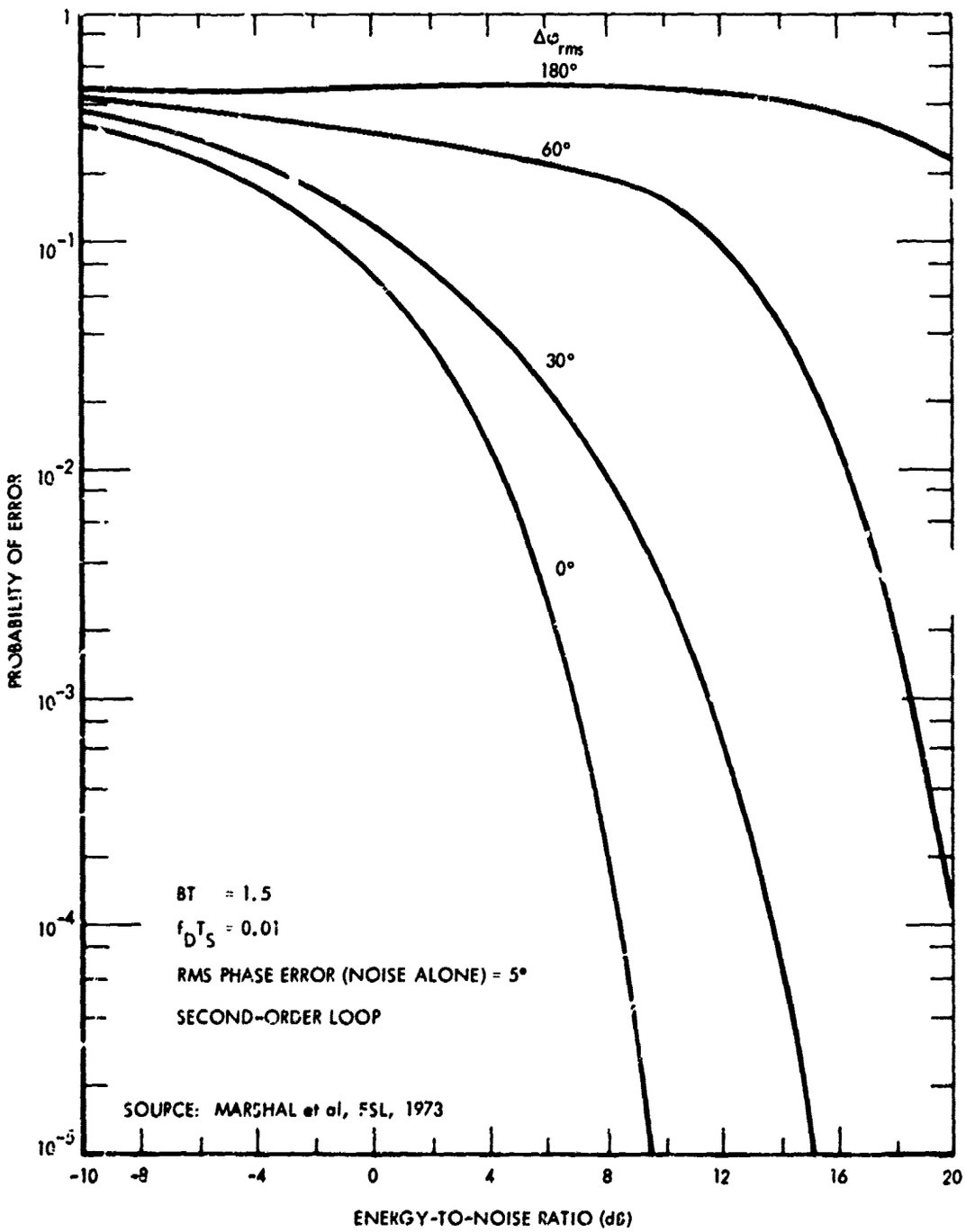

Figure 6-18. Probability of bit error for a BPSK signal due to phase scintillations, $f_D T_S = 0.01$.

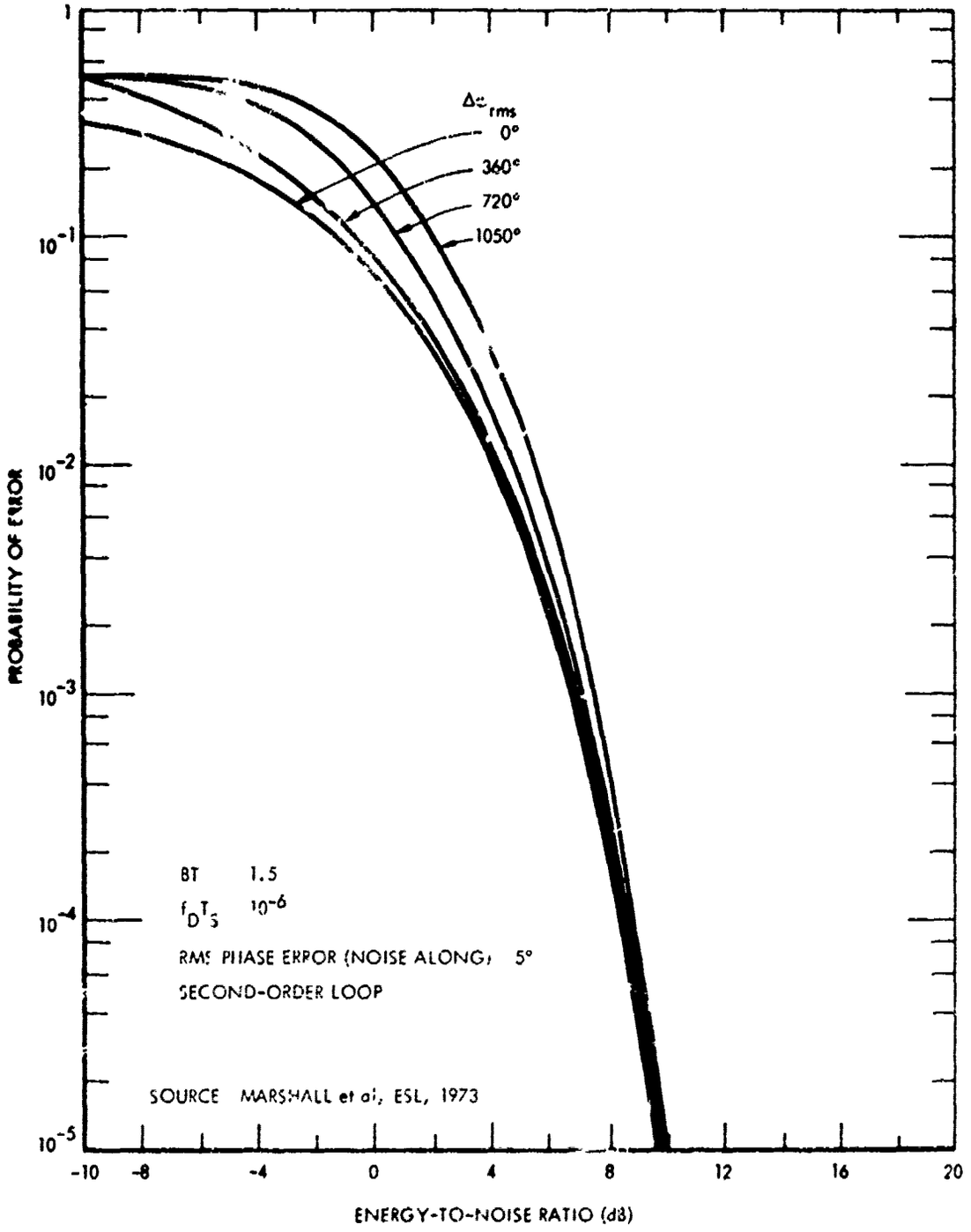

Figure 6-19. Probability of bit error for a BPSK signal due to phase scintillations, $f_D T_S = 10^{-6}$.

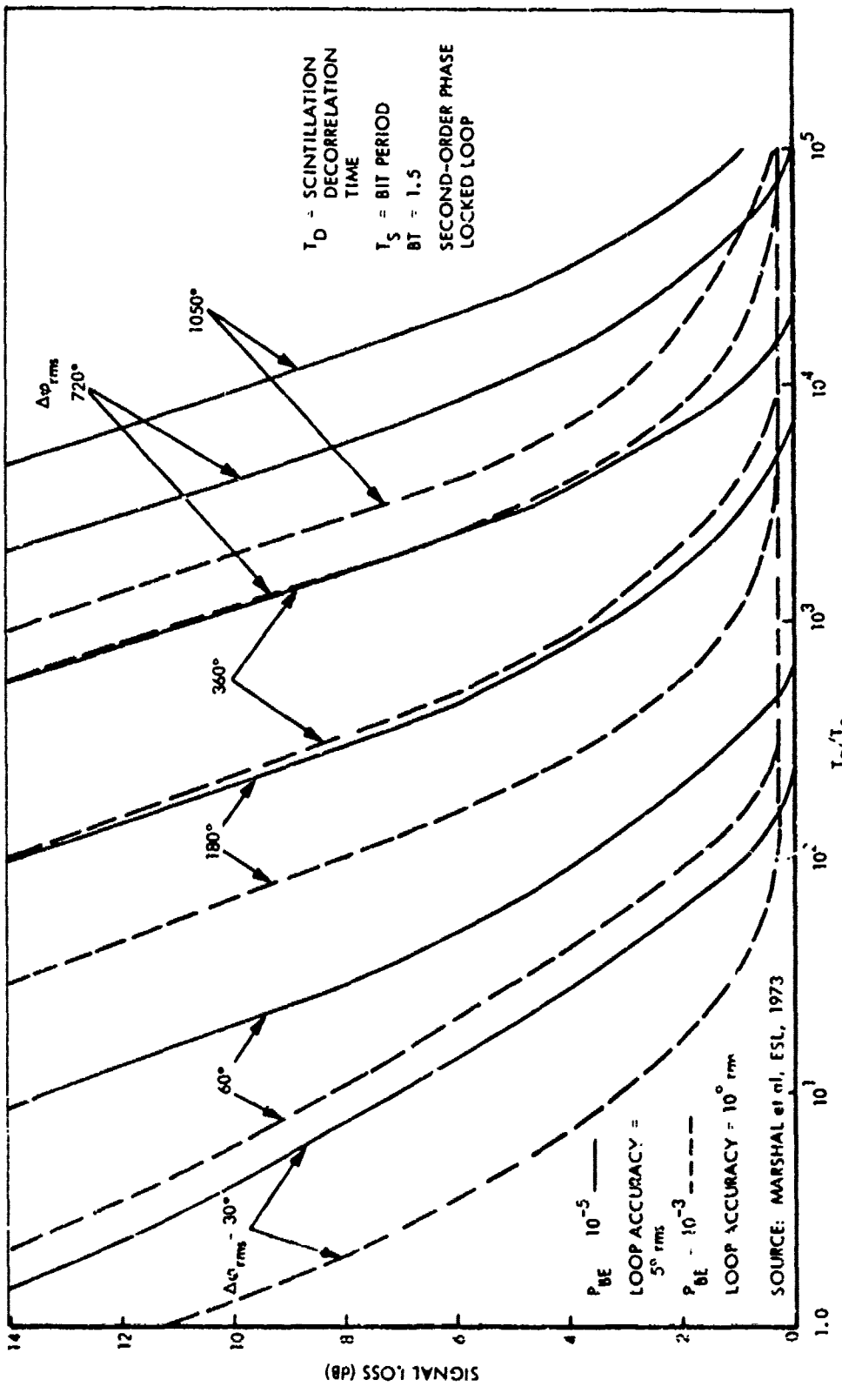

Figure 6-20. BPSK demodulation loss due to phase scintillation.

SECTION 7
NOISE

THERMAL NOISE

For an antenna with directivity $G(\vartheta,\phi)$ *viewing* a fireball, the antenna temperature T_{ANT} is

$$T_{ANT} = \int_{\theta}\int_{\phi} \frac{G(\theta,\phi)}{4\pi} T_s(\theta,\phi) \sin\theta \, d\theta d\phi$$

where

$$T_s = T_D\left(1 - e^{-L_o}\right) + T_{FB}e^{-L_o}\left[1 - \exp\left(-\int_d^{d+\Delta d} \alpha_{FB}\, dx\right)\right]$$

T_o is the temperature of the air between the antenna and the fireball, at a distance d from the antenna, T_{FB} is the fireball temperature, Δd the extent of the fireball, L_o the total absorption up to the fireball, and the α_{FB} the incremental absorption in the fireball. For a narrow beam antenna when T_s is approximately independent of angle over the beamwidth,

$$T_{ANT} = T_o\left(1 - 10^{-\frac{A_o}{10}}\right) + T_{FB}\left(1 - 10^{-\frac{A_{FB}}{10}}\right)10^{-\frac{A_o}{10}} ,$$

where A_o is the absorption in dB up to the fireball and A_{FB} is the absorption through the fireball.

If the fireball fills only a portion of the antenna beam, the contribution of the fireball emission is further reduced by approximately the ratio of the solid angle subtended by the fireball to the solid angle of the antenna beam.

SYNCHROTRON RADIATION

Electron trapping efficiency—see Figure 7-1.

Synchrotron noise power spectral density per unit solid angle per electron—see Figure 7-2.

Synchrotron noise power per electron versus frequency with electron energy as a parameter—see Figure 7-3.

Synchrotron noise power per electron versus electron energy with frequency as a parameter—see Figure 7-4.

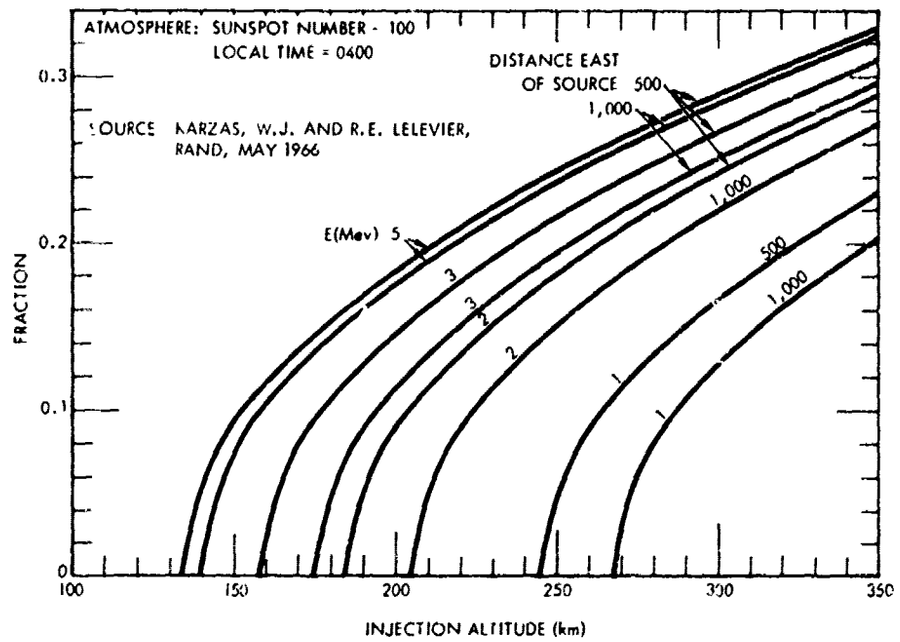

Figure 7-1. Fraction of injected betas of energy E that drift to 500 and 1,000 km east of injection point.

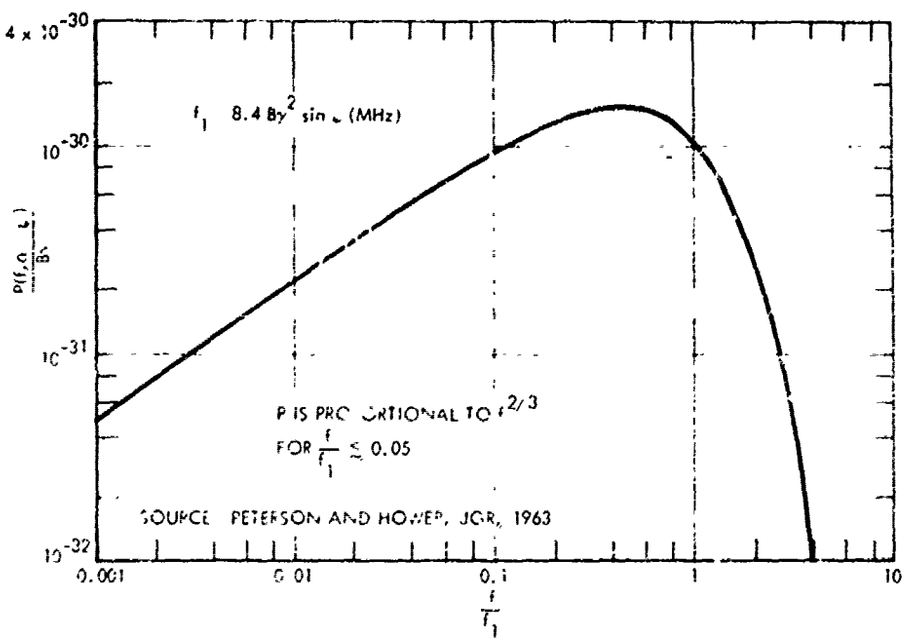

Figure 7-2. Synchrotron noise power spectral density per unit solid angle per electron in the orbital plane.

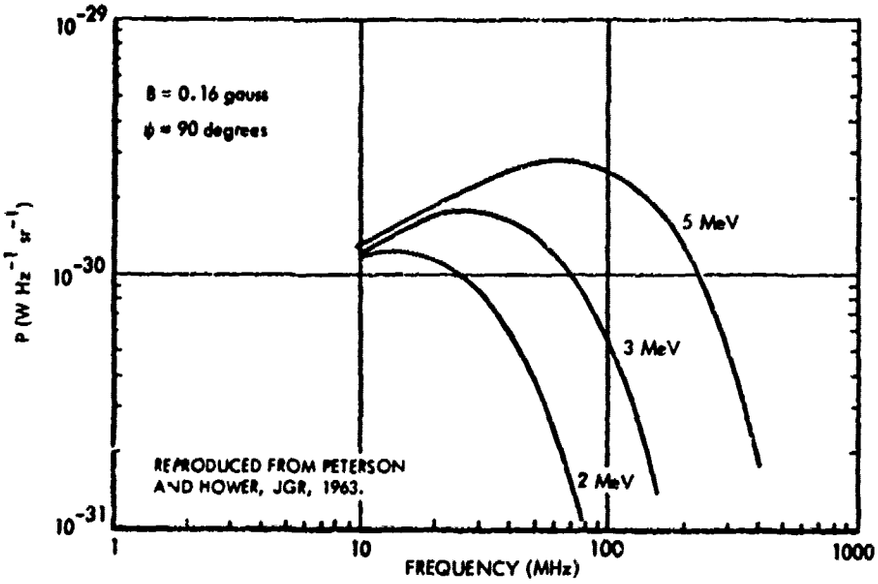

Figure 7-3. Power per electron versus frequency with electron energy as a parameter.

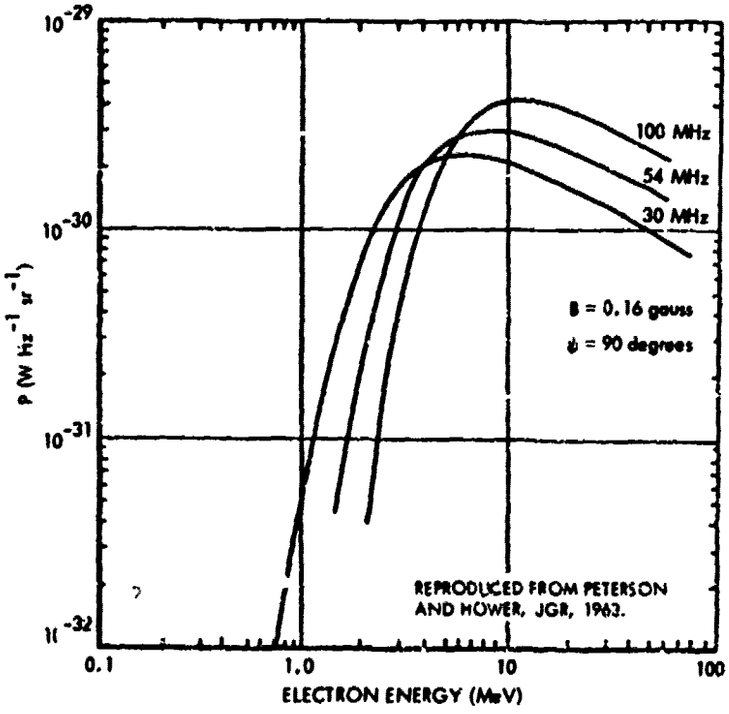

Figure 7-4. Power per electron versus electron energy with frequency as a parameter.

SECTION 8
PROPERTIES OF THE ATMOSPHERE

For the calculations carried out in this volume the U.S. Standard Atmosphere, 1962 is used for the altitude range 0 to 50 km; the COSPAR International Reference Atmosphere (CIRA), 1965 is used from 50 to 120 km—see Table 8-1.

D-region minor neutral species model—see Figure 8-1.

The CIRA 1965, Model 5, 8 hours is used for calculations from 120 to 800 km—see Table 8-2.

Since the completion of the calculations for this volume the new CIRA 1972 model atmospheres have been distributed. The model used for the present calculations is within 5 percent of the CIRA, 1972 Mean Reference Atmosphere from 0 to 120 km. Above 120 km the CIRA 1972 Mean Reference Atmosphere corresponds to an exospheric model which reaches 1000°K whereas the model in Table 8-2 approaches 1200°K. Comparison between the model used (Table 8-2) and the new CIRA 1972 Mean Model between 120 and 500 km can be made using Table 8-3. Also the density versus altitude for extremes in the CIRA 1972 Exospheric Temperature Model and the CIRA 1972 mean are compared with the CIRA 1965 Model 5, 8 hours in Figure 8-2.

Model ionosphere—see Figure 8-3.

25 Mass (M) penetrated between two points in atmosphere—see Figure 8-4.

Geomagnetic field (centered dipole approximation)—see Figure 8-5.

Geometric sunrise, sunset, and local noon zenith angle—see Figure 8-6.

Table 8-1. Properties of the atmosphere, 0 to 120 km.[a]

Altitude h (km)	Temperature T (°K)	Density ρ (gm cm^{-3})	Pressure p (dynes cm^{-2})	Pressure Scale Height H_p (km)	Mean Molecular Weight M	Particle Concentration n (cm^{-3})
0	288	1.23E-03[b]	1.01E 06	8.4	28.96	2.55E 19
2	275	1.01E-03	7.95E 05	8.1		2.09E 19
4	262	8.19E-04	6.17E 05	7.7		1.70E 19
6	249	6.60E-04	4.72E 05	7.3		1.37E 19
8	236	5.26E-04	3.56E 05	6.9		1.09E 19
10	223	4.13E-04	2.65E 05	6.6		8.60E 18
12	217	3.12E-04	1.94E 05	6.4		6.49E 18
14	217	2.28E-04	1.42E 05	6.4		4.74E 18
16	217	1.66E-04	1.04E 05	6.4		3.46E 18
18	217	1.22E-04	7.56E 04	6.4		2.53E 13
20	217	8.89E-05	5.53E 04	6.4		1.85E 18
22	219	6.45E-05	4.05E 04	6.4		1.34E 18
24	221	4.69E-05	2.97E 04	6.5		9.76E 17
26	223	3.43E-05	2.19E 04	6.6		7.12E 17
28	225	2.51E-05	1.62E 04	6.6		5.21E 17
30	226	1.84E-05	1.20E 04	6.7		3.83E 17
32	228	1.36E-05	8.89E 03	6.8		2.82E 17
34	234	9.89E-06	6.63E 03	6.9		2.06E 17
36	239	7.26E-06	4.98E 03	7.1		1.51E 17
38	245	5.37E-06	3.67E 03	7.3		1.12E 17
40	250	4.00E-06	2.87E 03	7.4		8.31E 16
42	256	2.99E-06	2.20E 03	7.6		6.23E 16
44	261	2.26E-06	1.69E 03	7.8		4.70E 16
46	267	1.71E-06	1.31E 03	7.9		3.56E 16
48	271	1.32E-06	1.02E 03	8.0		2.74E 16
50	271	1.04E-06	8.10E 02	8.1		2.16E 16
52	266	8.27E-07	6.30E 02	7.9		1.72E 16
54	260	6.54E-07	4.88E 02	7.7		1.36E 16
56	254	5.15E-07	3.76E 02	7.6		1.07E 16
58	248	4.03E-07	2.88E 02	7.4		8.39E 15

Notes:
[a] Values from 0 to 48 km are from U.S. Standard Atmosphere, 1962; above 48 km, from CIRA 1965.
[b] 1.23E-03 is 1.23 x 10^{-3}.

Table 8-1 (Continued).

Altitude h (km)	Temperature T (°K)	Density ρ (gm cm^{-3})	Pressure p (dynes cm^{-2})	Pressure Scale Height H_p (km)	Mean Molecular Weight M	Particle Concentration n (cm^{-3})
60	243	3.14E-07	2.20E 02	7.3	28.96	6.54E 15
62	238	2.43E-07	1 66E 02	7.1		5.06E 15
64	233	1.87E-07	1.25E 02	7.0		? 59E 15
66	227	1.43E-07	9.35E 01	6.8		2.98E 15
68	222	1.09E-07	6.94E 01	6.6		2.27E 15
70	217	8.23E-08	5.12E 01	6.5		1.71E 15
72	211	6.20E-08	3.75E 01	6.3		1.29E 15
74	204	4.63E-08	2.72E 01	6.1		9.62E 14
76	198	3.43E-08	1.95E 01	5.9		7.13E 14
78	192	2.51E-08	1.39E 01	5.8		5.23E 14
80	186	1.83E-08	9.75E 00	5.6		3.80E 14
82	186	1.28E-08	6.81E 00	5 6		2.65E 14
84	186	8.93E-09	4.77E 00	5.6	28.95	1.86E 14
86	186	6.25E-09	3.33E 00	5.6		1.30E 14
88	186	4.37E-09	2.33E 00	5.6		9.10E 13
90	186	3.06E-09	1.63E 00	5.6	28 94	6.37E 13
92	191	2.09E-09	1.15E 00	5.8	28 89	4.52E 13
94	196	1.45E-09	8.16E 01	5.9	28.83	3.02E 13
96	200	1.01E-09	5.86E 01	6.1	28.70	2.12E 13
98	204	7.11E-10	4.24E 01	6.3	28.52	1.50E 13
100	208	5.06E-10	3.10E 01	6.4	28.30	9.89E 12
102	216	3.57E-10	2.29E 01	6.7	28.02	7.61E 12
104	225	2.56E-10	1.71E 01	7.1	27.92	5.46E 2
106	233	1.86E-10	1.30E 01	7.4	27.82	3.98E 2
108	242	1.37E-10	9.93E 02	7.7	27.74	2.93E 12
110	251	1.02E-10	7.69E 02	8.0	27.66	2.19E 12
112	272	7.35E-11	6.05E 02	8.7	27.49	1.59E 12
114	293	5.45E-11	4.85E 02	9.4	27.34	1.18E 12
116	313	4.13E-11	3.95E 02	10.1	27.19	9.01E 11
118	334	3.19E-11	3.27E 02	10.9	27.08	7.02E 11
120	355	2.50E-11	2.73E 02	11.6	27.01	5.57E 11

Table 8-2. Properties of the atmosphere, 120 to 800 km.

Altitude h (km)	Temperature T (°K)	Density ρ (gm cm^{-3})	Pressure p (dynes cm^{-2})	Pressure Scale Height H_p (km)	Mean Molecular Weight M	$n(N_2)$ (cm^{-3})	$n(O_2)$ (cm^{-3})	n(O) (cm^{-3})	n(He) (cm^{-3})	n(A) (cm^{-3})
120	355	2.490E-11[a]	2.722E-02	11.6	27.01	4.000E 11	7.500E 10	7.600E 10	2.400E 07	4.500E 09
130	477	8.710E-12	1.312E-02	16.0	26.35	1.383E 11	2.325E 10	3.650E 10	1.801E 07	1.123E 09
140	573	4.046E-12	7.490E-03	19.7	25.74	6.302E 10	9.729E 09	2.154E 10	1.481E 07	3.960E 08
150	652	2.176E-12	4.690E-03	23.0	25.16	3.308E 10	4.746E 09	1.411E 10	1.273E 07	1.670E 08
160	721	1.281E-12	3.122E-03	26.1	24.60	1.891E 10	2.542E 09	9.817E 09	1.122E 07	7.854E 07
170	783	8.027E-13	2.173E-03	29.1	24.06	1.147E 10	1.454E 09	7.122E 09	1.006E 07	3.990E 07
180	839	5.283E-13	1.566E-03	32.0	23.54	7.284E 09	8.737E 08	5.335E 09	9.138E 06	2.150E 07
190	889	3.617E-13	1.161E-03	34.7	23.04	4.794E 09	5.463E 08	4.099E 09	8.385E 06	1.214E 07
200	933	2.557E-13	8.792E-04	37.3	22.55	3.249E 09	3.527E 08	3.216E 09	7.760E 06	7.113E 06
210	970	1.857E-13	6.783E-04	39.8	22.09	2.254E 09	2.336E 08	2.565E 09	7.232E 06	4.296E 06
220	1003	1.379E-13	5.313E-04	42.1	21.65	1.594E 09	1.581E 08	2.075E 09	6.779E 06	2.560E 06
230	1032	1.043E-13	4.214E-04	44.3	21.23	1.146E 09	1.088E 08	1.698E 09	6.385E 06	1.680E 06
240	1056	8.018E-14	3.379E-04	46.3	20.83	8.340E 08	7.596E 07	1.403E 09	6.037E 06	1.079E 06
250	1076	6.249E-14	2.735E-04	48.2	20.44	6.138E 08	5.367E 07	1.168E 09	5.728E 06	7.030E 05
260	1094	4.928E-14	2.232E-04	50.1	20.08	4.558E 08	3.829E 07	9.783E 08	5.449E 06	4.632E 05
270	1109	3.927E-14	1.834E-04	51.8	19.74	3.411E 08	2.755E 07	8.242E 08	5.195E 06	3.082E 05
280	1122	3.158E-14	1.516E-04	53.4	19.42	2.569E 08	1.996E 07	6.975E 08	4.963E 06	2.067E 05
290	1133	2.560E-14	1.261E-04	54.9	19.12	1.945E 08	1.455E 07	5.927E 08	4.749E 06	1.397E 05
300	1142	2.090E-14	1.054E-04	56.4	18.84	1.480E 08	1.066E 07	5.053E 08	4.550E 06	9.491E 04
320	1156	1.420E-14	7.451E-05	59.1	18.32	8.666E 07	5.797E 06	3.702E 08	4.191E 06	4.450E 04
340	1167	9.852E-15	5.347E-05	61.4	17.88	5.137E 07	3.195E 06	2.736E 08	3.873E 06	2.120E 04
360	1174	6.954E-15	3.884E-05	63.6	17.48	3.075E 07	1.779E 06	2.035E 08	3.589E 06	1.023E 04
380	1180	4.979E-15	2.850E-05	65.6	17.14	1.854E 07	9.991E 05	1.522E 08	3.331E 06	4.982E 03
400	1184	3.607E-15	2.110E-05	67.4	16.83	1.125E 07	5.650E 05	1.142E 08	3.097E 06	2.448E 03
420	1186	2.635E-15	1.570E-05	69.1	16.55	6.837E 06	3.200E 05	8.588E 07	2.682E 06	
440	1188	1.945E-15	1.180E-05	70.7	16.29	4.169E 06	1.829E 05	6.487E 07	2.685E 06	n(H)
460	1190	1.447E-15	8.920E-06	72.3	16.05	2.577E 06	1.050E 05	4.913E 07	2.503E 06	(cm^{-3})
480	1191	1.083E-15	6.786E-06	73.9	15.80	1.591E 06	6.058E 04	3.729E 07	2.335E 06	
500	1192	8.154E-16	5.193E-06	75.6	15.56	9.858E 05	3.507E 04	2.836E 07	2.180E 06	8.737E 03
520	1193	6.171E-16	3.998E-06	77.3	15.31	6.128E 05	2.038E 04	2.161E 07	2.037E 06	8.586E 03
540	1193	4.693E-16	3.097E-06	79.2	15.03	3.821E 05	1.188E 04	1.650E 07	1.903E 06	8.442E 03
560	1194	3.584E-16	2.414E-06	81.3	14.74	2.390E 05	6.952E 03	1.262E 07	1.780E 06	8.300E 03
580	1194	2.750E-16	1.894E-06	83.7	14.41	1.499E 05	4.081E 03	9.667E 06	1.665E 06	8.162E 03
600	1194	2.119E-16	1.497E-06	86.3	14.06	9.428E 04	2.404E 03	7.418E 06	1.558E 06	8.027E 03
620	1194	1.640E-16	1.192E-06	89.3	13.67	5.947E 04	1.420E 03	5.701E 06	1.458E 06	7.895E 03
640	1195	1.274E-16	9.564E-07	92.7	13.24	3.760E 04	8.417E 02	4.389E 06	1.366E 06	7.766E 03
660	1195	9.952E-17	7.742E-07	96.7	12.77	2.386E 04	5.004E 02	3.384E 06	1.280E 06	7.640E 03
680	1195	7.810E-17	6.325E-07	101.2	12.27	1.517E 04	2.984E 02	2.613E 06	1.200E 06	7.518E 03
700	1195	6.161E-17	5.216E-07	106.4	11.74	9.673E 03	1.785E 02	2.021E 06	1.125E 06	7.397E 03
720	1195	4.888E-17	4.344E-07	112.4	11.18	6.184E 03	1.071E 02	1.565E 06	1.055E 06	7.280E 03
740	195	3.901E-17	3.654E-07	119.1	10.61	3.963E 03	6.442E 01	1.214E 06	9.902E 05	7.165E 03
760	1195	3.135E-17	3.105E-07	126.6	10.04	2.546E 03	3.887E 01	9.429E 05	9.295E 05	7.052E 03
780	1195	2.537E-17	2.664E-07	135.0	9.46	1.640E 03	2.352E 01	7.334E 05	8.729E 05	6.942E 03
800	1195	2.068E-17	2.309E-07	144.3	8.91	1.059E 03	1.427E 01	5.713E 05	8.200E 05	6.834E 03

Note:

[a] 2.490E-11 is 2.490×10^{-11}.

Source: 1965 CIRA Atmosphere, Model 5, 8 hr.

Table 8-3. Some properties of the CIRA, 1972 mean reference atmosphere, 120 to 500 km.

Altitude h (km)	Temperature T (°K)	Pressure ρ (gm cm^{-3})	Pressure p (dynes cm^{-2})	Pressure Scale Height H_p (km)	Mean Molecular Weight M
120	335	2.44E-11	2.67E-2	11.6	25.45
140	549	3.85E-12	7.42E-3	20.6	23.65
160	703	1.24E-12	3-27E-3	28.2	22.26
180	798	5.46E-13	1.72E-3	34.0	21.11
200	859	2.79E-13	9.9E-4	38.6	20.14
220	901	1.56E-13	6.04E-4	42.4	19.32
240	929	9.25E-14	3.83E-4	45.6	18.63
260	949	5.74E-14	2.51E-4	48.3	18.07
280	963	3.68E-14	1.67E-4	50.4	17.60
300	973	2.42E-14	1.14E-4	52.6	17.22
320	980	1.62E-14	7.81E-5	54.3	16.91
340	985	1.10E-14	5.43E-5	55.8	16.64
360	988	7.62E-15	3.81E-5	57.1	16.42
380	991	5.30E-15	2.69E-5	58.3	16.21
400	993	3.73E-15	1.92E-5	59.4	16.03
420	994	2.64E-15	1.37E-5	60.6	15.84
440	995	1.88E-15	9.91E-6	61.7	15.65
460	996	1.34E-15	7.19E-6	63.0	15.45
480	997	9.64E-16	5.25E-6	64.4	15.22
500	997	6.97E-16	3.86E-6	65.9	14.95

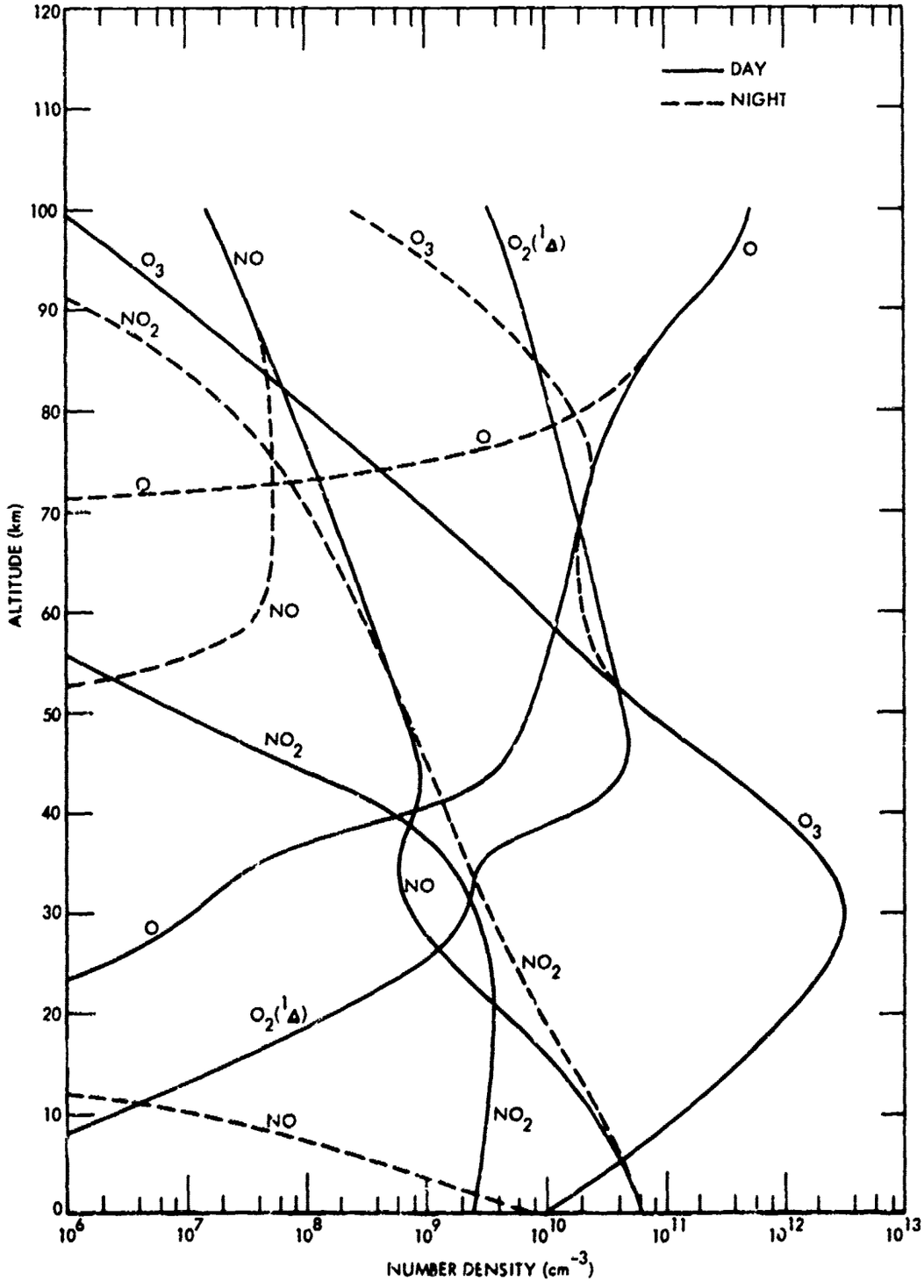

Figure 8-1. D-region minor neutral species model.

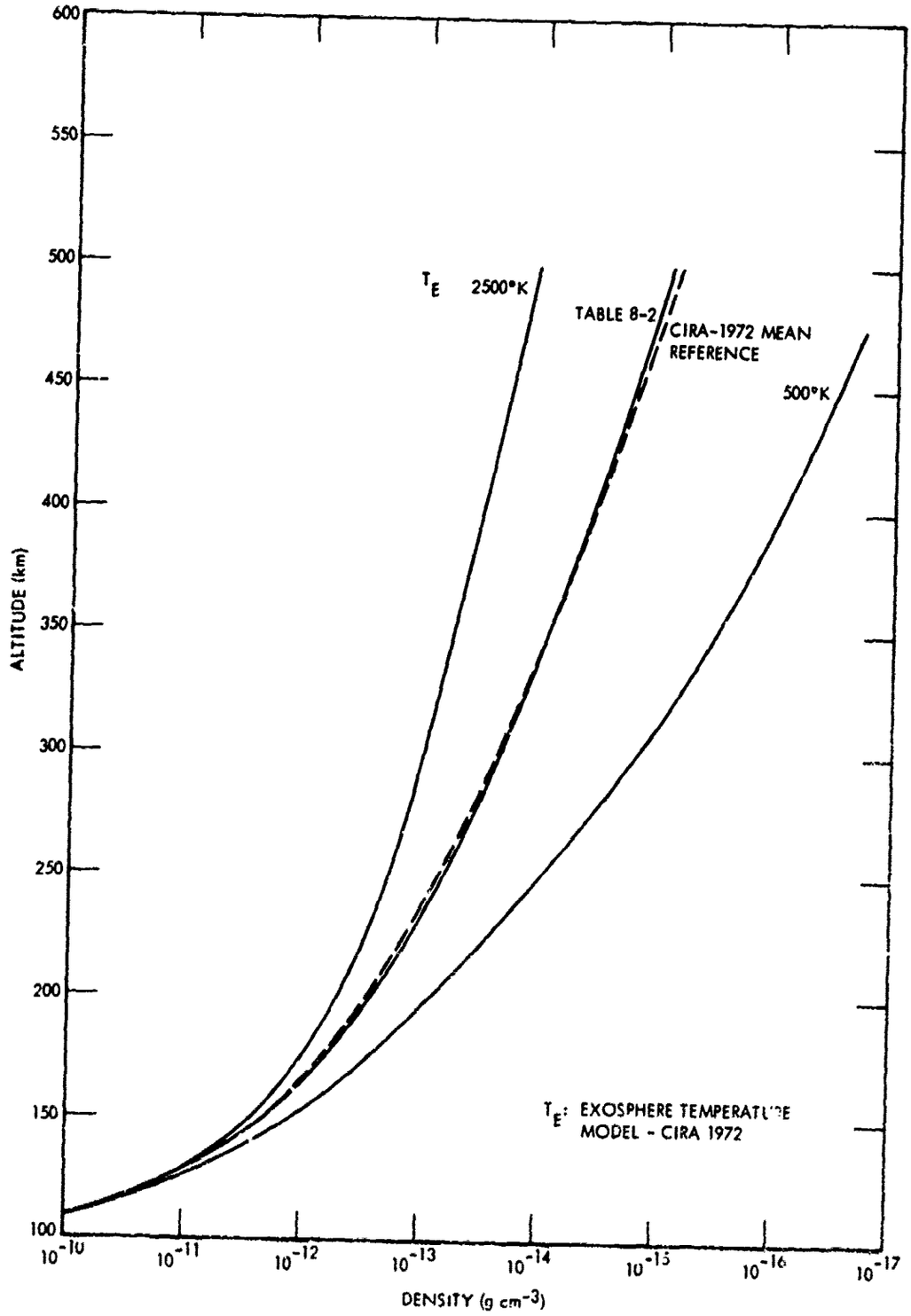

Figure 8-2. Density versus altitude for extremes of CIRA 1972 atmospheric models and for the CIRA 1972 mean and CIRA 1965 Model 5, 8 hour.

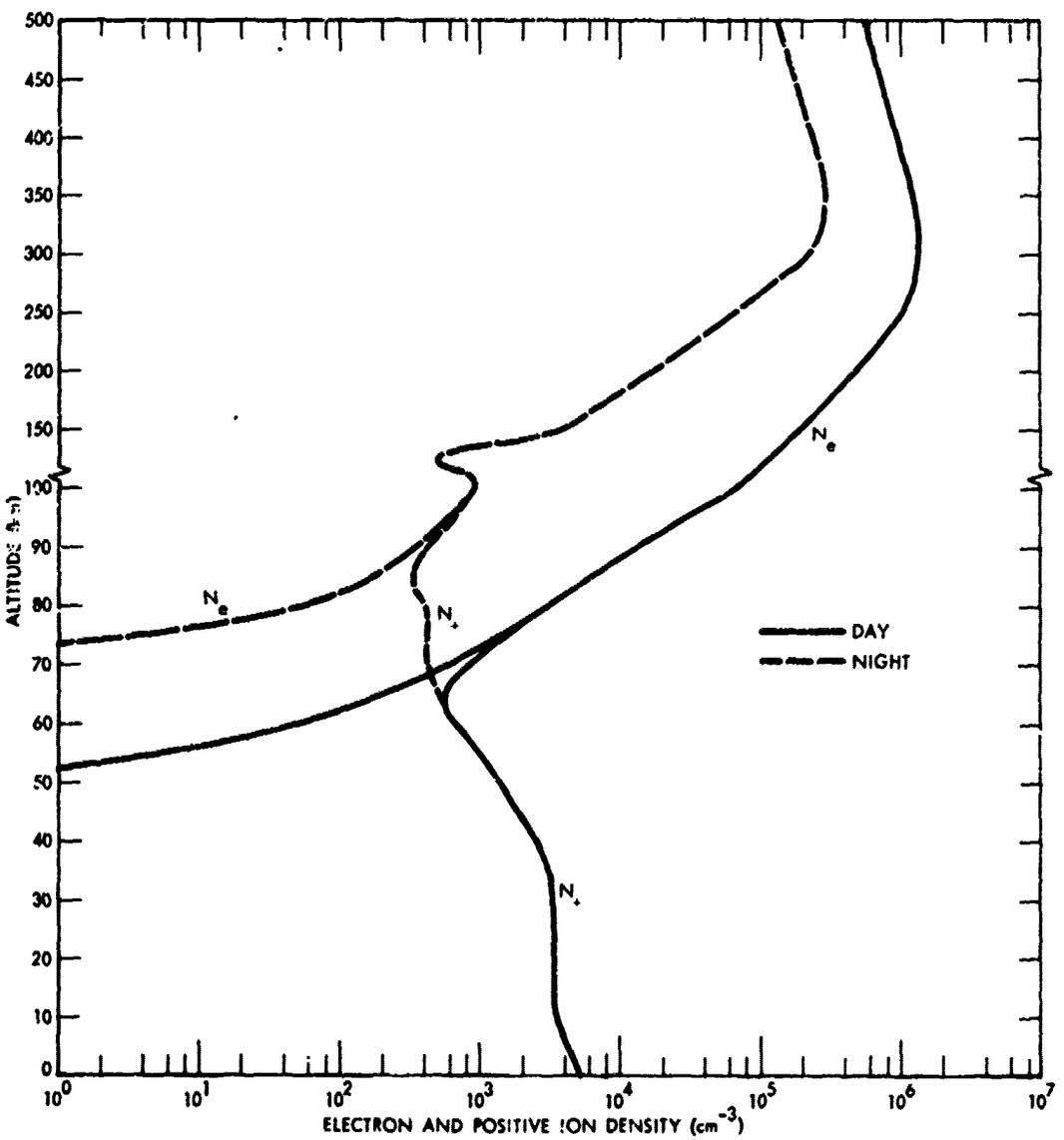

Figure 8-3. Model ionosphere.

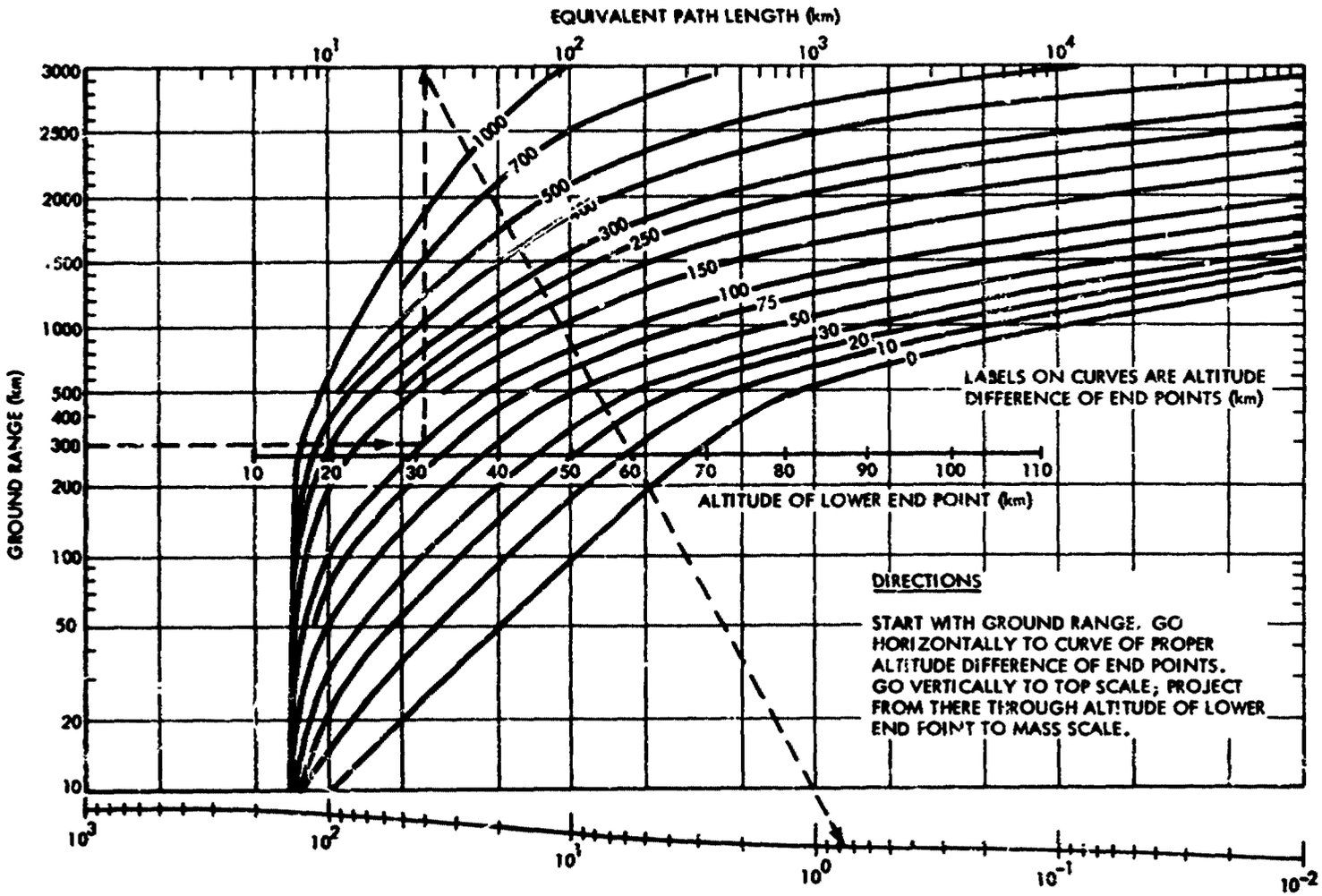

Figure 8-4. Computation of mass penetrated between two points in the atmosphere.

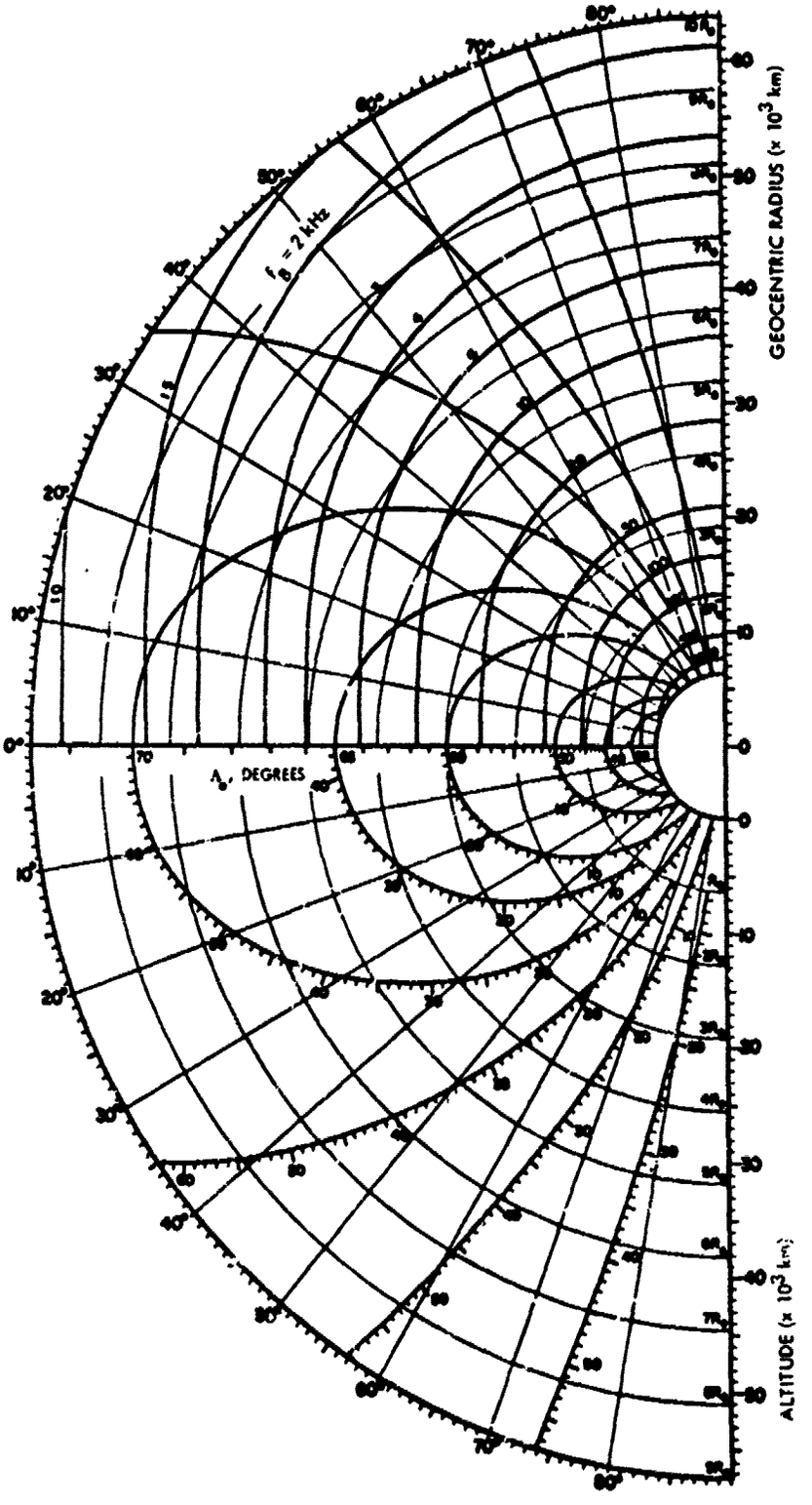

Figure 8-5. Dipole magnetic field.

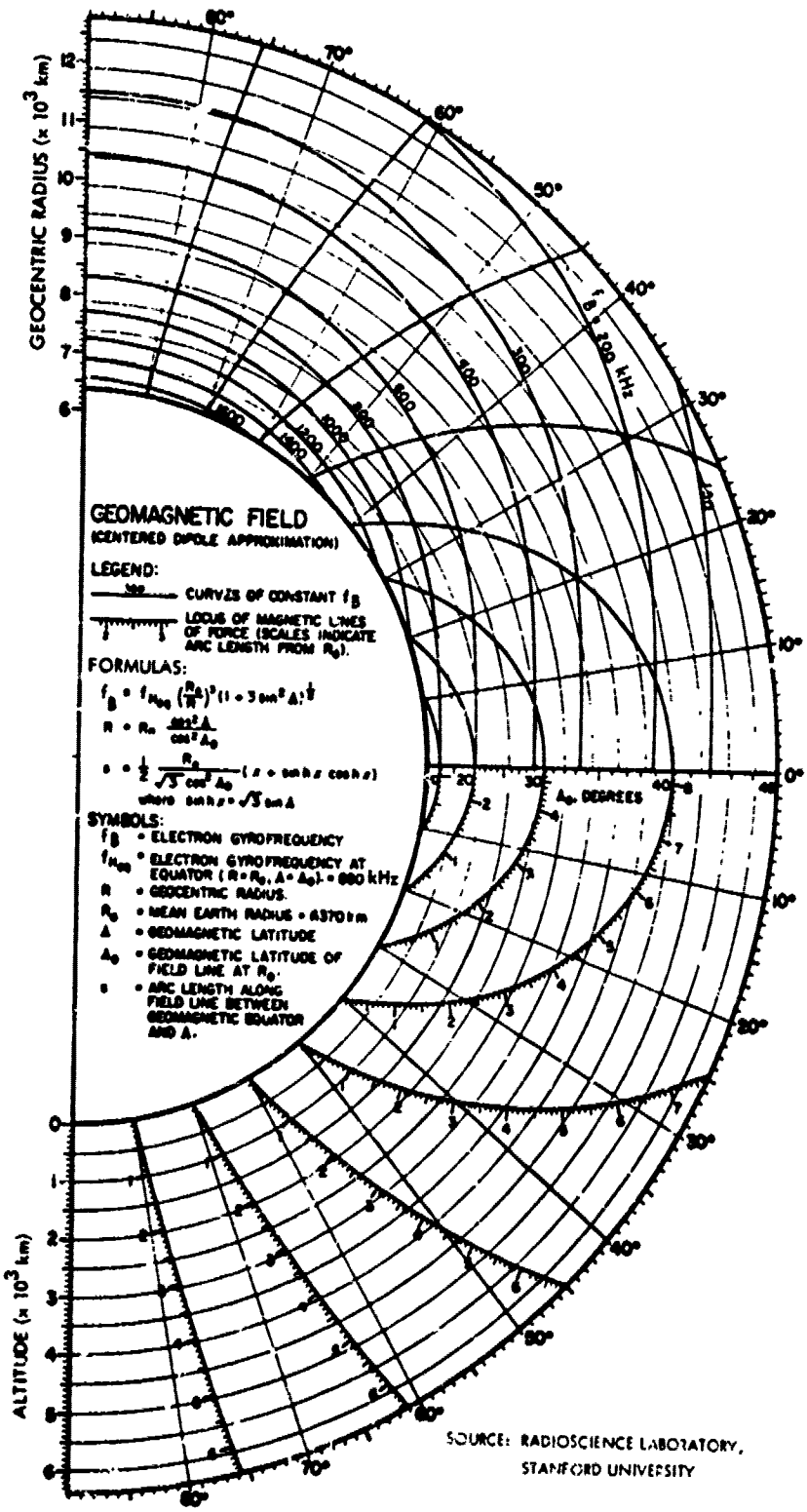

Figure 8-5. Dipole magnetic field (continued).

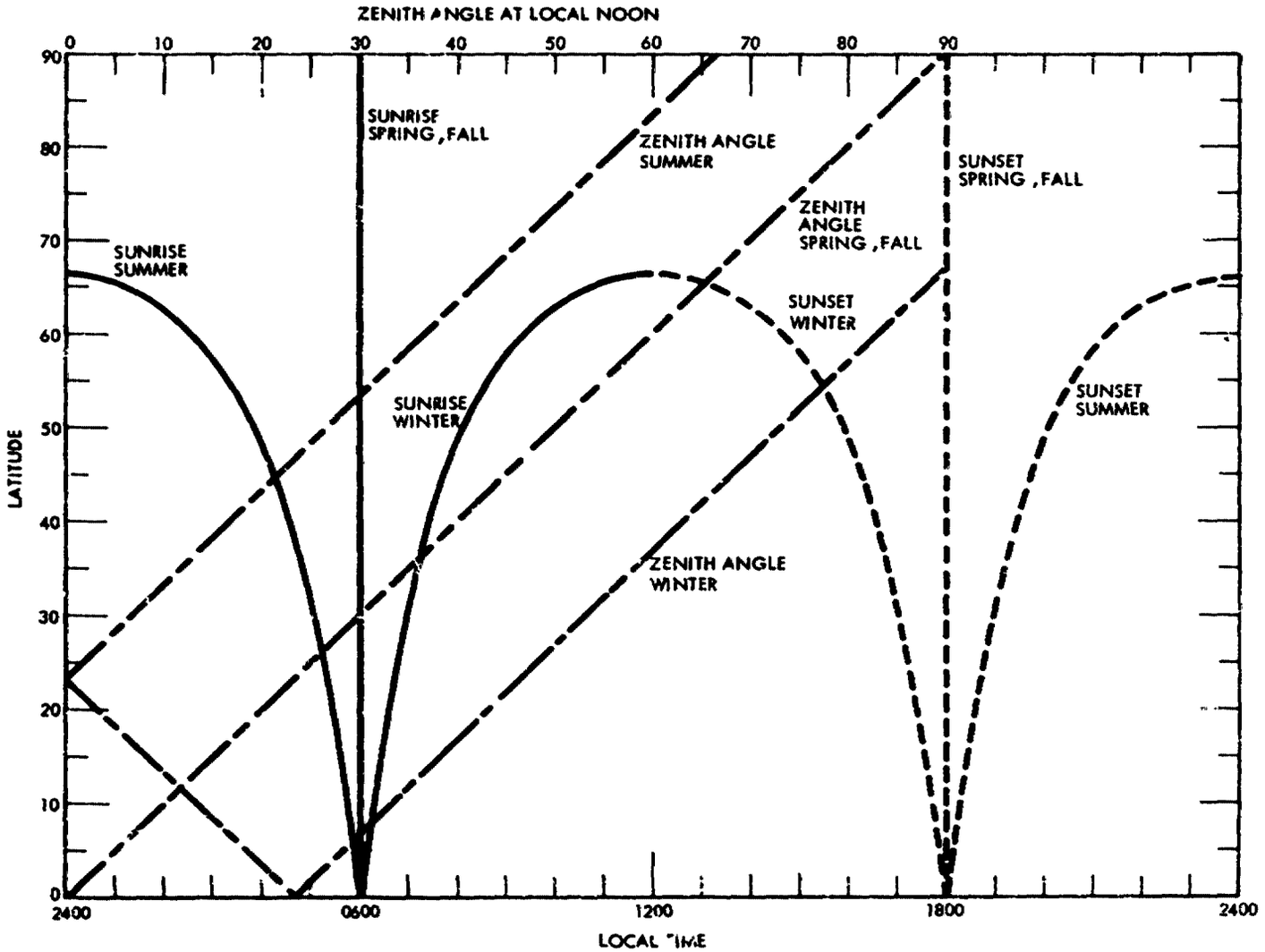

Figure 8-6A. Geometric ground sunrise, sunset, and zenith angle at local noon.

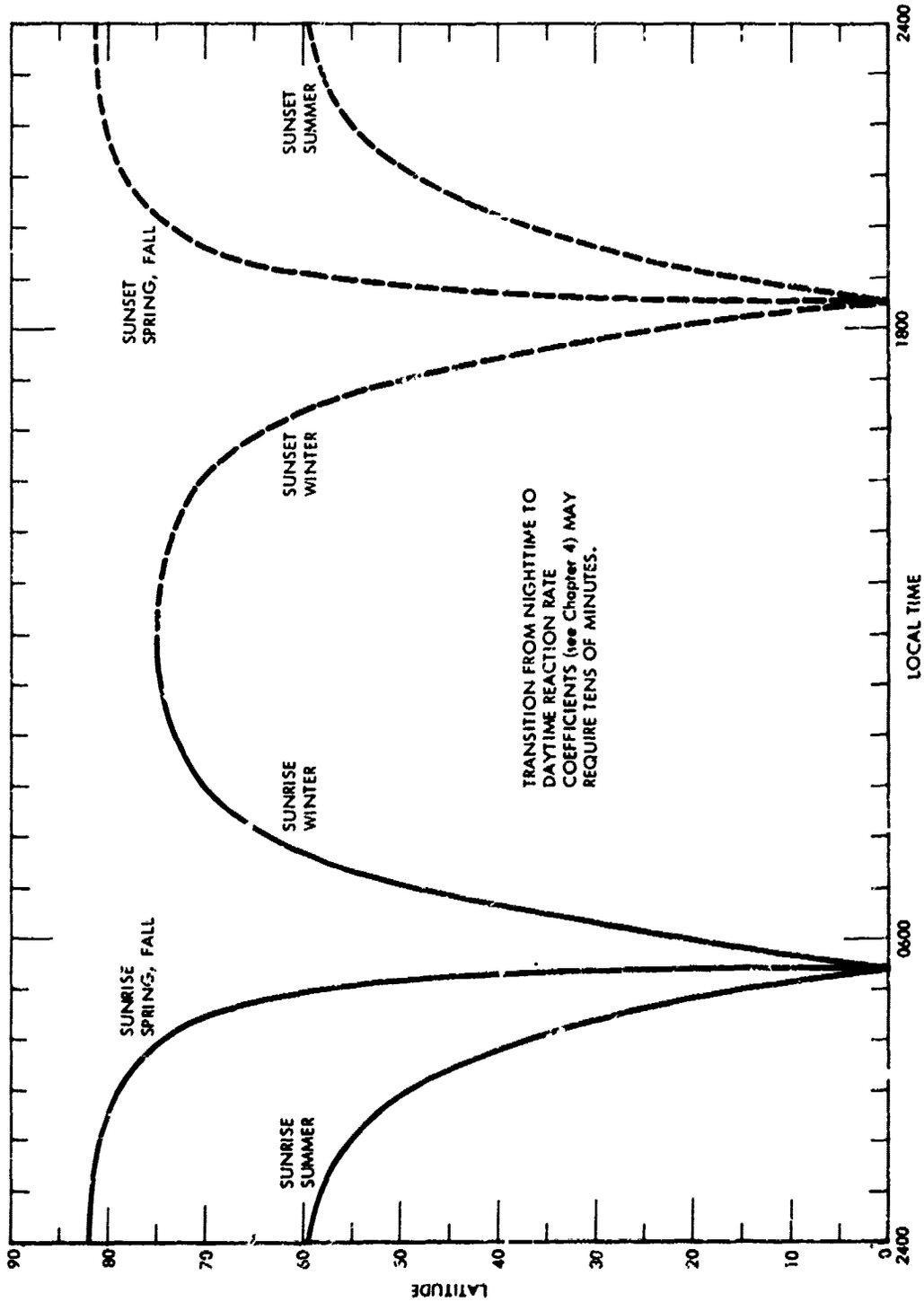

Figure 8-68. Geometric sunrise and sunset times at 65 km altitude.

SECTION 9
PHYSICAL CONSTANTS AND CONVERSION FACTORS

UNIVERSAL CONSTANTS

c	=	2.99793×10^{8}	m sec^{-1}	velocity of light in vacuum
e	=	1.602×10^{-19}	coulomb	electron charge
h	=	6.625×10^{-34}	joule sec	Planck's constant
	=	4.15×10^{-15}	eV sec	
hc	=	12.5	keV angstroms	
J	=	4.186	joules $(gm\text{-}calorie)^{-1}$	mechanical equivalent of heat
k	=	1.380×10^{-23}	joule $(°K)^{-1}$	Boltzmann constant
	$\approx$	$\frac{1}{11600}$	eV $(°K)^{-1}$	
h/k	$\approx$	4.8×10^{-11}	sec (°K)	
L_o	=	2.69×10^{25}	molecules m^{-3}	Loschmidt number
m_o	=	9.108×10^{-31}	kg	electron rest mass
$m_o c^2$	=	0.5110	MeV	
$\frac{e}{m_o c^2}$	$\approx$	2×10^{-6}	$volt^{-1}$	
N_o	=	6.025×10^{23}	$(gm\text{-}mole)^{-1}$	Avogadro's constant
r_e	=	2.818×10^{-15}	m	classical electron radius
R_o	=	8.317×10^{3}	joule $(kg\text{-}mole)^{-1}(°K)^{-1}$	gas constant

v	=	331.7	m sec^{-1}	velocity of sound (air STP)
ε_o	=	8.85×10^{-12}	farad m^{-1}	permittivity of free space
σ	=	5.669×10^{-5}	ergs cm^{-2} sec^{-1} $(°K)^{-4}$	blackbody emittance
	$\approx$	1	jerk $shake^{-1}$ cm^{-2} keV^{-4}	

CONVERSION FACTORS

Length

1 km = 1,000 m = 3.281 kft = 0.6214 mi

1 kft = 0.3048 km = 0.1894 mi

1 mi = 1.609 km = 5.280 kft = 0.8690 nmi

Cross Section

1 barn = 10^{-24} cm^2

Energy

1 eV = 1.602×10^{-19} joule = 1.602×10^{-12} erg

= 3.8×10^{-23} kcal

1 erg = 6.24×10^{11} eV

1 kcal = 4.186×10^{10} erg = 2.63×10^{22} eV

1 jerk = 10^{16} ergs

1 Rydberg = 13.605 eV

1 MT = 10^{15} calories

$\approx$ 4.18×10^{22} ergs

Other Energy Relations

1 rad = 100 erg gm^{-1}

For nonrelativistic particles:

$$E(eV) \approx 5 \times 10^3 A\left(\frac{v}{10^8}\right)^2$$

A = atomic weight

For relativistic electrons:

E(MeV)	v/c	E(MeV)	v/c
0.01	0.1956	0.1	0.5486
0.02	0.2727	0.2	0.6966
0.03	0.3293	0.3	0.7777
0.04	0.3751	0.4	0.8289
0.05	0.4138	0.5	0.8638
0.06	0.4474	0.6	0.8888
0.07	0.4771	0.7	0.9073
0.08	0.5037	0.8	0.9215
0.09	0.5277	0.9	0.9326
		1.0	0.9416

Time

1 shake = 10^{-8} sec

Pressure

1 atm = 1.0133 bars = 1.0132×10^{6} dynes cm^{-2}

= 14.70 psi = 760 torr = 29.92 in. Hg

1 torr = 1 mm Hg = 1.333×10^{3} dynes cm^{-2}

= 1.316×10^{-3} atm

1 dyne cm^{-2} = 9.87×10^{-7} atm = 7.5×10^{-4} torr

Temperature

1°C = 1°K = 1.8°F = 1.8°R

0°C = 273.16°K = 32°F = 459.72°R

Wavelength

1Å = 10^{-8} cm

1μ = 10^{-4} cm = 10^{4}Å

ATMOSPHERIC RELATIONS

M_o	=	28.9644	average molecular weight ($h < 100$ km)
n	=	$(N_o/M_o)\rho$	number density
	$\approx$	$2.08 \times 10^{22}\rho$	cm^{-3} ($h < 100$ km)
p	=	$(R_o/M_o)\rho T$	pressure
	$\approx$	$2.875 \times 10^{6}\rho T$	dynes cm^{-2} ($h < 100$ km) .